LASER INTERFEROMETER GRAVITATIONAL WAVE OBSERVATORY
- LIGO -

================================

LIGO SCIENTIFIC COLLABORATION

Technical Note	LIGO-T2200384–v2	2022/12/04
	Instrument Science White Paper 2022-2023	
	LIGO Scientific Collaboration	

Distribution of this document:

LIGO Scientific Collaboration

California Institute of Technology
LIGO Project, MS 100-36
Pasadena, CA 91125
Phone (626) 395-2129
Fax (626) 304-9834
E-mail: info@ligo.caltech.edu

Massachusetts Institute of Technology
LIGO Project, Room NW22-295
Cambridge, MA 02139
Phone (617) 253-4824
Fax (617) 253-7014
E-mail: info@ligo.mit.edu

LIGO Hanford Observatory
P.O. Box 159
Richland, WA 99352
Phone (509) 372-8106
Fax (509) 372-8137
E-mail: info@ligo.caltech.edu

LIGO Livingston Observatory
19100 LIGO Lane
Livingston, LA 70754
Phone (225) 686-3100
Fax (225) 686-7189
E-mail: info@ligo.caltech.edu

http://www.ligo.org/

Contents

List of Figures

1 Introduction

The inauguration of the Advanced LIGO detectors made clear that there are great opportunities to conduct new science by measuring gravitational waves. On September 14, 2015, when only at about 40 percent of the aLIGO design sensitivity, the aLIGO interferometers made the first detection of gravitational waves, GW150914 [16]. The discovery rate is accelerating; during the first and second Observing runs (O1 and O2), LIGO, in collaboration with the Virgo project, detected 10 binary black hole mergers [17, 18, 19, 20, 21] and the merger of two neutron stars [22]. In O3 the detection rate was about once per week, and the total count of gravitational-wave (GW) events from the coalescence of compact binaries now stands at 90. Improved detector performance will enable more detections and more accurate measurements of the astrophysical parameters encoded in the waveforms of the merging compact objects.

This Instrument Science White Paper describes the work by the LIGO Scientific Collaboration (LSC) to conduct research and development to improve the current generation of LIGO and GEO interferometers and to develop new concepts, prototypes, components, and to perform modeling for future interferometers. The LSC Operations White Paper [23] describes Detector Commissioning, Calibration, Computing, Detector Characterization, and the Joint Run Planning Committee – some of which straddle this document, particularly as ideas move from research into deployment at the detectors. The coordination of these efforts is described in the LIGO Scientific Collaboration Program 2022 [24]. Each subsection in sections 3-8 of this white paper refers to a particular topic in that document.

The success of Advanced LIGO, the A+ upgrade, and future upgrades and detectors requires a robust instrument science research program. This research program enables us to lay the foundation of upgrades to the detectors and to respond to the many challenges we discover while commissioning and operating some of the most sensitive scientific instruments ever built. This white paper represents the current best thinking of the LSC Instrument Science working groups:

- Advanced Interferometer Configurations Working Group (AIC) including Newtonian Noise and Interferometer Simulations.
- Quantum Noise Working Group (QNWG).
- Lasers and Auxiliary Optics Working Group (LAWG).
- Optics Working Group (OWG).
- Suspensions and Seismic Isolation Working Group (SWG).
- Control Systems Working Group (CSWG).

This white paper provides a survey of the current and planned R&D of these working groups; it will be updated yearly based on ongoing R&D and the experimental and observational results obtained.

Gravitational-wave detector development spans a number of different timescales and research areas. The most immediate effort is to improve the performance and understanding of the existing detectors and to reach the Advanced LIGO and A+ target design sensitivity. A somewhat longer term effort is to design, build, and characterize test systems and prototypes

for future detector upgrades and entirely new detectors. The research described in this Instrument Science white paper is focused on developing the very best gravitational wave detectors, but as we push the science of precision measurement forward, we are also looking for opportunities to impact other fields of physics.

This white paper uses a roadmap to describe the research and development for the instruments over the next 2 decades, 2020-2040, in order to focus effort and aid prioritizing tasks. This roadmap will be revised and refined yearly.

2 Roadmap 2020 - 2040 and Executive Summary

2.1 Detector Epochs

The first detection of gravitational waves [16] was a major scientific event and marked the birth of the science of gravitational wave astronomy. The need to probe further out into the universe and thus further backward in time is compelling instrument scientists and engineers to develop and deliver ever more sensitive GW detectors and will do so for generations to come. Tomorrow's global network of next-generation detectors will allow us to study novel astrophysics, cosmology and gravitational phenomena as described in many places including the Einstein Telescope Design Study [25], the Cosmic Explorer Horizon Study [26] and the GWIC science case [27].

The international gravitational-wave community is now planning for the next generation of observatories, known as third generation, or "3G" detectors. As we move towards these 3G observatories, we envision three epochs of detector operation spread over the next two decades. The first (and current) epoch is defined by enhancements to the existing Advanced LIGO detector, first to enable stable operation at the Advanced LIGO design sensitivity, and then to go beyond the Advanced LIGO design with the A+ upgrade. The second epoch will be devoted to maximizing the scientific benefits of the current LIGO facilities as we move towards the 3G detectors. This will be done by the proposed $A^\sharp$ upgrade (see 2.4), which is seen as the limit to what can be achieved in the LIGO facilities using detectors based on room temperature, fused silica optics. In addition to further improving the scientific reach of LIGO, $A^\sharp$ will also test key technologies for 3G detectors.

A third epoch is foreseen in the mid-2030s with installation of 3G detectors in new facilities. These are instruments capable of observing signals originating in the early universe. In the U.S., this is the Cosmic Explorer concept [28]. Research for 3G detectors is underway now. For Initial and Advanced LIGO, the time between initial conception and operation was 15 to 20 years, and we would expect a similar time span for 3G detectors. A typical detector cycle includes: assimilation of ideas and concepts; experimental laboratory work; conceptual design and prototyping; proposal writing and submission; engineering from concept to final design; construction and installation; commissioning; and observing. The research and development for new technologies to be implemented in such facilities needs to be done in the next several years to allow the design and timely funding construction of these projects.

The epochs of detector improvement are discussed below, with an emphasis on the critical research required to achieve the desired astrophysical performance. For discussion of the

system-level trades used to inform these designs, please see section 3 - Advanced Interferometer Configurations.

2.2   Achieving Advanced LIGO Design Sensitivity

The LIGO detectors alternate between periods of astrophysical observation and commissioning; the current schedule for the Observing Runs is described in Ref. [29]. A major goal of the LIGO Lab and the LSC Instrument Science teams is to achieve stable operation at the Advanced LIGO target design sensitivity. Figure 1 shows the fundamental noise sources that limit the Advanced LIGO design in its original high power, broadband tuning configuration [1]. The design sensitivity is limited by shot noise at high frequencies, by mirror coating Brownian thermal noise in the mid frequencies, and largely be quantum radiation pressure noises at low frequencies.

Aplus design curve - NSNS (1.4/1.4 $M_\odot$) 325 Mpc and BHBH (30/30 $M_\odot$) 2563 Mpc
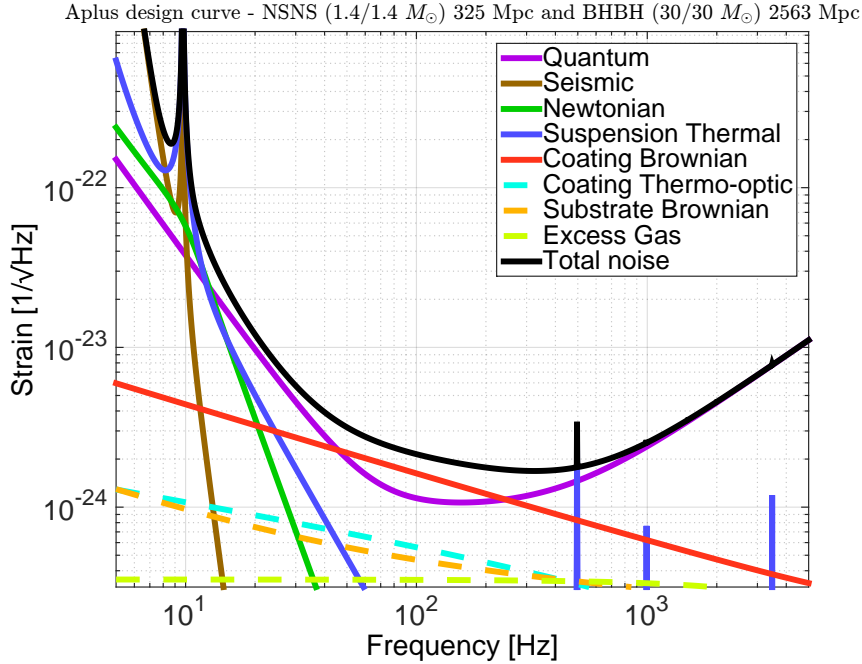
Figure 1: Design Sensitivity Curve for Advanced LIGO, from [1]. This is the baseline design, at full power (750 kW in the arms) and with broadband signal extraction tuning.

Since the A+ upgrade has now been partially implemented (see 2.3), that target sensitivity can be met at a lower power level in combination with frequency-dependent squeezing. That is the goal for the O4 run, for which the target range for binary neutron star coalescences is 160–190 Mpc. At the time of writing this document, the detectors are near the end of the installation work required for O4, and beginning the final commissioning period to achieve the O4 sensitivity goal.

There are a number of known technical issues which limit the performance of the detectors. There is also excess noise of unknown origin, and experience has shown that improving the detector sensitivity often reveals new noise sources. At this time, we know that the following

issues will have to be addressed in order to reach design sensitivity:

- Stabilize the interferometer controls as the power is increased.
- Reduce the noise and noise coupling of the laser system.
- Develop improved control techniques to reduce the control noise in the 10–25 Hz frequency band (particularly, but not limited to angular control noise).
- Reduce the impact of noise from scattered light.
- Understand and mitigate as needed noise from electro-static charge buildup.
- Improve the models for interferometer noise couplings.
- Identify and eliminate the (currently) unmodeled noise sources between 20 and 80 Hz.
- Monitor and control parametric instabilities as the power is increased.
- Monitor and compensate for thermal distortions as the power is increased.
- Characterize coating thermal noise in the interferometers.

In addition, we strive to improve the robustness and reliability of the detectors:

- Improve the overall duty cycle of the detectors.
- Improve the robust operation of the detector during large environmental disturbances such as high wind and earthquakes.
- Understand and mitigate the occurrence of instrumental transients (glitches)

The LSC and the LIGO Lab are working to bring the current Advanced LIGO detectors to the point where they will perform reliably at the Advanced LIGO design sensitivity. Knowledge of the current sensitivity limitations informs the research for next generation instrumentation, and lessons learned from improving the current detectors are already being incorporated into the upgrade plans.

2.3   The A+ Upgrade to Advanced LIGO

The LIGO Lab and its international partners have begun an upgrade to Advanced LIGO known as A+. This upgrade is planned to improve the binary neutron star inspiral range by a factor of 1.9× over Advanced LIGO (to around 325 Mpc), with a binary black hole range greater than 2.5 Gpc (see Figure 2). As noted, parts of the A+ upgrade are being implemented for the O4 observing run, and the complete upgrade will be in place for O5 [29]. The A+ upgrade includes:

- Frequency dependent squeezing using a 300 m filter cavity.
- Lower loss Faraday isolators and Active Wavefront Control.
- A larger diameter beamsplitter.
- Balanced homodyne readout and associated suspended steering mirrors.
- Test masses with mirror coatings that have a factor of 2 lower thermal noise than present coatings.

The first two items – squeezer filter cavity and elements to reduce squeezer losses – are being implemented for the O4 detectors. Maximum sensitivity improvement, however, requires
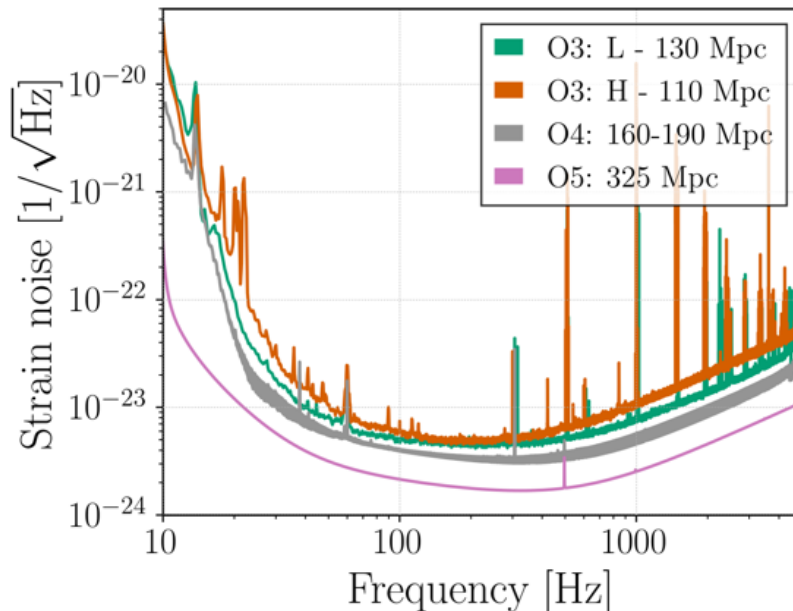
Figure 2: Strain sensitivities from Observation run 3 (O3), and the projected sensitivities for O4 and O5. The latter is the A+ design sensitivity [2].

reductions in both quantum noise and coating thermal noise [30], which will come with the second phase of the upgrade for O5.

There is ongoing R&D for A+ which includes:

- Development of improved amorphous coatings to reduce mechanical loss while maintaining optical quality, aiming for 4 times reduction in mechanical loss.
- Design and testing of the balanced homodyne readout system.
- Studying production of fused silica suspension fibers to ensure frequencies of violin modes are sufficiently matched.

2.4   Beyond A+: the A$^\sharp$ upgrade

In spring 2021 an LSC 'Post-O5 Study Group' was formed by the LSC Directorate, and charged with studying scenarios for upgrading the LIGO detectors beyond the A+ program [31]. The report issued by the group in fall 2022 recommends an immediate post-O5 upgrade design that goes by the working title of A$^\sharp$ [32]. The A$^\sharp$ design currently aims at a room temperature interferometer operating at $1\,\mu$m laser wavelength, with the following upgrades beyond A+:

- $100\,$kg fused silica test masses
- Fused silica suspension fibers operating at twice the current stress level
- Updated suspension designs to improve controllability and reduce cross-coupling to the angular degrees of freedom

- Improved seismic isolation for reduced control noise
- Subtraction of Newtonian noise
- Laser power increase to $1.5\,\mathrm{MW}$ arm power
- Squeezing increase to $10\,\mathrm{dB}$ broadband
- For higher power operation: improved thermal compensation; reduced coating absorption (uniform and point-like); improvements to parametric instability mitigation
- Coating thermal noise reduction
- Options for wideband signal recycling

More details on each of the above can be found in the Post-O5 report. The noise budget for this upgrade is shown in Fig. 3. For the targeted improvement in coating thermal noise, the report uses the projected thermal noise for a GaAs/AlGaAs crystalline coating as the example, although the improvement could alternatively come from amorphous coatings with reduced mechanical loss.
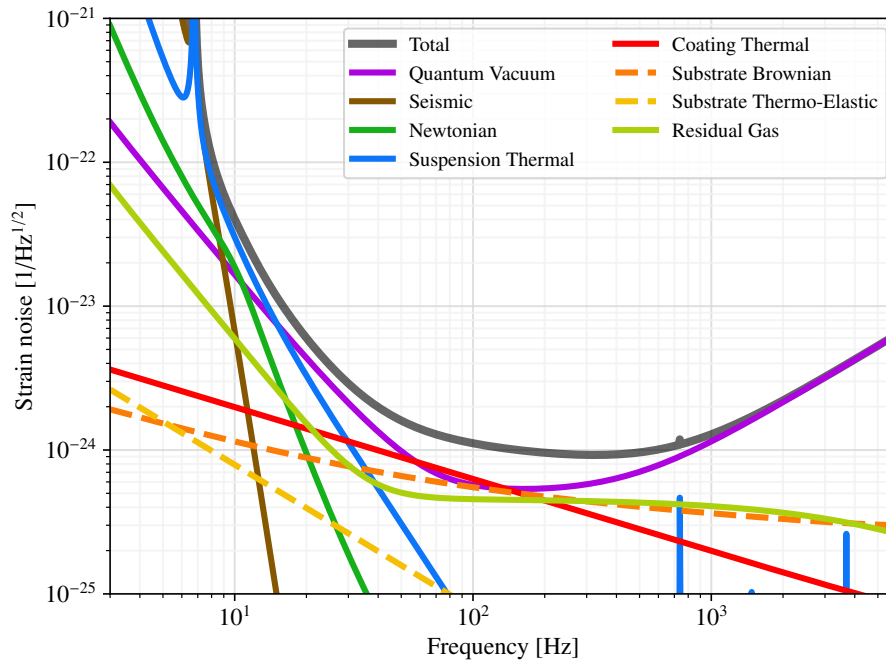
Figure 3: Strain noise for the A$^\sharp$ interferometer upgrade proposed in T2200287.

2.5 Cryogenic Operation and LIGO Voyager

Operation of gravitational wave detectors at low temperature offers potentially great benefits, as well as major challenges. The KAGRA detector [33] is designed to run at very low temperature (the sapphire test masses will be operated near 23 K), and the European Einstein Telescope design has one part of the detector working at low temperature. The LSC is exploring the Voyager concept, which has silicon test masses operating at 123 K and is designed to operate at the existing LIGO sites and in the existing vacuum envelope [34]. Voyager technologies are also seen as the basis of second generation detectors for the proposed new Cosmic Explorer facility.

Voyager offers a potential factor of 2.5-3 increase in BNS range beyond A+ (to 1100 Mpc), and is envisaged with a low frequency cutoff down to 10 Hz. Simulation and experimentation is underway now so that it could be possible to be operational in around a decade. See Figure 6 for the noise budget. A cryogenic upgrade to Cosmic Explorer would use the Voyager approach described below, and experience tells us that laying that groundwork early will have significant payoffs for the CE upgrade.

The LIGO Voyager design will improve sensitivity across the entire LIGO frequency band, 10 Hz to 8 kHz. However, substantial basic research is required to make the system design for Voyager a success because the subsystem improvements are tightly coupled: decisions made about one subsystem likely place requirements on other subsystems. For example, high frequency improvements achieved using increased laser power and low frequency improvements from reduced suspension thermal noise drive the need for low temperature operation. Low temperature will both reduce thermal distortions and lower the thermal noise of the mirrors. It also necessitates a change of the mirror substrate material (to silicon) and may also drive a change to the suspension material. The use of silicon optics drives a change to the laser wavelength to 2μm. The need to reduce scatter loss to maximize the effectiveness of squeezing across the spectrum may also be a driver for longer wavelength operation. In addition to new high-power lasers, the change in wavelength also drives a need for new optical components such as photodetectors, modulators, and Faraday isolators, all of which must meet LIGO requirements. The development of new optical coatings for low temperature with ultra-low optical and mechanical loss is also required. The R&D required for Voyager is laid out in the following sections for each working group.

It is difficult to overemphasize the technical challenge, complexity, and breadth of research and development required to operate gravitational wave detectors at low temperature. It is clear that research must be underway now and that the laser wavelength must be selected soon if technologies are to be ready for large-scale prototyping in roughly 5 years. Some of this work will be leveraged by the progress at KAGRA. Even if Voyager technologies are first implemented as an upgrade to CE, it is critical that LSC research be supported if these detectors are to be implemented.

2.6   Next generation of Gravitational wave Detectors and Facilities

As noted earlier, the U.S. concept for 3G detectors is Cosmic Explorer. The reference concept for Cosmic Explorer is a 40 km detector and a 20 km detector, both located in the United States. Both detectors would use a dual-recycled Fabry–Pérot Michelson interferometer, as in Advanced LIGO (and A+ and A$^\sharp$). Cosmic Explorer's increased sensitivity comes primarily from scaling up the detector's length from 4 to 40(20) km. With ten times the sensitivity of Advanced LIGO, Cosmic Explorer will push the reach of gravitational-wave astronomy towards the edge of the observable universe.

The science objectives and detector concepts are laid out in the Cosmic Explorer Horizon Study [26]. The reference detector concept for Cosmic Explorer is largely based on the evolution of technology currently deployed in LIGO and other gravitational-wave detectors. Nonetheless, significant instrument R&D is required to scale these technologies to Cosmic Explorer, and improve their performance in several key areas. The detector research required

for Cosmic Explorer is detailed in Ref. [35].

2.7   Structure of this White Paper

In the remainder of this paper, the six working groups each describe the R&D topics that fall under the aegis of that group. In addition, each topic is categorized as being either "Op", short for InfraOps, or Infrastructure and Operations, or "LT", short for Long Term. These designations are made using the definitions and guidelines in the LSC Program for 2022 [24].

3 Advanced Interferometer Configurations

The primary purpose of the AIC group is to coordinate the integration of interferometer systems into coherent wholes, which can then be studied to optimize trade-offs in future detectors. This includes studying broader configurations of detectors, length, angular, and higher order wavefront sensing schemes and how they impact the interferometer as whole. The following sections are organized in terms of the progress of detector technologies presented in the roadmap (section 2), followed by a sections on Newtonian noise mitigation and interferometer sensing and modeling, both of which describe R&D that is relevant to the configurations of the anticipated detector upgrades to LIGO. This R&D typically has strong overlaps with longer term design ideas such as Voyager and third generation observatories.

Op-3.1   A+

This work falls under section 2.3 of the LSC Program, "A+ Upgrade Project"
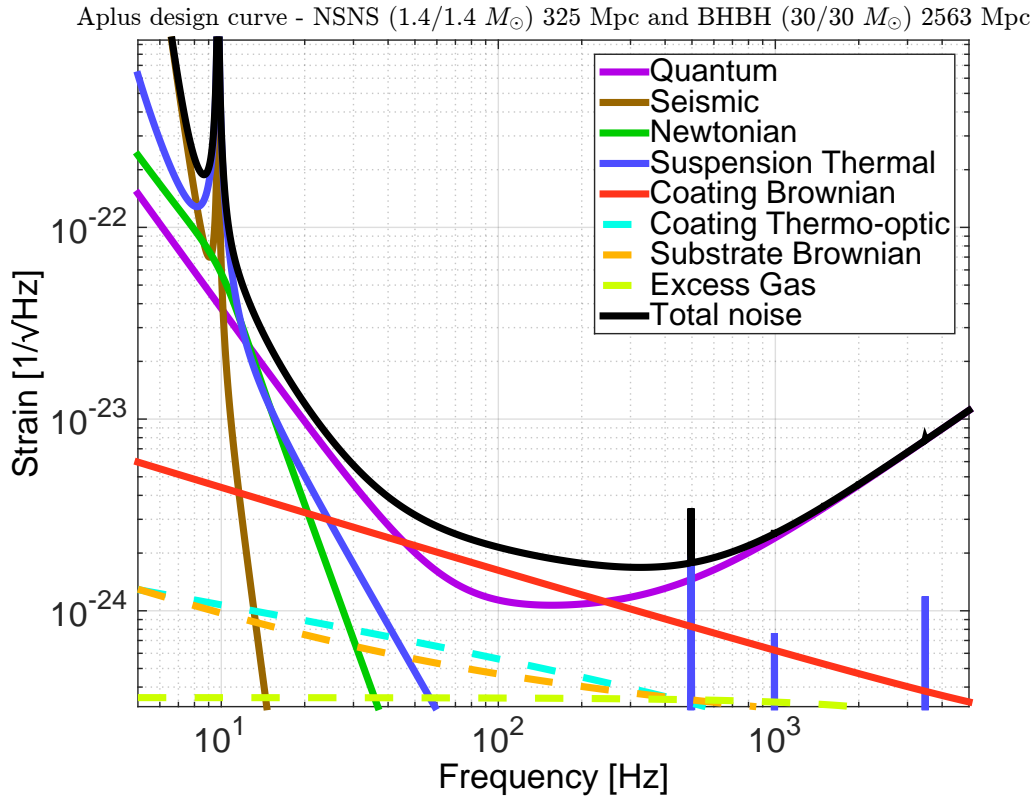
Figure 4: Design sensitivity of the A+ upgrade from [2].

A+ will be operational in 2023–2024. Figure 4 shows the A+ design sensitivity [2] using the parameters as given in Table 1. The A+ upgrade improves the two main limiting fundamental noise sources, namely quantum noise and coating Brownian noise.

Once operational, A+ will have a larger reach and therefore will survey a substantially larger volume of space than the unmodified aLIGO detectors would cover, by a factor of about 4-7

depending on the type of source, in effect collecting many years' science in each observing year. This will come with increased waveform resolution, to discern important physical details of loud event waveforms.

Gwinc Parameter	Value	Comment
ifo.Materials.Coating.Phihighn	$3.6 \times 10^{-4}/4$	tantala mechanical loss
ifo.Materials.Coating.Philown	$5 \times 10^{-5}/4$	silica mechanical loss
ifo.Laser.Power	125W	full power
ifo.Optics.Loss	37.5e-6	75 ppm round-trip
ifo.Optics.BSLoss	0.5e-3	
ifo.Optics.PhotoDetectorEfficiency	0.9	Improved readout loss
ifo.Optics.SRM.Transmittance	0.325	SRM transmission
ifo.Optics.SRM.Tunephase	0	SRM tuning
ifo.Optics.Quadrature.dc	90*pi/180	Readout phase
ifo.Squeezer.Type	'Freq Dependent'	Squeezing injection
ifo.Squeezer.AmplitudedB	12	SQZ amplitude [dB] (at the OPO)
ifo.Squeezer.SQZAngle	0*pi/180	SQZ phase [radians]
ifo.Squeezer.InjectionLoss	0.05	5% loss in SQZ path to IFO
fcParams.L	300m	filter cavity length
fcParams.Lrt	60e-6	round-trip loss in the cavity
fcParams.Te	1e-6	end mirror transmission
Gwinc Output	**Value**	**Comment**
Finesse	446	
Power Recycling Factor	43	
Arm power	750 kW	
Power on beam splitter	5.35 kW	
BNS range	325 Mpc	(comoving)
BBH range (30/30)	2.56 Gpc	(comoving, z = 0.7)

Table 1: Gwinc parameters for the A+ design curve [2].

Op-3.1.1   Frequency dependent squeezing and balanced homodyne readout

Squeezed states of light [36] have already been used to improve the sensitivity of gravitational-wave interferometers [37, 38]. However, any reduction in quantum shot noise at high frequencies is accompanied by a commensurate increase in quantum radiation pressure noise (for frequency independent squeezing).

By reflecting a squeezed beam from a detuned high-finesse optical resonator, known as a filter cavity, one can produce frequency dependent squeezing which can simultaneously reduce shot noise at high frequencies and radiation pressure noise at low frequencies [39, 40], enabling broadband improvements. In order to achieve the required bandwidth of the filter cavity and taking into account that mirror loss, backscattering and phase noise contamination set an upper limit on the allowed optical finesse, for A+ a finesse of 446 and a filter cavity length of 300 m was chosen.
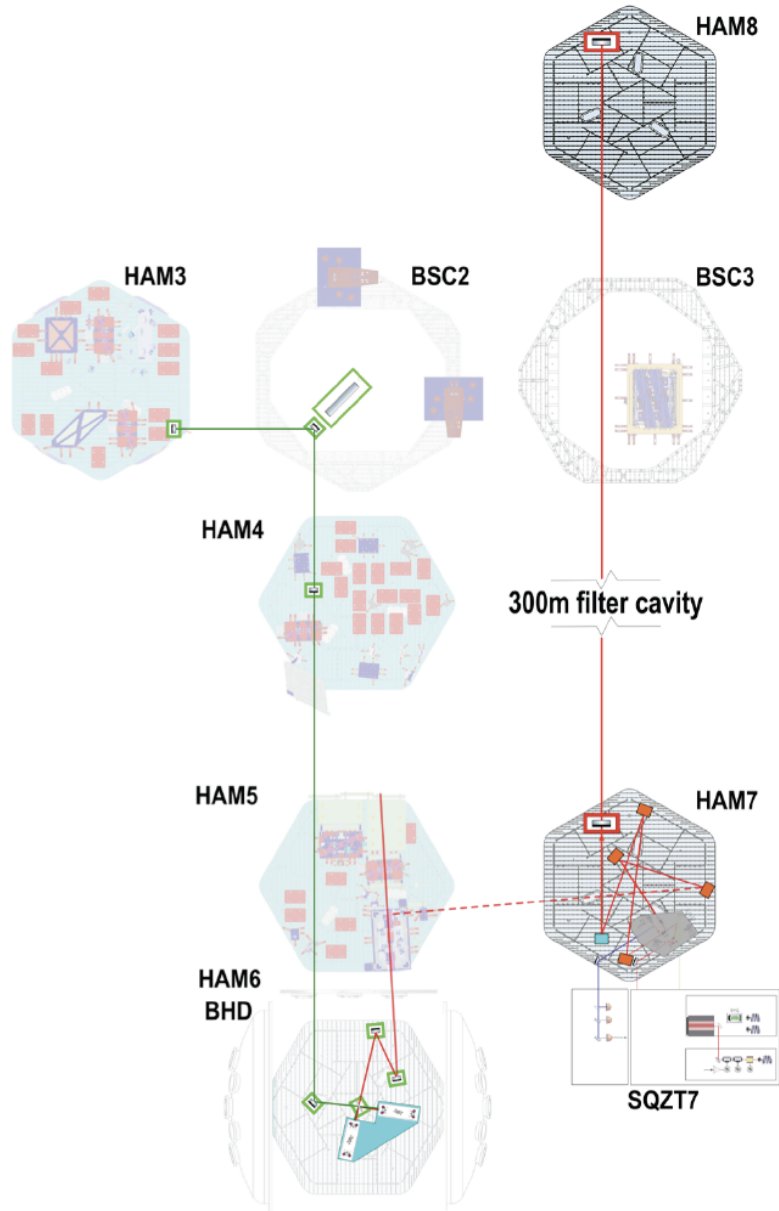
Figure 5: Sketch of optical layout of A+ detailing the filter cavity for the frequency dependent squeezing as well as the beam path relevant for the balanced homodyne readout.

In order to maximise the gain in quantum noise reduction, the A+ upgrades include a number of additional changes aimed to reducing the optical loss in the injection path, the main interferometer and the detection train. First of all the main beam splitter will be replaced by one with a larger free aperture (from currently 370 mm to 450 mm) to reduce clipping losses in the central interferometer from currently about 600 ppm down to about 100 ppm. Additional improvement of optical efficiency will be obtained by application of Faraday isolators with lower loss, improved mode matching between the various optical resonators (e.g. output beam to output mode cleaner etc) and adaptive mode matching elements to be integrated in the output train.

Finally, A+ will switch the main readout method from DC-readout to balanced homodyne detection (BHD). This will be installed in the later half of the A+ upgrade. BHD requires a local oscillator beam delivered geometrically separated from the signal beam. As shown in Fig. 5, for A+ the local oscillator beam will be derived from the POP port and then guided via several low-noise suspensions to the detection system, consisting of the separately suspended balanced homodyne beamsplitter and a suspended platform carrying two output mode cleaners and the relevant BHD photo detectors. BHD allows us to eliminate the need for static imbalance in the interferometer arms, and therefore reduces unwanted noise couplings to the GW signal channel. In addition, BHD affords the capability to fine-tune the reference phase in order to optimize squeezed light performance.

Op-3.1.2 Overview of AIC Research and Development for A+

The following list summarizes the R&D expected to be useful for A+, along with more minor improvements which are not directly related to the interferometer design.

- **Frequency Dependent Squeezing:** Quantum noise reduction R&D is discussed in section Op-4.2.1. In order to maximize the benefit from squeezing, it is crucial to minimize the losses between the squeezed light source and the gravitational wave photodetector in transmission to the output mode-cleaner (OMC). This requires developing ultra-low loss Faraday isolators, large diodes with high quantum efficiency, and a high throughput OMC. Moreover, at the interface between a squeezed light source and the interferometer, there are problems of alignment control and mode matching. Squeezing drives stringent mode-matching requirements which can only be met by a system capable of on-the-fly optimization. This will require a sensing scheme capable of measuring the mode-matching and feeding back to in-vacuum optics which can change the beam parameters. The mode overlaps of interest are those between the squeezed light source, the filter cavity, the interferometer, and the output mode cleaner (OMC).
- **Balanced Homodyne Detection:** Changing over the main readout system from DC-readout to BHD requires R&D in a variety of areas, including low phase-noise delivery of LO beam to the readout system; integrated arrangement of two output mode cleaners on a pre-isolated platform; low noise in-vacuum readout electronics of the BHD; control strategy for the BHD readout angle etc.
- **Newtonian Noise Subtraction:** All future detectors will benefit from Newtonian noise subtraction using seismometer arrays. While this may not be critical for A+, Newtonian noise coupling predictions vary, as does the seismic environment, making this an important form of risk reduction for both aLIGO and A+.
- **Scattered light:** Stray light control will need to be reevaluated for A+ due to its increased sensitivity.
- **Higher order wavefront sensing schemes** Increasing the circulating power in the arms for aLIGO has proved problematic. Further increasing the optical power stored in current and future detectors will require effective methods for mode-matching and mitigating the effect of point absorbers in coatings will be required. New methods and techniques in this area for allowing better and faster optimisation of detectors would be beneficial.

- **Optical Coating Quality:** Study of the three sources of optical loss and distortions to higher order mode resonances related to the coatings (coating thickness non-uniformity which leads to figure error, prompt scattering from micro-roughness and scattering from "inclusions" or "defects" in the coatings) will be necessary for A+ to succeed.
- **Charge Mitigation:** Charges on the test-masses are a potentially limiting noise source for aLIGO and future upgrades. Both as risk reduction for aLIGO, and to allow for the improved sensitivity of A+, research related to minimizing charging of (or removing charge from) the test-masses is of interest.
- **Maximum power:** So far aLIGO has struggled to reach its target design circulating power (800kW) within the arms. This is due to a combination of radiation pressure instabilities as well as well thermal deformations. R&D is required to better understand these limitations and possible solutions to allow us to reach full power.

Op-3.2   Beyond A+

This work falls under section 2.5 of the LSC Program, "Post-A+ planning and research"

There currently exists a multi-year gap between A+ (O5) and potential upgrades to 3rd generation technologies. It is clear that the physics and astronomy community will demand scientific output from the facilities for as long as they are operational. Over the coming years the AIC working group should explore potential configuration upgrades suggested by the post-O5 study group in more details. The aim is to develop the required knowledge so that a decision can be made when required for what happens beyond A+.

These upgrades should aim to maximise the current infrastructure and ensure we meet the designed A+ sensitivity or surpass it. There are a number of technologies under investigation which could improve detector performance within the current LIGO Observatory facilities while allowing room temperature operation.

There is ongoing conceptual design work and simulation to study the scientific impact of possible improvements to the detectors. This work has led to several interesting suggestions about upgrade paths at room temperature [41, 42, 43] which exploit the benefits of the following technologies now in development:

- Newtonian noise reduction

- Specially designed substrate surface figure error over the full aperture of large test masses while managing the residual substrate fixed lens and elastic distortion of the figure error when the mirror is suspended to control higher order optical mode resonances

- Improved thermal deformation correction and sensing and how these can be used in tandem to enable arm powers beyond 1MW

- Improved control and noise suppression for the length, angular, and mode-matching degrees-of-freedom which currently impact the detector noise above 10 Hz

- Explore new heterodyne readout schemes compatible with frequency dependent squeezing [44]

- Explore the possibilities of using folding in the arms to increase the effective arm lengths

- Alternatives to frontal modulation control schemes for SRC [45]

- Improvements to the Arm Length Stabilization (ALS) system may be needed to reduce complexity, possibly by injecting 532 nm lasers from the corner station instead of at the ETMs.

- Charge mitigation techniques including cold gas discharge and possible conductive coatings

- Reduction and subtraction of scattered light noise

LT-3.3   Voyager

This work falls under section 2.5 of the LSC Program, "Post-A+ planning and research"

The LIGO Scientific Collaboration (LSC) Instrument Science Working Groups held a workshop to study designs for third generation interferometers to be installed in the existing LIGO facilities. Subsequent studies of 3 straw-man designs (known as the Red, Green and Blue designs) showed that all of the designs shared many common requirements, some of which are anticipated in the A+ design described in the previous section. The most promising of the 3 straw-man designs has been dubbed "Voyager", and adopted as the baseline design for the next major upgrade in the current facilities [34], or as an upgrade to the Cosmic Explorer concept (see section LT-3.4). R&D required for a Voyager like detector also has a strong overlap with other future detector ideas targeting high-frequency GW signals, such as NEMO [46].

While not intended to exclude other options, a straw-man design for Voyager is used to understand potential benefits and expenses involved in upgrading beyond A+. The Voyager straw-man design mitigates the limiting thermal noise of aLIGO by replacing the fused silica mirrors and suspensions with silicon parts, and operating them at 123 K. The Voyager noise budget and the corresponding sensitivity described in this section are shown in Figure 6. The details of the Voyager design and descriptions of noise sources and design choices are in Ref. [34].

The main design features of the proposed cryogenic Voyager design are

- **Large cryogenic Silicon mirrors:** In order to obtain broadband improvement of the sensitivity, 120 - 200 kg Silicon mirrors at the operating temperature of 123 K are considered.

- **Silicon cryogenic suspension:** Silicon ribbons (and perhaps blade springs) in the final stage suspension at 123 K are employed.

- **Suspensions:**   The Voyager design will require new quadruple suspension systems (SUS) designed to support heavier test masses. In addition to supporting a heavier mass, the redesign efforts should also fix any features found to hinder aLIGO operation (e.g., bounce and roll mode damping, violin mode actuation, gas damping noise, etc.).
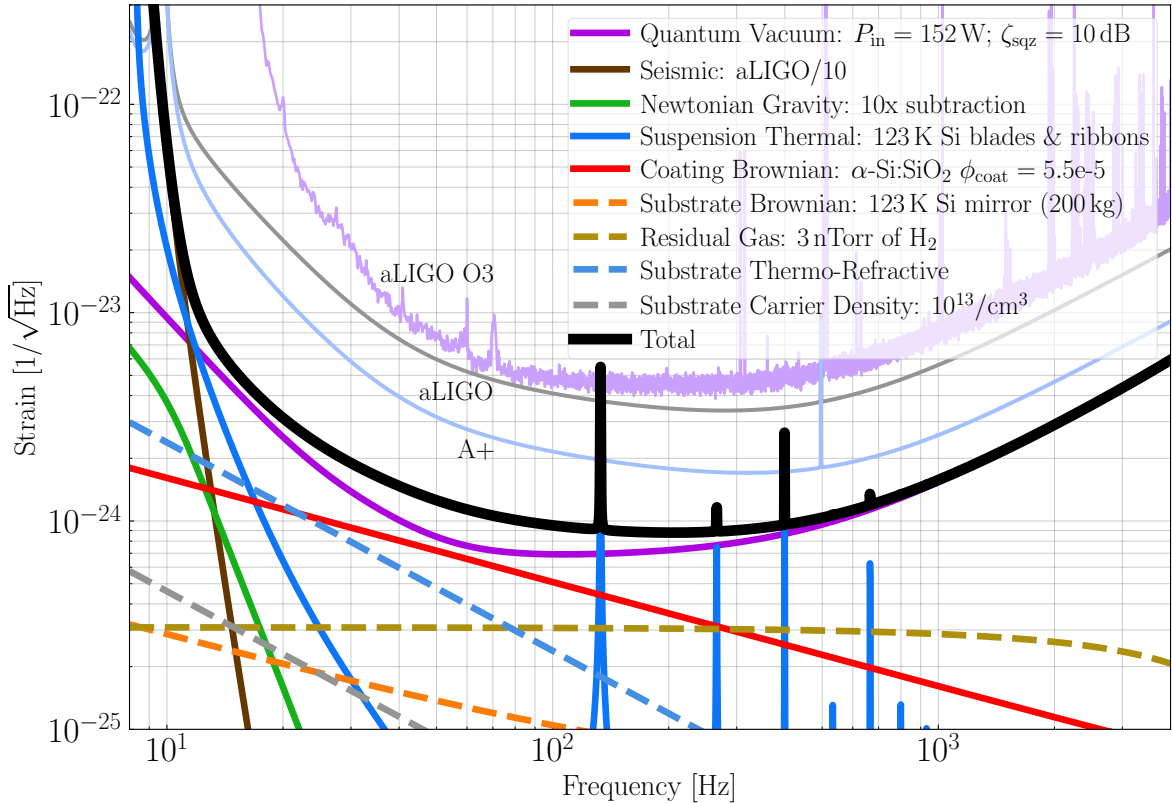
Figure 6: Strain Sensitivity of LIGO Voyager. $200\,\text{kg}$ silicon test masses at $123\,\text{K}$, and $3\,\text{MW}$ of arm cavity power. See https://dcc.ligo.org/LIGO-T1400226 for more details.

- **Newtonian noise:** Newtonian noise subtraction with seismometer arrays is included in the Voyager design, which assumes a factor of 10 suppression.

- **High power 1.5 - 2.0 μm laser:** 1.5 - 2.0 μm wavelength lasers operating at around $200\,\text{W}$ are employed. Arm cavity powers will reach $\sim 3\,\text{MW}$.

- **Coating Thermal Noise:** The beam spot size is increased by $\sim 25\%$ relative to the aLIGO size to lower thermal noise while avoiding optical stability issues and the baseline coating is assumed to be amorphous silicon / amorphous silica.

- **Quantum noise:** Squeezed light injection ($10\,\text{dB}$) and a $300\,\text{m}$ filter cavity for frequency dependent squeeze angle is assumed.

The move to the longer wavelength, motivated by the need for higher thermal conductivity to transport heat away from the optics, along with cryogenic operation offer the wide range of interesting research areas, listed below. **Note that while the wavelength is specified as 2000 nm for the noise calculations herein, wavelengths of 1500-2100 nm are being considered.** The final choice of wavelength will depend on the material properties of silicon, absorption in the HR coating, the availability of stable high-power lasers, and the quantum efficiency of photodetectors, among other things.

LT-3.4 Third Generation GW Observatories

This work falls under section 3 of the LSC Program, *"Advancing frontiers of Gravitational-Wave Astrophysics, Astronomy and Fundamental Physics: Improved Gravitational Wave Detectors"*

The current facilities, while extraordinary in their capabilities, present significant limitations to gravitational wave astrophysics. In particular, the length of the detectors is well below the optimal value, and the L-shaped vacuum enclosure only allows for the detection of one polarization of gravitational wave signal. A longer, triangular detector would relieve both of these constraints; making an order of magnitude improvement in sensitivity possible, and allowing for both gravitational wave polarizations to be measured with a single detector.

Currently, complementary design efforts are being carried out within the LSC for the Einstein Telescope (envisaged to be located in Europe) and Cosmic Explorer (envisaged to be located in the US or a combination of the US and Australia). Both of these projects are currently undergoing processes to start new collaborations with specific focus on each. The initial design of the Einstein Telescope was developed about a decade ago and is described in detail in the ET design study document [47]. The corner stones of the Einstein Telescope design are: A triangluar underground observatory consisting of three detectors of each 10 km arm length to provide full polarisation reconstruction, redundancy and null streams; each detector is comprised of two interferometers, a low-frequency, low power cryogenic interferometer and a high-frequency, high power interferometer.

The Cosmic Explorer design is based on a long, L-shaped observatory located on the earth's surface [48]. Cosmic Explorer aims to fully utilise A+ and beyond technology to achieve its goals. There is also the possibility of future upgrades to Cosmic Explorer that use Voyager technology. The astrophysical range of such a detector is shown in figure 7. Note that due to the detector's sensitivity to signals from most of the visible universe, it is necessary to express the range of such an instrument in terms of redshift at the detection horizon.

The designs used for CE make use of existing technology, or well defined extrapolations of existing technology, as a means of computing a *lower limit* to what can be done in a new facility. This should not be interpreted as a design target: Cosmic Explorer will make use of the best technology available in time for the final design process. This will certainly incorporate the results of Voyager R&D as well as other technological developments that occur in the intervening years. The design concept presented here should drive and not limit research into detector technologies and topologies useful in a very long baseline facility.

LT-3.4.1 R&D for third generation detectors

The R&D required for 3G observatories to suppress fundamental noise sources includes:

- **Large mirrors and relevant metrology :** CE and ET, depending on the exact design flavor, will require silica or silicon mirrors with diameters in the range of 0.5 m to 1.0 m.

- **Silicon cryogenic suspension:** operating at 123 K for CE and 10 K for ET-LF.
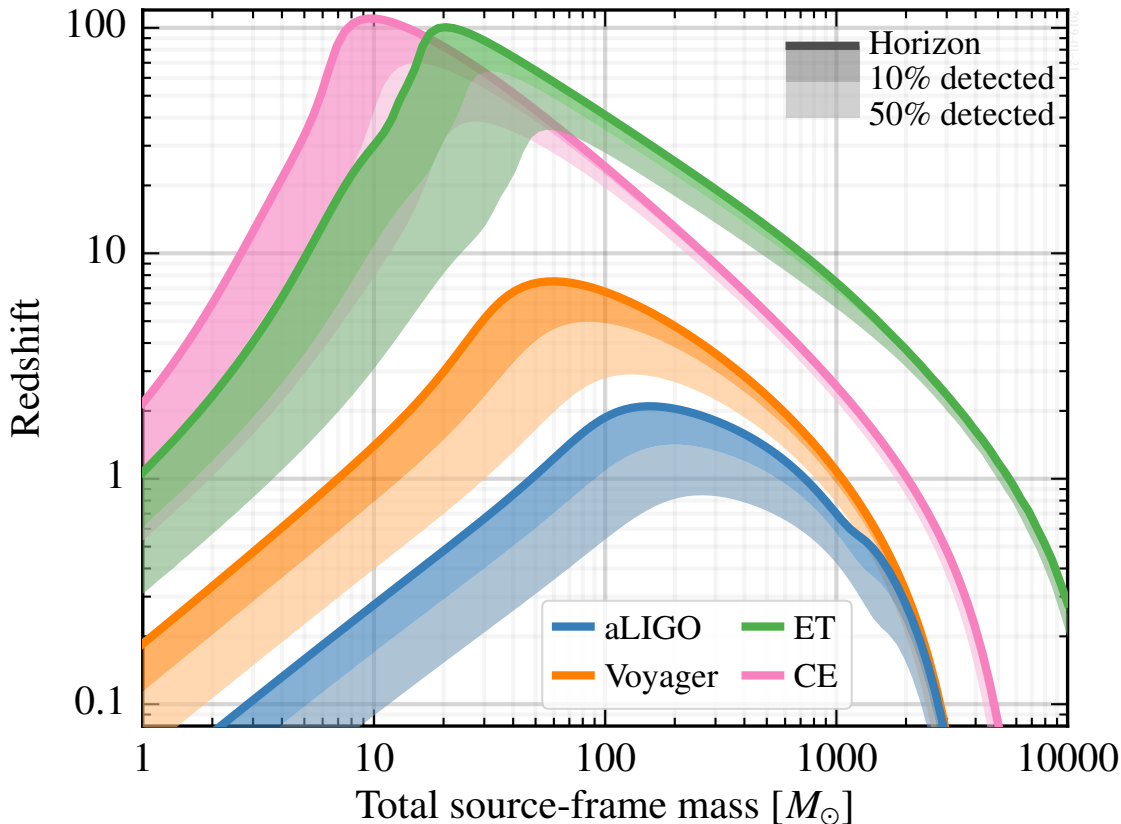
Figure 7: Astrophysical reach of various detector designs for equal-mass (non-spinning) compact binary inspiral systems. The maximum observable distance is shown as a function of the total intrinsic mass of the system. Baring a large number of primordial black holes, at redshifts larger than $z \simeq 10$ there will be few sources. Thus a horizon of $z > 20$ for a given mass should be taken to indicate that essentially *all* compact binary coalescence in the universe will be observable by a network of similar detectors, many with a high signal to noise ratio. Similar curves for the Einstein Telescope are shown for comparison. A Hubble constant of 67.9 km/s/Mpc and a ΛCDM model of expansion was assumed.

- **Suspensions:** need to be able to carry mirrors of several $100\,\mathrm{kg}$ for both warm silica (ET-HF) and crogenic silicon (CE and ET-LF). Also need to push suspensions modes to lower frequencies to allow sub $10\,\mathrm{Hz}$ sensitivity.

- **Newtonian noise:** Newtonian noise subtraction with seismometer arrays. Decomposition of seismic fields into different wave components. For more detailed description see section LT-3.9 .

- **High power laser:** Laser of various wavelength ($1064\,\mathrm{nm}$, $1550\,\mathrm{nm}$ and $2000\,\mathrm{nm}$) operating at the several hundred watt level are required to reach arm cavity powers of several MW.

- **Coating Thermal Noise:** The beam spot size will increase relative to the aLIGO size to lower thermal noise. New coating materials are required to provide low mechanical

and required optical parameters at cryogenic temperatures (123K for CE and 10K for ET-LF).

- **Quantum noise:** Frequency dependent squeezing with km-scale filter cavities form baseline designs. Alternative QND schemes may provide better sensitivity or reduced costs.

Moreover, there is a huge R&D effort required to reduce a multitude of technical noise source to a level compatible with the envisage 3G sensitivities, in particular in the sub 10 Hz band. This includes amongst others reduction of control and feedback noise, reduction of scattered light, laser noise, photo diode dark noise etc.

Finally, since 3G observatories will by definition be hosted in new facilities, there are various aspects related to site selection which require R&D:

- **Detector Network:** Given certain boundaries what is the best third generation network and how to optimally integrate Advanced + detectors?

- **Observatory Configuration:** Cost benefit analysis of single site with multiple detectors versus several sites with single detectors. This includes research on how to compare in a fair way sensitivity curves from for instance ET (several detectors) versus CE (single detector)

- **Low Frequency Cut-Off:** Analysis of the cost and benefits of extending the sensitivity into the sub-5 Hz range.

- **Integrated Cost Function for various science goals:** How to optimally combine figures of merit of several astrophysical targets (e.g. BNS range, BBH range, stochastic background, high frequency sensitivity for supernova core collapse model separation etc) into a single figure of merit which can guide the design of 3G detectors.

Op-3.5 Interferometer sensing in A+ and beyond

This work falls under section 2.3 and 2.5 of the LSC Program, "A+ Upgrade Project" and "Post-A+ planning and research".

Op-3.5.1 High power photo-detection

To achieve the required level of intensity stabilization of the input laser light substantial amounts of DC photocurrent must be detected. At low frequencies, photodiodes are subject to excess $1/f$ noise that degrades their performance. Research to characterize, understand, and improve upon photodiodes will be necessary to detect the signals from high power interferometers and at wavelengths from 1 to 2 micron.

In addition to the DC photocurrent, the RF power received by the RF detectors will also increase. Increasing the SNR in the RF detectors will directly reduce the auxiliary controls noise (a limit in nearly all GW interferometers) and so needs to be explored carefully.

Op-3.5.2   Output mode-cleaner

Moderate finesse mode cleaning cavities are used to filter the interferometer output beam to ensure that the output photodetectors sense only the interferometer's fundamental spatial mode.

The mode matching between the interferometer and the OMC is particularly critical for future interferometers in which losses will be critical due to increased use of squeezed light. Output mode matching presents a particular difficulty as it varies with the interferometer thermal state. Current research is exploring the use of thermal and mechanically deformable mirrors for adaptive mode matching [49]. Maximising the use of these new actuators by using appropriate sensing schemes will be required. Dithering, "Bull's Eye" wavefront sensing for measurement [50], and other RF sensing schemes are being explored [51, 52].

Op-3.5.3   Balanced Homodyne Detection for DARM

To measure high levels of squeezing, to allow for a tunable homodyne readout angle, and to avoid a variety of technical noises it would be advantageous to move away from DC readout for the interferometer's primary output (DARM). Balanced homodyne readout, standard practice in tabletop squeezing experiments, offers some advantages over DC readout (see P1100202, P1300184 and P1500091).

Work is underway on designing the balanced homodyne detection (BHD) system for A+ [53], and the Caltech 40m prototype is being outfitted with BHD [54].

Op-3.5.4   Wavefront diagnostics and corrections

Each of the mirrors in Advanced LIGO will have slightly different absorption characteristics and therefore will react differently when subjected to laser powers projected for Advanced LIGO (see T1100250-v2 [55]). Point absorbers in the test mass coatings are also limiting current interferometers [56, 57]. Sensing these point absorbers is currently achieved using the Hartmann sensors. Much work is being conducted to identify and remove these absorbers from the coatings at the source, however current and future non-cryogenic detectors may require higher order thermal actuators to compensate for deformations these absorbers induce. How different compensation schemes affect the interferometer should be considered.

In addition to the Hartmann style sensors, we may use phase cameras (essentially multi-pixel RF Wavefront Sensors). These could be used to implement real-time wavefront correction. Primitive phase cameras have been used in iLIGO and iVirgo, but there were problems due to the scanning induced backscatter. Future phase cameras should allow for wavefront sensing of individual sidebands simultaneously without any moving parts. Signifcant upgrades have been made to the phase cameras for Advanced Virgo [58]. Current research is also underway on using time-of-flight style sensors [59] as well as other non-mechanical schemes [60]. How to effectively use phase cameras in A+ and beyond should be investigated.

Op-3.6   Interferometer modeling / simulations

Op-3.6.1   Overview of Modeling

Interferometric gravitational-wave detectors are sufficiently complicated optical systems that detailed modeling is required for design and performance studies. The detector behaviour cannot be modelled with commercially available optical simulations because our requirements are very different from conventional systems. For example, the length scales involved in interferometric GW detection span 22 orders of magnitude. A variety of simulation tools has been developed by the GW community, successfully addressing the various problems encountered in interferometric GW detectors.

The planned upgrades to the detectors include either new technologies or envisage pushing detector parameters closer to their limits. In both cases the detector design and commissioning face new challenges, as previously used assumptions and simplifications can no longer be used. Simulation tools and the understanding of interferometer modelling have to be advanced ahead of time in order to be able to provide the essential design and commissioning support.

Simulations which use the FFT for propagating paraxial beams such as SIS [61] or OS-CAR [62] can be used to make detailed predictions about the impact of optical phase errors (surface roughness, phase distortions, etc.) and finite aperture sizes. FFT simulations are, however, too slow to simulate interferometer dynamics, and are therefore only used to find steady-state solutions. Potentially faster implementations of FFT based simulations can be performed using Linear Canonical Transforms (LCT) instead [63].

For understanding interferometer dynamics over a wide range of conditions which do not allow for linearization (e.g., not only at the operating point), time-domain simulations are the most appropriate tools. This type of simulation is important for lock acquisition studies and existing tools fill the need for most optical configurations [64, 65]. However, like FFT simulations, despite considerable optimization effort, time-domain simulations are slow and able to simulate only the lowest transverse-spatial modes. New simplified time domain tools are being developed to study particular non-linear angular sensing and control issues [66] and should be pursued further to provide new understanding of low-frequency behaviours.

For control system development, where we can assume that we are at a stable operating point and linearize around that point, frequency domain simulations such as Optickle [67] or Finesse [68, 69] prove an invaluable tool. Advanced LIGO control system development has depended on the Optickle simulation engine, which has been packaged for LSC design in Looptickle and later Lentickle, and for ASC design as Pickle. In addition to control system development, frequency domain simulation tools are also used to compute limitations to interferometer sensitivity due to fundamental noise sources (e.g., quantum noise) and technical noises (e.g., laser noise and auxiliary length degree of freedom control noise). Future tools should provide a simple and effective way to combine optical, mechanical and electronic systems to estimate control noise in the presence of multiple cross couplings. A new python based tool QLANCE [70] is being developed that wraps both Finesse and Optickle for modelling such control systems and cross couplings.

The commissioning of Advanced LIGO, as well as the design of further upgrades have shown that the combination of frequency domain simulations with paraxial beam propagation has become crucial to understand interferometer limitations. Geometric instabilities and thermal

beam distortions, both due to higher laser power, can dominate the interferometer behaviour. Modelling tasks related to alignment sensing and control, parametric instabilities, or simply the effect of mode mismatch or beam clipping on the control systems and ultimately on the gravitational wave signal have taken center stage. Simulation tools such as Finesse and MIST [71] use higher-order mode expansion to describe the laser beam properties and can combine the speed of frequency domain tools with the power of paraxial beam propagation. Such modal-modelling tools have become key tools in the commissioning of Advanced LIGO to date and will be used to transfer and apply aLIGO knowledge into the upgrade design process. Further development is ongoing to improve their performance and to add more advanced features.

The configuration level simulation, discussed in section LT-4.4, operates at a higher level in that the response of a given optical configuration is symbolically computed and parameterized [72]. A recent update has been written in Python, pygwinc [73]. This package offers a more usable and adaptable tool for computing noise budgets for a variety of interferometers. These symbolic computations can be compared with the more detailed numerical results given by frequency domain codes. While inappropriate for detailed simulation of the optical plant, this approach is very effective for an initial exploration of a parameter space for a variety of optical configurations. Further development of the GWINC configuration level simulation to accommodate the variety of optical configurations is currently under way for future detectors and will aid in down-selection and optimization.

To date these simulations have focused on the core of the interferometer, the optics, and have largely neglected the surrounding mechanical systems. A missing piece in detector simulation is a comprehensive mechanical simulation tool for the vibration isolation and suspension design (LSC Program section 3.2) which includes the capability to handle a variety of mechanical systems and the ability to compute of thermal noise for any given configuration.

In addition, development of the various simulation tools, future detector design and study will benefit greatly from a dedicated effort to organize and document these tools. Experience has shown that smaller, dedicated tools have been more effective that those tools trying to combine everything into one system. However, most tools come only with rudimental or outdated documentation, and code reviews or formal testing of simulation results are not common practice. In particular the main and established software tools should provide:

- An active maintainer who is responsible for the current code based and who can be identified and reached by any users of the software.

- A single webpage hosting the master version of the tool or code.

- Documentation about the implemented models and their limitations, including descriptions of mathematical algorithms, or parameter sets used.

- Training material, such as a set of examples and tutorials for new users, especially graduate students.

The effectiveness of simulation tools for the development of future detectors will be enhanced with some more high level organisation to coordinate the above requirements.

Simulation tools are strongly defined through the context in which they are used. Many of the priorities for the research and development directly translate into a priority task for modelling work or a required effort in developing new capabilities for simulation tools. Below we list a subset modelling challenges.

Op-3.6.2   Commissioning Advanced LIGO to reach design sensitivity

This work falls under section 2.2 of the LSC Program, " LSC Detector Commissioning and Detector Improvement activities"

Advanced LIGO has seen a rapid initial commissioning phase leading to the first detection. As expected, progress has now slowed because the origins of excess noise become harder to identify or eradicate closer to the final design sensitivity.

Advanced LIGO and future detectors will operate at higher light power so that thermal distortions of the optics and the change of the mirror suspension response due to radiation pressure will play a dominant role. In particular the transfer functions of any displacement signal into the detection ports will show the optical spring effects and higher-order mode resonances. Thus to model noise coupling of auxiliary degrees of freedom or auxiliary optics system into the gravitational wave channel we require models that include thermal effects and radiation pressure at the same time. For the rapid development of the control systems and noise mitigation strategies during the detector commissioning it is desirable that such simulation software is a fast, flexible and easy to use tool. Specific priority tasks include:

- Alignment sensing and control, modelling of mode sensing schemes, possibly using alternative sensors, in particular to improve noise around soft mode. Adding additional sensors to simulation tools, matching the models to experimental results, tools such as Lightsaber [74] are being developed to tackle this.

- Noise couplings at low frequencies: modelling of auxiliary optics and thermal distortions to mitigate coupling into longitudinal signals at low frequencies, modelling of beam jitter and beam size fluctuations. Including a more detailed mechanical coupling and feedback in optical modelling tools.

- Noise Budget Software: a simple tool (preferrably matlab or python) to estimate the current noise budget of the LIGO interferometers based on current data and parameters. Software to quickly and easily make measurements of noise budget traces (parent spectrum and non-linear coupling functions).

- High-power operation: modelling of parametric instabilities and thermal lensing to improve performance of mitigation systems, such as active wavefront control systems. Provide and test convenience functions for beam tracing and mode couplings.

- Knowledge transfer and training: providing documentation of modelling result, easy to use parameter files for the LIGO detectors and a forum in a simulation group will be important for recording the knowledge gained from commissioning and operating the first advanced interferometer and to train young scientists, towards the design of upgrades and new detectors.

Op-3.6.3   The A+ upgrade

This work falls under section 2.3 of the LSC Program, "A+ Upgrade Project"

The A+ upgrade introduces significant changes to the output optics, adding a balanced homodyne detector and frequency dependent squeezing. The design for these systems is under way. During the A+ upgrade a down-selection of coating options is required with the initial coating design being driven by models. The neccessary modelling tools are available but require the development indicated above. Current priorities for this phase include:

- Frequency dependent squeezing, modelling of non-linear optics in the squeezer and defects in the filter cavity and injection path to optimise system for maximum effective squeezing. Modelling of control signals for filter cavity and of injected squeezed light.

- Balanced homodyne detector, in particular coupling of signals and noise due to imperfections in core optics and auxiliary output optics. Modelling of control for auxiliary optics, the OMCs and the local oscillator phase.

- Coating thermal noise, combine various models into unified and accessible coating simulator, provide guidance for coating down selection.

- Improved models of the thermal state of the interferometer, not only the optical behaviour but more accurate finite-element analysis of thermo-refractive and -elastic effects.

Op-3.6.4   Post-A+ and possible further upgrades of current facilities

This work falls under section 2.5 of the LSC Program, "Post-A+ planning and research"

Each improvement in detector sensitivity will uncover new unwanted noise coupling mechanisms that typically require post-hoc mitigation strategies. This implies that for the designs of future detectors, we must model and study potential designs at greater depths than previous detectors. Voyager will introduce significant changes, such as cryogenic suspensions and a different laser wavelength. The main challenge will be the operation at very high circulating power (several MW). For the design of medium term upgrades such as Voyager a more consistent modelling of control noises is required to reduce the risk of low-frequency excess noise already at the design stage.

- High-power operation at low optical loss. Small asymmetries in absorption can increase the effective optical loss for squeezed states. Modelling of squeezed light in higher-order modes, improved thermal compensation systems, improved arm and mode matching techniques (LSC Program section 2.5, 3.5, 3.6).

- Parametric instabilities control, modelling of advanced mode dampers, development of a control scheme that allows tracking and selective damping of a large number of modes, requires more detailed modelling to predict individual modes.

- Scattered light control, modelling of backscatter of detection optics and internal interferometer scatter. Include injection of noise with specific coherence into interferometer modelling tools.

- Control design: better models of control schemes can be achieved by developing more effective tools for the analysis of in-loop cross coupling of a mixed mechanical, optical and electronic system. It is expected that modern control schemes as mentioned in section 8 will be used in a subset of systems at this time.

LT-3.7 Interferometer modeling / simulations: Third generation designs

This work falls under sections 3.7 and 3.8 of the LSC Program, "Topologies" and "Large Scale Facilities"

The 3G designs will introduce new facilities and therefore can potentially make use of very different optical configurations (very long arms, speed meters, very long auxiliary cavities) (LSC Program 2019-2020, section 3.7). Quantum noise reduction presents a challenge that will most likely have the strongest impact on the interferometer design. Newtonian noise reduction will be required. At the moment the main priority for interferometer modelling is to capture the knowledge from the current design and commissioning work to inform 3G designs. Other priority modelling task for this stage include:

- Advanced quantum noise schemes, development of a robust 'fundamental' quantum limit. Modelling of quantum correlations through complex MIMO (multiple in, multiple out) systems.

- Modelling of non-linear optical elements, such as crystals (squeezing), active optomechanical elements (unstable filters) etc. Development and implementation of realistic linearised couplings for these elements into optical models.

- Modelling of long-baseline and high-cavity finesse operation, including geometric consideration, control schemes and thermal effects.

- Study of optical configurations which rely strongly on polarisation schemes, requires the addition of light polarisation to interferometer models.

- Newtonian noise reduction, advanced modelling of local sensing (6D) and global control strategies, a more advanced implementation of mechanical systems and seismic and Newtonian noise coupling in interferometer models. Simulation of Newtonian noise based on ground noise measurements.

- Investigation of alternative beam shapes for thermal noise reduction, modelling of auxiliary optical systems to study feasibility.

Op-3.8 Newtonian Noise

This work falls under section 2.5 "Post-A+ planning and research" of the LSC Program.

Fluctuations of the gravity field due to terrestrial sources cause random displacement of test masses. This is generally known as Newtonian noise (NN), and it is predicted to limit the sensitivity of Advanced LIGO detectors between about 10 Hz and 30 Hz once their target sensitivity is reached [75]. According to current models, it is the contribution from seismic surface fields that will dominate at the LIGO sites [76]. Specifically, one can neglect atmospheric NN, NN from seismic body waves, and NN from vibrating structures. The main activities today focus on the development of a NN cancellation system as possible upgrade of the Advanced LIGO detectors based on monitoring of the seismic field by a seismic surface array [77].

Since NN increases steeply towards lower frequencies, and since its mitigation is a major challenge, NN must be considered early in the design of third-generation detectors, which will potentially extend the detection band to frequencies below 10 Hz. The outcome of these early analyses might strongly influence the detector design, i.e., they will inform decisions whether the detector should be built underground or above surface, or how aggressively the community should push the development of technologies to gain low-frequency sensitivity. Current efforts include the modeling of NN in underground environments, and characterization of underground seismic fields at the former Homestake mine [78]. Another major concern is that atmospheric NN might become a limiting noise source, which could potentially set an ultimate sensitivity limit especially to surface detectors [79].

Op-3.8.1 Beyond A+

This work falls under section 2.5 "Post-A+ planning and research" of the LSC Program.

Status quo A first comprehensive estimate of various NN contributions at the LIGO sites showed that seismic (ground vibration) NN strongly dominates (by about a factor 10 and more) over other NN contributions such as sound NN, and vibration of infrastructure [76]. These studies justify the focus of current activities on seismic NN characterization and cancellation. Only if NN is to be canceled by about a factor 10 (or more) will more careful studies of sub-dominant NN contributions be required.

Two array measurements were carried out at the LIGO Hanford site. The first array consisted of 44 Wilcoxon 731-207 sensors that were deployed in 2012 at the EY end station and took data for about a year [77]. The second array consisting of 30 L-4C sensors together with a tiltmeter from the Washington group was deployed in August 2016 at the corner station and also took data for about a year. Analysis of the array data showed that seismic fields are highly homogeneous, stationary in the NN band, and the dominant component is produced by local sources. This suggests that it will be relatively easy to cancel NN at the Hanford site, and that it is straight-forward to compute near-optimal array configurations in advance.

Further evidence of the efficiency of a future cancellation system came from noise-cancellation tests using a compact tiltmeter as target and seismometers as reference channels [80]. It had been shown previously that ground tilt under a test mass is fully coherent with acceleration NN under certain ideal conditions, and that it therefore serves as an ideal proxy of the actual NN and that a tiltmeter can be used to probe NN cancellation well before it is seen in GW detectors [81]. These tests were carried out with the result that the tilt signal fully canceled

in tiltmeter data. Performance limitation came from the tiltmeter instrumental noise.

Summary of required R&D activities   The development of a NN cancellation system as possible upgrade of Advanced LIGO requires activities in the following categories:

- Data characterization in the NN band

- Deployment of seismic arrays

- Static Wiener filters

- Optimization of array configurations

- Implementation in existing data-acquisition systems

Data characterization in the NN band   It is important to understand other noise contributions in the NN band to be able to predict and later analyze the performance of the NN cancellation system. Such studies should include long-term correlations between seismic sensors and the GW channel, search for coincident transients in the NN band between seismic channels and GW channel, and also further investigations of non-gravitational couplings between seismic data and the GW channel [82]. Some of the required tools can be derived from existing software developed in various LSC groups such as STAMP-PEM, KleineWelle, h-veto, etc.

Deployment of seismic arrays   Since one of the results of the array measurements is that the dominant seismic sources in the NN band are all part of the site infrastructure, one might argue that properties of the seismic fields at other stations can be inferred from the existing array data. While this might be true for the remaining Hanford end station, differences in geology between the Livingston and Hanford sites are substantial. Therefore, the recommendation is that at least one array measurement should be carried out at the Livingston site, preferably at the corner station, using a similar number of sensors as used at Hanford, ideally including a tiltmeter, and with data being recorded for at least two weeks.

Static Wiener filters   The simplest filter type that can be expected to achieve some cancellation of NN is the static Wiener filter [83]. It takes the data from a seismic array as input and maps them linearly to a single output, which represents the best linear estimate of the NN associated with the seismic field.

One needs to keep in mind that the optimization of the filter in this context does not include the optimal positioning of seismic sensors, on which the filter performance will strongly depend [75]. This problem is addressed in a separate task.

Preliminary results obtained from the Hanford array measurements suggest that better cancellation performance can be achieved if the Wiener filter is recalculated once per day, but the effect is minor (to be published). Such findings are important for the implementation of a noise filter since more options exist to implement a static filter.

The standard representation of a Wiener filter is a finite-impulse response (FIR) filter, but alternatives should be investigated. One might consider other static filters, Kalman filters, or adaptive filters. Even neural networks might be used to represent a filter, which has the potential advantage that a non-linear filter can in principle deal with more complicated structure in the data such as repetitive short transients.

Optimization of array configurations   The optimization of array configurations turns out to be the most challenging task for the development of a cancellation system. This will be true for A+, Voyager, and third-generation detectors. An array can be completely ineffective to cancel NN if the sensor positions relative to the test masses are chosen poorly. Optimization can be based on models of the seismic field, which are necessarily simple. In this case, algorithms have been developed to calculate optimal array configurations.

The problem is when the seismic field has certain features that are difficult to include in a physical model. Above all, seismic fields with significant inhomogeneity can typically be modeled only with computationally expensive finite-element simulations, which is not compatible with finding optimal configurations of arrays with many sensors being by itself a computationally expensive operation.

The easiest way to base the optimization on measurements is to pick the most effective seismometers from an array that has more sensors than required for cancellation and discard the rest. This has been successfully tested with the Hanford arrays. The open problem is to make use of array data to predict where the optimal sensor locations are, which do not have to coincide with the position of any of the sensors used for this analysis. A solution to this problem might lead to improvements of a cancellation system for A+, and Voyager, but it is absolutely essential for realizing a cancellation system for underground detectors, or surface detectors with very ambitious targets for NN suppression.

It should be emphasized that the two array measurements at Hanford suggest that optimization can in fact be based on relatively simple, homogeneous models of the seismic field, which greatly simplifies the problem.

Implementation in existing data-acquisition systems   This task concerns the strategy for developing a cancellation system. A cancellation system can be implemented by (a) using stored data, (b) using static filters that subtract in real time before data are stored, e.g., to improve sensitivity of low-latency GW searches, and (c) using filters that are adaptive or regularly updated. It seems feasible to start with either (a) or (b), and develop the system towards (c) as upgrade. Each option requires the development of software that should work autonomously even for option (a). An additional issue about option (c) is that it might require significant computational resources, which are not available in the existing data-acquisition system.

Op-3.8.2   Voyager

This work falls under section 2.5 "Post-A+ planning and research" of the LSC Program.

Status quo   Little work has been done so far that is specifically relevant to Voyager. One of the main tasks will be to understand the composition of the seismic field in detail in terms of surface and body waves. This can be done with existing Hanford array data. Work that has already started concerns the filter design. Neural networks were trained with reinforcement-learning algorithms with the goal to substitute the static Wiener filters. Such nonlinear filters might have fundamental advantages.

Summary of required R&D activities   The development of a NN cancellation system for Voyager would result from continuous enhancements of the A+ cancellation system. In order to achieve a factor 10 suppression of NN, the following additional tasks need to be included:

- Modeling of NN from seismic body waves and its cancellation

- Potentially, deployment of borehole seismometers

- Optional: modification of site infrastructure

- Optional: advanced filters (nonlinear, adaptive, ...)

Modeling of NN from seismic body waves and its cancellation   It is conceivable that the contribution of body waves to seismic NN can be significant if noise suppression factors of 5 or higher are to be achieved. In order to be prepared for this case, models have to be refined that combine NN from surface and body waves. The models must also provide methods to investigate possible array configurations to cancel NN from body waves if necessary. This task should also include an estimation of the effect of seismic scattering on NN and its cancellation, and the impact of local, near-surface geology.

Potentially, deployment of borehole seismometers   A possible result of the previous task is that a three-dimensional seismic array is required to cancel seismic NN in Voyager. This means that borehole seismometers need to be deployed. Since it is probably too costly to deploy borehole arrays for site characterization, the optimal three-dimensional configuration must be estimated from models and surface-array data.

Optional: modification of site infrastructure   A result of the previous array measurements at Hanford is that the dominant seismic sources in the NN band all form part of the site infrastructure. This is above all the air-handler fans at the end stations, and a variety of sources at the corner station. Any decrease of the seismic perturbation caused by these systems would result in a similar decrease of NN. It is therefore reasonable to consider modifications of the site infrastructure as part of the NN mitigation effort.

One approach would be to relocate the dominant seismic sources to increase their distance to the test masses, or to redesign their supports so that less energy is coupled into the seismic field. It was also suggested to dig recesses around the test masses that would remove most of the mass bearing the density perturbations of the seismic field. This could greatly reduce NN

from seismic surface waves. These schemes are more costly than NN cancellation, but they would guarantee a certain NN reduction, and they are complementary to NN cancellation.

Optional: advanced filters (nonlinear, adaptive, ...) Many potential alternatives to static Wiener filters exist. Wiener filters can be continuously recalculated, one can implement Kalman filters or generic, (quasi) linear adaptive filters, or even nonlinear filters for example based on neural networks. Enhanced filter designs might provide optimal noise cancellation even if two-point correlations of the seismic field change slowly, and some of the design options might even be able to deal with sudden changes of the field associated with seismic transients. It is therefore of interest to investigate alternative filter designs.

LT-3.9   Newtonian Noise: Third Generation

This work falls under section 3.2.C "Suspensions and Seismic Isolation" of the LSC Program.

Status quo Two third-generation projects are currently being pursued. First, finite-element simulations are carried out to investigate the impact of stratification and surface topography on NN and its cancellation. Second, an underground array was deployed and decommissioned at the the Sanford Underground Research Facility (the former Homestake mine). Analysis of the Homestake array data is expected to provide important insight into the composition of underground seismic fields. The Homestake array was taking data for about a year, and was mostly composed of STS-2 seismometers with 15 underground and 9 surface stations.

Summary of required R&D activities Research on NN for third-generation detectors has various new aspects compared to the A+ and Voyager cases. First, it can influence site selection. Avoiding a site with high seismic noise is the best way to mitigate NN. This also concerns the question whether a third-generation detector should be constructed underground. Furthermore, atmospheric NN needs to be considered. In general, greater attention needs to be paid to all tasks since an overall mitigation goal of more than a factor 100 NN suppression relative to the predicted level at the LIGO sites might be requested. In addition to all the tasks listed in the A+ and Voyager sections, NN research for the third generation includes:

- Modeling of atmospheric NN and its cancellation

- Modeling of NN from vibrating structures

- Identification of sites with low NN and/or beneficial to NN cancellation

- Study of the effect of facility designs on NN

- Study of underground seismic fields

- Algorithms to analyze data from three-dimensional seismic arrays

- Potentially, development of technology to cancel atmospheric NN, e.g., LIDAR based

- Investigation of Seismic and Acoustic Metamaterials

- Optional: designing low-noise site infrastructure

Modeling of atmospheric NN and its cancellation   It is possible that atmospheric NN will become a limiting noise source of third-generation detectors depending on how much the observation band will be extended towards lower frequencies. In order to develop a cancellation system of atmospheric NN, it is important to improve our current models. Especially, hydrodynamic simulations are required that can model turbulent air flow and atmospheric temperature fields. This task must also include a simulation of atmospheric NN cancellation based on yet-to-be-developed technologies.

Modeling of NN from vibrating structures   Newtonian noise from vibrating structures such as vacuum tanks or parts of the suspension system can typically be neglected, but this has only been shown to be true for Advanced LIGO (and this conclusion probably extends to Voyager). More careful analyses have to be done for third-generation detectors, where marginal limitation by NN from structural vibrations is conceivable. If identified as a relevant NN contribution, then cancellation of this component will be relatively straight-forward since a few sensors should suffice to monitor the vibration for the purpose of NN cancellation. While rough estimates are easy to obtain, a more detailed analysis requires finite-element simulations of the vibrating structures.

Identification of sites with low NN and/or beneficial to NN cancellation   Site characterization forms an important part of the development process towards the third generation. Candidate sites have to be evaluated based on many criteria, including an estimation of NN and the impact of local geology and topography on NN cancellation. With respect to NN, the site should have lowest possible seismic noise in the NN band, and be supported by a homogeneous ground with flat topography. The last two conditions make sure that seismic scattering can be neglected, which might otherwise cause NN cancellation to be unfeasible. Characterization of underground sites can be particularly time consuming and costly, and requires special, robust equipment for data acquisition.

Study of the effect of facility designs on NN   The Cosmic Explorer baseline sensitivity extends down to 5 Hz, with the gravity gradient contribution to the strain data subdominant at all frequencies. This assumes that the contribution from seismic Rayleigh waves can be subtracted from the data by a factor of 10; all other contributions are assumed to be mitigated by the design of the facility, which will most probably have the test masses on or near the surface. Newtonian noise models will be assembled to assess which Cosmic Explorer facility designs (if any) are compatible with the above assumptions, and perhaps relax the requirement of tenfold subtraction. So far this has focused on (1) adapting analytical Newtonian noise estimates that exist in the literature (e.g., for Einstein Telescope) to Cosmic Explorer, (2) running finite-element simulations for probable facility designs beyond

the usual infinite-half-space approximations (e.g., test masses on berms), and (3) looking at new ways to measure atmospheric density fluctuations beyond infrasound microphones. Some of these activities are applicable to Voyager as well, which is also a surface detector with similar requirements and challenges.

Study of underground seismic fields   There have been very few experiments with underground seismic arrays, especially with installations of high-quality, broadband seismometers. It is therefore important to gain experience with underground arrays, and to learn how to characterize an underground site and how to use the data to calculate accurate NN models.

The array design needs to be based on prior estimates of seismic speeds and depends on the frequency band where data are to be analyzed. As a rule of thumb, the array needs to have a spacing that does not exceed half a wavelength of the shortest waves of interest, and it should ideally have a diameter larger than the length of the longest waves of interest.

Algorithms to analyze data from three-dimensional seismic arrays   The analysis of data from a three-dimensional array is a complex task. The most important goal is to understand the average composition of the seismic field in terms of shear waves, compressional waves and surface waves so that the performance of a NN cancellation system can be predicted. The analysis can be further complicated by seismic scattering, and local seismic sources. Other goals include the estimation of seismic speeds, the measurement of propagation directions of waves in the field, identification of seismic sources, and cycles due to changes in seasonal and anthropogenic activity.

Potentially, development of new sensors and technologies to mitigate atmospheric NN.   No scheme has been proposed so far shown to be effective to cancel NN from the atmosphere, which means that atmospheric NN should currently be considered as the ultimate, low-frequency sensitivity limit. It is known that a surface array of microphones is ineffective to cancel NN from infrasound. A new idea is to monitor the atmosphere by a fiber barometer system, or by a LIDAR system. First estimates showed that current LIDAR systems do not have the required sensitivity at least to monitor infrasound, and so it needs to be investigated how much the sensitivity of these systems can be improved, however it is possible though that current systems are already able to monitor temperature perturbations with sufficient accuracy. Laser fiber barometers are under development and investigation to determine if they can be fabricated with the sensitivity required to monitor atmospheric NN, in particular the infrasound component. It is also necessary to simulate NN cancellation with fiber barometer, LIDAR systems and sensors limited by Atmospheric NN [84], to learn how practical constraints such as spatial resolution and range affect cancellation performance.

Investigation of Seismic and Acoustic Metamaterials   Advances in acoustic and seismic metamaterials offer intriguing applications to reduce the seismic and acoustic environment at the sites. Metamaterials are people-designed infrastructures that can be used to attenuate either the seismic or acoustic environments. Seismic metamaterials can be different configurations of boreholes, trees or buried resonators around the site. These structures

would be utilized to reduce the Rayleigh waves propagating near the detectors. Whereas, acoustic metamaterials may be a smaller structure attached to the vacuum systems themselves to reduce infrasound. The goal will be first to design a variety of seismic metamaterials and acoustic metamaterials. Then quantify the direct impact on the full spectrum of the interferometers.

Optional: designing low-noise site infrastructure Constructing a new site offers the possibility to improve its design compared to the existing sites with the goal to minimize NN. The goal is to keep seismic noise introduced by the site infrastructure at a low level. Seismic noise can be introduced in the form of vibrating machines such as air-handler fans, or by coupling of wind turbulence with the building walls. Seismic sources should generally be kept at greatest possible distance from the test masses, which not only reduces seismic noise at the test masses, but also facilitates cancellation of the associated NN. Wind-generated seismic noise is not an issue for the advanced detectors, but it should be investigated again for a third-generation detector if built at the surface.

4 Quantum Noise Reduction

LT-4.1 Introduction

The 2nd generation detectors, which are now being pushed towards design sensitivity (Advanced LIGO, Advanced Virgo, and KAGRA), are expected to be limited by quantum noise over nearly the entire GW band from 10 Hz to 10 kHz. By quantum noise, we refer to the quantum uncertainty of the electro-magnetic field at Fourier (sideband) frequencies in the GW detection band that beats with the monochromatic laser field (carrier field) to produce shot noise (photon counting noise, quantum imprecision noise) and radiation pressure noise (quantum back-action noise).

To upgrade those detectors it is essential to reduce the quantum noise. In this section techniques are discussed that go beyond scaling-up the carrier light power for reducing the (signal-normalized) shot noise and the test masses for reducing the (signal-normalized) radiation pressure noise. Both reduce the effects of quantum noise in 'classical' ways. There are several 'nonclassical' approaches that have been proposed within the community [85, 86, 87, 88, 89]. They can be put into four categories:

(i) Injection of externally produced squeezed vacuum states of light into the signal output port [37, 38, 90, 91, 92, 93, 94]. When the optimal frequency-dependent rotation of the squeezing angle is achieved either using external optical filters, or, the interferometer itself through the EPR squeezing idea [95, 96, 97], this technique yields a broadband quantum noise reduction [98].

(ii) Internal manipulation of the GWD cavities' gain bandwidth product by using negative dispersion media and internal squeezed state production including ponderomotive squeezing [98, 99, 100, 101, 102].

(iii) Reshaping the quantum noise spectral density by dynamical back-action from test-mass motion to intra-cavity light power and vice versa (coherent feedback) producing e.g. the optical bar effect or the optical spring effect (associated with detuned signal recycling) [103, 104]. It has recently been found this category is intimately related to (ii) and the sensitivity improvement can be equally attributable to the internal ponderomotive squeezing [105].

(iv) Reducing quantum back action by performing a QND measurement, e.g. by using a speed-meter interferometer [106, 107, 108, 109], or measuring the frequency-dependent mixture of phase and amplitude quadratures that is free from back-action (variational measurement) [98], or using auxiliary quantum systems with effective negative mass to cancel back-action noise [110].

These categories are not mutually exclusive and can be combined in different ways. Recent new understanding of the fundamental quantum limit (or the so-called quantum Cramér-Rao bound in quantum metrology community) unifies them together [111, 112, 113]. The fundamental quantum limit states that the detector sensitivity is bounded by the inverse of the quantum fluctuation of the optical energy inside the interferometer—a good sensitivity requires a large energy fluctuation (or energy). This is intuitively understood in terms of the time-energy uncertainty relation; we need a large energy fluctuation to measure the spacetime precisely. We now know that (i), (ii) and (iii) are different approaches to enhance

the energy fluctuation to lower the limit, similar to the "classical" approach of increasing the optical power, and (iv) is needed to achieve the fundamental quantum limit at different frequencies.

All four categories utilize correlations within the light's quantum uncertainty (with respect to the electric fields at different phases, the so-called field quadratures) to gain the nonclassical sensitivity improvement. Generally, optical states having quantum correlations are more sensitive to optical loss than coherent states [105]. This requires future detectors producing much less optical loss for light fields that enters the signal output port, travels along the arms and is back-reflected and detected by the photo diode. All categories also require introducing additional optics, increasing the complexity of the detectors, or even require a completely new interferometer topology.

In terms of readiness for implementation, (i) is the most mature technique. Frequency-independent squeezing has been implemented in GEO 600 [38, 93], and most recently Advanced LIGO detectors [114] and Advanced VIRGO [115]. In these cases only the shot noise was targeted, since radiation pressure noise was not dominant, which will change soon. We will utilize filter cavities to create frequency-dependent squeezing to reduce the radiation pressure noise. Frequency-dependent squeezing has recently been demonstrated with tens to hundreds meter filter cavities [116, 117], which consolidates the path for its implementation in A+, Voyager, and beyond. The other three approaches (ii), (iii) and (iv) are potentially implementable on LIGO Cosmic Explorer but are immature to be considered for A+ or Voyager. Intensive research and development is needed.

Op-4.1.1   A+

This work falls under section 2.11 of the LSC Program, "A+ Upgrade Project"

LIGO A+ includes the injection of frequency dependent squeezing at 1064 nm and a measured shot-noise squeezing of up to 6 dB. A list of loss contribution that allows for 6 dB of squeezing is given. This list is input for other groups, in particular to "optics" and "AIC". From Table 9 it is likely that 6 dB is achievable. Reaching the design performance of the aLIGO input Faradays and the aLIGO OMC, careful mode-matching and using now available photodiodes with quantum efficiency (QE) > 99% [118] should see 6 dB shot noise reduction using currently available squeezers.

From Table 9 we see that 6 dB noise reduction with a total efficiency of 77% (losses less than 23%) requires phase noise to be controlled to better than 17 mrad, which has been achieved in the experiment at LASTI with a 16 m cavity [116]. Operation of the squeezed light source in vacuum, recently demonstrated in [119], might be helpful for achieving this goal for A+.

R&D experimental tests include control system development for frequency dependent squeezing, optimizing squeezed light sources at 1064 nm and the characterization of low-loss Faraday isolators and mode-matching efficiencies.

Op-4.1.2   LIGO-HF

This work falls under section 2.5 "Post-A+ planning and research" of the LSC Program.

There can be some gap years between when A+ finishes and Voyager starts. The collaboration is considering ideas that can be explored during post A+ era and also be beneficial to Voyager. The LIGO-HF concept is to improve the high-frequency sensitivity of current facility to detect kHz GWs from the binary neutron stars at the merger [120, 121, 122, 123, 124]. As the sensitivity around kHz is mainly limited by shot noise, the key elements of LIGO-HF are squeezing, high optical high-power, and modification of the signal-recycling scheme, such as the long (twin) signal recycling. There is also a proposal to build a new facility in Australia specifically targeting at kHz [46], which also incorporates Voyager technology for reducing the coating thermal noise. In such detectors, the input test masses and end test masses can potentially operate at different cryogenic temperatures using radiative cooling, reducing the complexity of the overall test mass suspension systems [125].

The long signal-recycling idea requires an increase of the length and the finesse of the signal-recycling cavity (SRC). This allows a resonant coupling between the SRC and the arm cavity, which creates new longitudinal eigenmodes with two resonant frequencies. Having the upper and lower signal sidebands coincide with the new resonances provides a resonant enhancement of the signal response. The coupled-cavity resonance and its bandwidth are approximately given by

$$2.6\,\text{kHz} \left(\frac{T_\text{ITM}}{0.014}\right)^{\frac{1}{2}} \left(\frac{4\,\text{km}}{L_\text{arm}}\right)^{\frac{1}{2}} \left(\frac{300\,\text{m}}{L_\text{SRC}}\right)^{\frac{1}{2}}, \quad \text{bandwidth} \approx 2.0\,\text{kHz} \left(\frac{T_\text{SRM}}{0.05}\right) \left(\frac{300\,\text{m}}{L_\text{SRC}}\right). \quad (1)$$

A fundamental limit to the sensitivity of this configuration comes from the optical loss in the SRC. For a fixed coupled cavity resonance frequency, such a limit is independent of the arm cavity length. For example, if the coupled-cavity resonance is chosen to be 2.6 kHz, we obtain a sensitivity limit of

$$5.2 \times 10^{-25}\,\text{Hz}^{-\frac{1}{2}} \left(\frac{0.014}{T_\text{ITM}}\right)^{\frac{1}{2}} \left(\frac{4\,\text{MW}}{P_\text{arm}}\right)^{\frac{1}{2}} \left(\frac{\epsilon_\text{SRC}}{1000\,\text{ppm}}\right)^{\frac{1}{2}}. \quad (2)$$

The SRC loss mainly comes from the wavefront distortion on BS and ITM due to the thermal lensing, which can be partially mitigated by the thermal compensation system. Therefore, ϵ_SRC is power dependent and increasing the power doesn't necessarily improve the sensitivity, if the sensitivity is limited by the SRC loss. Research is needed to explore the thermal-lensing induced SRC loss and its mitigation strategy to implement the LIGO-HF idea.

Op-4.1.3   Voyager

This work falls under section 2.5 "Post-A+ planning and research" of the LSC Program.

For Voyager we propose the injection of frequency dependent squeezing at some frequency around $2\,\mu\text{m}$ and a measured shot-noise squeezing of 8 to 10 dB. A list of loss contribution that allows for such squeezing levels is given Table 9. We see that the total efficiency required for 10 dB is 91.3% requiring phase noise to be controlled to better than 4.4 mrad. Achieving the levels of stability will likely require operating the squeezer inside the vacuum envelope. Smaller and more compact designs of squeezed light sources will also help to reduce phase noise. A recent proposed scheme for controlling the phase noise could potentially achieve a sub-mrad stability [126].

Required R&D experimental tests: development of an audioband squeezed source of greater than 12 dB from 10 Hz to 10 kHz at 2 μm, which is promising given the recent advancement [127, 128]; control system development for frequency dependent squeezing at 2 μm, sourcing and characterize low-loss Faraday Isolators at at 2 μm, mode-matching efficiency, Brillouin scattering, and phase noise. Basically the state of the art for 1064 nm needs to be achieved at at 2 μm. Up to 12.3 dB of squeezing at 1550 nm has been demonstrated at the AEI, but only down to about 10 kHz. The extension to 10 Hz, however, should be straight forward using the techniques invented for 1064 nm. High efficiency generation and detection of squeezed states should be possible up to a wavelength of about 2.1 μm. The upper limit is set by the current availability of high-quantum-efficiency photo diodes.

LT-4.1.4   3rd generation GW detectors

This work falls under section 3.5 and 3.7 of the LSC Program, "Lasers and Squeezers" and "Topologies".
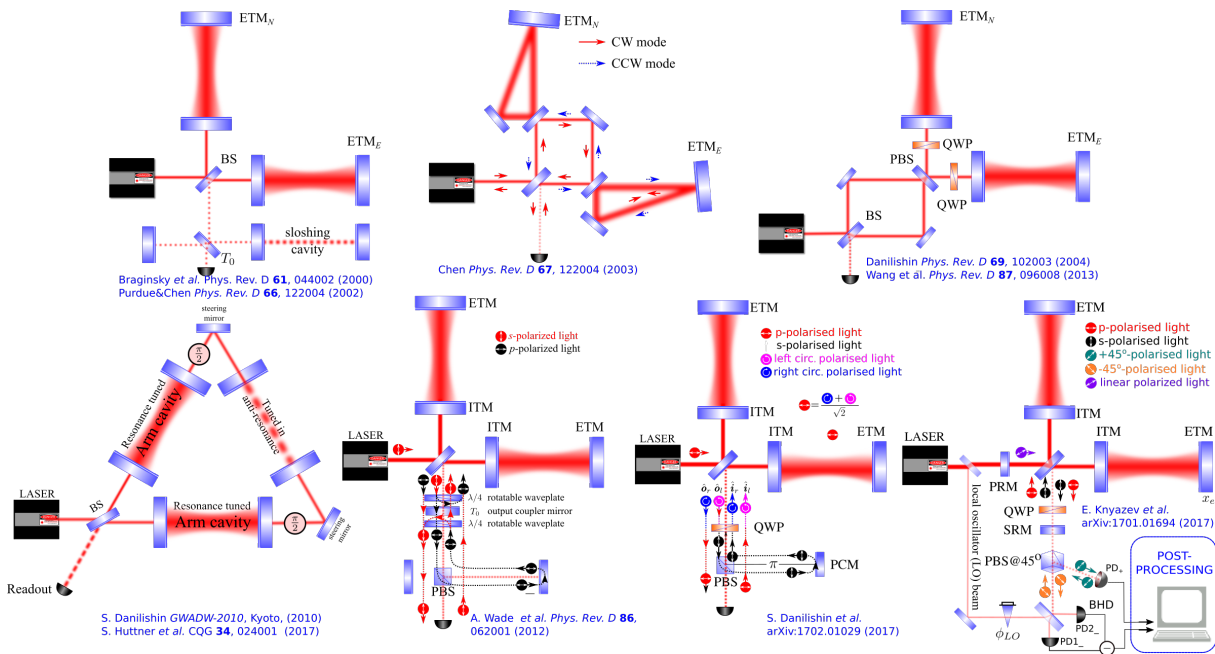
Figure 8: Different incarnations of speed meters [3, 4, 5, 6, 7, 8, 9, 10, 11, 12].

The longer term goal of 15 dB observed quantum noise reduction is extremely ambitious. From Table 9 we see that the total efficiency required is 97.4% requiring phase noise to be controlled to better than 2.5 mrad. Loss tolerances on the isolators, OMC, modematching etc far exceed anything currently achieved. 15 dB of squeezing was recently observed at the AEI [118] at 1064 nm at MHz frequencies. Similar results should be possible at 1550 nm and down to a few hertz, if photo diodes of the same high quantum efficiency are available. A photo diode quantum efficiency of greater 99.5% needs to be made available with surface areas suitable for GW detectors. Wavelengths around 2μm have been discussed. At these wavelengths squeezed light sources as well as photo-electric detection need to be researched.

Given the timeline for 3rd generation detectors, LIGO Cosmic Explorer and Einstein Telescope, the full list of quantum noise reduction concepts should be explored in addition to

frequency dependent squeezing and need to be extensively researched. The next section summarizes the currently proposed concepts.

Recently, a variety of new configurations featuring QND measurement of speed have been invented (see Fig. 8). Some of these concepts offer not only improved quantum noise and relaxed requirements for filter cavities, but also the possibility of reduced coating thermal noise [10] and the introduction of negative inertia [6, 9]. Some can be implemented with minimal changes to the main Michelson interferometer infrastructure by means of using 2 orthogonal polarizations of light at the same time and by adding a few polarization optical components to the readout port [8, 11, 12]. Individual design studies are required to evaluate the technical challenges, infrastructure requirements and various benefits of these configurations.

Op-4.2   State-of-the-art squeezed-light sources

This work falls under section 2.5 "Post-A+ planning and research" of the LSC Program.

Squeezed vacuum states of light [94] are produced by cavity-enhanced type I optical-parametric amplification (OPA), also called cavity-enhanced type I parametric down-conversion (PDC), sometimes also type I optical-parametric oscillation (OPO) below threshold. The most efficient source is a (second-order nonlinear) periodically poled KTP (PPKTP) crystal placed in a cavity that is pumped with second-harmonic light (below oscillation threshold). At threshold such a device produces, theoretically, an infinite squeeze factor, if the optical loss is zero and if the pump power is infinite. Great progress has been made over the last 10 years in the generation of squeezed vacuum states of light at 1064 nm and 1550 nm [92]. For Voyager and LIGO Cosmic Explorer, squeezed-light sources at wavelengths around $2\mu m$ are also needed, which has been recently demonstrated experimentally with PPKTP [127, 128].

1. Both ANU and AEI have measured squeezing of around 10 dB down to 10 Hz at 1064 nm. The AEI has observed greater than 12 dB at MHz frequencies at both 1064 nm and 1550 nm [129, 130]. Recently, the AEI together with the ILP Hamburg observed 15 dB of squeezing at 1064 nm at MHz frequencies [118].

2. GEO 600 has been operated now for several years [38] at a time regularly observing more then 3.5 dB sensitivity improvement with a highest value above 4 dB [131, 132]

3. An ANU designed squeezer was installed on the LIGO H1 detector operating in the S6 configuration. Sensitivity enhancement was observed above 200 Hz with 2.1 dB improvement above a few hundred hertz. Importantly, no excess noise was seen below 200 Hz and no additional glitching was found.

4. Photodiodes with quantum efficiency in excess of 0.99 at 1064 nm are now available [118].

Any absorption/scattering between the squeezing resonator and detection reduces the level of squeezing. Starting with a suitable source of squeezed light, Table 9 presents a comprehensive list of potential loss sources along with levels required to observe 6 dB, 10 dB and 15 dB of

quantum noise reduction. The final column of the table presents the numbers achieved during the H1 squeezing test. The numbers are presented in terms of efficiencies (1 - loss). A filter cavity (see section Op-4.4.1) is needed to achieve broadband quantum noise suppression or to at least reduce the squeezing ellipse to a coherent state at frequencies where shot noise does not dominate.

As the level of squeezing is increased the requirement on stability of the squeeze angle is increased. As the angle rotates away from the detected quadrature angle the level of measured squeezing is reduced. In the presence of phase fluctuations the average squeeze factor is reduced. The effect gets worse as the level of anti-squeezing increases. Due to optical loss, the anti-squeeze factor is always larger than the squeeze factor. The tolerance on phase noise will decrease as larger squeeze factors are applied. This is depicted in Fig. 10 where measured squeezing loci are plotted for different values of total loss and total phase noise.

Op-4.2.1 Low-loss input and output optics

Utilizing externally generated squeezed vacuum states of light requires additional input and output optics. The most prominent ones are the Faraday rotator in combination with one polarising beam splitter for input/output coupling the squeezed mode, the detuned narrow linewidth filter cavity for engineering the frequency dependent rotation of the squeezing ellipse that allows for simultaneous squeezing of shot noise and radiation pressure noise, and the output modecleaner right before photo-electric detection. All these components should have a transmission of greater 99%, where the exact value depends on the squeeze factor aimed for and very low scattering. The Faraday rotator needs to provide precisely 45 degree rotation with high transversal homogeneity and very good anti-reflection coatings (cf. section Op-7.2.2). The extinction ratio of the polarising beamsplitter is another issue as well as the impedance-matching of the output modecleaner.

A general issue of GW detectors at signal frequencies below 100 Hz is given by parasitic interferences due to carrier light that is back-scattered from moving surfaces [133, 134]. Generally, parasitic interferences can be mitigated through optics having higher surface qualities, by dumping and absorption of scattered light, and by reducing the motion of back-scatter surfaces. Recently, a new readout scheme was proposed and experimentally investigated that allows for a subtraction of back-scatter noise, if a model can be fitted to the parasitic interference [135]. The injection of squeezed vacuum states requires new optics that can produce additional scattering. In order to avoid parasitic interferences from the squeezing resonator, the optical pass between the squeezing resonator and the signal recycling/extraction mirror must be kept constant. Additional Faraday isolators in between may be required.

The filter cavity concept is outlined in Op-4.4.1, also see the AIC Chapter. For a given filter bandwidth γ_{filter} (to be determined by the needs of input/output filtering), when realized by a cavity of length L, the total loss $\mathcal{E}$ is determined by

$$\mathcal{E} = \frac{4\epsilon}{T} = \frac{\epsilon c}{\gamma_{\text{filter}} L} \tag{3}$$

where T is the input-mirror power transmissivity [related to bandwidth by $\gamma_{\text{filter}} = Tc/(4L)$] and ϵ is the loss per round-trip. It is therefore the ratio ϵ/L that determines the goodness

	Loss source	H1 experiment	Near term goal (6dB)	Longer term goal (10 dB)	Dreaming(15dB)
1	OPO escape efficiency	96%	98%	99%	99.8%
2	Injection path optics	80%	99.7%	99.7%	99.99%
3	viewport	99.8%	99.8%	99.8%	99.99%
4	3 faraday passes	94%, 94%, unknown	97% each (aLIGO input Faradays)	99% each	99.7 % each
7	RF pick off beamsplitter (beam for ISCT4)	98.8%	99%	99.5%	99.8%
5	Reflection off of Signal recycling cavity@100 Hz	arm cavity and michelson =98%	97.5%(Tsrm=35%)	99.2% (Tsrm=50%)	99.5%
6	Circulator for filter cavity	NA	98%	99.5%	99.8%
8	Squeezer mode matching to OMC	71% (inferred from total)	96%	98%	99.7%
10	OMC transmission	82%	97%	99.5%	99.7%
11	QE of PDs		99%	99.7%	99.99%
	Total efficiency (escape * detection)	40-45%	77.6%	91.3%	97.4%
	Total phase noise allowable		17mrad	7 mrad	2.5 mrad
	Measured squeezing (dB)		6	10	15.25

For numbers in the H1 column- red numbers were measured during the experiment, numbers in black were made before installing components or estimates of losses that were too small compared to the total to measure accurately with the uncertainty in our measurements.

Figure 9: Table 11 Maximum acceptable losses to achieve 6 dB, 10 dB and 15 dB of observed quantum enhancement. From Dwyer [13]

Measured Squeezing
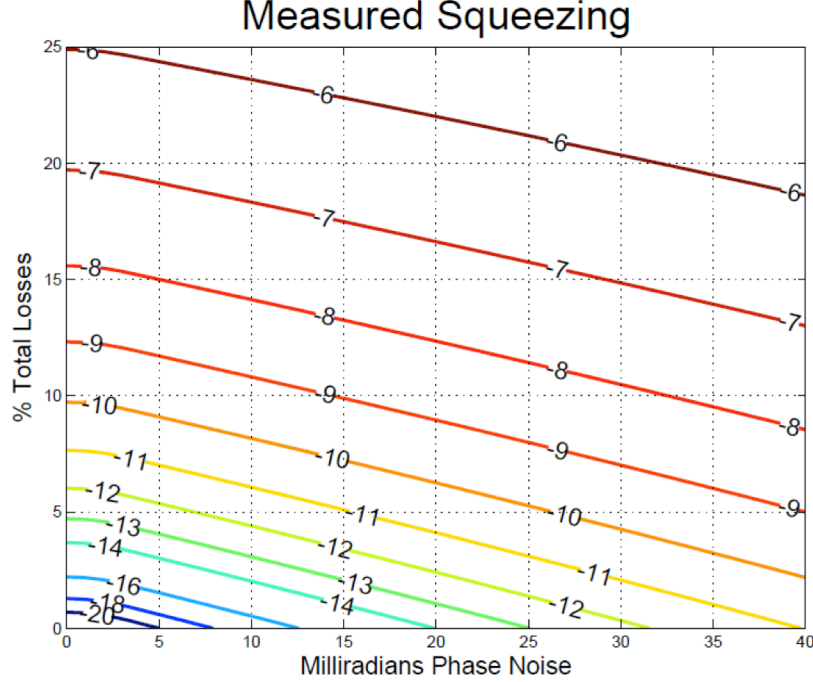
Figure 10: Measured squeezing for different values of total losses (the product of escape efficiency and detection efficiency) and total phase noise. For each value of phase noise, the nonlinear gain in the squeezing resonator is optimized to maximize the measured squeezing, but the nonlinear gain is capped at 90, (pump power at 80% of threshold). Operating the squeezing resonator closer to threshold doesn't improve the measured squeezing very much, but could make stable operation of the squeezer difficult. From Dwyer [13]

of the filter. Since the per-round-trip loss ϵ depends on the beam spot size, which in turn depends on L, an optimization is need to find out the optimal length and design of filter cavities [136].

The effect of losses is further amplified if back-action evasion is required, in which case the signal strength in the quadrature being detected is significantly less than conventional situations. A rule of thumb for this limitation is available from Kimble et al. [98], where we have

$$\sqrt{S_h/S_h^{\mathrm{SQL}}} \geq (e^{-2q}\mathcal{E})^{-1/4} \tag{4}$$

where $\mathcal{E}$ is the power loss, and e^{-2q} is the power squeezing factor. Assuming $\mathcal{E}$ to be 0.01, and 10 dB squeezing, we have a SQL-beating limit of 0.18.

Figure 11 shows the effect of round-trip loss on the degradation of squeezing for a filter cavity with 22 Hz detuning and bandwidth. The colors correspond to the quantum-noise spectral density along the minor axis of the noise ellipse relative to coherent vacuum noise. It can be seen that round-trip loss over 50 ppm degrades the squeezing to a level comparable to coherent vacuum around frequencies near the filter resonance. Here and in the following, round-trip loss are considered excluding the transmission of the input mirror. The input transmission is comparatively large (about 550 ppm for the filter calculation of Fig. 11) and does not directly contribute to squeezing degradation. Round-trip loss is dominated by optical scatter loss from imperfect mirrors in combination with finite aperture size. The goal
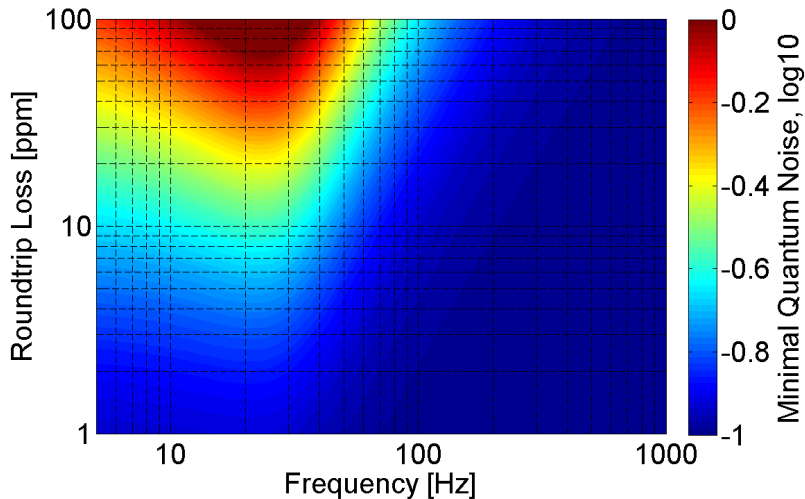
Figure 11: Degradation of 10 dB external squeezing reflected from a 300 m filter cavity as function of round-trip loss (in addition to input transmission) and frequency.

is to minimize scatter loss.

Scatter loss in cavities is determined by properties of the individual mirrors such as mirror size, mirror curvature, mirror surface abberations and defects, and by the optical path length of the cavity. Scatter loss in cavities is not fully understood yet. A concerted effort of high-finesse cavity experiments, scattering measurements, numerical simulations and theoretical work is required to form a consistent picture between loss models and observations. Practically speaking, ultra-low losses (around 1 ppm) have been achieved on the mirrors of fixed cavities [137, 138]. However, the lowest loss measured on the large, test-mass-sized beams are more usually in the 50-100 ppm range. FFT simulations have shown that the loss for large beams is dominated by the large scale figure error of the substrate, while the losses for small beams are dominated by point defects in the coatings. Since the low frequency performance of the QND schemes so strongly depends on the loss for intermediate sized (∼mm) beams, it is vitally important to develop ultra-low loss mirrors for this beam size. The modern polishing technology is already good enough.

Additional more specific problems that need to be investigated include small-angle scatter loss in cavities, coherent loss versus incoherent loss, and round-trip loss as a function of cavity aspect ratio. Coherent scatter loss designates the effect when the spatial pattern of higher-order modes resonating inside the cavity matches the pattern of light scattered from a mirror. In this case scattered light can build up resonantly provided that the overall loss in these higher-order modes is not too high. In general, higher-order modes experience more loss since they describe a wider spatial intensity distribution that directs additional light power beyond the mirror aperture compared to the target mode of the cavity, which is usually the Gaussian shaped TEM_{00} mode. For this reason it is also necessary to understand how much round-trip loss is influenced by the cavity aperture, or better by the cavity aspect ratio, which is the aperture divided by the cavity length. Coherent scatter loss can potentially lead to a significant increase of the total scatter loss, and it is no more describable by simple perturbative scatter models.

Losses in mirrors are also addressed in the Optics section 5.

Op-4.3 High-quantum-efficiency photo-electric detection

This work falls under section 2.5 "Post-A+ planning and research" of the LSC Program.

Op-4.3.1 PIN photo diodes

Photo-electric detection in the output of a GW detector is done with unity gain semiconductor PIN photo diodes, where PIN stands for positive-intrinsic-negative. Such a detector ideally elevates exactly one photo electron to the conduction band for every incident photon. An imperfection is treated as optical loss. Already GW detectors operated with light in coherent states require photo diodes with high quantum efficiency since the square root of its signal normalized shot-noise spectral density scales with $1/\sqrt{n}$, where n is the number of *detected* photons per second. For a GW detector that uses any nonclassical techniques the effect of imperfect quantum efficiency is stronger [94].

Recently, the quantum efficiency of a custom-made InGaAs photo diode was calibrated to $(99.5\pm0.5)\%$ [118], where two identical such photo diodes were used in a home-made balanced homodyne detector arrangement. The two photo diodes were manufactured from the same wafer material as the photodiode that has been used in GEO 600 since 2011 [38, 93]. The photo diodes allowed for the observation of 15 dB squeezing from a squeezing resonator with about 1% escape efficiency, negligible phase noise and access noise, and propagation loss of another 1% including imperfect modematching between the squeezed vacuum mode and the optical local oscillator of the balanced detection scheme.

At 1550 nm custom-made photo diodes with quantum efficiencies greater 99% might already exist. An indication for that is the observed squeeze factor of 12.3 dB at this wavelength [130]. The response of standard InGaAs photodiodes show a cutoff at 1600 nm, but extended InGaAs is available that allows photo-electric detection to wavelengths as long as 2.5 µm. For LIGO Cosmic Explorer it needs to be investigated up to what wavelength quantum efficiencies of close to 99% can be realized. Further discussion on the development of high efficiency photodiodes can be found in section Op-7.3.2.

Quantum efficiency and losses can potentially be mitigated by parametrically amplifying the squeezed state before detection on the photodetector. By parametrically amplifying the squeezed state (anti-squeezing the squeezed state with a 2nd squeezer), the squeezed quadrature can be shifted to above the vacuum level. While the concept was initially proposed for 1 µm, the technique is wavelength agnostic and is applicable to longer wavelengths such as 2µm. To fully take advantage of this approach, additional optical loss from the mode mismatch and the 2nd squeezer cavity shall be kept low.

Op-4.3.2 Balanced homodyne detection (BHD)

All table-top experiments that observed squeeze factors of greater than 8 dB used two identical PIN photo diodes as a balanced receiver. In this arrangement the dim squeezed signal

beam is overlapped with a modematched local oscillator of the same carrier wavelength on a balanced beam splitter and the different voltage from the photo diodes is recorded. Ideally the signal beam does not contain any carrier component. In any case, the power ratio of local oscillator (LO) and signal beam should be as high as possible.

The main advantage of a balanced homodyne detector compared with a single photo diode is that an arbitrary (frequency independent) field quadrature can be detected, which is required in many nonclassical approaches, such as detuned signal recycling, variational input/output and speed meters. Ideally the local oscillator mode corresponds to the carrier mode inside the interferometer to avoid any differential phase noise. Tapping such a local oscillator, e.g. from the AR-coated surface of the beam splitter or the POP port, and delivering it with the required low phase noise to the detection system is the main challenge and it will involve additional hardware in terms of low noise suspensions for beam delivery and an addition output mode cleaner [139].

The BHD scheme, however, provides additional advantages. The local oscillator, assumed to be in the ideal transverse mode, acts as an output mode cleaner. Also the BHD scheme allows for interferometer operation exactly at the dark fringe. Recently, noise couplings in the BHD scheme were experimentally investigated in the context of GW detectors [140].

LT-4.3.3   Heterodyne detection

Recently, there is a revived interest in using heterodyne detection scheme to achieve the dark-port operation, the same as BHD. With the introduction of a stable tuned signal-recycling cavity in Advanced LIGO, issues associated with unbalanced radio frequency (RF) sidebands and parasitic higher order optical modes are significantly improved compared with LIGO. One nice aspect of the heterodyne detection is that it does not require an additional optical path for introducing the local oscillator, in contrast to BHD. At the fundamental level, heterodyne readout measures sidebands near the carrier frequency and twice the RF modulation frequency away from the carrier. Because the latter does not contains GW signals, heterodyne readout introduces additional quantum noise that is absent for BHD. It has been shown that such an additional noise can be suppressed using squeezing, which however requires a broadband squeezing source spanning up to RF modulation frequency [141]. A more recent proposal tries to completely eliminate the additional noise by introducing an additional carrier at twice of the modulation frequency [142]. Further detailed studies are needed to investigate the broadband squeezing and the technical noise couplings to justify heterodyne readout as a viable alternative to BHD.

LT-4.4   Interferometer techniques supporting nonclassical quantum noise reduction

This work falls under section 3.7 of the LSC Program, "Topologies".
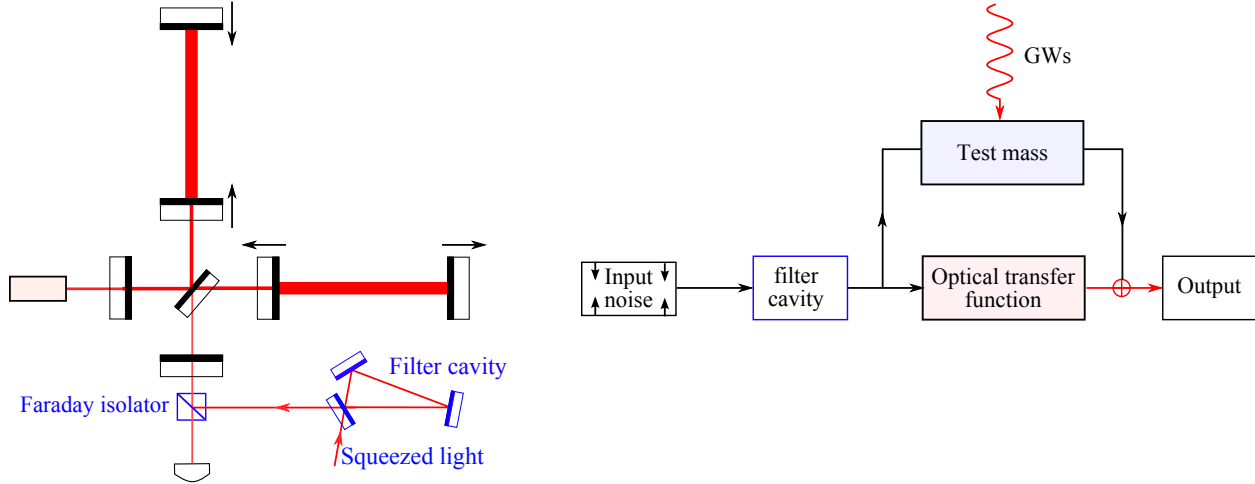
Figure 12: Schematics showing the frequency-dependent squeezing scheme (left) and its associated flow chart (right).

Op-4.4.1   Frequency-dependent squeeze angle (input filtering)

The first scheme is 'frequency-dependent squeezing' (as discussed in the previous sections). This term refers to a broadband spectrum of squeezed vacuum states for which the squeeze angle is frequency dependent and optimized for the cancelation of back-action noise and for achieving the optimum signal to noise ratio. The frequency dependence of the squeeze angle can be achieved by reflecting off the squeeze spectrum from a detuned narrow band cavity. There might be other ways how the same frequency dependence can effectively be achieved. Research on alternatives might be very valuable for future gravitational-wave detectors.

As shown schematically in Fig. 12, it utilizes an optical (filter) cavity to rotate the amplitude and phase quadratures, or equivalently the squeeze angle, in a frequency-dependent way. If the parameters of the filter cavity is appropriately specified, one can rotate the squeeze angle such that the quantum noise spectrum is reduced by an overall factor that is equal to squeeze factor.

For illustration, in Fig. 13, we show the resulting noise spectrum in *the ideal case without optical loss*. As we can see, the squeeze angle rotates in such a way that at low frequencies the fluctuation in the amplitude quadrature is squeezed—thus reducing the radiation-pressure noise, while at high frequencies the phase quadrature is squeezed—thus reducing the shot noise. In order to achieve the desired rotation of squeeze angle, the filter cavity needs to have a bandwidth that is comparable to the detection bandwidth—this indicates a high-finesse cavity is necessary if the cavity length is short. The specification for the filter cavity can almost be analytically calculated by using the method outlined in [108].

In reality, the optical loss will affect the performance of input filtering, as shown in the left panel of Fig. 14. Additionally, parameters of the filter cavity, in particular, the transmissivity of the mirrors and the detuning, cannot be exactly set to the optimal value, and their variation will influence the sensitivity in a similar manner to the optical loss, as illustrated in the right panel of Fig. 14.
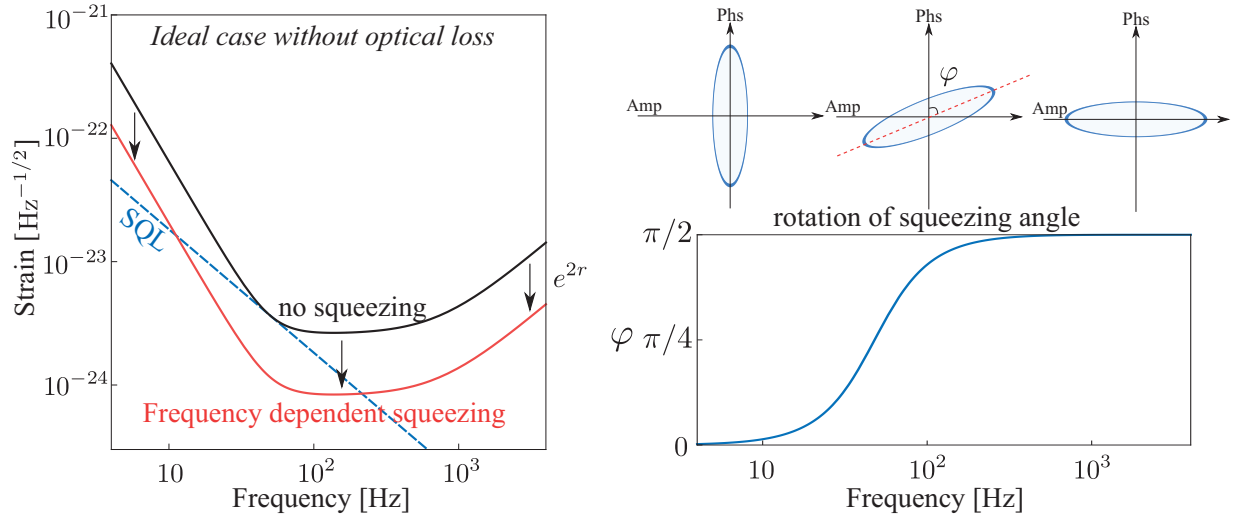
Figure 13: Noise spectrum for frequency-dependent squeezing (left) and rotation of the squeeze angle (right).
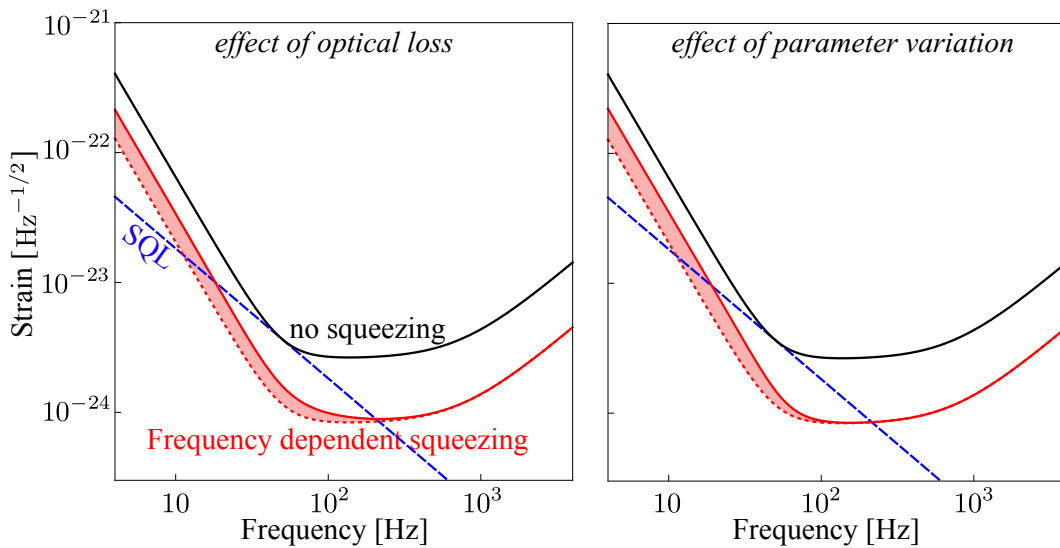
Figure 14: The effect of optical loss (left) and the parameter variation of the filter cavity (right) for input filtering. The shaded regions illustrate the degradation in sensitivity. Here we have assumed the total optical loss of 20% (round-trip loss multiplied by the number of bounces inside the cavity) and parameter variations of 10%.

LT-4.4.2   Frequency dependent readout phase (output filtering)

A close related counterpart to the input filtering is the variational readout, and as shown schematically in Fig. 15, it uses an optical cavity to filter the detector output which allows one to measure different optical quadratures at different frequencies. The filter cavity has the same functionality as in the case of the frequency-dependent squeezing—the only difference is that it rotates the optical quadratures of the output instead of input. In the ideal case, this scheme can coherently cancel the radiation-pressure noise at low-frequencies, and give rise to a shot-noise only sensitivity [98]. In Fig. 16, we show the resulting noise spectrum in
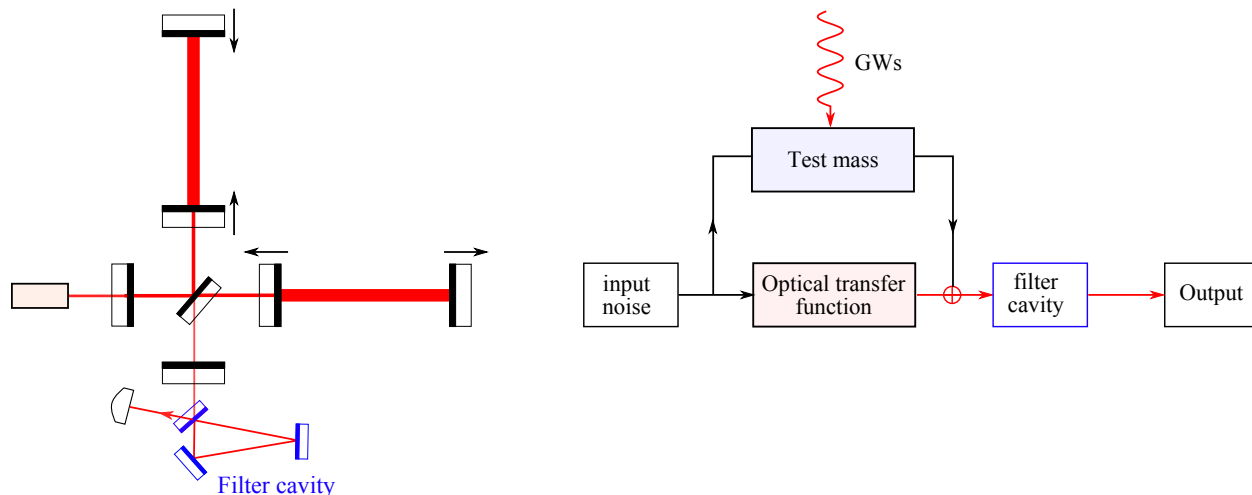
Figure 15: Schematics showing the frequency dependent (or variational) readout scheme (left) and its associated flow chart (right).
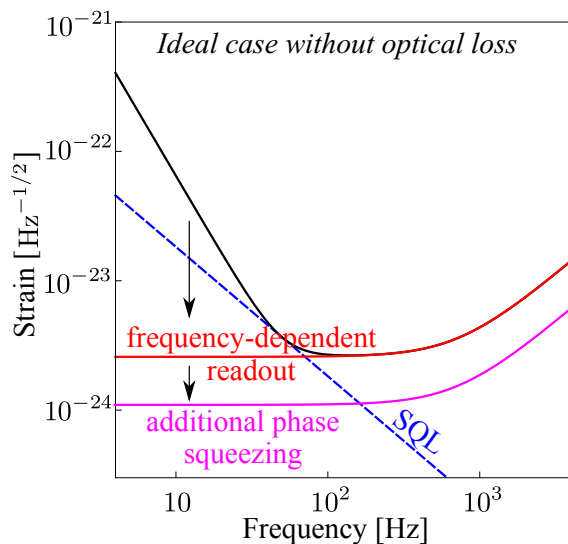
Figure 16: The noise spectrum for the frequency-dependent readout scheme.

the ideal lossless case. In reality, due to the presence of optical loss and parameter variation of the filter cavity, such a cancelation cannot be perfect, as illustrated in Fig. 17.

As this technique leads to reduced signal (but increased signal/quantum noise) at low frequencies it is far more sensitive to optical losses compared with input filtering.

LT-4.4.3   Conditional Squeezing

Conditional squeezing is a new concept that was proposed to achieve frequency-dependent squeezing without an additional filter cavity [95]. The concept is based on Einstein-Podolsky-Rosen entanglement that exists within a single squeezed cavity mode as demonstrated in [143]. The entanglement is utilized by separating the upper and lower sidebands and using two balanced homodyne detectors with different local oscillator frequencies. The new
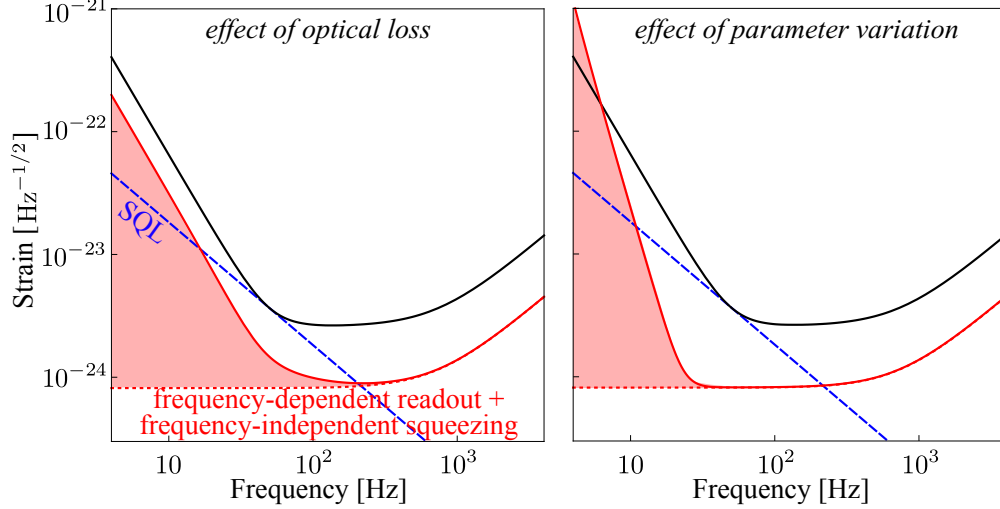
Figure 17: The effect of optical loss (left) and parameter variation of the filter cavity (right) for frequency-dependent readout (output filtering). Similar to Fig. 14, we have used a total optical loss of 20%. In contrast, the parameter variation is chosen to be only 10^{-4} in order to produce reasonable sensitivity, as it is much more sensitive than input filtering.

concept uses two local oscillators with a frequency difference of about a multiple of the free spectral range of the signal extraction cavity. The observed frequency dependent squeezing is conditional because it is revealed only after combining the noise from both readouts.

Implementation of this new concept in a large scale GWD implies separate readout and injection channels for both entangled beams. A thorough analysis of the the effect of losses throughout the interferometer, arm length asymmetries, and imperfect separation of the signal and idler beams were considered for the GEO600 interferometer in [144]. This study has shown that conditional squeezing results in comparable performance to frequency dependent squeezing with filter cavities, yet at a price of 3 dB extra squeezing and with rather stringent constraints on injection and readout loss. Experimental table-top tests of the concept (outside the radiation pressure noise regime) have been successfully demonstrated at Hamburg University [96] and ANU [97].

LT-4.4.4   Twin (long) signal-recycling

Twin signal recycling (TSR) refers to a signal recycling scheme in which upper *and* lower signal sidebands are resonantly enhanced simultaneously (balanced) providing a spectral density which is reduced by up to a factor of two [145]. TSR requires a an additional signal recycling mirror, most likely in a long-baseline arrangement. Squeezed states, however, can be used without setting up another long baseline filter cavity if only to reduce the shot noise at the resonance[146]. One filter cavity is needed if low-frequency radiation pressure noise were to be suppressed.

TSR is equivalent to the long signal-recycling cavity scheme in the LIGO configuration [147], where the two cavities in TSR are replaced by the arm cavity and the signal-recycling cavity (SRC). This idea has been explored in the LIGO-HF concept to achieve a resonant enhancement of the detector sensitivity at kHz [121]. Because both the arm cavity and SRC
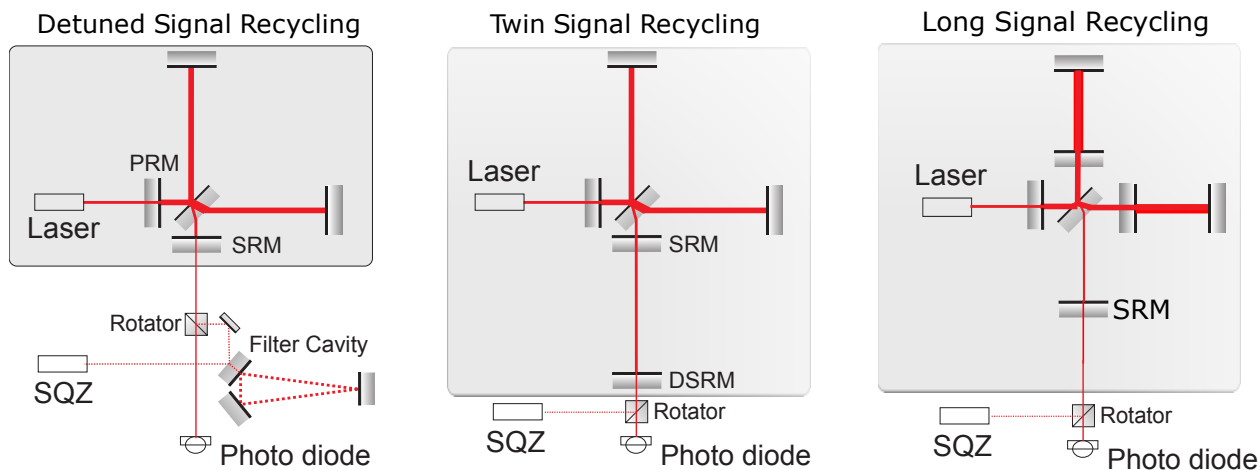
Figure 18: (Color online) Top left (shaded): Topology of the current gravitational wave detector GEO 600. The mirror in the laser input port (PRM) realizes so-called power-recycling. The signal-recycling mirror (SRM) in the output port establishes a carrier light detuned single-sideband signal recycling cavity. Bottom left: Extension for a broadband shot-noise reduction utilizing squeezed states. Middle: twin signal recycling. Two optically coupled cavities are formed with the help of an additional mirror DSRM. Their resonance doublet enables balanced dual-signal-recycling resulting in lower shot noise. Squeezed states can be used without additional filter cavity for reducing the shot noise only. Right: long signal recycling. It shares the same principle as twin signal recycling. The two coupled cavities are the arm cavity snd the signal-recycling cavities.

are tuned, the control scheme and the frequency-dependent squeezing implementation are the same as A+.

LT-4.4.5   Speed meter

Normally, a GW detector measures the test mass position at different times to infer the signal. However, position at different times does not commute with the Hamilton operator of a free mass. According to quantum measurement theory [148], such a measurement process inevitably introduces quantum back action and perturbs the test mass motion. (In the context of GW detectors, the back action is the radiation-pressure noise.) In order to evade back action, one needs to measure the conserved dynamical quantity of the test mass—the momentum. The latter is (approximately) proportional to speed, which is why a *speed meter* is ideal for measuring gravitational waves with greatly reduced radiation-pressure noise [106].

Several practical speed-meter configurations were proposed over the last 15 years (see Fig. 8) which fall into 3 distinct categories by the shape (frequency dependence) of their response to the GW signal. These are the *Sagnac-type speed meters* [5, 7, 12, 109], *sloshing speed meters* [8, 10, 149], and a recently proposed scheme that uses *EPR-type* entanglement between different polarizations [11].

In Fig. 19, we show the two simplified schemes of a sloshing and Sagnac-type speed meters. The sloshing speed meter, proposed in Ref. [149], uses a sloshing cavity. We can gain a qualitative understanding of how such a scheme allows us to measure the speed of the test
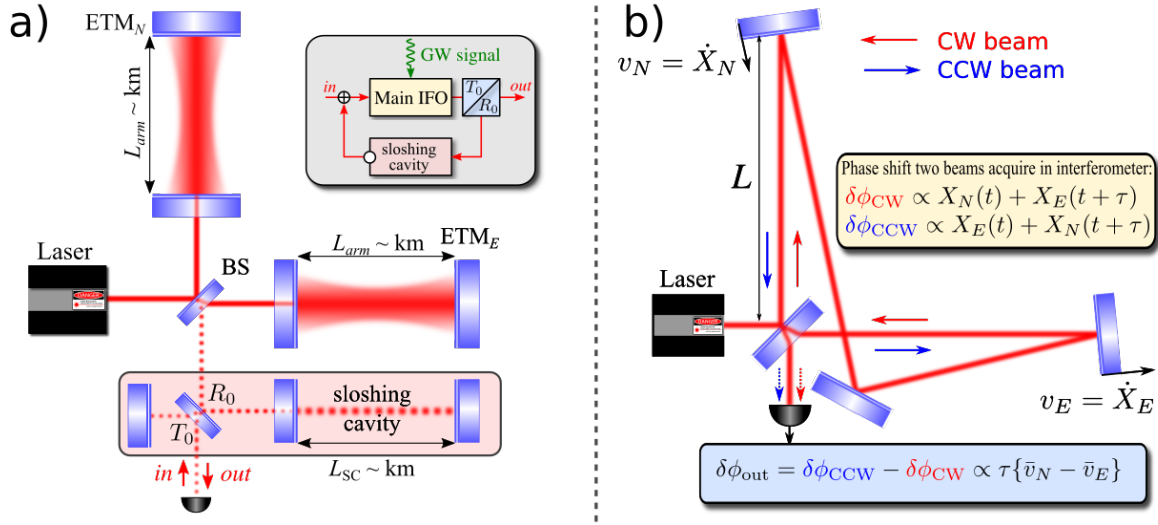
Figure 19: Two variants of implementation of speed meter interferometers, (a) the sloshing speed meter, and (b) the Sagnac speed meter. Inset in the grey rectangle in (a) represents the block diagram of the sloshing speed meter principle of operation. Here ETM stands for end test mass, BS is a beam splitter, and $T_0 = 1 - R_0$ is the (power) transmissivity of the output coupling mirror.

mass. Basically, the information of test mass position at an previous moment is stored in the sloshing cavity, and it coherently superposes (but with a minus sign due to the phase shift in the tuned cavity) with the output of the interferometer which contains the current test mass position. The sloshing happens at a frequency that is comparable to the detection frequency, and the superposed output is, therefore, equal to the derivative of the test-mass position, i.e., the speed.

The zero-area Sagnac speed meter derives the speed signal from the subtraction of the two counter-propagating light beams at the main beam-splitter. The light beams visit both arms and interact with the test masses sequentially, but in an opposite order. As a result, the phase of the beams carries the information about displacement of the test masses, but with a delay τ that takes light to travel between the arms. When the two beams recombine at the beam splitter, the phase at the readout port of the interferometer turns to be proportional to the relative mean velocity of the differential arm motion, $\delta\phi_{out} \propto \tau\{\bar{v}_N - \bar{v}_E\}$.

The typical noise spectrum of speed meters is shown in Fig. 20. The low-frequency spectrum has the same slope as the standard quantum limit, which is a unique feature of speed meter. When the optical power is high enough, we can surpass the standard quantum limit.

As a rule, no filter cavity is needed for the speed meter configuration, as the radiation pressure noise at low frequencies is cancelled. However, such a cancellation is achieved by choosing the homodyne detection angle that is deviated from the phase quadrature, therefore decreasing sensitivity at high frequencies. The deviation is proportional to the optical power. With frequency-dependent squeezing, we can reduce the effective optical power seen by the test mass, which allows us to measure the quadrature closer to the phase one, and thus enhance the high-frequency sensitivity. Similarly, the frequency dependent readout allows us to cancel the low-frequency radiation pressure noise without sacrificing the high-frequency
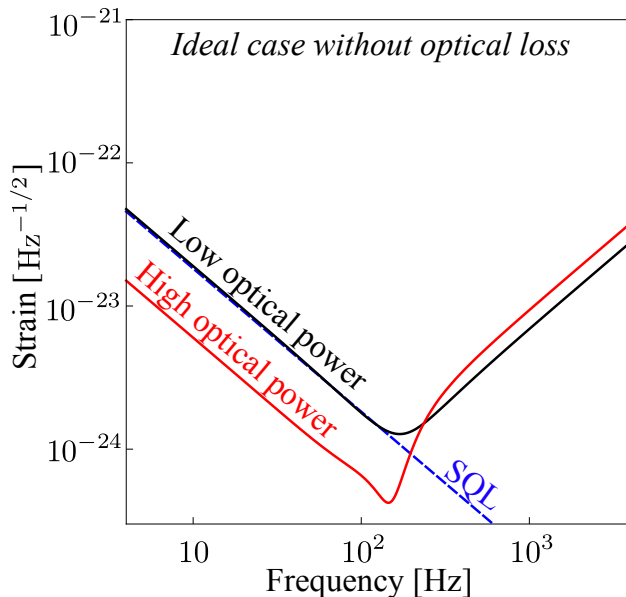
Figure 20: Plot showing the noise spectrum for the speed-meter configuration for two different optical powers.

sensitivity by rotating the readout quadrature to the phase one at high frequencies.

LT-4.4.6   Local Readout / Optical Bar

The local-readout scheme is shown schematically in Fig. 21. It is a special case of a dual-carrier scheme—the second carrier light is only resonant in the power-recycling cavity and is anti-resonant in arm cavity (barely enters the arm cavity). The local readout scheme was first proposed in Ref. [150] and was motivated by trying to enhance the low-frequency sensitivity of a detuned signal-recycling interferometer, which is not as good as the tuned signal-recycling due to the optical-spring effect.

The idea of the local readout is based on that of the *optical bar*, proposed by Braginsky and co-authors [103]. At frequencies below the optomechanical resonance, the input test masses (ITMs) and end test masses (ETMs) are connected in a rigid way via dynamical backaction. For this reason, at these low frequencies, the distance to the ETMs due to a gravitational wave result in a local motion of the ITMs. This first of all reduces the sensitivity at these frequencies. The idea behind the local readout is to measure the motion of the ITMs locally and to use this information in the data processing.

LT-4.5   Numerical Optimization and Comparison

This work falls under section 3.7 of the LSC Program, "Topologies".

To find out the possible candidate that is feasible for upgrading the sensitivity of aLIGO, we made a systematic comparison of those configurations mentioned before, and the results has been reported in Ref. [147]. Here we will just show the main result and one can refer to reference for more details.
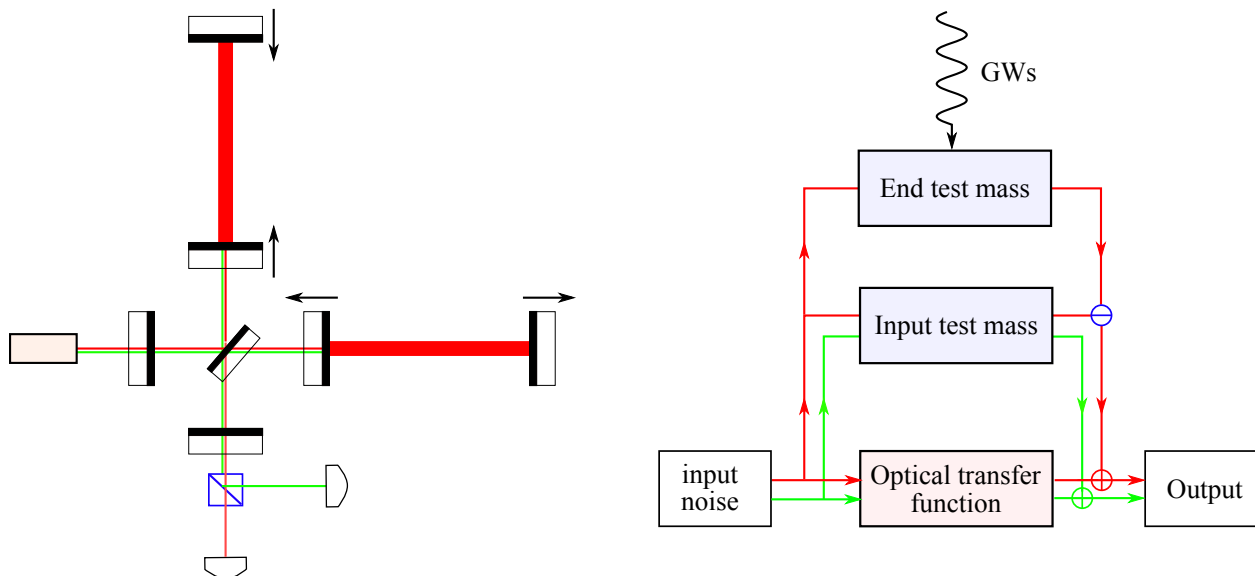
Figure 21: Diagram of the local-readout topology (left) and the resulting feedback loops (right).

The final optimization result critically depends on the cost function. In the literature, optimizations have been carried out by using a cost function that is source-oriented—trying to maximize the signal-to-noise ratio for particular astrophysical sources. Here we apply a rather different cost function that tries to maximize the *broadband* improvement over aLIGO. This follows the same philosophy of designing aLIGO which aims at a factor of 10 broadband improvement over initial LIGO.

For optimization, we also take into account the various classical noise sources (to be distinguished from the quantum noise). In particular, we consider Brownian thermal noise in the mirror suspensions [151, 152], seismic vibrations propagating to the mirror [153], terrestrial gravitational fluctuations [76, 154], and Brownian thermal fluctuations of the mirror (and mirror coating) surface [155, 156].

The results of the numerical optimization are shown in Figs. 22 and 23, where we plot the total noise spectra (the quantum noise + the classical noises) for different configurations with frequency dependent squeezing (input filtering) and frequency dependent readout (output filtering), respectively. In producing Fig. 22, we assume a moderate reduction in the thermal noise and the same mass and optical power as those for aLIGO. In producing Fig. 23, we assume a more optimistic reduction in the thermal noise, the mirror mass to be 150 kg and the maximum arm cavity power to be 3 MW.

As we can see, by adding just one filter cavity to the signal-recycled interferometer (aLIGO topology), we can already obtain a broadband improvement over aLIGO. Limited by thermal noise at low frequencies, the difference among these configurations is not very prominent. This leads us to the conclusion that adding one input filter cavity to aLIGO seems to be the most feasible approach for upgrading in the near term, which is the one adopted by A+. If the low-frequency thermal noise can be reduced in the future, the speed meter and the multiple-carrier scheme can provide significant low-frequency enhancement of the sensitivity. This extra enhancement will, for some low enough thermal noise, be enough to compensate
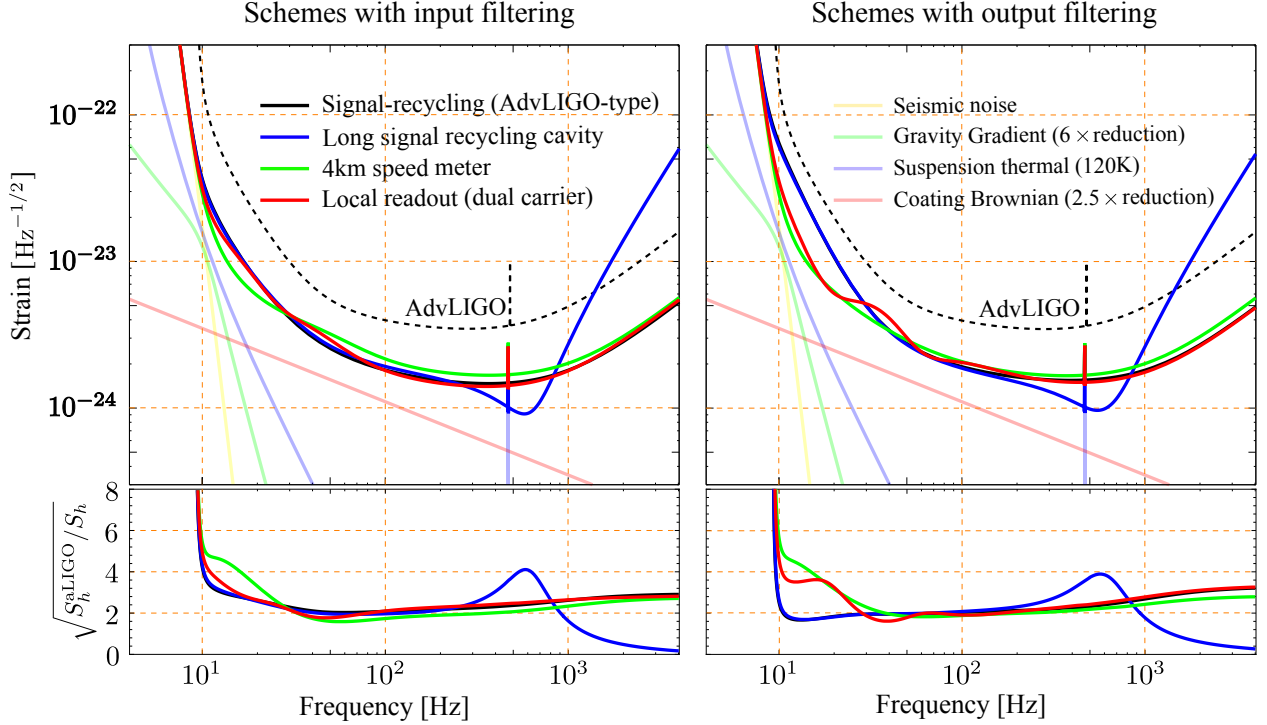
Figure 22: The optimized total noise spectrum for different schemes assuming a moderate improvement of the thermal noise compared with aLIGO baseline design. The lower panels show the linear strain sensitivity improvement over aLIGO.

for the extra complexity.

LT-4.6   Development of a QND apparatus which is quantum radiation pressure dominated

This work falls under sections 3.5 and 3.7 of the LSC Program, "Lasers and Squeezers" and "Topologies".

The implementation of these advanced ideas in the next generation detectors, in particular in the Einstein Telescope and LIGO Cosmic Explorer, cannot be done without first demonstrating them in a lab on the prototype facilities. The first experimental demonstration of quantum radiation pressure noise and its suppression using squeezed light at audio bands with a movable 55-ng mirror have been done at LSU [157, 158]. Efforts to demonstrate QND interferometry are crucial to understanding what is achievable, to learn about problems which could mask such phenomena and how to beat such limits. Recent demonstration with Advanced LIGO proves that in principle we can surpass the SQL by using the quantum correlation [159], a milestone for confirming the principle underlying all QND techniques.

There are also major activities planned or underway at the AEI 10 m prototype; the University of Birmingham; MIT; the University of Tokyo and LSU. The Glasgow 10 m, the Gingin Facility and the ANU have embarked on testing optical spring dynamics. More effort is needed toward observing QRP noise. The first serious effort to demonstrate a quantum
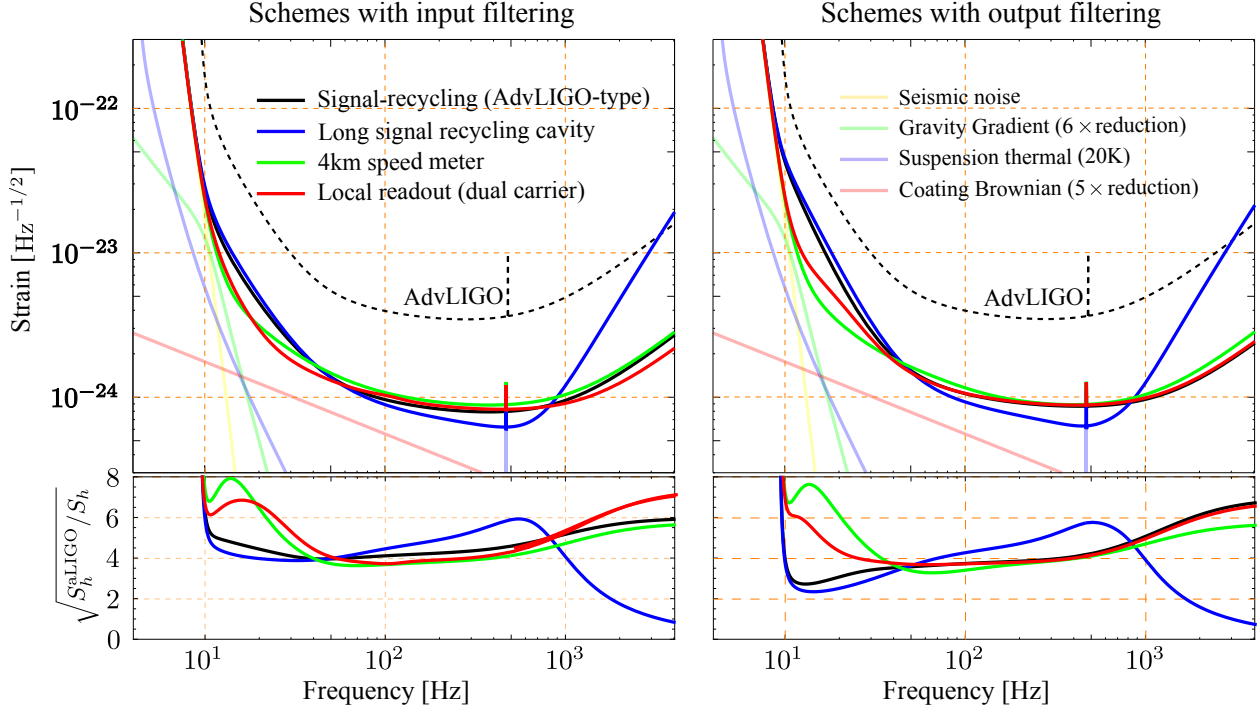
Figure 23: Optimization results for different schemes assuming more substantial thermal noise improvements, increasing the mirror mass from 40 to 150 kg, and increasing the arm cavity power from 800 to 3000 kW.

speed meter is under construction at the University of Glasgow. As such experiments run up against excess noise sources and thermal noise they will inform activities across other working groups.

Obviously, without QRP noise and SQL limited apparatus, no direct tests of these ideas can be performed. However, measuring transfer functions, demonstrating low-loss manipulation of squeezed states and variational readouts can be performed with shot noise limited systems. Plans are underway for such an experiment at MIT and AEI. More effort is needed.

LT-4.7   Development of other signal-to-quantum-noise enhancement techniques

This work falls under sections 3.5 and 3.7 of the LSC Program, "Lasers and Squeezers" and "Topologies".

LT-4.7.1   External source of ponderomotive squeezing

Squeezed light can be produced by mirror motion under radiation pressure — this is called ponderomotive or opto-mechanical squeezing. Ponderomotive squeezing was demonstrated recently [160]. A squeezed factor of $1.7\,\mathrm{dB}$ at about $1.5\,\mathrm{MHz}$ was achieved, in a setup with a SiN membrane. A ponderomotive squeezing experiment at MIT has recently achieved a milestone of showing squeezing of $0.7 \pm 0.1\,\mathrm{dB}$ at 47 kHz [161]. See Fig. 24 for a sample configuration.
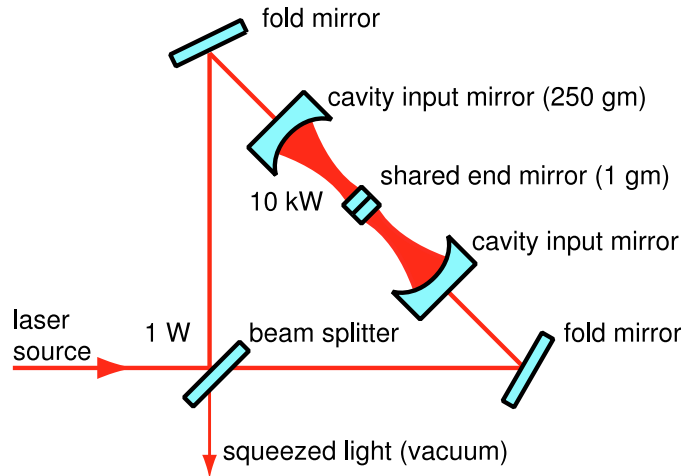
Figure 24: Ponderomotive Squeezer, taken from Corbitt et al. [14]

LT-4.7.2 Intra-cavity squeezing and white-light cavity

Independent of the injection of externally produced squeezed light, intra-(signal-recycling) cavity squeezing might result in an additional signal to quantum noise improvement [102]. Intra-cavity squeezing modifies the peak sensitivity - bandwidth product in a non-trivial way, from which the sensitivity of signal-recycled gravitational-wave detectors could benefit. When the interferometer is used in a signal-extraction tuning, intra-cavity squeezing allows the expansion of the detection bandwidth by producing squeezed light at high frequencies without affecting the low-frequency sensitivity [162]. Such intra-cavity squeezing can also be used to control and modify the optical spring effect by adjusting the squeezing angle and strength [163, 164]. Theoretical as well as experimental work is required to research and develop appropriate schemes based on crystal squeezers.

It was theoretically shown that negative dispersion can result in a white light cavity without significantly adding quantum noise [165, 166, 167]. Traditionally, the type of mediums which provides negative dispersion are atomic media, but they introduce an additional constrain on the wavelength a gravitational-wave detector can be operated at and a thorough investigation of all noise sources of such systems is required. It should be investigated whether solid state optical systems at suitable wavelengths can also provide the same property. Recently, unstable opto-mechanical filters were proposed [168], however, such filters are susceptible to the thermal noise of the mechanical oscillator, which puts stringent requirements on the quality factor of the mechanical oscillator and the environmental temperature that the filter operates at. This thermal noise issue might be mitigated with the idea of optical dilution, or using high quality factor mechanical oscillator at cryogentic temperature [123], or replacing the mechanical oscillator by a nonlinear crystal [169]. Additionally, the details of the control scheme to stabilise the system still needs to be carefully researched. The Caltech group has recently proposed a new scheme [170], similar to the one considered in Ref. [171]. When properly choosing the parameters based upon the principle of PT symmetry, it allows sensitivity improvement and at the same time does not have the issue of instability. Further research into the general principle

LT-4.7.3   Opto-mechanically Induced Transparency

Opto-mechanically induced transparency (OMIT) [172] corresponds to electromagnetically induced transparency (EIT) in atomic vapors with more freedom in choosing the laser wavelength. OMIT can slow down light, possibly improving high finesse optical filters [173]. With enough slowing, one can almost eliminate the need for long filter cavities. This research needs to be pushed into a direction that does not introduce an unrealistic constrain on the gravitational-wave detector wavelength [174].

LT-4.7.4   Negative-mass/frequency systems

The idea of using a negative mass system to coherently cancel the quantum back action noise was proposed theoretically in Ref. [175] for general optomechanical devices, and explored in more detail specifically for the GW detector in Ref. [176]. For a negative-mass system, the radiation-pressure noise introduced into the probing light has a sign opposite to the one in the GW detector. If coupled to the detector's input or output, the negative-mass system can effectively undo the ponderomotive squeezing from the test mass, which cancels the radiation pressure noise.

The negative-mass system can be realised by using a nonlinear crystal as in the original proposal [175], or equivalently a negative-frequency atomic spin ensemble [110, 177, 178]. The negative-frequency atomic spin ensemble for cancelling the back action noise has been demonstrated experimentally [110]. It can also be used to create the frequency-dependent squeezing without a filter cavity [179, 180].

Atomic spin ensembles, however, are very selective in terms of light wavelength, as it has to match the certain transition frequencies between the atomic energy levels, and to date no atomic ensemble that works with 1064 nm, 1550 nm or 2 μm wavelength is identified. This problem can be solved by using entangled dual-frequency squeezed beams like in the case of conditional squeezing. A scheme of GW detector based on this idea was proposed in [179]. It offers a similar broadband suppression of quantum noise as the conditional squeezing scheme but with an advantage of a simpler readout optics. The preliminary estimation of loss influence on its performance was done in Refs. [179, 180], yet the design of a practical scheme based on this principle requires further theoretical and experimental R&D and prototyping.

LT-4.7.5   Other

There is the general question of whether atom interferometry offers a competitive topology for a third generation detector. Whilst this research area is not a fundamental activity of the LSC we should keep a watching brief on this technology and provide scientific support and advice when and where we can.

5 Optics

The Optics Working Group (OWG) of the LSC pursues research related to the development and implementation of optical components for ground-based gravitational wave detectors. This includes work on optical components being installed in Advanced LIGO, to better understand their behavior during commissioning and operation; possible upgrades to subsystems of Advanced LIGO including core optics, input optics, and auxiliary optics; and longer term research into ways around significant limitations in current detectors to be implemented in future generations of interferometers.

The OWGs work can broadly be divided into the following categories:

Mirror coating research   The high-reflection (HR) coatings on the test masses must satisfy a number of performance criteria including low absorption, low scatter, high uniformity, high reflectivity at two wavelengths, low mechanical loss, and low thermo-optic noise. Of these, mechanical loss and optical absorption provide the greatest sensitivity limits, and thus the most significant opportunity to improve performance.

The majority of coating research is focused on understanding and reducing the thermal noise arising from the HR coatings because it is a leading noise source in Advanced LIGO's central frequency range and a major design hurdle for all future detectors. However the anti-reflective (AR) coatings also present some challenges such as optical absorption.

Coating research encompasses the following areas:

- **Materials Investigations:** Measurements of the physical characteristics (Mechanical loss, Thermo-optic loss, Young's modulus, optical absorption etc) for coating material candidates for A+ LIGO and LIGO Voyager. This research includes investigations of how these characteristics change through processing, composition, temperature, etc.

- **Structural Measurements and Modeling:** Research to determine the coating structure by measuring or modeling the distribution of atoms and bond configurations, which can then be used to identify correlations to mechanical loss and other material properties. These investigations aim to understand the mechanisms of coating mechanical loss, and identify ways of reducing its effect through a materials-by-design process.

- **Direct Thermal Noise Measurements:** Use of precision interferometry to directly measure thermal noise from coatings made from new materials, techniques, designs, etc. to verify predictions coming out of material investigations. This is an important step to both test predictions and test coating performance before use in actual gravitational wave detectors.

Mirror substrate research   Mirror substrate research encompasses the following broad areas:

- **Substrate material properties:** The mirror substrates for gravitational wave detectors must meet many requirements including low mechanical loss, low optical absorption, low scatter losses and appropriate figure. While previous experience with fused silica substrates is directly relevant for A+ LIGO, the proposed change to silicon substrates for LIGO Voyager requires significantly more research and development. The proposed change from silica to silicon substrates for Voyager is largely driven by the increase in mechanical loss of fused silica at cryogenic temperatures. In addition, silicon mirrors will experience less thermal lensing for the same laser power, potentially allowing the use of higher powers in the arm cavities with silicon mirrors. Silicon is not transparent at 1064 nm, so a change in interferometer laser wavelength, possibly to 1550 nm or higher, would also be required. Low optical absorption is important in a cryogenically-cooled mirror to minimize the heat load and allow the required operating temperature to be maintained. In addition, other optical effects in silicon need to be considered, including two-photon absorption and noise associated with both intrinsic and generated free carriers.

- **Parametric instabilities:** The build-up of parametric instabilities in the arm cavities related to the high laser power levels are a potential problem from high optical power in aLIGO and beyond, with parametric instability already having been observed in the Livingston aLIGO detector. These undesirable effects result from exchange of energy between light stored in cavities and acoustic modes of the mirror which define the cavities, and can result in high excitation of particular acoustic modes of the mirrors, leading to control problems and in extreme cases loss of lock of the interferometer. Research focuses on understanding parametric instabilities and developing methods of reducing the effects.

- **Charging:** There are various mechanisms by which the mirrors in an interferometer can become charged, and interaction between charges on the mirror and charges on nearby surfaces can generate force noise on the mirror. In addition, charging may lead to interferometer control problems through interactions with the electrostatic drives. Charging research focuses on measurements of charge noise and identification and testing of methods for charge mitigation.

Op-5.1 Coatings and Substrates for A+ and room temperature upgrades

This work falls under sections 2.3 and 2.5 of the LSC Program, "A+ Upgrade Project" and 'Post-A+ planning and research.

Op-5.1.1 Coating Research: Coatings for A+ LIGO and room temperature upgrades

Coating thermal noise is related to several properties of the coating including the mechanical loss, the Young's modulus and the thickness, and to the radius of the interferometer laser beam and the temperature of the mirror. For A+ LIGO, a number of different techniques are expected to be capable of providing some reduction in coating thermal noise, including using a larger beam radius, optimizing coating designs (including composition, layer thicknesses and possible exploitation of differences in the loss angle associated with shear and bulk

motion) and possible reductions in mechanical loss via optimizing doping, annealing or via the use of promising alternative coating materials. It seems likely that a combination of a number of these techniques may be used to produce the best possible coating for the A+ LIGO detectors.

Beyond the A+ detectors, it may be possible to develop improved technologies that would enable increased performance at room temperature. For the detector optics, this means further reductions in thermal noise. The use of a larger laser beam radius in the interferometer (along with the use of appropriately larger mirrors) is one of the most obvious methods for reducing coating thermal noise. However, the use of larger mirrors will have a significant impact on the mirror suspensions and seismic isolation systems, so detailed trade-off studies in collaboration with the suspensions working group are required. In addition, detailed discussions with coating vendors are required to determine how much development is required to enable coatings of the required uniformity to be deposited on larger optics.

Further improvements to amorphous coatings would aim for beyond the factor two decrease in thermal noise targeted by A+. Due to a significant decrease in absorption of some materials, e.g. amorphous silicon, a change from 1064 nm to longer wavelength may be beneficial, opening up the possibility to use a variety of new coating materials with low mechanical loss. While a wavelength change is rather complex, the potentially great benefit makes it worthwhile to explore possible material and wavelength options.

Op-5.1.2 Coating Research: aLIGO Coatings

It is important to ensure that the thermal noise and optical performance of the aLIGO mirror coatings is fully understood, in order to enable an accurate baseline for the development of coatings for A+ LIGO. Understanding the variations in coating mechanical loss measured on different substrates, and how this relates to direct thermal noise measurements on test mirrors and to the magnitude of thermal noise expected in the aLIGO mirrors is a research priority. Similarly, a full understanding of the scattering characteristics of the aLIGO coatings is required to assist with fully characterizing scatter loss, and potential related noise sources, in the detectors.

Op-5.1.3 Coating Research: Mechanical Loss

For room temperature mirrors at 1064 nm, the coatings with highest optical quality are ion beam sputtered (IBS) amorphous coatings, where the high index material is typically a metal oxide (i.e. Ta_2O_5 or TiO_2) and the low index material is usually silica.

The thermal noise due to the mirror coatings can be calculated from the coating mechanical loss using the Levin method [181]. Two methods are currently employed to measured the mechanical loss. The first method measures the loss via ringdown of small coated cantilever samples over the temperature range of $0 - 300$ K. These measurements map out the Debye loss peaks and determine the activation energy of the loss mechanism. This knowledge can then be used as a constraint in models of the coating structure (see Section Op-5.1.7) By accurately modeling the coating structure, one may be able to identify the microscopic causes of internal friction and design coatings with minimal loss. Thus, while temperature

dependent coating loss measurements are also of interest for cryogenic coatings for LIGO Voyager, these measurements are also relevant to understanding loss mechanisms in room temperature coatings for A+ LIGO.

The second method measures the mechanical loss of coated thin silica disks at room temperature over a wide frequency range (typically $3 - 20$ kHz). The frequency dependence allows separation of the bulk, surface and thermoelastic losses. Characterizing the mechanical loss at a wide range of frequencies and temperatures is valuable both as a search for new materials and to better understand the causes of thermal noise in amorphous thin film oxides.

The high index materials that have been explored include: tantala, titania, niobia, hafnia, and zirconia. Silicon nitride, Si_3N_4, also may be promising. Low index materials include silica and alumina. As applied, the high index materials have losses ranging from $3 - 7$ $\times 10^{-4}$.

The loss in the silica coating layers, while several times less than the high-index layer, is not negligible. For coating geometries, the loss in silica is dominated by surface and stress-induced losses. The latter loss can be minimized through a slow annealing process. However, this process typically destroys a multilayer coating by either crystallization of the high index material or adhesion failure due to differential thermal expansion. Thus the loss in the silica layers will depend on the geometry and thermal history of the multilayer coating. The loss in alumina is dominated by thermoelastic loss and is not currently suitable for room temperature coatings.

The most commonly used model for loss in these glassy materials [182] assumes an asymmetric, double-well bond potential formed by two nearly degenerate bond states. In silica, for example, the O bond potential has an angular dependence that is described by nested, asymmetric potentials [183], where the activation energy depends on the atomic distribution. In this model, one may minimize the loss by removing the potential's double-well (i.e., doping to change the bond potential or annealing to allow the material to assume its lowest energy state).

Doping   Doping can reduce the mechanical loss by favorably changing the bond potential and by stabilizing the matrix against crystallization. For example, doping the tantala layers with titania has been shown to reduce mechanical loss by about 40%. This reduction allowed titania-doped tantala/silica to be selected for the Advanced LIGO coatings. Silica-doped titania has shown promise for reduced thermal noise, and was considered a fallback coating for Advanced LIGO. A trinary alloy of titania/tantala/silica as the high index material may allow for benefits from each material. Silica, while effective at stabilizing high-index materials and thus allowing for higher annealing temperatures, also reduces the index of refraction, thus requiring thicker coating layers. Effective medium theory may be of use in modeling alloys and doping, and comparing Q measurements to predictions of effective medium theory are an important next step in verifying this approach.

The use of dopants in tantala, titania, hafnia and zirconia are being explored as a means of understanding and reducing the mechanical dissipation. While it is crucial that any new materials also satisfy the stringent optical requirements of LIGO interferometers, there are advantages of initially just pursuing lower mechanical loss.

Shear and bulk loss angles   Amorphous materials, including fused silica, tantala, titania doped tantala, and other oxides under consideration as coating materials have two independent elastic moduli, and thus two independent loss angles. Work at Caltech by Yanbei Chen's group suggests that it should be possible to design coatings with reduced Brownian thermal noise by having the thermal noise generated by different loss angles partially cancel out. Whether this is practical or significant depends on the values of the loss angles for the coating materials, which can only be determined experimentally. Measurement of torsional and bulk mechanical losses of coating materials will provide necessary input for these designs.

Annealing   Ion beam sputtering forms coatings with high compressive stress, and comparatively high mechanical loss and absorption. Annealing these coatings will reduce the stress and correspondingly reduce the absorption and mechanical loss. Typically the annealing temperature is limited by either the crystallization temperature for the high index material or shear failure from the differential expansion of the coating layers. If these failure mechanisms can be avoided, annealing could potentially provide significant improvements in mechanical loss and absorption.

The mechanical loss in silica coatings has been reduced by about $8\times$ through high temperature annealing. In addition a zirconia/silica coating has been demonstrated to survive a $1000°$ C annealing without shear failure. Annealing has also been shown to reduce the absorption in zirconia coatings by a factor of several. Work is currently underway to use doping to stabilize the coatings against crystallization, which leads to unacceptable scatter. Silica doping suppresses crystallite growth during annealing in titania [184], hafnia and zirconia [185]. Coating designs to withstand high temperature annealing could see significant improvements in their absorption and their mechanical loss. Planar layered composites consisting of alternating nm-scale Titania (or hafnia) and silica (or Alumina) layers can be annealed to much higher temperatures compared to (un-doped) materials [186, 187]. Recent results have suggested that heat-treatment of zirconia-doped tantala coatings can reduce the mechanical loss, and heat-treatment at temperatures up to $800°$ C is possible without crystallization occurring [188, 189]. Further measurements and repeat coating runs are required to fully characterize this material. It is interesting to note that zirconia was also identified as an interesting dopant by atomic modeling work carried out within the LSC. This work showed that titania doping increased the flexibility of ring-structures found in the coating, and suggested that zirconia doping would increase the flexibility further, possibly resulting in lower mechanical loss [190]. The strategy of using a doped material consisting of the correct proportions of two high-index materials to stabilize against crystallization appears promising and should be further investigated with other material combinations.

Elevated temperature deposition   Deposition of amorphous silicon coatings onto heated substrates can reduce the mechanical loss by orders of magnitude [187], possibly due to the material forming a more ordered amorphous state referred to as an 'ideal glass'. Evidence suggests that a larger loss reduction is possible with elevated temperature deposition than with post-deposition annealing, possibly due to the coating atoms having more freedom to move during the deposition process. Since post-deposition annealing is already known to reduce the mechanical loss of oxide coatings such as silica and tantala, deposition at

elevated temperatures may also be a promising technique for significantly reducing the loss of these materials and also of other materials, including non-oxides. In pure tantala, however, deposition at high temperature only marginally improved the loss angle over post-annealing at the same temperature [191]. Alternative methods of providing more energy to the coating atoms as they are deposited on the substrate may also be of interest, for example the use of ion-assisted deposition where a secondary ion-source is used to bombard the substrate with an ion beam during coating deposition. It sometimes has adverse effects, however: in pure tantala, applying a bias during sputtering deposition led to a deterioration of the loss angle, or no improvement [192].

Interface Effects Early experiments on loss in Initial LIGO's tantala/silica mirror coatings [193] demonstrated that the loss was primarily due to the tantala layers. No significant loss could be attributed to the coating interfaces. Measurements conducted at LMA on the Advanced LIGO coating initially indicated some excess loss associated with the coating interfaces, but that conclusion was not borne out in subsequent measurements. Nevertheless, for any proposed change in coating material a study of interface losses should be conducted [194].

Op-5.1.4   Coating Research: Optical Properties

Optical Absorption Absorption of light in the coatings will result in thermoelastic distortion of the optics and will ultimately limit the circulating light power in the interferometer. When coupled to the bulk absorption in the input test masses, this leads to significant surface deformation of the test masses and bulk thermal lensing in the input test masses. Coating absorptions as low as 0.3 ppm have been reported in undoped silica/tantala coatings, while titania-doped tantala and silica-doped titania coatings have been shown to have absorption at or below 0.5 ppm. The coatings used in aLIGO made of silica/titania doped tantala have an absorption of < 0.4 ppm [195]. Further improvements beyond this level will make thermal compensation easier for A+ LIGO, and detailed studies of absorption are essential for any coating materials considered for use in current or future detectors.

Studies aimed at understanding and improving coating mechanical loss may involve working with coatings with relatively high absorption during a research phase e.g. to understand why a particular dopant affects the mechanical loss. Further research into the absorption of anti-reflection coatings is also required, as these coatings consistently have a higher absorption (up to 10 ppm) than high-reflectivity coatings (typically below 1 ppm).

Optical Loss from Scattering It is important to minimize the optical scatter

- to maintain the high power in the arm cavities as optical losses reduce the achievable power build up,

- to reduce phase noise from backscattering,

- and to realize more sophisticated quantum non-demolition (QND) topologies as explained in section Op-4.2.1 for the case of filter cavities.

Scatterometer measurements should be conducted for proposed coatings and new coating materials. Studies of the dependence of scatter on coating materials and manufacturing are important in determining the lowest possible scatter. One of the important sources of optical loss is scattering from mirror-surface aberrations. These are traditionally investigated by measuring the angular distribution of scattered light (i.e. measurements of the bidirectional scattering distribution function (BSDF)), or scanning the surface with lasers and integrating the scattered light in spheres. As much as these measurements are important to link scattering from mirrors with losses in optical systems like cavities, they do not give direct information about the cause of scattering.

Scatter loss in (future) optical systems with sizes up to a few hundred of meters will likely be dominated by point-defect scattering as the quality of substrate polishing has advanced to a level that makes residual surface-roughness scatter loss negligible in most cases. These conclusions are based on numerous simulations and partially on scattering measurements in first-generation GW detectors. Even though it is believed that very low-loss systems can be realized in the near future with scatter loss around 10 ppm per mirror, the question is how much further the loss can be decreased. Loss estimates play a major role when deciding between the various candidate QND configurations for future GW detectors. Whereas input filters (see section Op-4.4.1) are relatively robust against optical loss, output filters (see section LT-4.4.2) that can potentially eliminate all back-action quantum noise are known to be highly susceptible to loss. A few ppm loss per mirror typically destroys the entire advantage that output filters have over input filters (eventually making them even worse in performance). Similar problems are encountered with alternative QND schemes.

Assuming that point-like defects residing in the mirror coatings are the dominant source of scatter loss, one has to investigate individual defects for their material compositions, morphologies, and structures. The answers can be used to understand the origin of the defects with the goal to improve the coating process and, in case of damage induced defects, also the handling of the coated optics. Various analysis methods are available. Defect morphology can be studied optically or with force microscopy depending on defect size. Defect materials can be investigated spectroscopically. The analyses should progress from larger to smaller defects since the larger defects dominate the point-defect scatter even if they are significantly less numerous.

Op-5.1.5   Coating Research: Other Coating Properties

Thermo-optic Noise   Coating Thermo-Optic (TO) noise is the apparent motion of the surface of a mirror due to stochastic temperature fluctuations. These temperature fluctuations drive two separate but correlated effects, commonly known as coating Thermo-Elastic (TE) and coating Thermo-Refractive (TR) noise [196, 197]. The power spectral density of these temperature fluctuations has been calculated in various places [196, 198].

The first effect (TE) is physical motion of the surface of the mirror due to the thermal expansion of the coating. This effect requires knowledge of the effective Coefficient of Thermal Expansion (CTE) for the coating materials. We say 'effective' because the coatings are attached to large substrates, therefore not free to expand laterally; Poisson ratio effects and substrate behavior need to be accounted for. The coatings are also under great stress so

that any change in the Young's modulus with temperature could conceivably couple into out-of-plane expansion of the layers.

The second effect (TR) is apparent motion of the surface of the mirror as measured by a laser beam, due to changes in the mirror's complex reflection coefficient. Since the mirrors used are generally high reflectors, the magnitude of the reflectivity does not change when the temperature changes (varying the optical path length of the individual layers and thus the superposition of the reflected light field), but the phase picked up on reflection does change to first order in the temperature change. For historical reasons this effect is referred to as TR, but physical expansion of the layers also plays a role here.

It is expected that these two effects will partially cancel [199], and there is evidence that this is indeed the case [200, 201]. In [199], it was argued that with nominal values the cancellation would put the level of TO noise roughly an order of magnitude below coating Brownian noise. No noise floor data out of the LIGO interferometers has contradicted this estimate.

However, the relevant thermal / thermo-optic parameters involved (specifically the CTE and dn/dT for the thin-film high- and low-index materials in the coating) are known to differ from bulk values, and measurements of these values exhibit wide variation (up to an order of magnitude, see e.g. [202, 203, 204, 205, 206]). The situation is complicated by the fact that the parameters could conceivably depend on deposition technology, doping, and layer structure. This is particularly unfortunate for two reasons:

- First, it makes predicting this noise level challenging. For TE and TR effects to cancel so that the sum is of order 10% of either effect alone, it is necessary that the magnitudes of the TE and TR effects are within 10% of each other to begin with. Since these parameters are not known at the 10% level, as we move forward it will be important to check individual coating TO responses. We currently have capabilities within the collaboration for making such measurements (using the technique described in [200]), but are interested in other methods of making the measurement as well.

- Second, it makes design of future coatings with greater degrees of cancellation (or design of coatings to jointly minimize say TO noise and Brownian noise) effectively impossible until we have better measurements of the individual parameters themselves. A method for extracting individual parameters from measurements on a set of differing coating structures was shown in a proof-of-principle manner in [200], but we still need trusted measurements for these parameters as they will appear in our coatings. To the extent possible, coating material, chemistry, deposition process, substrate, and coating layer structure should be held as close as possible to the materials, processes, and designs used in the LIGO mirror coatings until these various factors' impacts on the TO parameters of the coating materials can be teased out. Studies of these effects (both experimental and theoretical) that help us understand their impacts on coating TO parameters are also of serious interest as they can then help us in the selection and design of future coatings.

Young's Modulus and Stress   The Young's modulus of a coating is required both for the analysis of mechanical loss measurements and for calculations of the level of coating

thermal noise. It is therefore important to obtain accurate values of Young's modulus for every coating, and post-deposition coating treatment, studied. Residual stress in coatings is likely to be an important property, and there is interesting evidence suggesting that stress can alter the mechanical loss of coatings, particularly in silicon nitride. Therefore studies of the effects of residual stress on the loss and of methods of altering the stress in particular coatings are of interest. The use of several measurement techniques can be beneficial in these studies, as each technique has different systematic errors and, for example, different sensitivity to the properties of the coating substrate material. In addition to measuring these properties at room temperature, where possible the capability to measure the temperature dependence of these properties should be developed.

Young's modulus and dissipation measurement method with sub nanometer spatial and depth resolution has been developed by Konrad Samwer. This method shows that the Young' modulus in glasses has a position-dependent spread as wide as 30 % (and the local loss factor is also poorly defined), and that the spread is reduced with annealing, while crystals have constant Young's modulus everywhere. It has also been shown that fused silica, which is the glass with the lowest known mechanical loss, has a substantially narrower Young's modulus spread than other glasses. The method can either explore small shallow volumes, or wider and deeper volumes, up to several hundreds of atomic spacings in dimension. The capability of this method to scan the Young's modulus with sub-nanometric resolution offers a new way to explore the uniformity of our coatings, as a function of annealing, and perhaps shine some light on some loss mechanisms.

Uniformity It has also proven to be challenging to maintain coating thickness uniformity across the large face of Advanced LIGO optics. Non-uniformity in thickness leads to non-uniformity of transmission and scatter of light out of the cavity mode to other optical modes. This also leads to limits on optical power and squeezing, as the higher spatial frequency scatter discussed in the previous section. Even larger optics are possible in future detectors, making maintaining coating uniformity even more challenging and thus an important research topic. The limitation on obtainable uniformity can come from metrology limitations, making improved metrology an important research direction. An additional research direction is to explore corrective coatings, which place additional coating material onto a coated optic after uniformity measurements have been made.

Op-5.1.6   Coating Research: Coating Deposition Parameters

Variations in the optical and mechanical loss of nominally identical coatings from different vendors have been observed, suggesting that the precise deposition parameters may be important in determining the loss. Thus more detailed measurements of the effects of parameters such as ion energy, sputtering ion, oxygen pressure and thermal treatment may be valuable. While ion beam sputtering produces the lowest optical loss coatings, the mechanical loss of coatings deposited by other techniques has not been extensively studied. Studies of coatings deposited by different techniques (e.g. magnetron sputtering, e-beam evaporation, atomic layer deposition) may enhance understanding of the relationship between loss and structure in these materials.

Coating layer thickness may also prove an important variable in determining amorphous material properties, especially mechanical loss. There are suggestions that making traditional quarter-wavelength coating layers from a sub-structure of much thinner layers of two materials may enable improvements in mechanical loss and may allow higher treatment temperatures to be realized without crystallization occurring [207]. If this effect can be confirmed and understood, it may be possible to design high reflective coatings with much lower thermal noise using known materials like tantala and silica (see **nm-Layered Composites** in Sec. Op-5.1.10).

Op-5.1.7 Coating Research: Structural Studies

The mechanical loss is fundamentally connected to the atomic structure of the amorphous film, and therefore experimental and theoretical tools for characterizing the atomic properties form an important area of research. Until recently the experimental scattering methods have primarily yielded information on short-range order ($< 0.5\,\mathrm{nm}$). Recent theoretical insights show that structural motifs on several nm spatial scales are responsible for the elastic losses at frequencies and temperatures of interest here. Thus, theoretical and experimental methods for characterization of medium range order ($0.5 \sim 5\,\mathrm{nm}$) are essential for understanding and predicting elastic losses in these films.

Experimental Structure Characterization   Experimental structure determinations are based on x-ray or electron scattering methods, both of which have been employed. The data collected can be converted to statistical averages of local atomic environments, often described in terms of pair distribution functions (PDFs). Electron PDF (e-PDF) and extended x-ray absorption fine structure (EXAFS) have been used to gain an understanding of the short range order in doped and heat-treated tantala [208, 209, 210, 211]. In more recent work, grazing incidence pair distribution functions (GI-PDF) has been used to reach higher resolution on unprocessed titania and zirconia doped tantala thin films [212]. Fluctuation electron microscopy (FEM), which uses a focused electron beam to enable characterization of the variance in local environments, is a measurement that is more sensitive to medium range order than conventional e-PDFs [213].

Atomic Modeling   Molecular dynamics methods allow numerical simulation of the atomic structures of amorphous solids obtained by cooling the corresponding liquid phase [214]. The calculated energy landscape obtained through suitable processing of the structures computed from multiple such numerical experiments allows calculation of the elastic loss. In addition to comparing the calculated losses to experimental data, the simulations can also be tested by comparison with the PDFs of these model structures with those obtained from experiment. For titania-doped tantala, these calculated losses correctly captured the trends vs Ti doping and the absolute values at cryogenic temperatures, but were less accurate for room temperature data. Similarly, the simulated PDFs were close to experimental data for short range order, but were less successful for capturing the medium range order [215].

To address these issues, reverse Monte Carlo (RMC) methods have been used to compute the atomic structure from experimental scattering data. By including the measured variance

and/or the high resolution data from GI-PDF measurements as the constraints on the RMC, atomic structure models have been developed which represent the short and medium range order with higher accuracy than was previously possible [216]. These models have provided novel insights into the atomic structure of coatings and effects of annealing or elevated temperature depositions on coating structure. Through correlating changes in structure with measured mechanical loss data, inferences about low loss materials have been drawn. For example, by observing that the content of edge-sharing (ES) and face-sharing (FS) polyhedra in ZrO_2-doped Ta_2O_5 is correlated with mechanical loss at room temperature, GeO_2, which has almost no ES and FS polyhedra, was identified as a potential low RT loss high-index layer material. Subsequent deposition and loss measurement confirmed this prediction [217, 218]. Further experiments identified Ti as a promising doping material to make a dielectric stack with low thermal noise with SiO_2 as low index layer. Modeling efforts and GIPDF measurements are now focused at finding suitable Ti-concentration in GeO_2 that would yield the lowest thermal noise. A key step in this plan is the development of accurate inter-atomic potentials for the TiO_2-doped GeO_2 or any other material of interest. We have developed inter-atomic potentials for TiO_2-doped GeO_2; we plan to develop further refined interatomic potentials using a machine-learning based approach.

In a-Si, a simpler material, simulations based on searches for two-level systems in the energy landscape allowed to identify mechanisms for mechanical dissipation, the majority of them being related to bond hopping or bond exchange [219]. Loss angle values found are in agreement with experiment.

Deposition Simulation   Another key theoretical approach is the direct MD simulation of vapor deposition processes. Such a tool would be invaluable to reduce the large parameter space of substrate temperatures, deposition rates, materials and dopants to a promising subspace that could be synthesized and characterized efficiently. Recent reports of such simulations using simple model potentials showed promise for this approach [220, 221]. Such simulations will be implemented using the accurate atomic potentials, to obtain realistic predictions to guide experimental work.

Op-5.1.8   Coating Research: Direct Thermal Noise Measurements

Direct measurements of thermal noise are of interest to compare with the predictions obtained from mechanical loss measurements and to test the improving theories of coating thermal noise [222].

Fixed Spacer Cavities   Coating thermal noise measurements are now being carried out using fixed spacer cavities, which are limited by coating thermal noise over a wide frequency band and are significantly easier to operate than a suspended mirror system. These systems will use standard size (1 inch diameter) substrates and can provide a convenient test-bed for the development of low thermal noise optics.

AEI 10 meter prototype   The 10 meter prototype interferometer at the Albert Einstein Institute in Hannover Germany will be able to directly measure coating thermal noise. It

will have the ability to change the size of the laser spot on the mirrors to allow for a direct test of spot size dependence, which is an important driver of the desire for larger optics in future detectors.

Op-5.1.9 Coating Research: Crystalline Coatings

In addition to amorphous coatings, development of large area AlGaAs/GaAs crystalline coatings and the transfer process necessary to apply them to silica substrates is likely possible, although a development phase of 3 years and *circa* \$20M is currently anticipated [223] (see Section 5.2.1, which describes development for Voyager crystalline coatings, but is also applicable to room temperature).

Op-5.1.10 Coating Research: Coating Design

nm-Layered Composites Planar layered composites consisting of nm-scale alternating films of Titania and Silica are increasingly stable against crystallization, as the (Titania) layers thickness is reduced [207]. These composites behave as homogeneous materials as regards their optical and viscoelastic properties, for which simple and accurate modeling is available. Crystallization inhibition up to very high annealing temperature has been also observed in nm-layered Hafnia-Alumina composites [187].

Optimized Coatings Since the thermal noise in the coatings typically scales as the total thickness of the more lossy material, reducing this thickness while maintaining the optical properties will reduce thermal noise. Constrained numerical optimization codes have been shown to produce high reflectivity coatings while reducing the volume of high index materials by as much as 20%. Thermo-optic noise from thermoelastic and thermorefractive effects is included in this optimization. The mechanical loss of the low index (silica) material takes on a larger role for thickness optimized coatings, as optimization typically makes the high index (titania- tantala) contribution equal to the low index. Such an optimized design was proposed for use in Advanced LIGO [224, 225]. Greater understanding of mechanical loss in thin film silica and/or other low index materials is crucial to exploiting the full potential of this optimization. Thickness optimization should be generalized to incorporate the dopant concentrations (which affect both the optical and viscoelastic properties of the materials) in the parameters to be optimized, in the perspective of designing minimal noise coatings based on doped (or nm-layered) mixtures.

Designing coatings that take advantage of different loss angles for bulk and torsional motion will be important once numerical values are found. This optimization will need to be done while including thickness effects on Brownian thermal noise as well as thermo-optic noise.

Multi-material coatings The use of multi-material coatings to take advantage of the properties of different materials has been proposed [226, 227]. In particular, it may be possible to exploit the fact that most of the incident light intensity is reflected by the first few bi-layers of a coating, potentially allowing coating materials with higher optical absorption, but lower mechanical loss, to be used in the lower layers of a coating stack without

significantly increasing the total absorption of the coating stack. It should be noted that multi-material coating designs, coupled with the low optical absorption observed in amorphous silicon coatings deposited using a novel ion-beam sputtering process at the University of the West of Scotland, may potentially allow the use of amorphous silicon layers in mirror coatings for use at 1064 nm for A+ [228]. Amorphous silicon is an attractive coating material due to its low mechanical loss and high refractive index: see section Op-5.2.1 for more details.

Crystalline layers in amorphous coatings   It has been proposed to use crystalline silicon layers, created by the silicon-on-insulator (SOI) technology which can produce thin and homogeneous silicon layers, on top of an amorphous coating [229]. Such a layer can potentially have very low optical absorption at 1550 nm and reduce the absorption in amorphous layers underneath significantly using the same principle as multi-material coatings (see previous paragraph). This could allow for the use of materials with low mechanical loss, but high optical absorption. SOI with multiple sets of alternating layers of crystalline silicon and SiO_2 has also been shown for semi-conductor applications, making this technology even more interesting for GW applications. For A+ upgrades, this principle could be of interesting either at 1064 nm with some amorphous bilayers for absorption reduction on top, or at a longer wavelength, e.g. 1550 nm, where the absorption of crystalline silicon is lower.

Op-5.1.11   Mirror substrate research

Fused Silica   Experiments to measure mechanical loss in silica versus annealing parameters, including ramp down and dwell times have led to improvements in the substrate thermal noise. In order for the fused silica thermal noise to pose a problem in the future, the thermal noise of the coating would have to be reduced by more than an order of magnitude. This makes silica substrate mechanical loss studies a lower priority than coating mechanical loss.

Larger fused silica test masses in the range of $\sim$80 - 200 kg could be employed as a way to reduce thermal noise. This would require improved substrate surface figure error over the area of the larger test masses, while managing the residual substrate fixed lens and elastic distortion of the figure error when the mirror is suspended. There would also need to be improved coating thickness uniformity over the larger area of the larger test masses.

Op-5.1.12   Mirror Substrate Research: Parametric Instabilities

The build-up of parametric instabilities in the arm cavities due to the high laser power levels are a potential problem in Advanced LIGO and beyond. These undesirable effects result from the exchange of energy between the light stored in the optical cavities and the acoustic modes of the mirror which define the cavities.At high optical powers, the radiation pressure force of scattered high order optical cavity modes can couple strongly to the mechanical modes of the test masses, resulting in a parametric instability. High excitation of the mirror's acoustic modes can result in difficulties in the controls engineering and at very high amplitudes can lead to lock loss. Unfortunately, the requirements for high sensitivity are commensurate with the conditions under which parametric instability occurs. These include high optical power and low mechanical loss materials in the mirrors.

Using finite element methods, it is possible to start developing a quantitative understanding of this problem by modeling the modes and parametric gain for different test mass configurations, as well as investigate methods for mitigating the instabilities. In order to make a realistic estimate for the parametric gain, it is necessary to also include the full field calculations of the dual-recycled interferometer [230].
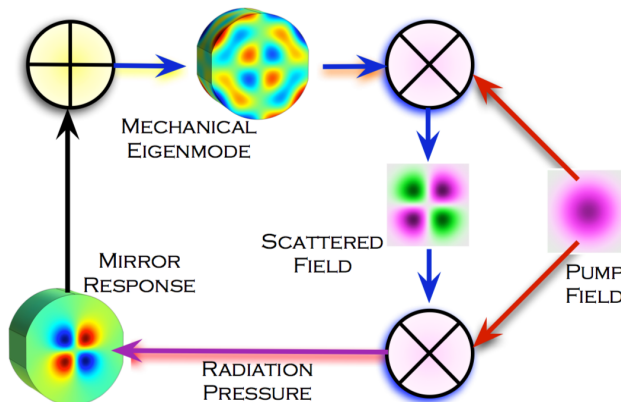
Figure 25: Schematic diagram of the parametric instability mechanism [15].

Starting with O3, acoustic mode dampers have been added to the barrels of the test masses to reduce the Q factors of the test mass modes above 15 kHz. In addition, active damping has been employed using the electro-static actuators on the test masses. The parametric instability situation will need continued investigation as the laser power level is increased for O4 and O5. This includes making more measurements of test mass modal Qs and frequencies and modeling the gain of relevant modes as the power is increased.

Small scale suspended test mass experiments are also underway to study parametric instability. The larger scale experiments will be useful in testing noise performance of various parametric instability suppression schemes, the small scale experiments will be useful to validate the theory of parametric instability and for proof-of-principle test of suppression schemes. The small scale experiments using millimeter scale test masses in a tabletop configuration using coupled cavities and/or specially designed near-concentric cavities can be done using a standard NPRO laser and standard 1" optics. The small scale resonator experiment at UWA has reached the threshold of parametric instability. These experiments are valuable but, because of its applicability to Advanced LIGO and A+ LIGO, the emphasis of parametric instability research should be on suppression schemes.

Modeling [231, 232, 233] already showed that 3MI signal gain had extreme sensitivity to metrology errors. This result carried the message that 3MI monitoring could be very sensitive, but its usefulness was not recognized because the main concern at the time was to suppress the few interactions for which the parametric gain could exceed unity as these represent parametric instability. Using selected modes with gain between 10e-1 and 10e-3 that have been shown experimentally to be easily observed with excellent signal to noise ratio, we would be able to monitor the interferometer global state variations. Because of the complexity of the information that the 3MI provides, further efforts in modeling and experimental research is required to make the 3MI to be a practical monitoring tool.

Op-5.1.13   Mirror Substrate Research: Charging on the Optics

Surface charge may build up on the test masses through a variety of mechanisms, such as contact with dust (particularly during pump down) and/or the earthquake limit stops, removal of First Contact used to keep the optic clean during transport, cosmic ray showers, the ion pumps near the test masses, or handling.

One noise mechanism is static charge distribution on either the optic or the earthquake stop will couple motion of the earthquake stop into forces on the optic [234]. Another mechanism is the noise caused by time-varying charge distributions on the optic (or the earthquake stop) resulting in time-varying forces on the optic. Gaussian noise from this mechanism can be described by a Markov process [235]. The result depends on the magnitude of the deposited charge and the correlation time of the deposited charge, with a smaller actuating noise for correlation times far from the reciprocal of the frequency at which the noise is being measured. These correlation times are being measured using scanning Kelvin probes operated in vacuum which measure the magnitude and distribution of surface charges and their rate of motion across a sample.

Charge may also interact with the electro-static drive causing noise or reduced effectiveness of the drive. Modeling has been started to study this, and experimental work at LASTI has begun to better understand the role of charge with the electro-static drive. There have also been two experimental verifications of a charging contribution from dielectric polarization of the fused silica [236, 237]. Further experimental and theoretical work is planned on polarization noise. Calculations have also been carried out to estimate the force noise that might be expected from Coulomb interactions between charge accumulations on the test mass and various components in the suspension system. The earthquake stops being the closest to the test mass surfaces are of greatest concern for most issues with charge on the optic [234].

Ongoing work will focus on different cleaning and handling methods (including ways of applying and removing First Contact), discharging the optics using ionized gas, and conductive coatings. Understanding what sensitivity limits might come from charging is crucial for A+.

Discharging using ionized gas   The primary solution to mitigating charge in the advanced detectors involves blowing nitrogen gas across needles at 4kV AC, which ionizes the gas externally to the vacuum chamber [238, 239, 240]. The nitrogen ions, which comprise both polarities, travel through an aperture and into the vacuum tank. This is currently installed and used in aLIGO, and will remain in A+.

Conductive coatings   Developing and testing finite conductivity coatings is also an important area of research. Here, the influence of charge on the coating surface will be reduced by having a lightly conductive coating under the dielectric stack, which will support a compensating image charge plane. This will mitigate the effect of surface charges interacting with nearby support structures, particularly the earthquake stops. The conductive coating can then be effectively grounded by UV photoemission conduction, between the optic and support structures. Work is ongoing on conductive ion beam sputtered layers composed of alumina doped zinc oxide (AZO), and measuring the relationship between electrical conduc-

tivity, optical absorption, and mechanical loss. In addition, atomic layer deposition (ALD) of zinc oxide is also under investigation, and show promise for being conductive with extremely thin ($\approx$10 nm) layers. To discharge the optics with conductive coatings, a 'UV electron photoemission wireless conduction' system has been developed, and tests verify that it can ground the test mass to less than a 10 V potential. The UV source will consist of UV GaAs LED's and photoelectrons will be generated – implemented on the barrels of the optics, or possibly the earthquake stops.

Charge noise measurements It would also be useful to directly measure noise from charging, to confirm both the Weiss Markov-process noise model and the parameters found from the Kelvin probe work. Torsion balances, which have been used for laboratory gravity experiments and to test noise models of LISA, offer another possibility to verify Markov noise from charges. Torsion balances are well suited to this since they reach their highest sensitivity at frequencies where Markov charge noise is expected to be large. For charging studies, the torsion pendulum will need to be made entirely of an insulator, likely fused silica, which is a departure from previous experience. The LSC group at the University of Washington, which has experience with torsion pendulums through LISA and other research programs, has performed studies of charging noise [241]. Additional torsion balance experiments are also being developed at University of Glasgow [242] and Moscow State University. In Glasgow, a torsion bob comprising fused silica discs is being utilized to study charge motion on the surface of fused silica and the level of charge deposition when fused silica surfaces come into contact. A Kelvin probe located within the vacuum tank also allows the correlation time to be measured. Initial results suggest that the Weiss theory does give an accurate estimation to the level of charge noise [243, 244]. Further tests are planned with zinc oxide coatings which have the possibility of providing well defined characteristic correlation times, thus allowing the level of charge noise to be varied in a reproducible way. Research at Moscow State University is focusing on the exploration of noise associated with dielectric polarization induced when an electrostatic drive (ESD) is operated near a fused silica test mass [245]. The experimental setup includes a monolithic torsion oscillator with frequency of 63 Hz fabricated entirely from fused silica.

Op-5.2   Coatings and Substrates for LIGO Voyager

This work falls under section 2.5 of the LSC Program, "Post-A+ planning and research".

The proposed use of silicon mirrors operating at 120 K and operating wavelength of 1550 nm or possibly 2000 nm will require further research into silicon as an optical material, continued development of suitable low thermal noise coatings and measurement of a wide range of properties of these coatings at low temperature. Many of the research areas and techniques mentioned in the previous section are relevant to LIGO Voyager, but research on different materials and with many of the measurements carried out at low temperature.

Op-5.2.1   Mirror coating research: Mechanical Loss

The thermal noise of a mechanical system depends on the temperature and mechanical dissipation. For many optical coating materials, the mechanical loss increases at cryogenic

temperatures [246, 247]. Thus using coatings designed for room temperature at cryogenic temperatures will see less improvement in the thermal noise than one might naïvely assume. Thus the shift to cryogenic operation will require the development of new mirror coatings.

Crystalline Coatings Single-crystalline coatings grown by molecular beam epitaxy are of significant interest as a possible alternative to current amorphous coatings. This is likely to be of particular relevance for low-temperature detectors, as the cryogenic dissipation peaks observed in current silica and tantala coatings are thought to be related to the amorphous structure of the materials [215]. There are multiple crystalline coatings under investigation within the LSC; among them are aluminum gallium arsenide, AlGaAs, and aluminum gallium phosphide, AlGaP. General factors which require investigation for crystalline coatings include adhesion to substrates at cryogenic temperatures, light scattering, and fabrication on curved mirror substrates.

Aluminum Gallium Arsenide (GaAs:AlGaAs) coatings[248] have been studied as free-standing micromechanical resonators for use in quantum optomechanical experiments, and have been shown to have very low mechanical losses (as low as 4.5×10^{-6}) at cryogenic temperature [249]. However, these coatings are grown on GaAs substrates, and must be transferred and bonded onto appropriate mirror substrates for use in gravitational wave detectors. Current ongoing experiments with AEI Hannover are exploring larger area coatings at 48 mm in diameter, with larger coatings over 200 mm diameter planned for the future [**?**]. The application of this technique to curved mirrors will require development effort, and it is essential to study these coatings after transfer to appropriate substrates to evaluate any additional mechanical loss and light scatter which may be associated with the bonding process.

Aluminum Gallium Phosphide (GaP:AlGaP) coatings are lattice-matched to silicon, allowing a reflective coating to be grown directly on to a silicon mirror substrate, eliminating the need for coating transfer and bonding [250]. Initial measurements of the mechanical loss at room temperature were limited by thermoelastic damping in the silicon substrate: however, these measurements did allow an upper limit of approximately $< 2 \times 10^{-4}$ to be placed on the coating loss at room temperature [251]. Continuing to characterize the loss and optical properties of these coatings at cryogenic temperatures is of high priority. These coatings are more typically grown on GaP substrates, and thus further development of the techniques for growing these coatings on silicon substrates will be necessary [250].

Amorphous Coatings In addition to the proposed design of Voyager operating at 120 K planned future detectors such as the Einstein Telescope in Europe and KAGRA in Japan will operate at cryogenic temperature to reduce thermal noise. It is therefore essential to fully characterize the performance of coating materials at cryogenic temperatures. In particular, the mechanical loss can be a strong function of temperature and low temperature loss peaks have been observed in silica, tantala and titania-doped tantala coatings [246, 247, 252], there is still some benefit to operating these coatings at cryogenic temperature. For example cooling to 20 K would provide a reduction in coating thermal noise by a factor of about 2, rather than the factor of 4 improvement which would be expected if the coating loss was constant with temperature [246].

Cryogenic mechanical loss measurements of coating materials are a valuable tool for exploring the microscopic processes responsible for energy dissipation. Identification and analysis of Debye-like loss peaks allows key parameters of the dissipation mechanisms to be calculated and, coupled with atomic modeling and structural measurements, may allow the association of loss peaks with particular types of atomic motion within the coating structure.

There has recently been significant progress in understanding the loss mechanisms in tantala coatings, with analysis of cryogenic loss peaks providing information about the dissipation mechanisms, and structural studies and atomic modeling revealing correlations between structure, doping level and loss. The level of loss in tantala below 100 K is strongly dependent on heat-treatment and doping level, and continued studies to optimize coating composition and post-deposition annealing may yield further improvements in coating thermal noise. The results are consistent with a model in which transitions of atoms between energetically stable positions are responsible for the loss, and suggest that the atomic structure of the coating is a key factor in determining the loss.

To enable further reductions in coating thermal noise there is an ongoing effort to identify coatings with a lower mechanical loss at cryogenic temperatures. A number of research paths are being pursued, including further improvement of current silica/tantala coatings, the use of alternative coating materials, particularly amorphous silicon high-index layers, silicon nitride, tantala doped titania, silica doped hafnia and titania, nm-layered silica/hafnia and silica/titania composites.

For cryogenic coatings, amorphous silicon is a leading candidate for a high index material. Amorphous silicon (a-Si) coatings can have a particularly low mechanical loss, with recent measurements placing a conservative upper limit of 5×10^{-5} on the loss angle of ion-beam sputtered a-Si below 50 K [253]. In addition, the high refractive index of silicon allows thinner coatings with fewer layer pairs. The use of a silicon/silica coating could potentially reduce coating thermal noise by a factor of 2.4 at 20 K compared to a silica/tantala coating. However, the first measurements of optical absorption in these coatings suggest that significant efforts to understand and reduce the optical absorption may be required. However, the effect of the high absorption could be significantly reduced through the use of 'multi-material' coatings Op-5.2.7 (see Sec. Op-5.1.10), and the use of heat-treatment has been shown to be effective in significantly reducing the absorption of a-Si films. Recent work carried out within the LSC has shown that amorphous silicon films deposited using an ion-beam sputtering system with a novel electron cyclotron resonance ion source can have optical absorption a factor of up to 50 lower than other, commercially available ion-beam sputtered a-Si coatings [254]. Finally, the absorption of a-Si can be a factor of $\sim$7 lower at 2000 nm than at 1550 nm [255], so a move to a $\sim$ 2000 nm laser could also be necessary to enable the use of a-Si coatings.

It has been shown that infusing hydrogen in the silicon coating can significantly reduce the optical absorption, thought to be related to passivating dangling bonds. Studies to test this for ion-beam sputtered coatings and to evaluate the effect of hydrogenation on the optical absorption should therefore be carried out. However, the hydrogen can diffuse out of the silicon, reversing this effect. Nevertheless, the usefulness of dopants to improve the mechanical loss is clear. Recent work also suggests that deposition of a-Si films at elevated temperature (400°C) can result in significant reduction of the mechanical loss due to an increase in the structural order of the film. The effect of deposition at elevated temperatures

on the optical absorption is therefore an important area of study.

Studies of different deposition methods for a-Si are also of great interest. In particular, chemical vapor deposition is a more mature technology for a-Si deposition than ion-beam sputtering (used, for example, for solar cells) and allows for relatively straightforward tuning of the deposition process including control of doping and stress.

Measurements of hafnia coatings indicate that, even when in a partially poly-crystalline form, this material has a lower loss than tantala at temperatures below 50 K. Preliminary results [256] seem to indicate that amorphous TiO_2 may also be almost exempt from a cryogenic loss peak. Experience with tantala suggests that poly-crystalline structure may significantly increase the loss. One method of preventing crystallization of hafnia films is doping with silica and it has been shown that this does not significantly increase the loss at room temperature. Silica doping is also effective in stabilizing Titania against crystallization [184]. Layered nm-scale silica-titania (and alumina-hafnia) can also be annealed at high temperatures. Low temperature loss measurements of silica-doped hafnia coatings are underway. Cryogenic loss measurements on tantala and Silica doped Titania, and nm-layered hafnia/silica and Titania/Silica composites are also being planned.

There have been reports on the particularly low cryogenic mechanical loss of stressed amorphous silicon nitride films [257, 258]. The composition of this material is highly process-dependent and is possible to make both high and low refractive index SiN_x films by varying the composition, leading to the possibility of an entirely CVD-grown, SiN_x based HR coating.

Silicon oxynitride shows a low extinction coefficient (in the mid 10^{-6} range), and lower cryogenic mechanical loss than silica [259]. The refractive-index can be tuned from nitride-like (high index) to silica-like (low index) which enables the production of multilayers structures of silicon(oxy)nitrides with high area uniformity, but also makes it an interesting partner material for a variety of other high- or low-index materials and is therefore worth being explored in more detail.

Diamond-like carbon (DLC) coatings may also be of interest for further study, as there is evidence in the literature that the loss of this material is very low, with some films having a lower loss than amorphous silicon.

Studies of other possible alternative amorphous coating materials should continue, and where possible the choice of material (or treatment regime e.g. dopant, doping level, heat-treatment) will be informed by the results of structural measurements and modeling. While most of the effort to date has focused on developing alternative high-index coating materials for use at low temperature, it should be noted that silica coatings also have a cryogenic loss peak of a similar magnitude to that observed in tantala. Thus more studies of possible alternative low-index materials are required. In this connection, silica doped Hafnia (or nm-layered Hafnia-Silica composites) could be an interesting candidate low-index material, with a refractive index of ≈ 1.5. This could be used with Tantala doped titania (or silica doped titania, or nm-layered titania-silica composites) for the high-index material (with refractive index ≈ 2.15), to achieve a contrast comparable to that of the silica/tantala HR coatings presently in use, hopefully featuring much better cryogenic behavior.

Shear and bulk loss angles   Understanding the mechanical loss angles associated with bulk and shear motion is of interest for any candidate coating for LIGO Voyager, and suitable finite element modeling will be required to support experimental investigations. Extension of this work to crystalline coatings, where separate loss angles are expected to be associated with each crystal axis, is required.

Op-5.2.2   Coating Research: Optical Properties

Optical absorption   Measurements of coating optical absorption at cryogenic temperatures will be necessary to provide the information necessary to select coatings for the proposed Voyager design. Just as with mechanical loss, the optical absorption can be strongly dependent on doping and annealing. These dependencies will need to be investigated for any proposed coating in order to minimize both mechanical loss and optical absorption. As noted above, aSi is one of the most promising low mechanical loss coating materials for use at low temperature, however, the absorption of aSi coatings is currently significantly higher than will be required for Voyager and further development is required.

Optical Loss from Scattering   In order to maintain the highest optical power in future detectors, it is important to minimize the amount of scatted light. Scatterometer measurements should be conducted for proposed coatings and new coating materials. Studies of the dependence of scatter on coating materials and deposition parameters will be important in determining the lowest possible scatted light levels. Realizing more sophisticated quantum non-demolition (QND) topologies also requires extremely low-loss optical systems as is explained in section Op-4.2.1 for the case of filter cavities. One of the important sources of optical loss is light scattering from mirror-surface aberrations. These are traditionally investigated by measuring the angular distribution of scattered light (i.e. measurements of the bidirectional scattering distribution function (BSDF)), or scanning the surface with lasers and collecting the scattered light with integrating spheres. As much as these measurements are important to link scattering from mirrors with losses in optical cavities, they do not give direct information about the cause of scattering.

Assuming that point-like defects residing in the mirror coatings are the dominant source of scatter loss, one has to investigate individual defects for their material compositions, morphologies, and structures. The answers can be used to understand the origin of the defects with the goal to improve the coating deposition process. Various analysis methods are available. Defect morphology can be studied optically or with force microscopy depending on defect size. Defect materials can be investigated spectroscopically. The analyses should progress from larger to smaller defects since the larger defects dominate the point-defect scatter even if they are significantly less numerous.

Op-5.2.3   Coating Research: Other Coating Properties

Young's Modulus and Stress   The Young's modulus of a coating is required both for the analysis of mechanical loss measurements and for calculations of the level of coating thermal noise. It is therefore important to obtain accurate values of Young's modulus for every coating including post-deposition annealing. Measuring the temperature dependence

of Young's modulus will be of particular importance for LIGO Voyager, and this capability should be developed.

Residual stress in coatings is likely to be an important property, and there is interesting evidence suggesting that stress can alter mechanical loss of coatings, particularly in silicon nitride. Therefore studies of the effects of residual stress on the mechanical loss and of methods of altering the stress in coatings are important. The use of several measurement techniques can be beneficial in these studies, as each technique has different systematic errors and, for example, different sensitivity to the properties of the coating substrate material.

Uniformity As discussed in Op-5.1.5, coating uniformity is important to avoid the scattering of light out of the cavity mode and into other optical modes, which leads to limits on the optical power and squeezing. With the larger optics proposed for Voyager, maintaining coating uniformity will be even more challenging and thus an important research topic. Moreover, the limitation on obtainable uniformity can come from metrology limitations, so improved metrology is an important research direction. An additional research direction is to explore ion beam million and corrective coatings, which remove or place additional coating material onto a coated optic after uniformity measurements.

Op-5.2.4   Coating Research: Coating Deposition Parameters

Variations in the loss of nominally identical coatings from different vendors have been observed, suggesting that the precise deposition parameters may be important in determining the loss. Thus more detailed measurements of the effects of parameters such as ion energy, sputtering ion, oxygen pressure and thermal treatment may be valuable. While ion beam sputtering produces the lowest optical loss coatings, the mechanical loss of coatings deposited by other techniques has not been extensively studied. Studies of coatings deposited by different techniques (e.g. magnetron sputtering, e-beam evaporation, atomic layer deposition) may enhance understanding of the relationship between loss and structure in these materials.

Op-5.2.5   Coating Research: Structural Studies

There is currently little understanding of the mechanical loss mechanisms in amorphous or crystalline coatings, although it seems likely that in the amorphous case the loss mechanism is related to the local atomic structure and may involve transitions of two-level systems as is believed to be the case in fused silica. Studies of the structure of amorphous coatings, aimed at understanding links between structure, composition, loss and optical properties, are a critical part of the research required to develop coatings suitable for use in LIGO Voyager. The suite of structural investigation and atomic modeling techniques discussed in Op-5.1.7 will also be applied to interesting candidate materials for Voyager, and used to inform the mechanical loss studies outlined above. Understanding structural defects in crystalline coatings is also likely to be an important area of research.

Op-5.2.6 Coating Research: Direct Thermal Noise Measurements

Direct measurements of thermal noise, as described in Op-5.1.8, are also of interest on coatings suitable for use in LIGO Voyager. In cases (e.g. crystalline coatings) where thermo-optic noise cancellation is required to get the thermo-elastic or thermo-refractive noise below the Brownian noise, Q measurements alone cannot truly probe the thermal noise limits.

Op-5.2.7 Coating Research: Coating Design

nm-Layered Composites Planar layered composites consisting of nm-scale alternating films of titania and silica can be more and more resistant to crystallization, as the (titania) layers thickness is reduced [207]. These composites behave as homogeneous materials as regards their optical and viscoelastic properties, for which simple and accurate modeling is available [260]. Crystallization inhibition up to very high annealing temperature has also been observed in nm-layered hafnia-alumina composites[187]. Recent work has shown that nano-layer structures of silica and titania can suppress the characteristic loss peaks found in silica films [P1800102].

Optimized Layer-Thickness Coatings Since the thermal noise in the coatings is dominated by the total thickness of the more lossy tantala layers, reducing this thickness while maintaining the optical and mechanical properties will reduce thermal noise. Constrained numerical optimization codes have been shown to produce high reflectivity coatings while reducing the volume of high index materials by as much as 20% [261]. Using this optimization method, a coating thermal noise reduction of 9% has been experimentally verified through direct thermal noise measurements [262].

Multi-material coatings The use of multi-material coatings to take advantage of the properties of different materials has been proposed [226, 227]. In particular, it may be possible to exploit the fact that most of the incident light intensity is reflected by the first few bi-layers of a coating, potentially allowing coating materials with higher optical absorption, but lower mechanical loss, to be used in the lower layers of a coating stack without significantly increasing the total absorption of the coating stack. This type of design may allow the use of aSi in the lower part of a coating stack, taking advantage of both the low mechanical loss and high refractive index of this material. This principle can possibly be extended to including one or more crystalline layers – see Sec. Op-5.1.10.

Op-5.2.8 Reduced Coating and Coating Free Optics

Several ideas have been proposed to reduce the mirror thermal noise by reducing the required coating thickness or removing the coating altogether, including:

- Corner cube style retro reflectors

- Brewster angle prism retroreflectors

- Khalili cavities as end mirrors

- Diffraction gratings

While some of these techniques may be more appropriate for consideration for use in LIGO Cosmic Explorer, some of them may provide possible alternative solutions to the coatings for LIGO Voyager. Corner reflectors and Brewster angle mirrors would allow for no coatings to be needed and Khalili cavities would allow for much thinner coatings than conventional mirrors. Experimental work is needed to test some of these concepts for practical limitations. A bench experiment has been done forming a cavity with one Brewster angle mirror and one conventional mirror on fixed suspensions to see if a high finesse cavity can be formed. Follow on work with suspended mirrors will be necessary to evaluate the mechanical stability of such a system.

Op-5.2.9   Ice Growth On the Mirrors

In KAGRA, the growth of an ice layer on the core optics has been observed [263], caused by a non-perfect vacuum. This ice layer increases the coating thermal noise [264], the optical absorption and changes the reflectivity [265]. By further reducing the residual pressure, the ice growth can be significantly reduced. However, at wavelengths relevant for e.g. LIGO Voyager, the optical absorption is much higher than at 1064nm (used in KAGRA). This makes investigations into the characterization and mitigation of such an ice layer of interest.

Diffraction gratings   All-reflective interferometers using diffraction gratings as optics avoid problems associated with the transmission of large laser powers through optical substrates. Moderately high finesse optical cavities have been demonstrated using small gratings. The challenge will be to scale up the optical aperture to what is required for a large detector. In addition, absorption by the grating surface can distort its surface profile, possibly resulting in changes in the beam profile as well as power-dependent changes in the diffracted beam shape and efficiency. Modeling has been done along with sample produced, but these effects need to be investigated more in depth. Investigations of mechanical loss in gratings are needed to verify thermal noise levels as are direct thermal noise measurements. Demonstration of high reflectance values is also important.

Op-5.2.10   Mirror substrate research

Silicon   The OWG is investigating alternative materials to fused silica for use as test mass substrates and which can be used in low temperature detectors. Both silicon and sapphire potentially offer superior performance at cryogenic temperatures and/or specific frequency ranges. Different substrate materials, operating temperatures, and laser wavelengths may also require and/or allow for different coatings and suspension connection techniques.

Previous research efforts on silicon have largely focused on acquiring and fabricating cylindrical test specimens and investigating their mechanical properties as a function of doping. Studies of silicon properties, including mechanical loss for predicting thermal noise, of different crystal orientations are valuable. In addition, silicon cantilever micro-resonators with

resonant frequencies in the sub-kHz range have been fabricated to explore dissipation mechanisms in a regime where thermoelastic effects are significant. Surface loss effects are also emphasized by the large surface-area to volume ratio of the micro-resonators. Preliminary experiments measuring the dissipation have been carried out and reveal disagreement with theoretically predicted loss.

Understanding the optical loss of silicon at 1550 - 2000 nm is also an active area of research. The high thermal conductivity of silicon could significantly reduce the effects of thermal loading of transmissive components if the optical loss is low enough. Understanding the temperature dependence of the optical absorption along with all other thermo-optic and thermo-physical properties is important. Research will be required to develop suitable components if a change in wavelength is considered. Silicon mirrors and suspension elements have an advantage of being conductive thus control of charging effects may be easier to implement. Nonetheless, charging will need to be investigated since doping and especially coatings can influence the charging properties.

Investigations of the wavelength dependence of the absorption of silicon is of interest, as it may be beneficial to consider operating at a longer wavelength to reduce or eliminate two-photon absorption effects.

Sapphire Recent efforts have yielded information about the mechanical and optical properties of sapphire, methods for growing and processing large sapphire blanks, and ways to achieve high homogeneity, low absorption sapphire. Studies on annealing for improved optical absorption have been extended to elucidate further details of the kinetics of the out-diffusion process. Gathering experimental data at low temperature is important to predict the performance of cryogenic sapphire test masses. The KAGRA project is pioneering this effort. Room temperature sapphire is also a potential mirror substrate for detectors optimized at higher frequencies. Measurements of mechanical properties including mechanical loss as a function of crystal orientation are also important for predicting substrate and coating thermal noise.

Op-5.2.11 Mirror Substrate Research: Parametric Instabilities

As discussed in Op-5.1.12, parametric instabilities are a potential problem arising from high laser power. These undesirable effects result from exchange of energy between light stored in cavities and acoustic modes of the cavity mirrors. Experimental research and modeling of parametric instabilities, and possible suppression techniques, in silicon mirrors at high power levels will be required.

Op-5.2.12 Mirror Substrate Research: Composite Masses

Increasing the mass of the test masses reduces the influence of both classical and quantum radiation pressure noise. Beyond a certain size, however, it is impractical to fabricate mono-lithic masses. Using large masses made as a composite of multiple, smaller pieces could circumvent this problem. Non-cylindrical mass distributions could also be used to increase the total mass and total angular moment of inertia without increasing the optical path length

within the substrate. The larger translational and angular moments of inertia would reduce the radiation pressure noise and the influence of the Sidles-Sigg instability. Thermal noise issues related to mechanical loss from the interfaces will have to be understood.

Op-5.2.13   Mirror Substrate Research: Charging

The use of semi-conductor silicon optics will require several new areas of research into charging.

- Silicon resistivity at low temperature. Determination of the resistivity and time constants of charge motion on silicon at cryogenic temperatures. At these low temperatures the free carriers begin to freeze out. Research should assess the charge mobility on high purity silicon substrates with resistivity at the level few thousand ohm-m using Kelvin probe, 4-terminal measurements and electromechanical oscillators.

- Coating charging. R&D is necessary to assess the time constant of charge motion on the surface of coatings necessary for cryogenic detectors. Materials include amorphous silicon and crystalline coatings based on AlGaAs and AlGaP. Pushing the performance of future detectors to lower frequencies (1-10Hz) will require the assessment of charge noise mechanisms. These include surface charge with low mobility on the surface of coatings, charge motion in silicon surface/substrates and the interaction of these charges with the electric field of the ESD and nearby grounded hardware.

- Study of discharge mechanisms including (i) utilising He gas rather than N2, (ii) mono/multi layers of gas adsorbed on surfaces (iii) pumping time at low temperature (iv) charging mechanisms.

- Noise mechanisms for semiconductors. The interactions between crystalline silicon and electric fields, e.g. the electrostatic drive and stray environmental fields, should be studied.

While optics research targeted at LIGO Cosmic Explorer is rather more speculative and long term, it is clear that research on optical components for future ground-based interferometers must begin well in advance of any complete conceptual design. One important consideration will be the operating temperature of LIGO Cosmic Explorer, and research into the temperature dependence of both the thermal noise and the optical proprieties of coatings and mirror substrates will be critical in informing this choice. Thus all of the research avenues detailed in the previous sections for substrates and coatings for use at room temperature and at cryogenic temperature are potentially of relevance for Cosmic Explorer.

It should be noted that some of the promising technologies discussed in the LIGO Voyager section, in particular AlGaP and AlGaAs crystalline coatings, involve a larger time and cost commitment than other options. The maximum available diameter of GaAs substrates on which AlGaAs can be grown may potentially restrict the use of these coatings in Voyager. On the time-scale of Cosmic Explorer, it seems more likely that some of these technical issues may be overcome. In addition to this, research into improved amorphous coatings should continue to be pursued. As discussed above, some amorphous coatings (e.g. aSi)

have already been demonstrated to have mechanical loss factors that are equivalent to or better than those measured for crystalline coatings, and further progress with modeling and theoretical understanding of the properties of these materials may allow both mechanical loss and optical absorption to be optimized. Finally, other concepts for making mirrors without coatings (e.g. waveguide mirrors, consisting of coating-free structured surfaces), or with a much reduced coating thickness, are also of interest and further research into the application of these methods to large-scale interferometer mirrors is of interest.

6 Suspensions and Seismic Isolation Systems

The research of the Suspension and Seismic Isolation Working Group (SWG) is aimed at providing the necessary isolation, alignment, and control of the interferometer optics from seismic and mechanical disturbances while simultaneously ensuring that the displacement due to thermal noise of the suspended systems is at a suitably low level. To first order we can divide the research into two broad subdivisions, suspensions and isolation, both of which involve mechanical and control aspects. Suspension research involves study of the mechanical design of the suspensions, the thermo-mechanical properties of the suspension materials and suitable techniques for damping suspension resonances and applying signals for interferometer control. Isolation system research involves mechanical design and active control for isolation and alignment. The overall isolation of the optics comes from the product of the two systems.

The isolation and suspension system for the most sensitive optics in Advanced LIGO is comprised of three sub-systems: the hydraulic external pre-isolator (HEPI) for low frequency alignment and control, a two-stage hybrid active & passive isolation platform designed to give a factor of ~ 1000 attenuation at 10 Hz, and a quadruple pendulum suspension system that provides passive isolation above a few Hz. The final stage of the suspension consists of a 40 kg silica mirror suspended on fused silica fibers to reduce suspension thermal noise.

The R&D for baseline Advanced LIGO isolation and suspension sub-systems is complete. These systems are in operation at the LIGO facilities, and were successful during Advanced LIGO's first three observing runs. Upgrades to the Suspension and Seismic Isolation and Alignment System are grouped into four broad categories: In section Op-6.1 we describe ongoing work on immediate improvements and risk reduction for the baseline Advanced LIGO detector. In section Op-6.2, we describe the A+ (and beyond) improvements which can improve the baseline sensitivity without substantially altering the existing equipment. In section LT-6.4 we describe the Voyager R&D which will make more substantial changes and allow us to operate with cooled optics, and finally in section LT-6.5 we describe the long term work on suspension and isolation systems which build the foundation for the ultimate ground-based gravitational wave detectors.

Op-6.1 Vibration Isolation and Control R&D for Incremental Upgrades to Advanced LIGO

This work falls under section 2.2 of the LSC Program, "Detector Commissioning and Detector Improvement activities", and under section 2.3 "A+ Upgrade Project".

There is ongoing R&D work to provide incremental improvements to Advanced LIGO to improve performance of the aLIGO vibration isolation and suspensions, and improving the stable operation of the observatories by making the instruments more capable of withstanding high winds and teleseismic earthquakes. This type of work is designed to be easily incorporated with the existing detector systems with minimal disruption of the Observatories. These upgrades include work to add additional environmental sensors and incorporate them into the controls, adding more sophisticated control algorithms to improve performance during unusual environmental conditions, small mechanical changes to damp vibration modes, and

relatively modest changes to the facilities.

Op-6.1.1   Tilt/horizontal coupling and advanced sensors

Tilt-horizontal coupling causes a variety of problems and is a basic limit to the performance of the isolation systems at low frequencies (below 0.3 Hz) [266]. Seismic motion in the 10-300 mHz region is governed by the microseism, wind, and earthquakes. Excess motion in this band affects the locking of the interferometer and consequently the duty cycle of the observatories. It may also affect noise in the GW band by frequency up-conversion through non-linearities in the interferometer control and excess RMS motion.

Beam Rotation Sensors developed and built by the University of Washington have now been installed at both LHO and LLO. They are now fully incorporated in the seismic controls and have significantly reduced tilt-injection and improved duty cycle of (at least) the Hanford observatory [267]

A compact and UHV-compatible rotation sensor is the logical next-step. Such an instrument could be mounted on the BSC-ISI, potentially improving angular controls of the ISI and further reducing low-frequency differential motion between platforms. In particular, it would allow closing RX and RY control-loops on the BSC-ISI-ST2, a known cause of broadband motion. A current candidate device is the Cylindrical Rotation Sensor (CRS), a revised version of the compact BRS (cBRS) [268].

Other inertial rotation sensors are being developed, and are described in section LT-6.3. The goal now is to measure these ground tilts reliably and with low noise. Several rotational sensors have been investigated in the past [269, 270, 271, 272].

Op-6.1.2   Wind Mitigation

The largest driver of tilt on the technical slabs at the LIGO Observatories is the wind. In addition to measuring the tilt as described in section Op-6.1.1, work was undertaken in Oct 2019 to reduce the wind driven tilt of the End Stations at LHO. The tilt effects are seen in all the buildings, but are most visible at the End Stations where the End Test Masses are located. The wind causes tilting of the slab between at least 10 mHz to 1 Hz.

Based on LSC modeling efforts [273], large wind fences were installed at both Hanford end stations in Oct. 2019. Studies comparing the wind driven tilts of O3a (before the fences) and O3B (after the fences) show that the fences reduce the wind driven tilts of the building, and complement the BRS sensors [274]. This study and ongoing measurements will be used to evaluate the need for additional wind protection, and to help inform the design of future facilities.

Op-6.1.3   Pier Motion Control

The motion at the top of the HEPI piers is significantly higher than the ground motion, especially in the horizontal direction. A set of solutions have been suggested to address the problem [275]. We have recently shown that the amplification is due to motion of the

bending piers and the attachment of the payload to the pier top [276]. The FE model is being updated with new experimental results. These results shed considerable light on an old problem, and enable research on how to address the problem. Solutions to mitigate this motion amplification will be proposed and studied. Both passive (reinforcement, truss, cross beams, cables) and active solutions (feedback shaker on the chamber, active tendons) should be considered.

Op-6.1.4   Control System Enhancements for the Existing System

Advanced LIGO has an impressive array of sensors and a flexible control system. Most of the baseline Advanced LIGO control schemes use local information to control the seismic platforms and Interferometer readouts to control the interferometer lengths and angles. As system integration proceeds, studies need to be conducted to investigate optimal ways to combine all the sensor information to achieve the best interferometer performance. For example, using feedforward to directly cancel the contribution of ground motion signals which appear in the interferometer signal was demonstrated in Enhanced LIGO [277]. Studies on the coherence between various channels from the ground, up through the seismic platforms and suspension systems to the various interferometer readouts should be conducted. When coherent contributions are found, they could be used to inform the development of advanced control techniques to be layered onto the existing controls. Alternatively, the complementary filters used to combine the sensors can be designed using H_∞ synthesis in order to find the combination that provides the lowest sensor noise at each frequency [278]. Other control improvements have also been suggested such as optimally distributing the control authority between the isolation stages [279] to improve system locking and robustness, and advanced multi-input multi-output (MIMO) control approaches for better decoupling the suspension system [280].

Models of the isolation system exist, but these need to be improved to allow us to better understand the performance of the existing systems and to better design and evaluate the impact of modern control tools and new sensors.

Another improvement consists of changing the control laws in real time in response to changing environmental conditions [279, 281]. We often experience variations in the local environment arising from many difference sources such as wind at the Hanford Observatory, storms in the Gulf of Mexico which cause large microseismic motions, logging near the Livingston Observatory, and teleseismic earthquakes (those far from the Observatories). We can now accurately predict the arrival time of teleseismic waves, although the amplitude predictions are less certain [282, 283]. We have implemented an updated control scheme to better compensate for the motions [284, 285]. This system has improved the robustness of both detectors. Work is underway to evaluate and improve the performance of this system by improving the automation of the responses, improving the warning systems, understanding the current performance limits during earthquakes, and creating staged responses to small and large events.

Another question which needs to be answered is "what in particular limits the upper unity gain frequencies of the isolation control loops for the Advanced LIGO seismic isolation platforms?" A clear understanding of the practical limits could be used to inform a campaign

to modify the platforms to achieve better isolation performance, particularly in the 5-40 Hz band. For example, a numerical study has shown that a high frequency blend with a force sensor (even a virtual force sensor) may help to increase significantly the controller bandwidth of the active isolation stages,without compromising the isolation [286, 287]. This technique will be further studied on more elaborate models.

An interesting risk reduction idea would be to develop a fail-operate control system for the seismic isolation platforms. These systems use position sensors, geophones and seismometers in their control loops. While these instruments have very low failure rates, we cannot exclude the possibility that one of them could stop working during operations, thus compromising the functioning of the platform and the interferometer. It is therefore important to study methods to monitor performance of the sensors, actuators, and the mechanical plant to help mark when the behavior of a component begins to degrade, and to identify which component is malfunctioning. A set of basic Matlab scripts have been developed to perform this task [288] but those functions are difficult to use in the observatory environment and can only be used while the interferometer is offline. A realtime estimator system could be developed to continuously compare the expected and actual performance of the system so that diagnostics could be run continuously in the background. Development of realtime state-space tools to allow this to be implemented in the LIGO realtime computers is now being pursued jointly by the Controls working and is described in section Op-8.2.6. In the event of a problem, it is also important to study "emergency control schemes" that would allow the platform to keep operating with a malfunctioning sensor. Feedforward techniques to either compensate for the loss of performance, or possibly reconstruct the lost signal are good candidates. Control schemes accounting for the failure of each type of sensors should be proposed and studied.

There is ongoing research on the controls for the Suspension system. We have recently demonstrated a technique called 'Global Damping' to reduce the sensor noise from the Suspension which couples into the Interferometer [289]. Global damping also reduces the interdependence of damping and IFO length control. This technique could be incorporated into the control system at the Observatory and studies should be done to investigate its utility for the full-scale interferometer.

We have also modeled the benefit of implementing feedforward control from the ISI table to the top stage of the suspension at frequencies near the microseism. This control will need to apply both force in the longitudinal direction and torque in the pitch DOF to generate the necessary control force for the pendulum, so the controllers must be individually tuned [290]. Implementation at the sites will allow us to ascertain the long term benefit and performance of this system.

Testing of adaptive control schemes have been done [279] to automatically adjust the trade-off between damping strength and feedthrough of sensor noise in the GW band. Tests are also planned to study damping methods of the bounce and roll modes within the monolithic section. As described above, studies of how to distribute the control authority (hierarchical control) are underway, both for control of a pendulum chain, and also for offloading pendulum control to the seismic isolation system.

Op-6.1.5   RMS motion reduction

In 2021 a low frequency workshop was held to discuss some of the ongoing challenges and R&D efforts within this area. A report can be found at [291].

Motion below 10 Hz couples to DARM through a variety of complex mechanisms. Rather than work to investigate each mechanism serially, reducing the low-frequency and RMS motion seen by ISC degrees of freedom should be a priority, with a focus on RMS velocity (to reduce scatter upconversion), peak displacement (to reduce saturations) and motion close to 10 Hz.

There are several ongoing projects that have substantially improved interferometer operations by reducing low-frequency motion. The effectiveness of the BRS system in improving duty-cycle, especially at LHO, is well documented and covered in the previous section. Applying differential controls signals during earthquakes [285] has significantly improved the probability of staying in lock by reducing motion from 30-100 mHz. The recent implementation of 'R0 tracking' at LLO has seen a large decrease in glitch rate, even with only a modest factor of a couple in the reduction of relative motion from 0.01-0.3Hz [292]. Work on modelling SRCL performance and HAM-ISI motion identified that motion from 3-4 Hz was driving the SRCL UGF up, increasing coupling to DARM at 30 Hz. A relatively simple modification of the ISI controls reduced the motion in this band significantly [293], [294].

Techniques such as 'CPS-diff' have already being implemented on-site [295], [296], [297], and there is potential for similar controls techniques, and for the use of additional sensors, eg [298]. Recent work on the residual motion of SRCL provides a useful example of how the source of low-frequency motion can be investigated [299]. Emphasis should always be placed on addressing causes of motion seen by ISC loops.

Op-6.1.6   Violin Mode Analysis

Extensive analysis of the violin modes of the monolithic suspensions, with Q's in the order of a billion, is underway. Long term tracking of their amplitude, phase and frequencies for the fundamental and higher order harmonics, together with more accurate FEA models of the actual installed suspensions, will contribute to the characterisation of the monolithic suspensions and long term monitoring of their state [300, 301]. This work has already proven to provide temperature sensitivity of the suspensions which has been used to associate violin modes harmonics with individual suspensions and fibres, in a non-invasive way. We are enhancing our understanding of the effects of the complex geometries of the ends of the suspensions fibres, horns and ears with violin mode phenomena such as inharmonicity, frequency spread, which are well understood, together with frequency splitting which is an area of ongoing research. Future research will include monitoring violin mode Q values over time (believed to increase) to refine our understanding of the mechanical loss mechanisms of the suspension fibres fused silica material. Also searches for non-Gaussian events on the monolithic suspension are to be carried out. This regime of research will ultimately provide tighter bounds on the contributing mechanical loss terms for characterising thermal noise of each individual installed suspension.

Op-6.1.7   Suspension Design Updates

Upgrades to specific suspension designs are being considered as potential near-term improvements for Advanced LIGO [302]. First, the current size of the beamsplitter optic (37 cm diameter) was established early in the Advanced LIGO design, and is the limiting optical aperture. Retrofitting the detector with a larger beamsplitter optic would enhance optical performance [303]. This will require design changes to the beamsplitter triple suspension itself and its supporting structure [304, 305]. A larger beamsplitter is now included in the currently proposed design for A+ as discussed in section Op-6.2.

Actuation of the beamsplitter optic is now part of the A+ design. Currently global control signals are applied to actuators at the middle mass of the beamsplitter triple suspension. Actuation directly on the optic will allow wider bandwidth operation to improve lock acquisition.

Secondly, noise in the signal recycling cavity (SRC) length coupling into the GW readout may be a greater noise source than we would like. In particular the highest vertical and roll modes (around 28 and 41 Hz) in the small and large HAM triple suspensions (HSTS and HLTS) potentially add noise in the GW band. This noise could be addressed by adding a third stage of cantilever springs at the middle masses of the HSTS and HLTSs, taking the vertical mode below 10 Hz and increasing the overall vertical isolation. Preliminary design work has begun on this possible modification [306]. However given that the HAM-ISI isolation performance is better than the design requirements, this proposed modification is not being taken further at present [307]. An alternative is the addition of passive dampers which would reduce the peaks at the highest vertical and roll modes at the expense of modest increase in thermal noise performance on the wings of the peaks. A design based on the bounce and roll dampers (BRDs) developed for the quad suspensions, discussed below, has been developed and tested on both an HSTS and an HLTS [308, 309]. They could provide a reduction in Q of a factor of about 10. At present further work on this is on hold.

Thirdly some improvements to the original design of test mass quadruple suspensions have been undertaken. Work by colleagues in the LISA area and subsequent follow-up by LSC groups has shown that enhanced gas damping in small gaps could lead to excess noise in aLIGO suspensions [310, 311, 312]. A new design of reaction mass, called the annular end reaction mass (AERM), was developed which is donut shaped to reduce the squeezed film damping associated with this small gap. [313]. These AERMs have now been installed at both observatories.

Two other developments for the quad suspensions have been implemented, associated with damping high Q modes. A non-magnetic damper for the upper intermediate mass blades to suppress the thermal excited motion at the internal modes of the blade have been installed [314]. We have also installed passive dampers, so-called BRDs (bounce and roll dampers), to reduce the size of the bounce and roll mode peaks around 10 and 13 Hz associated with compression and extension of the silica fibers between the test mass and penultimate mass. [315]. The BRDs are able to reduce the quality factor of the bounce and roll modes from 500,000 to less than 10,000, reducing the time taken for the modes to damp down from several hours to a few minutes or less. [316].

BRDs have also been developed for the beamsplitter suspensions [317] [318] and have recently

been installed at LHO and LLO. The target damped Qs for the bounce and roll modes are in the range 100 - 200. It is expected that damping these modes will lead to better plant inversion for better MICH feedback

A further addition to the quad suspensions is under development: the use of passive violin mode dampers (VMDs)([319, 320]). The violin modes of the quad suspensions (fundamental plus higher harmonics) have very high Qs (of order 10^9) which can become significantly excited by earthquakes or other disturbances. Methods to actively damp them have been developed and are in use. However the feedback loops require manual tuning and this can take time and can be challenging when the modes are close in frequency. The use of passive tuned mass dampers attached to the PUM could alleviate the situation. For example reducing the Qs down to $\sim 10^7$ would reduce decay time of excited modes to ∼hours.

Op-6.1.8   Mechanical Upconversion: Crackling Noise

Some sources of gravitational waves produce short, impulsive events in an extremely large body of data, and so characterization and reducing "background" transients of technical origin is important. Investigations of non-thermal noise originating in the fused silica fibers has been carried out with no non-thermal noise being seen at modest sensitivity (insufficient to exclude it as a significant noise source for aLIGO). Work has been done to study the noise associated with the violin modes of the silica suspensions in GEO 600 [321]. Further work has started to extend these studies by modeling and analyzing data from O1 and future engineering or science runs to put upper limits on this noise component in Advanced LIGO. Direct experiments to characterize the level of and/or put upper limits at a meaningful sensitivity level to potential non-Gaussian transient events associated with the Advanced LIGO suspension system are challenging. However new ideas for carrying out such experiments are encouraged.

One approach which is being pursued to observe impulsive releases of energy or acoustic emissions ("creak effect") is to strain the element statically while also driving the element through a large amplitude motion at low frequency below the measurement band, while interferometrically measuring the element at high sensitivity in band (above 10 Hz). By large amplitude motion we mean much larger (100∼1000 times) than the out of band motions estimated through modeling. We will drive the large amplitude low frequency motions in a common mode fashion between two identical devices under test while measuring the noise which will be uncorrelated between the two elements. Experiments of this type are underway to measure or put upper limits on noise from maraging steel cantilever blades [322, 323, 324, 325] and separately for silicate bonds.

Furthermore, these techniques can be applied to study low frequency mechanical noise in glassy metals, potential materials for use in the suspensions of future low-frequency interferometers.

Op-6.1.9   Maraging flexure robustness studies

Maraging steel is the material used for the construction of crucial passive isolation components in the ground-based detectors. In VIRGO and KAGRA the operating stresses are high

and in the region of 1-1.5 GPa. Most of the aLIGO suspension blades are stressed to around 1 GPa [326], and the aLIGO seismic system has stress levels which are roughly 50% lower. There have been occurrences of cantilever blades failing in Virgo and KAGRA. Initial studies point to hydrogen embrittlement [327] in the maraging steel which can lower the ultimate tensile stress. Furthermore, it appears that the hydrogen can migrate towards regions of highest stress. It is of interest to study the reasons of these failures to avoid further damage to both present and future suspensions.

Op-6.1.10   LLO site-wide ground motion resonance at 4.164 Hz

A site-wide ground motion resonance has been found at LLO with a frequency in the range 4.164 ± 0.002 Hz. While the current program is focused on ground motion since the start of O3b, the resonance is visible at least as far back as November 2015. The frequency is close to a known resonance in one of the cryobaffles [328] but an association with $h(t)$ glitches associated with the cryobaffle resonance has not been found for this feature. Evidence from the Corner Station BRS channels suggests that the disturbance is a Rayleigh wave moving in the x-direction [329] indicating that the disturbance may be associated with the pipeline crossing the site. Additional investigations are in progress to confirm or refute this association and to identify any other impacts of this resonance.

Op-6.2   Research and Development for LIGO A+

This work falls under section 2.3 of the LSC Program, "A+ Upgrade Project"

Funding has been secured from the National Science Foundation and the UK Science and Technology Facilities Council, with participation of the Australian Research Council for the construction of A+. A+ seeks to expand the volume of the universe observable by Advanced LIGO by factor of approximately 6.6 and 4.1, for $1.4 \, M_\odot$ neutron star binaries and $30 \, M_\odot$ binary black holes, respectively. With funding starting in late 2018, the upgrade could be complete by early 2023 and enter observations in 2024. The details of the A+ submitted design can be found in [330, 331]. The A+ baseline for suspensions includes a larger beamsplitter suspension, new compact triple suspensions for relaying the balanced homodyne signals, and the possibility of actuation changes for the beamsplitter and thinner fused silica fibres.

Op-6.2.1   Models and controls for HAM Relay Triple Suspensions (HRTS): required for A+

A new, compact triple-suspension has been designed to FDR for A+, see the UK WP3 Document tree [332]. The suspension will need a matching state-space model of the mechanics and damping filters. The damping filter design should reflect the vibration requirements of the BHD beam paths, which are somewhat more relaxed than the core-optics.

Op-6.2.2   Thinner Fused Silica Fibers

Work is currently underway in the UK to enhance the robustness and dimensional reproducibility of the fused silica fibres used in the final stage of the QUAD suspensions. The A+

proposal includes the option to install thinner fibres operating at 1.2 GPa stress to lower the vertical bounce mode to 7 Hz and increase the first violin mode to above 600 Hz. This work utilises laser stabilisation techniques which have been shown to improve the median fibre strength [333]. A programme of work has been undertaken at LIGO Hanford in 2019/2020 to upgrade the fibre pulling machine, allowing the stabilisation techniques to be utilised. The was completed in February 2020.

Op-6.2.3   Larger Beamsplitter

The original aLIGO beamsplitters are 370mm in diameter, leading to aperture losses in the range of 600 parts per million (PPM). The A+ optical budget requires much smaller beamsplitter aperture loss which will be achieved by enlarging the beamsplitters to 450 mm diameter. The increased diameter will require adaptation of vendor production tooling and of LIGO installation and metrology fixtures, in addition to a redesign of their triple suspensions. This effort, along with fabrication of the revised suspensions and production of the beamsplitter optics themselves, is currently being undertaken by UK partners.

Op-6.3   Research and Development for beyond LIGO A+

This work falls under section 2.5 of the LSC Program, "Post-A+ Technology Development"

More generally, there are also activities to develop technologies that go beyond the A+ baseline, using the same LIGO infrastructure as per A$^\sharp$. The development of these technologies require sufficient time for appropriate engineering solutions. The technologies implementations will require more substantial changes to the Suspension, Isolation, and Alignment subsystems. For example, suspensions may be replaced to take heavier test masses. In addition to the improved isolation from ground motion, improved rejection of thermal noise is also being studied, although the system will remain at room temperature. The seismic isolation systems will remain largely unchanged, but could be improved with higher performance sensors. The only adjustment would be to the pier mountings, to allow more space for proposed longer suspensions. The total mass of the QUAD suspension would remain unchanged, but the relative masses of different components would change to cater for a larger test mass (e.g. 80 kg). Some of these technologies could be installed as part of the A+ upgrade, but they are not part of the A+ project.

Op-6.3.1   Seismic Platform Interferometer: A+ and beyond

It is possible to improve the performance below 1 Hz with an auxiliary system which reduces the differential motion and tilt of the various optical tables in the detector. This type of approach has been discussed for many years, and is traditionally called a 'Suspension Point Interferometer' (SPI), i.e., an interferometric sensor which measures between the points which suspend the arm mirrors [334].

The systems under investigation are slightly different; the method involves controlling the relative motion of the optical tables, and hence an alternative name is Seismic Platform Interferometer. The relative motion of the tables for this system will need to be measured in

at least 3 degrees of freedom, namely length, pitch, and yaw. This will allow the detectors to be mounted securely to the table, and will also allow the benefits to be shared by multiple suspensions on the same table, a common situation on the HAM optical tables.

A prototype system has been demonstrated at Stanford [335, 336] using a fiber coupled 1.5 micron laser, which used a Mach Zender interferometer to measure the inter-platform length motion and an optical lever to measure differential angles. At the AEI 10m prototype, another SPI prototype is being used successfully. It is based on a set of Mach-Zender interferometers, and uses a LISA-pathfinder style phasemeter for readout [337]. The rotational degrees of freedom (DOFs) are sensed via differential wave-front sensing. The target sensitivity is 100 pm/$\sqrt{\text{Hz}}$ and 10 nrad/$\sqrt{\text{Hz}}$ at 10 mHz for displacement and rotational DOFs respectively. A third SPI prototype is being developed at the Australian National University using Digital Interferometry [338] [339]. This is a parallel extension to the work for improved local suspension sensor development (see section .

In addition to the SPI, optical levers are being investigated, which may improve the resolution of the angular DOFs.

Considerable work remains to adapt these systems for use with Advanced LIGO (e.g. stable mechanical coupling to stage 1 of the HAM-ISI or stage 0 of the BSC-ISI, reliable UHV compatible fiber coupling, control integration). In addition, were this system to be used for the 4 km arms, then considerable work would be required to achieve the necessary laser frequency stability required to realize a beneficial system.

It should be noted that improved rotational sensing described in Section Op-6.1.1 and the SPI are complementary approaches to the low-frequency noise issue. It is also important to realize that since the optical tables for Advanced LIGO are controlled in all 6 degrees of freedom, once new SPI or tilt sensors become available, they can be incorporated into the existing control system easily, because the seismic tables will not require modification.

Op-6.3.2 Hybrid Suspension Sensing

The SRCL [299] study clearly shows that improvements to the seismic systems are necessary, but it also shows we need to improve the performance of the suspensions. As the observatories improve the performance of the existing isolation platforms to match the new HAM7/ HAM8 ISIs [340], this situation will be even more critical. Under this new HAM-ISI performance, the OSEM noise is expected to exceed the undamped optic motion for all frequencies above 0.8 Hz, except at the undamped suspension modes. The implication is that any measurement in these regimes will be dominated by sensor noise. For example, for the Filter Cavity suspensions at 4 Hz we would be injecting noise that is 20 times bigger than the undamped optic motion we are attempting to control.

One possible solution to this situation is to leverage the GS-13 inertial sensors installed in the HAM-ISIs, together with our detailed dynamical model of the suspensions, plus the OSEM and actuator data to create a model-driven suspension sensor using steady-state Kalman filtering. This scheme could be deployed with the existing LIGO CDS tools, and it would require little fine-tuning to generate reproducible results.

Preliminary work [341] suggests this could be a promising path for damping the suspension

resonances. At the time of writing, the scheme is in the process of being tested in a prototype facility to demonstrate its readiness. Additional details, such as the potential advantage of inertial vs. relative damping, the eventual incorporation of measured transfer functions into the model, as well as the introduction of additional sensors into the estimator is a subject of ongoing research.

Op-6.3.3   Improved OSEMS: A+ and beyond

Op-6.3.1

The sensors for local damping of suspensions should be improved. Optical Sensor/ Electro-magnetic Motors (OSEMs) are used to provide actuation and local sensing for the Advanced LIGO suspensions. Improved sensors can increase the damping of pendulum modes without compromising the performance, but making practical, low-cost units which have better performance than the existing OSEMs is a challenge.

The April 2021 LIGO 'Low-Frequency workshop' saw presentations by several groups developing novel low-noise displacement sensors. The workshop summary and report [291] presents a table showing six possible options that employ interferometric sensors. For a summary of compact interferometers including many of the techniques employed in the LSC, see [342]. Two further options presented are 'differential OSEMs' and Rasnik.

The most mature of these options at the moment is to place HoQI sensors [343] in parallel to BOSEMs on the middle stage (M2) of the new Big-Beamsplitter-Suspension . The HoQI interferometer has been miniaturised to fit in the 'tablecloth' of the suspension [344] and integrated into CDS and demonstrated in low noise operation [345]. It is now ready to undergo LIGO vacuum compatibility testing.

Another interesting technique to study for the realisation of compact readout interferometers is Deep-Frequency Modulation interferometry [346], [347], as developed for space-mission test-mass readout, which can also provide an absolute signal for the test mass position. Aspects regarding the achievable noise levels and dynamic range have to be studied further to fully assess the potential benefits and shortcomings. A compact optical head design has recently been proposed and will be investigated experimentally [348] and a simplified readout algorithm that requires less computational resources is being tested. Further enhanced schemes using resonant optical layouts might enable to achieve sub-femtometer sensitivity.

A further pathway for interferometric sensing of local suspensions is using Digital Interferometry, with early testing underway [338] [339]. This technique measures displacement via differential phase readout of pseudo-random modulated signals at different time-of-flight delays. The development of digital interferometric coding hardware/ software compatible with LIGO site infrastructure, and fast-hardware capabilities with the aim of shorter time-of-flight separation distances, need to be explored.

UCLouvain, together with Nikhef, will further develop Rasnik [349], a 3-point alignment system already operation at CERN (e.g. 6000 systems are in the ATLAS detector), that can operate as a displacement sensor. It has now proven flat sensitivity of 7×10^{-12} m$/\sqrt{\text{Hz}}$ [350] and will be improved to below 10^{-12} m$/\sqrt{\text{Hz}}$ sensitivities. Only image blurring and the photon flux quantum fluctuation falling onto the image sensor pixels is limiting at the moment.

By replacing the used LED by a UV one, the refractive objective by a reflective one, and the pixel sensor by the one that can take in more light, the spatial resolution improves by a factor 7. Further software improvement will result in sub picometer sensitivity. Rasnik reconstructs all 6 degrees of freedom (the 2 perpendicular to the optical axis with the most precision, the other 4 roughly three orders of magnitude less precise) out of 1 single image. Therefore, no cross coupling is possible.

Op-6.3.4   Improved Seismic Sensors: A+ and beyond

Some of the technical noises in Advanced LIGO are currently more than an order of magnitude above the instrument fundamental limits at 10 Hz [351], masking many important GW events. A recent proposal [352] shows a path towards detecting gravitational waves at 10 Hz and at lower frequencies. An important component for such an upgrade is a substantially improved vibration isolation system. In the context of that work, the 6D isolation system [353] [354] is presented as a viable option, motivated by improved tilt sensing, low suspension thermal noise, and HoQI readout noise.

Improvement in seismic isolation performance can also be achieved through novel sensors with either improved sensitivity, such as inertial rotation sensors discussed above, or lower noise.

Several LSC groups are working on instruments, most commonly employing laser-interferometer readout. For use in LIGO, instrument design should consider: sensitivity to temperature gradients, suspension thermal noise, sensitivity to environmental and actuator electromagnetic fields, sensing noise, and UHV compatibility. Both horizontal and vertical instruments will be necessary for future seismic isolation upgrades.

L4C seismometers have been modified to include a compact interferometer as a sensing scheme [355], such sensors show a factor of 60 higher resolution than their non-modified counterparts at 10mHz and work is underway to further quantify their performance at higher frequencies. These sensors have not yet been tested in vacuum and will require to be placed inside a vacuum pod to pass LIGO vacuum requirements. Substantial modelling work has been conducted on evaluating these sensors on HAM-ISIs, where a factor of 70 and 10 reduction in the RMS motion of the platforms is predicted at 0.1Hz and 1Hz respectively [356].

Several improved inertial sensors are now being studied e.g. [357], [358]. The monolithic Watt's linkage with an interferometric readout [359] shows a displacement sensitivity of $8{\times}10^{-15}$m/$\sqrt{\text{Hz}}$ between 30-100 Hz and will reach $3{\times}10^{-15}$m/$\sqrt{\text{Hz}}$ between 10-100 Hz.

1D Interferometric inertial sensors are also being investigated in [360] and [361] towards improving the performance of the seismometers currently employed in Advanced LIGO such as the GS13, L4C and T240. The potential of using the interferometric inertial sensor for seismic vibration isolation has been experimentally studied, where a reduction of the transmitted motion of up to 60 dB in a frequency range from 100 mHz to 10Hz was obtained [362].

Additional technologies, such as quasi-monolithic 1D accelerometers [363], can provide additional benefits with regards to low-frequency inertial sensing. The readout of such ac-

celerometers with centimetre-scale optical resonators can be realised by combining high-dynamic range, FPGA-based frequency readout [364] with suitable, compact laser frequency references [365].

The SWG has recently launched R&D activities with regard to the development of highly compact monolithic optomechanical seismic sensors [366]. These novel instruments target sensitivities comparable to the currently used commercial seismometers, however, in much more compact and light-weight form factors and yielding straightforward compatibility with vacuum or low temperature environments. Currently, there are no inertial sensing alternatives that are readily available to operate in these conditions, which are required for future gravitational wave detectors, such as A$^\sharp$and LIGO Voyager. Performance of these instruments are at levels of $10^{-9}\mathrm{ms}^{-2}/\sqrt{Hz}$ to 10^{-10} $\mathrm{ms}^{-2}/\sqrt{Hz}$ in terms of acceleration noise floor over measurement frequencies between 10 mHz to approximately 50 Hz. Study of appropriate low loss materials allowing micro-fabrication of such devices is necessary to identify the path towards cryogenic- and vacuum-compatible optomechanical seismic sensors beyond A+.

Op-6.3.5   Tilt Sensor Development: A+ and beyond

As noted in section Op-6.1.1 there are a number of alternative approaches to tilt sensing, which are described below;

1. Suspending a horizontal seismometer is work currently being studied at MIT/Cardiff University. This approach is distinct from the others in that the seismometer is made to passively reject tilt noise, thus producing a tilt-free horizontal sensor [272].

2. A new liquid absolute tiltmeter prototype is being investigated at University of Brussels [367]. This tiltmeter will measure the absolute inclination with respect to local gravity by using a laser beam reflected at the surface of a liquid.

3. The University of Western Australia has designed and built a tilt meter coined 'A Low Frequency Rotational Accelerometer' or ALFRA. It uses a beam balance style mechanism supported by cross flexures. It is read out by a Walk-off style optical sensor and has achieved a readout sensitivity of a few $\mathrm{nrad}/\sqrt{\mathrm{Hz}}$ above 20 mHz and 0.1 $\mathrm{nrad}/\sqrt{\mathrm{Hz}}$ above 50 mHz [368]. The cross flexure design allows positioning both vertically and horizontally which enables measurements of all angular degrees of freedom. The ALFRA will be used to reduce ground tilt to translation coupling. Additionally, it is compact enough to be installed on any isolation stage to deliver in-loop error signals for all three angular degrees of freedom.

Op-6.3.6   Larger Main Optics: beyond A+

Studies are underway to explore the design of improved suspensions for the 4 main optics (the 'Test Masses') of Advanced LIGO. The SWG has created a sub-working group and mailing list (https://sympa.ligo.org/wws/info/heavy_sus) to focus activities for large optics suspension. It has been shown that by increasing the mass from 40 kg to 80 kg, and increasing length of the final suspension fiber to 120 cm, the thermal motion of the optic can

be lowered by a factor of 2 from the current design [369]. By using 160 kg test masses and 120 cm long final suspensions, the thermal noise of the suspension can be improved so that it is 3 times better than the current design. However, work needs to be done to optimize the entire suspension design [370] so that it has good overall seismic isolation. Work needs to be done to show how to fit this larger, heavier suspension onto the existing Seismic Isolation Platforms. One possibility is mount the longer suspension to the top of the final stage of the seismic isolation system, rather than the bottom, and interleave the suspension through the isolation system. A second option would be to raise the entire seismic isolation system up on its existing support structure. Since the optical table would need to move up substantially, it is not clear what the performance impact would be and it requires investigation.

Op-6.3.7 Alternative Control Approaches for Larger Suspensions: A+ and beyond

The design and installation of larger optic suspensions gives an opportunity to revisit the design of the caging, sensing, and control of the pendulum system. One alternative approach is to merge a portion of the suspension cage and the reaction chain [371]. This is a major design change, but could result in improved access and alignment and it would allow all the pendulum DOFs to be sensed and controlled. The reduced mass of the combined cage and reaction structure would allow a more massive main optic.

Op-6.3.8 Studies of the monolithic final stage: A+ and beyond

Extensive characterization (strength, dimensions, mechanical loss) of fused silica fibers as suspension elements [372, 373], produced using both oxy-hydrogen and laser-based pulling techniques [374], has been done. Welding techniques and silicate bonding techniques including characterization of associated losses [375] has been done, along with extensive exploration on the ear shape and fiber shape.

Several monolithic suspensions (4 per detector since O1) have been installed in Advanced LIGO, with the end test masses having undergone re-installation in the downtime between O2 and O3, to enable test masses with improved coatings and annular reaction masses. Integration of the suspensions into the Advanced LIGO interferometers has significantly reduced the low frequency thermal noise, to allow access to the 10 Hz to 40 Hz range of the interferometer. As the interferometer noise is improved, participation of experts will be critical to understanding the interferometer performance.

Several areas of research could yield enhancements to Advanced LIGO suspensions. Further understanding and characterizing of losses in silica fibers including investigations of non-linear thermoelastic noise and of surface losses could lead to improvements. Changes in fiber neck shape including shorter neck and thicker stock could lead to enhanced thermal noise performance. Research is also underway to further understand the role of weld loss in addition to techniques to observe and ameliorate stress in the weld regions. Furthermore, an increase in strength of the fibers could allow reduction in cross-section and in vertical bounce frequency, enhancing isolation. Investigations of the silicate bond mechanical loss and strength as a function of time and following temperature treatments are underway to reduce further the loss contribution and optimize ear design. As noted in 3.1.4, increased fiber stress can move the bounce/roll modes below 10 Hz which reduces the requirements on passive or

active damping of these modes. A test suspension has been hanging at 1 GPa for over 3 years at LIGO Hanford, and a further series of tests at stresses up to 1.5 GPa will verify the robustness of an engineered suspension. Such an upgrade can easily be incorporated into a 60 cm aLIGO QUAD system operating at higher fibre stress (to lower the vertical bounce mode out of band and increase the violin modes) such as in A+, or an upgraded longer/heavier system for beyond A+.

Suitable prototype long fibres manufactured from thicker diameter stock material have been demonstrated, and the necessary prototype upgrades to fibre pulling and characterisation equipment have been undertaken. Laser welding, which has been proven on larger test ear horns, has been tested and provisionally shown to work. The research has led to the demonstration of the first four fibre 1.2m long heavy mass (120-200kg) suspension, and this 4 fibre large mass test hang was successfully undertaken in September 2018. This suspension continues to hang successfully, 23 months after installation, with 1.2m fibres, under stress of 1-1.2GPa and suspending 140 kg. These fibres have geometries for thermoelastic noise nulling already highly developed. In addition, long term fibre stress corrosion experiments are ongoing to demonstrate and characterise the longevity of fibres supporting a higher working stress, in the stress regime of 1-5 GPa [301].

Op-6.3.9   Studies of Glassy Metals and Low Frequency Isolation: A+ and beyond

The University of Western Australia (UWA) has been developing and using Euler springs for vertical vibration isolation for decades [376]. Relatively light springs allow for high internal mode frequencies and the buckling concepts allow for compact low-frequency solutions. New developments include contouring of the blades and geometric use of the blades [377]. The former entails using glassy metal rectangles and cutting away material where it is least needed, *i.e.* in regions of low von Mises stress. The latter is simply putting the blades under some angle to optimize for low overall natural frequency and operating range. One ultimate goal would be the development of a vertical pre-isolator, much like the role the LaCoste stage in the UWA isolator currently has.

UCLouvain is further collaborating with the MIT group to investigate the use of Euler springs in the Cosmic Explorer suspension. In particular, they want to use them instead of conventional blades as the vertical suspension components for the test mass fibres, in order to move the main mode to lower frequencies as well as the blade internal modes to higher frequency.

LT-6.4   LIGO Voyager

This work falls under section 3.2 of the LSC Program, "Suspensions and Seismic Isolation", and 3.4 "Cryogenics".

The LIGO Voyager design represents a major shift in the LIGO design with adoption of cryogenic test masses [378]. Investigations of moving to cryogenic temperatures have shown that they can provide significant improvements in the thermal noise, even with test mass temperatures as high as 120 K to 130 K. The LIGO Voyager design is based on the ideas presented in the 'Blue Team' design and incorporates a 150 to 200 kg silicon optic which

is radiatively cooled to about 123 K with a cold-shield held at around 77 K. Increasing the mass of the interferometer mirrors will linearly reduce the displacement noise due to radiation pressure noise. Changing the size, mass, temperature, and material for the optic requires many changes across the detector, and especially close collaboration between the Optics Working group (see Section 5) and the Suspension and Isolation Working Group.

This design requires test masses and heat links (either to the mass or to the cooling shield) with excellent thermal and vibration properties. These are likely copper, but might also be silicon or sapphire. Any cold system will require an ultimate heat sink. Current cryocoolers, even those designed for gravitational wave detectors [379] are not free from vibration, and the heat transport properties of heat links are limited. Thus, it is essential that studies of systems with suspension elements of suitable design and dimensions to provide an efficient path for required heat conduction while still maintaining good thermal noise and mechanical isolation performance be carried out, and followed with experimental demonstrations. A possible way to reduce the requirements of the heat links is to shorten them by having flowing liquid nitrogen in pipes within the main vacuum system. Chilling the nitrogen could further reduce the requirements on these heat links.

Research on cryogenic upgrades is vital to both the Voyager concept and the potential cryogenic upgrade to 3G detectors like Cosmic Explorer (see section LT-6.5). Cryogenic operation of 3G detectors is a significant challenge which is why the research to ensure the success of these observatories is underway now.

LT-6.4.1   Experimental Demonstrations of Cooled Optics

Cooling the optics without compromising their vibration performance is a significant challenge, and experimental demonstrations are critical to the long-term engineering success of the program. These experiments are now underway [380, 381, 382, 383, 384]. It has recently been realized that the scattered light from the optic will be a significant heat load for the cryogenic shield. It is critical that we demonstrate technology capable of removing the heat from both the absorbed laser power in the optic and the scattered power from the optic which is incident on the cryoshield – while maintaining vibration levels small enough to prevent upconversion of the scattered light returning from the shield back into the interferometer beam.

Another of the challenges to implementing a cryogenic silicon suspension is extracting the required heat in a reasonable amount of time. A purely radiative cooled suspension with a 150 to 200 kg silicon test mass will require cool down periods to 120 K on the order of weeks at best to months at worst. Research is currently underway to investigate the benefits and feasibility of introducing a cool down period which incorporates aggressive cooling technology that would not be permitted during Observing Runs. Current research is focussing on the methods of convectively cooling the suspension in a dry atmosphere and contacting the suspension stages with a movable cold link [380].

Methods of maintaining room temperature detector infrastructure near the cold suspension stages should be pursued. This issue is particularly relevant for Advanced LIGO hardware that will be reused in a future cryogenic system. Notable components that might be influenced are suspension springs, electronics, and sensors and actuators.

Materials   Investigations of materials suitable for construction of elements of the isolation and suspension systems with good properties for use at cryogenic temperatures should be studied e.g. silicon carbide which has excellent stiffness to weight ratio (specific stiffness) and low thermal expansion constant and silicon, which has excellent thermal conduction properties and high specific stiffness.

Passive damping of structures at low temperatures is also an area of concern. Viton is quite lossy at room temperature, and is vacuum compatible, and so is used extensively in Advanced LIGO to help control structural vibrations above 80 Hz. Unfortunately, handbook values [385] indicate that it is not effective at cryogenic temperatures, so investigations into replacements should be undertaken.

Integrated Control of Cryogenic Suspensions   The design and installation of new optic suspensions should be accompanied by a careful design of the caging, sensing, and control of the suspension and final optic. One alternative approach to the Advanced LIGO design is to split the suspension cage into a warm and cold section and to combine the structures of the cold portion of the cage with the cryogenic shield [383].

Cooling Options   During the detector operation the test mass needs to be kept at a temperature of about 123 K. Therefore, it will be necessary to extract up to 10W of heat absorbed by the test mass from the laser beam under high vacuum conditions. This can be done by means of radiative cooling. However, the thermal emissivity of the silicon test mass and the optical coatings deposited upon its face is too small to provide the necessary rate of radiative cooling. The emissivity of a barrel of a cylindrical test mass can be increased by using a high-emissivity coating such as DLC (Diamond-Like Carbon) coating [386], Acktar Black coating [387] or the carbon nanotube NASA Goddard black coating [388]. However, any coating of the test mass introduces additional mechanical loss and additional thermal noise associated with this loss. It was found that Acktar Black coating results in up to 10% increase of the total strain noise of LIGO Voyager design [389]. Carbon nanotube black coating gives significantly lower noise level but it can be damaged under mechanical influence [390]. Choosing a promising coating with low mechanical loss and high resistance to external influences remains an important task.

LT-6.4.2   Inertial Sensing at Cryogenic Temperatures

Future ground-based gravitational wave observatories are planned to operate at cryogenic temperatures. As in Advanced LIGO, highly sensitive inertial sensors are relevant to characterize passive vibration isolation and will also enable active vibration isolation. Commercially available sensors compatible with these operating conditions would require significant sensitivity improvements to be incorporated in future observatories, and the systems currently utilized in Advanced LIGO are not compatible with low temperatures. Optomechanical accelerometers that are microfabricated in silicon-based materials are currently being investigated to develop inertial sensing systems that provide the required sensitivity and are readily compatible with low temperature operation (e.g. Arizona group).

Inspired by the room temperature monolithic interferometrically read out accelerometer

[359], a new proposal [391] aims to improve the 10^{-15} m/$\sqrt{\text{Hz}}$ sensitivity down to 0.5 Hz and 10^{-11} m/$\sqrt{\text{Hz}}$ at 10 mHz. The sensor self-noise features a fiftyfold reduction of thermal suspension noise over the previous design by increasing the mechanical Q factor by not using magnets in the actuator. Using superconducting coils and proof mass material exploits the Meissner effect, which reduces eddy current damping. Additionally, the temperature necessary to turn the mechanics material, Niobium, superconducting is < 9.2 K, which further reduces thermal noise. The penultimate mass of the Einstein Telescope main optics suspension will likely be close to liquid-Helium temperatures. This is a perfect environment to use the proposed sensor and access the unprecedented inertial sensitivity. The sensor output can be used for monitoring passive suspension seismic isolation performance and possibly low frequency control of the highest cryogenic stage in the suspension chain.

LT-6.4.3 Low noise cantilever blade springs and improved suspension thermal noise

There are a variety of techniques being explored which could improve the room temperature thermal noise of the suspensions [392]. It is possible to improve dissipation dilution by increasing suspension length or thickening fiber ends to enhance energy distribution (e.g. 5 mm stock rather than 3 mm stock).

Studies are also underway to understand how to lower the first 'bounce' mode of the test mass. Development of fused silica or silicon blade springs which could be incorporated in the final monolithic stage for improved vertical isolation compatible with lower thermal noise is an attractive option to explore for possible upgrades to Advanced LIGO and future interferometers. Sapphire is also a possible material choice. Experiments are already underway to investigate the breaking stress for such materials when used as blades. In addition to robustness tests of silicon/sapphire as a spring material, work on protective coatings, mechanical loss and thermal conductivity also need to be pursued.

Experiments are also underway to directly measure Silicon thermal noise at room and cryogenic temperatures [393].

LT-6.4.4 Silicon and Sapphire Suspensions

Silicon has attractive thermal and thermo-mechanical properties making it a strong candidate for the suspension elements in future detectors possibly operating at cryogenic temperatures to reduce thermal noise. It is also conductive which may have advantages for controlling charging effects (discussed elsewhere). The high electrical resistivity of pure silicon may cause additional mechanical losses associated with an electric field of an electro-statics actuator, which require further investigations [394]. Development and measurement of suitable suspension flexure elements, including studies of the optimum material, thermal noise properties, and the geometry and assembly of elements including methods of bonding to test masses are being pursued [369]. Analysis techniques include the use of FEA to study the various contributions to thermal noise such as surface loss and bond loss. Investigation of fabrication techniques, properties of silicon- silicon bonds such as strength and thermal conductivity and thermo-mechanical properties of silicon, for example as a function of doping, are examples of areas which can be addressed. Sapphire should also be studied as this is a potential backup/alternative material, having the benefit of low thermal noise but allowing

the use of 1064 nm transmissive optics. This is the material of choice in KAGRA.

Suspension elements are being fabricated via two methods (i) laser heated pedestal growth, and (ii) mechanical fabrication from wafers. The laser heated pedestal method is being pursued in both sapphire and silicon. With this technique surface tension is used as the "crucible", resulting in the purest fibers. It is expected that the strength and thermal conductivity of these pristine fibers should be high, and this will be tested once samples are available. Sapphire is an easier material in principle to grow as it absorbs efficiently at $10.6\mu m$, from the CO2 heating laser. Silicon undergoes a "metallic" phase transition resulting in a change in emissivity during melting, and this might prove an interesting control problem to maintain the melt temperature. Mechanical etching/machining of silicon ribbons has already been used to make short (5 cm) suspension fibers. This technique has been shown to reduce fiber strength by approximately one order of magnitude (300 MPa) compared to the pristine material (4 GPa). This is likely to be caused by a damage layer. Oxidizing/ wet etching the samples has been shown to improve the strength by a factor of 2, possibly due to healing these damaged layers.

As an alternative protective coating, diamond-like carbon (DLC) has been investigated alongside thermally-grown oxide coatings and magnetron sputtered silica coating. In addition, the effect of edge polishing the silicon flexures and argon plasma pre-deposition treatment was investigated [395]. It is likely that silicon surface quality is the dominant factor in determining both its tensile and flexural strength. However, it was shown that application of a multilayer DLC coating combined with an extended pre-deposition argon etching process can increase average tensile strength by around 80%, with some outlying data points suggesting yet greater improvement is possible. Edge polishing appears to slightly degrade the strength of silicon, likely due to creation of edge defects; however, application of a 3μ DLC multilayer coating can more than compensate for these effects, possibly due to the conformal nature of the coating process and the coating 'filling in' cracks or chips introduced by polishing. Additionally, DLC coatings on silicon were shown to provide a high level of protection from abrasion, which may facilitate easier handling / assembly of silicon suspension components, making them generally more robust. Similar coatings could also be considered for relevant silica and sapphire components. Thermal noise calculations showed that replacing the current maraging steel blades of aLIGO with DLC-coated silicon blade springs could offer a 6.4-fold reduction in vertical thermal noise at 10 Hz, with significant improvement across all frequencies above 3.5 Hz

There is currently some activities underway in both the UK and Australia to develop small scale silicon prototypes. In the UK, work is ongoing to build a small-scale 1 kg prototype silicon suspension. This work includes handling, assembly and transport of the suspension and supporting structure as well as bonding and fabrication techniques of the suspension elements. This suspension and its supporting elements are designed to operate in a cryogen-free cryostat down to 4 K. In Australia the plan is to suspend a small scale optic from a torsion fibre. Both of these activities are complimentary and a very useful first step towards understanding the challenges faced when building up suspensions from crystalline materials.

A slightly modified version of silicate bonding for the attachment of interface pieces to silicon test masses is well underway. Strength measurements at both cryogenic and room temperatures of these bonds has shown it is a viable attachment technique and investigations

are ongoing to further understand the influence of different parameters on strength like the nature and thickness of the oxide layer required. Bond loss measurements on silicon test masses are also underway, with groups from Moscow and Glasgow fabricated tuning forks from silicon ribbons, which were then silicate bonded. They have found the upper limit of the bond loss at the temperature of 123 K [396]. Further research is aimed at improving the technology of silicon ribbon fabrication and their bonding for creation of prototypes of quasi-monolithic silicon suspension.

The collaboration should also look at opportunities to operate larger prototypes at 123 K. For example, there has been some discussion about the possibility of turning the Caltech 40 m prototype into such a testbed. More recently Maastricht University is setting up a 10m cryogenic prototype, while the University of Glasgow 10m is looking at options to reconfigure its infrastructure as a cryogenic prototype.

LT-6.5   R&D for LIGO Cosmic Explorer and other 3rd Generation Instruments

This work falls under sections 3.2 and 3.8 of the LSC Program, "Suspensions and Seismic Isolation" and "Large Scale Facilities".

Sensitivity studies are now well underway to understand some of the design implications for future 3rd generation detectors. These include the Einstein Telescope Design Study [25] and the Cosmic Explorer Horizon Study [26].

The Einstein Telescope proposes a xylophone configuration, operating both low temperature and room temperature instruments in the same facility, in a triangular configuration. At an Einstein Telescope meeting in 2018, the science team also looked at the trade-offs of operating the instrument in a single 123 K configuration. The ET consortium is currently applying to have ET included in the ESFRI (European Strategy Forum on Research Infrastructures) roadmap. Site studies at two possible locations, Sardinia (Italy) and South of Limburg (north east Europe) are also underway.

The baseline concept for Cosmic Explorer [26, 397] is a 40 km L-shaped facility on the Earth's surface. The general design is based on a room temperature detector, lending on much of the R&D that has been discussed in the sections above (longer silica suspensions, larger test masses, improved isolation performance). A potential future path (well in the 2040s) the instrument can potentially switch to a cryogenic silicon detector, leveraging R&D that is currently underway for LIGO Voyager and other detector concepts (e.g. the Einstein Telescope).

In the previous sections the main technologies for dealing with the 3rd generation technologies have been identified, and below we refer to the areas which require active research. It is important to note that technologies typically take 10-15 years to reach maturity, from lab scale demonstration to an engineered solution which can be installed at a site, and thus for a >2030 timeframe this R&D must be developed now.

LT-6.5.1   Seismic Noise

As the coupling of vertical motion to the sensitive direction of the GW detector increases linearly with detector length (due to the curvature of the Earth), the GW strain resulting from a fixed vertical displacement noise level is insensitive to detector length [26]. The active seismic isolation concepts and systems developed for Advanced LIGO must be adequate to support these new suspensions, though inertial sensors and tilt sensors with lower noise will be necessary if the suspension modes were reduced to lower frequencies. The capacity of the inertial seismic isolation systems and suspension must be adequate to support any increase optic mass and care should be taken to ensure low frequency resonances of the structure do not pollute the detection band.

The implementation of beam rotation sensors, to monitor tilt and to correct the horizontal inertial sensors, will be an important ongoing development effort.

LT-6.5.2   Suspension Thermal Noise

Current research into test-mass suspensions is focused on supporting larger masses to reduce the challenges of quantum noise, and longer suspensions for reduced thermal and seismic noise both in the horizontal and vertical directions. Vertical thermal noise can be further reduced by lowering the vertical resonance frequency of the last stage of the suspension, possibly by introducing monolithic blade springs into the suspension designs. Research needs to focus on robust techniques to engineer these larger suspensions. This includes techniques to handle masses of the order 150-300 kg (see Table **??**), robustly bond and fabricate suspension fibres (both fused silica and crystalline silicon/sapphire), and build a suitable protocol for mating/installation to the inertial seismic isolation system.

LT-6.5.3   Material Characterisation

There is much effort in the collaboration devoted to measuring and characterising the thermo-mechanical properties of fused silica, sapphire and silicon. This effort needs to continue as the most robust thermal noise models require a full understanding of the suspension, including thermal conductivity, optical absorption, mechanical loss and tensile strength. This is particularly the case for the test mass optics, suspension fibres and potential spring materials which may move away from maraging steel (due to its higher loss angle of 10^{-4}).

Silicon tensile strength work is ongoing at Glasgow, investigating various surface treatments to laser cut silicon samples and look at practical, affordable and scalable techniques to remove surface damage in the hope of increasing the ultimate tensile strength. This will allow for greater flexibility in pushing the suspension violin modes frequencies out of the detection band while supporting a heavier test mass and increasing the safety factor. Thermal conductivity and thermal extraction experiments are to be conducted on the aforementioned Glasgow prototype silicon suspension which, in conjunction with thermal finite-element simulations, will lead to a better understanding of the thermal extraction capability of the bonded suspension elements.

LT-6.5.4 Cooling Strategies

There is significant work that needs to be put into techniques to cool the next generation mirror suspensions. While this is an issue that must be approached for LIGO Voyager, the larger scale of the test mass may add some additional complexity. There are ongoing activities in both the US [398] and Brazil [399] to understand the technical challenges of cooling to both liquid nitrogen and liquid helium in a seismically quite environment.

In the past years there has been significant advances in measuring the emissivity of silicon [400] [401] as a function of temperature, which is an important property to measure for estimating the cooling time of a LIGO Voyager optic.

LT-6.5.5 Environmental Noise

While there is still uncertainty about the location and fabrication strategy for a Cosmic Explorer type instrument, it is important to note that the collaboration should be working on mitigating environmental noise as a high priority. This includes the choice of seismically quiet sites, sites with low wind noise (if systems are located above ground), and low microseismic, infrasonic and anthroprogenic noise.

7 Lasers and Auxiliary Systems

The Lasers and Auxiliary Systems working group (LAWG) developed out of the Lasers working group. In addition to all types of *classical* lasers (squeezing is part of the Quantum Noise WG), this group now includes auxiliary systems which encompasses all technologies which are not part of any of the other working groups.

The following sections are organized in terms of the needs and requirements for lasers and auxiliary systems according to the road-map (section 2) It lists the identified technologies and research areas with respect to aLIGO, A+, LIGO Voyager and LIGO Cosmic Explorer and closes with research areas and R&D that is relevant to all envisioned detectors.

Op-7.1 Achieving Advanced LIGO Design Sensitivity

Op-7.1.1 Advanced LIGO PSL

This work falls under section 2.2 of the LSC Program, "LSC Detector Commissioning and Detector Improvement activities"

The original high-power oscillator developed for and installed in Advanced LIGO [402, 403] will not be used going forward (in O4 and beyond). Instead, the 2 W Nd:YAG non-planar ring-oscillator (NPRO) master will be amplified with two neoLASE neoVAN 4S-HP solid state amplifiers in series, a configuration which was developed and tested by the GEO group in Hannover (Laser Zentrum Hannover (LZH) and Max-Planck-Institut für Gravitationsphysik / Albert-Einstein-Institut AEI).

These new laser systems need to be installed and tested at both LIGO observatories in the upgrade period between O3 and O4. Continuing technical support for the PSL system will be necessary, to address problems that arise from continuous running over long times and to further monitor the long term stability and operating parameters of the laser.

Op-7.2 A+

This work falls under section 2.11 of the LSC Program, "A+ Upgrade Project"

The following section lists R&D areas that are relevant for the A+ time frame.

Op-7.2.1 PSL upgrades

The A+ design still requires the full laser power originally planned for Advanced LIGO, which means a 200 W laser source. Thus amplifier options to generate a low noise 200 W laser need to be developed for O5. Promising candidates are additional solid state amplifiers and high-power fiber amplifiers, or coherently combining outputs from either type of amplifier.

Given the lower noise goals for A+, the need to reduce the noise of the PSL and investigate noise sources will persist. Beam jitter fluctuations and amplitude fluctuation are two such noise sources that may need to be improved within the PSL.

Other tasks and goals for A+ are to provide continuing technical support for the PSL system, to address problems that arise from continuous running over long times and to further monitor the long term stability and operating parameters of the laser.

Op-7.2.2   Faraday Isolator in Squeezing Systems

Faraday isolators are required to separate the counter-propagating beam from the incoming beam. The aLIGO Faraday isolators use TGG as the Faraday material. The TGG rotates the polarization angle by an amount proportional to the length of the crystal, the Verdet constant, and to the applied magnetic field. The main issues with the Faraday isolator are beam distortion due to laser heating and subsequent thermal lensing, a reduction of the optical isolation due to depolarization and changes in the temperature dependent Verdet constant. This is further complicated by the fact that the FI is usually placed inside the vacuum chamber following the suspended input optic mode cleaner.

The power handling capabilities of the output Faraday isolator are far less critical. However, the optical losses inside the Faraday would currently limit the amount of usable squeezing. Since squeezing is one of the leading ideas to 3rd generation detectors, any improvement in the optical losses could directly improve the range of these detectors.

Figure 26 shows how the losses in the squeezed beam path are strongly affecting the amount of squeezing detectable in the interferometer and therefore the improvement in the sensitivity. With 10 dB of squeezing injected, for instance, the losses need to be less than 20% in order to be able to detect at least 6 dB of squeezing.
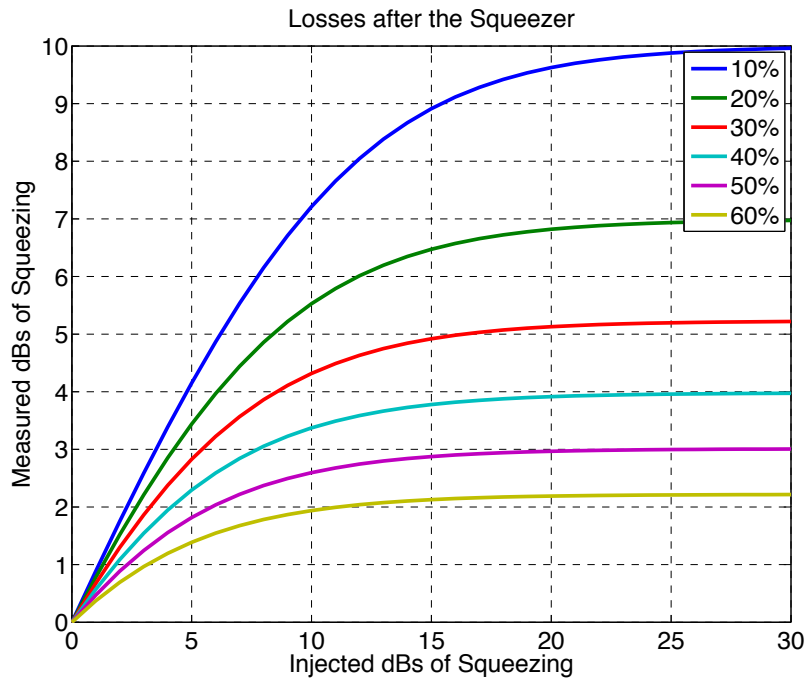

Figure 26: Measured squeezing as function of the injected squeezing for different levels of losses in the squeezed path.

In a typical layout for injecting squeezing in the interferometer the squeezed beam needs to

pass through not only the main output Faraday of the IFO (twice), but also at least one additional Faraday to isolate the interferometer from the squeezer and mitigate noise from back scattered light. The losses of the new Advanced LIGO Faraday have been measured to be $\sim 4\%$. Similar measurements in initial LIGO Faradays give losses of 4 - 6%. With the current losses the Faradays themselves will account for about 15% of the losses in the squeezed path. In order to maximize the benefit from the injection of squeezed light, it is important to reduce the losses of a single Faraday to 1 - 2%.

For the main dark port Faraday, it is also important to reduce the amount of light which leaks into the squeezed beam path, as this is a source of noise once it is back scattered back into the IFO from the squeezer source. In the new Advanced LIGO Faraday about 0.5% of the light which passes through the Faraday is reflected by the thin film polarizer. By improving the mechanical design of the Faraday one can hope to reduce this percentage down to $\sim 0.01\%$.

Op-7.2.3   Laser Stabilization

Power stabilization will probably be the most demanding laser stabilization task in future gravitational wave detectors. Technical power noise on the laser can couple via many paths into the gravitational wave channel. Advanced LIGO requires a relative intensity noise (RIN) of around $10^{-9}/\sqrt{\mathrm{Hz}}$ in the interferometer input beam. The accurate sensing of the needed 500 mW laser power at that location is difficult and the signal is still contaminated by pointing, polarization, and potentially even frequency noise. Ongoing research is needed to understand these couplings and reach the required stabilities.

Op-7.3   Post A+ planning / LIGO Voyager

This work falls under sections 2.5 "Post-A+ planning and research", and also 3.4 "Cryogenics", 3.5 "Lasers and Squeezers", and 3.6 "Auxiliary Systems" of the LSC Program.

The Post A+ and LIGO Voyager design mitigates limiting noises of aLIGO by allowing moderate changes to the LIGO detectors without affecting the vacuum envelop but with possibly including cryogenic temperatures of 120 K. The following section describes the planning and needed R&D related to those improvements.

Op-7.3.1   PSL System

The road map for the general description in section 2. The designs call for laser wavelengths of 1.5 μm and longer to be compatible with silicon optics at cryogenic temperatures. As the final sensitivity depends on the power inside the interferometer the input power can be traded against power recycling gain without affecting the fundamental noise limits. However, the power recycling gain is limited by the optical losses inside the arm cavities as well as the contrast defect at the beam splitter. Typical power levels for the lasers required for LIGO Voyager are envisioned to be about 200 W.

High power concepts: 1550-1650 nm Erbium doped fiber lasers and Er:YAG lasers emit between 1550 and 1650 nm where the absorption in silicon is expected to be very low. Commercially available erbium fiber systems include a master laser and a fiber amplifier and achieve output powers of 10 W in single mode, single frequency operation and higher power levels are expected in the near future.

The GEO group achieved more than 100 W of output power by an off-resonant pumping scheme. The Adelaide group has completed a high-resolution spectroscopic investigation of Er:YAG at cryogenic temperatures, where it is a 4-level gain medium, and demonstrated a 5 W cryogenic Er:YAG laser at 1617 nm. Power scalability as well as the free running noise performance and the robustness of this system needs to be investigated. Further stabilization concepts for these kind of amplifier systems have to be developed.

High power concepts - 2 μm and longer Another interesting region for gravitational wave detector wavelengths, especially to avoid 2-photon interaction in silicon, is 2 μm or slightly longer. Ho:YAG and Tm:YAG lasers, either as systems with discrete crystals or fiber based [404], are possible candidates but more research is needed to find the most suitable laser medium and to demonstrate the feasibility of a 2 μm PSL. Development is also needed for a low-noise, single-frequency source at 2 μm to serve as a master oscillator [405]. In all cases power scalability as well as the free running noise performance and the robustness of these systems needs to be investigated.

Narrowband frequency concepts An alternate method for realizing narrow line seed lasers in the 1500-2100 nm wavelength range is the fiber distributed Bragg reflector (DBR) configuration. Matched fiber Bragg gratings (FBGs) fabricated with conventional phase masks or with direct femtosecond laser inscription is spliced with short piece of heavily doped fiber (ytterbium/erbium/thulium or holmium based on the required emission wavelength) in between to form a Fabry Perot cavity operating in the single longitudinal mode [406, 407, 408]. Writing the gratings directly onto the doped fiber would be an option to minimise the cavity loss. Careful control of the length of the fiber (mounted on the piezoelectric transducers) helps achieve wavelength tunability [409]. Linewidth control may be further possible with a feedforward technique [410]. These single longitudinal mode lasers are suitable for further fiber amplification [406].

Additional Requirements Many different applications drive the laser development worldwide and it appears that nearly every year improved laser systems become commercially available. However, there is currently no application which has similar stringent requirements on the temporal and spatial stability as gravitational wave detectors. Hence a laser development programs for 3$^{\text{rd}}$ generation detectors is needed to design and build a reliable laser with sufficiently low free-running noise, an appropriate spatial beam profile and good controllability. Programs that have been initiated are going to require continued support.

Op-7.3.2 Photodiodes

Advanced LIGO is currently using four in-vacuum photodiodes in parallel to measure the required 500 mW of light for intensity stabilization of the input beam [411]. This is a sub-optimal arrangement for several reasons including reliability and alignment issues. To get a quantum limited measurement of the power fluctuation of 500 mW of light, new photodetectors need to be developed with sufficient power handling capability, spatial uniformity and quantum efficiency. First experiments showed that back-illuminated InGaAs diodes show promising features. However neither the spatial uniformity nor a sufficiently high quantum efficiency has been demonstrated so far. Furthermore current power stabilization experiments seem to be limited by 1/f electronic noise in photodiodes. The origin of this noise needs to be better understood and either the noise source has to be reduced or easily applicable selection criteria need to be found to get the best devices from the available vendors.

High efficiency photodiodes are especially important when using squeezed light, as described in section Op-4.3.1 of the quantum noise research. Further R&D in close collaboration between the material and device experts, electrical engineers and groups that can test the photodiodes is needed to develop better photodiodes for LIGO Voyager and later generation gravitational wave detectors, especially with respect to the longer 1.5 μm to 2 μm wavelength range where quantum efficiency is currently inferior to 1 μm systems.

Op-7.3.3 Electro-Optic Modulators

Length and alignment sensing schemes rely heavily on the generation of optical sidebands which co-propagate with the carrier field into the interferometer. These sidebands are currently generated by RTP-based electro-optic modulators which withstand several 100 W of continuous laser power without degrading the beam profile. LIGO Voyager and LIGO Cosmic Explorer detectors are likely to work at different wavelengths and/or at higher power levels for which suitable electro-optic modulators are not yet available or have not been tested. The main problems encountered in high power applications are photo refractive damage and variations in optical path length across the beam profile caused by the residual absorption of the laser beam.

Photo refractive damage has a fairly well defined threshold in specific nonlinear crystals and can be increased by doping the crystal. The most promising family of crystals in the near infrared region are crystals belonging to the MTiOXO$_4$-family such as RTP; M is an alkaline metal such as K, Rb, or Cs, and X is either P or As. These crystals have fairly large electro-optical coefficients, good thermal properties, and, in principle, very low optical absorption coefficients between 1 and 2 μm laser wavelength. Optical absorption in the MTiOXO$_4$-family increases at lower wavelength and potentially limits the laser power to a 10's of watts for visible lasers.

β-barium borate (BBO) and its derivatives are often used in the visible and near-UV region of the spectrum. BBO is uniaxial and has a very high damage threshold. Values larger than 3 kW/cm^2 for cw-light have been quoted by multiple vendors. It's negative thermo-optical coefficient prevents self-focusing. However, the electro-optical coefficient is low compared to other electro-optical crystals and BBO appears to be of limited value unless the laser wavelengths is reduced to well below 500 nm.

Magnesium-oxide doped lithium niobate ($MgO:LiNbO_3$) might be a potential alternative for IR lasers. The doping increases the photo refractive damage threshold significantly [412] and the crystal has a ~10% larger modulation coefficient than RTP. However, going to laser powers beyond 1 kW and laser wavelength below 1 um requires significant testing of electro-optical materials to ensure that electro-optical modulators will be available for LIGO Voyager and future detector generations.

Op-7.3.4 Faraday Isolators

The aLIGO Faraday isolator uses two TGG crystals, a quartz rotator, and a waveplate to compensate the depolarization inside the TGG crystals. It is optimized to suppress thermal effects that would distort the laser mode. Scaling this to kW-class power levels requires further reductions in the optical absorption in TGG while the large number of components already increases the number of ghost beams significantly. Other options are to increase the polarization rotation through the use of stronger magnetic fields, by cooling the crystal, or by finding materials that have a larger Verdet constant.

One recent approach used to increase the magneto-optical effect is doping TGG single crystals and ceramics, or other garnets with rare-earth elements such as Ce^{3+}, Dy^{3+}, Tb^{3+}, and Pr^{3+}. This method improves the Verdet constant by 20%-70%, keeping absorption levels similar to TGG single crystals. Terbium-doped Y_2O_3 ceramics investigated in the 380-1750 nm range showed more than 3 times higher Verdet constant than TGG crystals and ceramics. High power studies are needed for a complete evaluation of these materials.

Increased absorption in TGG will likely prevent the use at wavelength longer than 1.3 μm and in addition make the crystals very long. At 2 μm the crystals would need to be twice as long as the 12 mm crystals used in aLIGO, but the telecommunication sector developed ferromagnetic rare earth iron garnets (RIGs) such as yttrium iron garnet (YIG) and more recently $\{BiRE\}_3(FeGaAl)_5O_{12}$ to rotate the polarization. Unlike paramagnetic Faraday materials, these ferromagnetic materials can be magnetized such that they don't require any external magnetic field. These materials are typically grown in sub-mm thick films on lattice-matched substrates such as GGG for 45 deg rotation. However, the absorption is still in the 1-10 ppm/cm range at interesting wavelengths which prohibits high power laser operation. At shorter wavelength, optical absorption increases in all materials pronouncing thermal effects.

In general, new materials need to be found and investigated to achieve strong Faraday rotation while minimizing absorption and the resulting thermal effects. Candidates are potassium dihydrogen phosphate (KDP) and its isomorphs. Various other potential alternatives are EuF_2 crystals and Dy_2O_3 ceramics, or Ce:YIG films grown on GGG substrates with different crystallographic orientations. Another alternative are thin ferromagnetic films such as iron or cobalt. They show a strong Faraday effect in the visible and near infrared, but currently the strong optical absorption of these type of materials needs further optimization. This list is not exhaustive and no candidate materials should be excluded if they show promise to satisfy the requirements as shown above.

Strong thermal gradients also have a negative effect on the performance of Faraday isolators. Creating an optical contact between a strongly absorbing magneto-optic material and a low

absorbing material, for example TGG and sapphire, in a sandwich structure could allow to reduce thermally induced effects.

A targeted research program to study these materials at higher power levels at all interesting wavelength (1.06 μm, 1.5 μm and 2 μm), is required to develop Faraday isolators for the next generation of gravitational wave detectors.

Op-7.3.5   Cryogenics

It has long been known that cryogenically cooled test masses can have much improved material parameters which lead to significant reductions in thermal noise. However, operating at cryogenic temperatures presents multiple new challenges which need to be addressed. The most pressing is to find ways to cool the temperature, to isolate the mirrors from their hot surroundings and to constantly extract the deposited laser heat without short-circuiting the suspension and seismic isolation system. Detailed thermal models have to be developed and tested to maximize radiative and conductive cooling paths.

An additional challenge is the strong possibility of contamination through condensation on the surfaces. Methods will need to be developed to (i) mitigate the level of contamination in cryogenic mirrors, (ii) quantify the magnitude and type of contaminants, and (iii) if necessary, clean contaminated mirrors in situ. One idea which should be pursued is to use femtosecond laser spectroscopy to identify the contaminant and potentially also to remove it.

Cryogenics: Radiative Cooling   Operation at cryogenic temperatures poses formidable challenges including heat extraction from the cooled test masses, required both under steady state operation and for cooling from room temperature in a reasonable time. The system needs to work without adding noise or short-circuiting the mechanical isolation. In the steady state, the circulating power may be in the range 0.5 to 3 MW, and with anticipated coating losses of 0.5 to 1 ppm, power loss in the arm coatings is of order 0.3 to 3 W per optic. For cooling, a reasonable estimate is between 2 and 100 W of heat conduction from the test masses to the cold environment.

Studies are underway of a novel method of heat removal: near-field radiative coupling between two objects: one hot and one cold. The basic idea is that many thermal fluctuations in the hot object do not couple to radiation; instead, they produce evanescent fields outside the object. If a cold object with appropriate properties is introduced into this evanescent field region, energy is transferred, cooling the hot object. This approach is potentially capable of removing more than 200 W from a test mass. The heat transfer can be greatly enhanced using a small gap but this is accompanied by force coupling and this effect needs to be taken into account. Room-temperature experiments to explore this method of heat transfer have observed and are characterizing in detail the heat transfer in the near-field regime. Cryogenic experiments are planned, as are measurements to determine the effects of coatings on the heat transfer, and to attempt to optimize the coatings for maximum transfer with spacing around 0.1-1 μm.

LT-7.4 LIGO Cosmic Explorer

This work falls under sections 3.5, and 3.6 of the LSC Program, "Lasers and Squeezers" and "Auxiliary Systems"

The current LIGO facilities, while extraordinary in their capabilities, present significant limitations to potential long term improvement. The Ultimate stage will allow for a complete redesign and major expansion of the detector. The following topics are future developments within this project phase.

LT-7.4.1 PSL for LIGO Cosmic Explorer

Most ideas regarding the LIGO Cosmic Explorer detectors target the low frequency performance where the sensitivity is limited by radiation pressure noise, thermal noise and Newtonian noise and not by shot noise or the available laser power. The laser needs for silicon test masses for these detectors can probably be met by LIGO Voyager PSLs assuming that the lasers will be developed in time, except for an increase in output power.

High power concepts: 1550 nm to 2 μm and longer The main difference between Voyager and Cosmic Explorer is that the typical power levels for the lasers required will go up from several 100 W up to 1 kW. To further explore the high frequency region of the GW-spectrum, further increases of the laser power will be required and the laser concepts as outline in the Voyager section will need to brought to the 1 kW level.

If new test mass materials other than silicon become available changes towards a shorter wavelength might be advantageous. Shorter wavelengths generally require thinner coating layers which could reduce coating thermal noise; however, it should be kept in mind that shorter wavelength also generate smaller beam sizes for identical cavity g-parameters. The general scaling of coating thermal noise with thickness of coating layers and beamsize is in first order independent of the wavelength (for identical cavity g-parameters). The most obvious way to reduce the wavelength is via frequency doubling a powerful 1064 or 1030 nm laser. Other concepts could be viable to achieve the desired power levels, for example coherent beam combination, but technical realization and beam properties, and laser stability will need to be investigated..

High power concepts - 1030-1064 nm In the future, if kilowatt class lasers become necessary for frequency doubling, Yb doped YAG, which operates at 1030 nm, could replace the Nd system because of its higher efficiency, lower quantum defect, better thermal management and potentially longer-lived laser diode pumps. Its main disadvantages are that it is a quasi-3-level system at room temperature and thus more sensitive to increased temperatures within the gain medium, and that it has a much lower pump absorption coefficient. However, at cryogenic temperatures, the quasi-3-level system turns into an efficient 4 level system. The Adelaide group demonstrated already 200 W, with diffraction limited beam quality for all power levels, requiring no thermal compensation, at 1030 nm from a cryogenic Yb:YAG laser using a single zig-zag slab [413]. There is a substantial commercial interest

driving the development of both Yb solid state and fiber lasers, amplifiers and their pump diodes for very high power applications.

Another option is the coherent beam combination of two or more 200W class lasers. Either solid state high power systems or Yb:doped fiber amplifiers with identical or independent seed laser sources are potential candidates to generate the 200 W output power. The characterization and stabilization of coherently combined systems at intermediate and high power levels should be investigated. The beam combination option is a possibility for all wavelengths that are mentioned in this section.

High power concepts - spatial mode filtering and adaptive optics   To convert distorted laser beam profiles into the target eigenmode of the interferometer either static or dynamic wave front correction systems or passive filtering will be required. Advanced LIGO uses optical cavities (the mode cleaner) to filter the fundamental 00-mode and suppress all higher order modes. This technology is slowly reaching its limits as the high power build up inside these optical cavities starts to distort the filter cavities themselves. Other spatial modes such as Laguerre Gauss 33-modes or Mesa beams require modified filter cavities which are resonant only for these specific spatial modes.

For higher power levels intrinsic problems are expected with the filtering method and hence dynamic adaptive beam correction methods should be designed. These could be based on well known Shack-Hartmann detectors and adaptive optic techniques currently employed in astronomical telescopes. These techniques have also significant commercial potential for many other high power laser applications.

Op-7.5   General R&D

This work falls under sections 2.2, and 2.11 of the LSC Program, "LSC Detector Commissioning and Detector Improvement activities" and "A+ Upgrade Project"

The R&D projects listed in the following section require constant improvements and are relevant to all envisioned detector generations, from A+ to LIGO Cosmic Explorer.

Op-7.5.1   Auxiliary Lasers

Auxiliary lasers serve several functions in interferometric gravitational wave detectors.

- CO_2 lasers at 10 μm are used to write a heating pattern into the compensation plate placed next to the ITM.

- Diode lasers at various wavelengths are used together with Hartmann sensors to sense thermal deformations in the test masses and the compensation plate.

- Frequency doubled Nd:YAG lasers are injected at the end stations for lock acquisition of interferometer length degrees of freedom.

- Nd:YLF, 1047 nm lasers coupled with acousto-optical modulators and custom designed photo-detector systems are used in concert as the primary absolute reference system, the so-called "photon calibrator" (Pcal) system [414].

The status and planned R&D on these laser types is described as part of the subsystems they are used in: CO_2 lasers as part of the TCS actuation in Section Op-7.5.2, diode lasers for Hartmann sensors as part of TCS sensing and control in the AIC working group, frequency doubled Nd:YAG lasers as a part of the lock acquisition in Section Op-8.1.1, and Nd:YLF 1047 nm lasers provide the basis on which the calibration of the interferometers is formed, discussed in Section Op-7.5.5 (and in the greater context of the calibration working group in Section Op-8.1.3).

Op-7.5.2   Thermal Correction System

The goal of the Thermal Correction System is to optimize the spatial mode inside the interferometer. This spatial mode can be degraded by imperfections in the mirrors caused by radii of curvature or surface figure errors as well as non-homogeneous heating of the optics by the science beam. Untreated, this will reduce the mode matching between the two arm cavities and the recycling cavities and change the beam size inside the interferometer. Advanced LIGO uses ring heaters to optimize the radii of curvatures of the ITMs and ETMs and CO_2 lasers to compensate the thermal lens in the ITM substrate by acting on the compensation plate [415].

Ring Heater   The ring heater has to meet several requirements. It has to generate a homogeneous heating profile with minimal heating of the suspension structure. Its location very close to the test masses requires that it has to meet very stringent cleanliness requirements. Advanced LIGO is currently using a ringheater which uses nichrome wire wound around a bent glass rod, an alternative design developed by the UF group sandwiches the nichrome wire between two alumina coated aluminum surfaces [416]. Both heaters are embedded inside a gold coated thermal shield to maximize the heat transferred to the mirror and minimize the radiative heat transfer into the suspension.

The heat loss at the end points due to thermal conductivity generates an asymmetric heating profile which will also distort the mirror surface and the thermal lens inside the substrate. At higher heating powers, these asymmetries will start to reduce the optical build-up inside the arm cavities and increase the contrast defect at the beam splitter. The development of ring heaters which produce more symmetric heating profiles could already be crucial for high power operation in Advanced LIGO.

One way to reduce the heating by the ringheater or even eliminate it is to coat the barrel of the optic with a thin layer (a few microns) or an IR reflecting metal such as gold [415]. This would reduce the radial heat flow and homogenize the temperature distribution inside the substrate. Adding a gold barrel coating to the optics would have implication for other aspects of the design, notably thermal noise, charge mitigation, and parametric instabilities. Measurements of the mechanical loss of a thin gold coating indicate that the gold coating can be applied without adversely affecting thermal noise. Gold coating applied to the barrel for thermal

compensation purposes might not reduce the optics modal Q's enough to cause significant improvement in parametric instability performance. Tests of a gold coatings interaction with possible charge mitigation schemes, including UV, should be explored. Results of these tests might require follow-ups with other materials and/or coating methods or with additional modeling. This technique may be ready for use in a 3rd generation detector.

CO$_2$ laser   Power fluctuations of the CO$_2$ laser are one of the dominant noise sources associated with the TCS. Commercially available CO$_2$ lasers do not meet the stringent requirements on power stability for Advanced LIGO during high power operation (125 W input power in the science beam) and R&D has started to develop better CO$_2$ lasers for Advanced LIGO.

A scanning (or, more generally, a directed-beam) thermal compensation system that can vary the compensation profile in real time without injecting noise into the signal band would be very valuable to correct non-radial symmetric beam distortions. Such a system could already be important for high power operation in 3rd generation detectors. This will require research on carbon dioxide or other potential heating lasers, to reduce noise and possibly boost power, and potentially on measurement and control issues. In addition, by moving to shorter wavelengths it might be possible to develop MEMS or other technology based spatial light modulators to allow a programmable heating beam profile.

Op-7.5.3   Active Wavefront Control

Several technologies, notably squeezing, assume improved mode-matching (see table of losses in 9) is available for these systems. The limits assumed in these scenarios are beyond static polishing and placement uncertainties for mode-matching optics. Therefore, active wavefront control (AWC) is required to maximize mode-overlap between cavities. This control is in addition to the Thermal Correction System. Although there is some overlap between the two systems, TCS is predominantly needed for correcting dynamic changes wavefront errors and AWC is used for correcting static wavefront errors. Future adaptive control research is needed to address:

- A possible redesign of SRC/PRC configuration to improve mode-matching actuator orthogonality.

- Adaptive mode-matching on output optics addressing thermally adaptive optics for low spatial frequency curvature errors (astigmatism and defocus) and higher spatial frequency (point sources and polishing errors). Extreme mode-matching targets of larger than 99.5% may require correction of polishing errors beyond spherical correction.

- Other adaptive optic techniques capable of macroscopic motion of the order of tens of centimeters within the output chain.

- Improved sensing techniques for SRC/IFO, SRC/OMC and FC/IFO mode-matching.

- General adaptive optics for in vacuum use. A generic, low noise, high range small adaptive optic element, either mechanical or thermal based, is needed.

Op-7.5.4 Beam Shaping

Mirror thermal noise is one of the fundamental factors limiting the sensitivity of gravitational wave detectors. A Gaussian beam profile is not the best shape to average over thermal fluctuations and different, carefully chosen shapes allow for sensitivity improvements. Non-spherical mirrors, shaped to support flat intensity mesa profile beams, have been designed and fabricated using specialized coating techniques. These mirrors are being tested on a dedicated interferometer to assess ease of mode-matching and locking. Recent efforts have shown that the tilt sensitivity of the fundamental mesa mode agrees with expectations. It is possible to extend this study, producing useful alignment correction signals via the wavefront sensing technique. The Sidles-Sigg tilt instabilities must also be examined. In addition, continued modeling needs to examine how thermal effects alter the mode profile in a detector arm cavity and help develop thermal compensation strategies. One option involves depositing a static thermal compensation profile to mitigate these effects.

Modeling and experimental work is being carried out on Laguerre-Gauss and other optical modes that show promise for reducing thermal noise. Laguerre-Gauss modes may avoid some of the instability issues that cause concern with mesa beams. There are, however, questions about the strict requirements on the figure and polish of the optics necessary for these higher order modes. There has been modeling of the effects of different beam shapes on parametric instabilities. Further modeling and experimental testing will be necessary to truly evaluate the potential and limitations of these beam shapes.

Op-7.5.5 Photon Calibrator

The following is a list of activities that serve to *improve* the existing design and integration with the global network of photon calibrator systems. For discussion and description of the *maintenance* of the existing Pcal systems across the global detector network, see the Operations White Paper [23]. For discussion of the how the R&D of the Pcal system fits in the greater context of the calibration working group, see Section Op-8.1.3.

- Explore options and proceed with update of Pcal transmitter modules, including lasers and maybe AOMs.

- Increase frequency of primary power standard calibrations with NIST

- Fabricate updated transimpedance amplifiers with integrated temperature sensors; implement and characterize laser power transfer standards

- Characterize the temperature dependencies of the laser power transfer standards

- Test proposed novel method for assessing Pcal center of force offset on detectors test masses to reduce uncertainty due to unintended rotation

- Assess results of bilateral comparison between NIST and PTB and consider scheduling additional comparisons.

We expect the above mentioned upgrades to (and continued maintenance of) the Pcal systems will allow them to meet the requirements of the LIGO detectors through O4 and O5 (i.e.

the A+ era). There is no planned efforts at this time to explore the design of a Pcal system that would meet the needs of a Voyager or Cosmic Explorer-like detector.

8 Control Systems

This work falls under sections 2.2 and 2.7 of the LSC Program*, "Detector Commissioning and Detector Improvement activities" and "Detector Calibration and Data Timing"*

The Control Systems Working Group (CSWG) covers fundamental and applied research in control systems as it relates to GW interferometers, including:

- system identification
- modeling
- synthesis
- analysis
- optimization
- performance assessment
- hardware and software implementation

The role of the CSWG is unique within the LSC's instrument science working groups. The use of control systems is pervasive within, and enabling to, the work of many of the other instrument science working groups. In addition to supporting its own fundamental research in cutting-edge control system techniques, the CSWG should support and enable the research of other LSC WGs. In particular, as next generation detectors are researched, control system considerations should be included at the very beginning as an integral aspect of the system.

An important task for the CSWG is to enable as much as possible contributions from all members of the LSC. To achieve this goal, the CSWG will organize tutorial session on topics related both to the theory and practice of control systems, and to the actual implementation in LIGO. Those tutorials will be recorded and made available for reference.

The following sections describe the control system challenges in implementing the roadmap, and then R&D focus areas for the group which are relevant to all of the anticipated detectors. Although the discussion concentrates on Interferometer sensing and control, there are similar control challenges in many of the other interferometer subsystems as well, such as our principal "actuator" systems - SEI, SUS and TCS.

Op-8.1 Interferometer Sensing and Control (ISC)

The Interferometer Sensing and Control (ISC) consists of four areas (LSC, ASC, CAL, and CDS). The dominant issue of ISC is to maintain IFO stability while not introducing control noise. The following is an overview of the four subsystems:

Length Sensing and Control (LSC): Length sensing and control refers to management of resonance conditions of the fundamental degrees of freedom in the suspended interferometer while maintaining a high sensitivity to gravitational waves. The longitudinal distances between the mirrors (or the lengths of resonant cavities) are controlled to minimize length changes.

Alignment Sensing and Control (ASC): The ASC primarily controls the 1st-order optical modes in the interferometer by adjusting the angular orientation of the mirrors. In addition to the LSC, this system is also necessary to maintain interferometer sensitivity. Although the angular motion of the mirrors are locally stabilized by the vibration isolation and the suspension systems, the global control is necessary in order to realize stable interferometer operation.

Calibration (CAL): The calibration of the detectors' LSC degree of freedom most sensitive to gravitational waves, the differential arm length (DARM), is the essential interface between the instrument and the consumers of its astrophysical output. This precision engineering involves detailed, highly precise, and accurate characterization of each component of the loop from aspects as complex as the detector's opto-mechanical response to differential arm length changes, down to the simplest electronics inside anti-aliasing chasses. This must be done over the entire, many kHz, frequency band of the detector and its validity must be maintained over $\mathcal{O}(\sim 1 \ yr)$ duration observation runs. At its core, this requires development of an extremely stable, precise, and accurate set of references from which the calibration is derived.

With these references, the detector's response to gravitational waves is characterized and monitored, informing models which produce a data stream which estimates the DARM displacement of the detector free of controls, divided by the average length of the arms, a.k.a. strain. The production and maintenance of the response model, the strain data, estimates of the systematic error and uncertainty in that data, and all of the surrounding infrastructure are discussed in the LVK Operations White Paper [?] (one may also find VIRGO instrument science goals in this paper). Addressing the impact of systematic error and uncertainty in the strain data is a research area currently under rapid development and discussed in the LVK Observational Science White Paper [?].

Controls and Data Systems (CDS) The computational system involved in sensor data receiving and control distribution is an critical part of any modern control system. In this context, subjects covered below refer to research and development that includes improving the data acquisition system for specialized needs and advanced control topologies as well as taking full advantage of the existing capabilities of the digital infrastructure.

Op-8.1.1 Length Sensing and Control (LSC)

The Advanced LIGO interferometers consist of five coupled cavities that must resonate simultaneously to reach the operating point. The LSC receives the length sensing signals from the photodiodes and sends commands to the actuators on the suspensions so that those five degrees of freedom stay at the operating point. Between the sensing and the actuation, the signals are processed by servo filters so that stable feedback control of each loop is established. The LSC system for the Voyager and Cosmic Explorer detectors will also rest on the above technologies.

The aLIGO LSC employs a combination of RF heterodyne detection and DC readout [417]. This RF sensing scheme comprises the Pound-Drever-Hall technique, Schnupp modulation,

and third harmonic demodulation technique [418] as a baseline design. The DC readout scheme provides sensing of the GW signal with shot noise performance superior to that of RF detection, along with more immunity to laser noises when combined with an Output Mode Cleaner (OMC). DC readout also clears the way for the use of squeezed light injection to reduce quantum noise.

These sensing techniques have been independently demonstrated by the Enhanced LIGO [37, 419] and GEO600 [93, 420] interferometers, and other prototype interferometers [421, 422, 423]. The task for the aLIGO interferometer commissioning team is to integrate these well known techniques and find any hidden issues. As a scale model of the full aLIGO interferometers, the Caltech 40m prototype plays an important role in this effort by giving us a first look at potential problems.

An example of an upcoming ISC challenge is the filter cavity which will be required for filtering squeezed light before it enters the interferometer. This cavity will require length control via a carrier frequency which is not the same as the carrier light circulating in the interferometer (to avoid polluting the squeezed state with scattered photons). The filter cavity will also present an alignment control problem similar to the input mode-cleaner. Similarly, the phase of squeezed light source itself must be controlled with respect to the interferometer.

For LIGO Cosmic Explorer, the idea of the Suspension Point Interferometer [334] may also be investigated as it could be a practical solution to mitigate the vibrational noise caused by the heat link of the cryogenic cooling system.

Lock acquisition   A new feature of the aLIGO LSC is the use of independent laser sources in the Arm Length Stabilization (ALS) system [424, 425, 426]. This system enable us to lock the long arm cavities in a deterministic way with the guidance of auxiliary beams injected from the end mirrors.

Advanced LIGO achieves lock using two single arm interferometers to control the arm cavity mirrors independently of the Michelson and signal recycling cavities, known as Arm Length Stabilization (ALS). The arm cavity locking uses frequency-doubled lasers at each end station, with each laser frequency referenced to the master laser in the vertex.

It may be possible to significantly improve the robustness of the ALS system by injecting the frequency doubled laser beams from the vertex.

Machine Learning (ML) and Reinforcement Learning (RL) techniques are under investigation for the lock acquisition of the corner interferometer. A prototype is under construction at Caltech to test new ML and RL ideas for lock acquisition [427].

Op-8.1.2   Alignment Sensing and Control (ASC)

Sidles-Sigg instability   High circulating power in a kilometer-scale Fabry-Perot cavity can lead to an alignment instability in which a radiation pressure driven anti-spring overcomes the mechanical restoring force of the cavity's suspended optics (Sidles-Sigg instability) [428]. The Advanced LIGO interferometers were designed to avoid instability, but this is still a

potential threat for the Voyager/Cosmic Explorer detectors. Essentially, higher power leads to greater instability which can only be suppressed with high-bandwidth active alignment control. As the bandwidth of the ASC loops approaches the gravitational-wave band of the detector, noise from the alignment control signals is introduced into the detection band and can spoil the interferometer sensitivity. The investigations to mitigate this instability should be carried out in both practical and innovative aspects: reduction of the control noise level of the ASC system and exploration of any new scheme to directly suppress the instability (e.g., optical trapping of alignment degrees of freedom).

Towards ASC of Voyager/Cosmic Explorer detectors   As the optical system incorporates more components, the Alignment Control System gets increasingly complicated. Already in current interferometers, we will be required to develop new techniques to control the alignment of the OMC [429], the squeezed light source, and the filter cavities, in addition to the already complicated ASC of the main interferometer.

The higher power operation of the interferometer in future detectors will involve coupling of the higher order modes into the field content at the dark port. This coupling will depend on the angular motion of the mirrors and will make the ASC requirements more stringent. To address the issue, deep investigation of the interferometer behavior with simulation is required in the design phase.

Historically, the control noise of the ASC system has consistently been one of the main limiting technical noises in the low frequency band for all interferometric gravitational wave detectors. As the band of gravitational-wave detection moves down, and the bandwidth of alignment control increases, both for suppressing higher-order modes and optical instability, the ASC problem becomes increasingly difficult.

The CSWG should address the interfaces between ASC and other subsystems, such as suspension and seismic isolation, to ensure that the design of the new suspensions and seismic platforms takes into account controllability and noise performance of the ASC loops.

System identification techniques as well as linear an non-linear noise subtractions algorithms need to be studied to improve the low frequency sensitivity of the detectors by optimizing the ASC loops or by subtracting their control noises.

Op-8.1.3   Calibration (CAL)

As the detectors improve sensitivity, the signal-to-noise ratio increases for known sources and the possibility for exciting new astrophysics increases. With this improvement comes the need for increased precision on individual detector calibration [430, 431, 432, 433, 434, 435**?**]. As the gravitational wave network adds new members, the need for accuracy between observatories becomes heightened [436]. And finally, as previous detections have revealed, there is ever more a push to improve the calibration out to the highest possible frequencies [434, 437, 438]. This section describes the R&D projects that must take place for us to move beyond the current capabilities of the calibration hardware[1].

---

[1]The ongoing calibration for the current detectors is described in the Operations Whitepaper[23]

Upgrades the Photon Calibrator System   The primary reference for measuring the global sensing and actuation upon the detector's DARM degree of freedom in Advanced LIGO has been the Photon Calibrator [414]. While this system has allowed us to achieve 2-3% magnitude, 1-2 deg phase accuracy in detector response over the instrument's most sensitive, 20-1000 Hz, band [439, 440], its life-span is finite and maintaining the high-level of precision requires a rigorous maintenance schedule [441]. Improvements to the system are being considered in order to reduce implementation uncertainty. See further discussion of activities in section Op-7.5.5.

Calibration Precision/Accuracy beyond "1%"   The photon calibrator is primarily limited by (a) its absolute calibration of the system's reference received from NIST, and (b) its alignment into the interferometer, to a level of 0.41% [442]. Section Op-7.5.5 discusses improvements to the system that might allow the photon calibrator to *only* be limited by its reference uncertainty. However, propagating that uncertainty through several combined measurements of the interferometer (to-date) adds up to the current estimates of systematic error in (i.e. the accuracy of) detector response to DARM changes of 2-3% in magnitude, with an 68% confidence interval (i.e. the precision) of that estimate that can be as large as 10%. These levels of detector response precision and accuracy are depend on the detector configuration and limited by the ability to quantify unknown frequency dependence [440]. Much of the astrophysical information from SNR $\tilde{1}00$ events – expected to be prevalent at the design sensitivity of 2G detectors, and even more so in 3G detectors – would be limited by these levels of precision and accuracy. Thus, we must explore improvements to the current reference itself, in the use of the current reference through the detector, and/or better ways to characterize the detector response frequency dependence, while being mindful of the detector configuration. In doing so we shall also consider supplementing the photon calibrator reference with others in order to harness the full capability of improved sensitivity, for example by improving systems for direct gravitational interaction between a LIGO test mass and an externally modulated gravitational reference as is planned for KAGRA and VIRGO in O4 [23, 443, 444], or by attempting entire new methods exploiting the 532 nm lasers from the lock-acquisition system [445]. See further discussion of activities in section Op-8.2.8.

Detector Calibration Above 1 kHz   Virtually all force-actuator references are / will-be limited in actuation strength by the f^{-2} displacement response of the test mass suspensions. However, gravitational waves from supernovae and colliding neutron stars are expected to yield exciting information above ∼1 kHz. The two-fold inhibitors – high noise and low actuation strength – mean obtaining even sparse confirmational measurements at these frequencies takes days to weeks. The results are further confused by previously negligible aspects of the detector as discussed in Section 4.4 of [440]. Research to account for such effects in the model, conducting multi-week measurements, and considering modifications to the characterization hardware are on-going.

Op-8.1.4   Control and Data Acquisition System (CDS)

Noise Cancellation   Noise cancellation techniques are already been widely used in the Advanced LIGO interferometers and will be even more important for future detectors. Ba-

sically, noise cancellation based on Wiener filters eliminates the noise in a target signal correlated to witness channels.

This family of techniques has a wide area of application such as seismic noise reduction, Newtonian noise subtraction, and magnetic/acoustic noise cancellation. Residual coupling of auxiliary LSC degrees of freedom to the main GW signals, which presented a sensitivity limit in the initial and Enhanced LIGO interferometers, may also be reduced by noise cancellation.

Up to now, a basic scheme with linear adaptive noise cancellation is being tested on the CDS system at the 40 m prototype [446]. This technique has also been applied to seismic noise subtraction during Enhanced LIGO [446].

Linear [447] and non-stationary [448] noise subtraction techniques have been already implemented offline to improve the sensitivity of the LIGO detectors during O2 and O3.

In the future, in addition to the linear noise subtraction, subtraction of bilinear noise should also be investigated as it may prove useful in removing a variety of noise sources from the GW signal. Machine learning (artificial neural networks, deep learning) may be able to learn non-linear and non-stationary couplings in interferometer noise for the purpose of subtracting this noise from signals[449].

Many of the noise subtraction applications to date have been performed off-line. The focus for the controls working group will be applications that benefit from on-line, real-time, adaptive subtraction (filtering).

Automatic Optimization As the interferometer configuration gets more complicated, the difficulty of optimizing system parameters increases significantly. For example, we have to deal with the different range and frequency dependence of the multiple sensors and actuators at each stage of the suspension and isolation system, as opposed to the single pendulum suspensions use in iLIGO. Optimization of hierarchical control will depend on the noise level of the interferometer, which may change in time, making the traditional approach of by-hand optimization untenable.

Many of the optimization procedures in the future interferometers will need to be automated within the interferometer control system, and some may need to be dynamically adjusted. This approach should be applied in Advanced LIGO and expanded in the future detectors with continuous effort toward automatic optimization or "machine learning". New involvement and collaboration with researchers of this particular field is encouraged.

Modern control Along with adaptive noise cancellation and automatic optimization, other applications of modern control theory to interferometer gravitational wave detectors should be considered.

Feedback control of interferometer gravitational wave detectors has mostly relied on the classical control theory up to now. The classical control theory, developed in the 1950s, is still effective as one of the approaches for control applications. However, control theory has continued over the intervening 60 years and significant improvements to the classical approach are available. Modern control theory, offers various possibilities to improve the

interferometer control.

An example application of modern control theory is the modal-damping work done on the aLIGO suspensions at MIT [279]. The challenge faced in suspension control, and also elsewhere in aLIGO and similar detectors, is that of combining multiple sensor signals with a variety of noise levels and response functions to provide a controller which is effective in the control band while minimizing noise in the gravitational-wave detection band. The currently employed approach of classical controls requires experts to spend considerable time diagonalizing the system and constructing near-optimal (really just "good enough") filters for each degree of freedom of the system.

Modern Control techniques can also be used to combine the information from multiple sensors and dynamics models to create more complete information about the state of various systems which are being controlled. A simple version of this technique using classical techniques is the sensor blending and sensor correction used by the ISI to very good effect.

A possible application using modern control tools would be to improve the suspension damping by leveraging the GS-13 inertial sensors installed in the ISIs, together with our detailed dynamical model of the suspensions, plus the OSEM and actuator data to create a model-driven suspension sensor using steady-state Kalman filtering. This scheme could be deployed with the existing LIGO CDS tools, and it would require little fine-tuning to generate reproducible results. This could be extended to include improved OSEMs as they are added to various suspensions and is consistent with modal damping.

Preliminary work [341] suggests this could be a promising path for damping the suspension resonances. At the time of writing, the scheme is in the process of being tested in a prototype facility to demonstrate its readiness. Additional details, such as the potential advantage of inertial vs. relative damping, the eventual incorporation of measured transfer functions into the model, as well as the introduction of additional sensors into the estimator is a subject of ongoing research.

These technologies can be first investigated by simulation and then applied to prototype facilities. Once effectiveness of these advanced control is demonstrated, it can be implemented to the aLIGO interferometers in order to accelerate the interferometer optimization.

Virtual Interferometer   The flexibility of the Advanced LIGO CDS system, and recent changes to the RCG software allows, for the first time, the beginnings of the "Virtual Interferometer". The recent RCG changes support a "virtual" IOP with the RCG code running in user space (instead of the kernel).

Future detectors should have a computer facility which enables us to login and run the control system for the test of operating and diagnosing tests without having the actual detector equipment. At the beginning this can only be a tool for the commissioning and development, as seen in the "Simulated Plant" concept being tested at the 40m prototype [450], but eventually can provide various realtime tests of the interferometer behavior by cooperative interaction with the other simulation tools. This should include the test of the online data production for mock data challenges.

Op-8.2 Research Areas

Our research efforts in the near term are focused on the following topical areas, each described in the subsections below:

- Application of Machine Learning to Controls

- Length-to-Angle (L2A) decoupling

- Feedback optimization

- System Identification

- Interferometer robust configuration for earthquakes

- State space control for Real-Time Code Generator (RCG) Software

- Angular Sensing & Control

- Calibration

Op-8.2.1 Application of Machine Learning to Controls

Interferometer lock loss is a significant contributor to interferometer downtime and generally represents missed opportunities to collect science data. Lock losses occur for a variety of reasons, many of which are unknown or poorly understood. An automated system that can categorize lock losses or diagnose proximate causes can yield valuable information about where to focus commissioning efforts to improve detector stability. Considering the large amount of auxiliary data produced by the interferometers, machine learning and data mining methods may find use in the development of such an automated system. One example of an automated system to help explain lock losses is the Lockloss Monitor [451].

In the future, it would be desirable to have a system that could analyze the DARM channel along with a number of auxiliary channels to diagnose and predict lock-losses even before they occur; with enough forewarning, the interferometer controls configuration could be quickly adjusted to prevent the lock-loss from ever occurring, i.e. lock maintenance. Such a system is being designed specifically for earthquake events; see section Op-8.2.5.

The difficulty in automatically locking an optical cavity (especially a high finesse cavity) is that there is no signal to use for feedback until very near the resonance condition. When the mirrors are swinging uncontrolled, the system is effectively 'blind'. This is motivation for the (lower finesse) Arm Length Stabilization (ALS) system, which uses light which is frequency doubled main laser light (i.e. green light), as a first step in getting the Fabry-Perot arm cavities close to the main laser light resonance condition. Machine learning techniques may be able to perform state estimation on these nonlinear plants (resonant cavities) and serve to provide guidance to a control system [449]. An experiment to train a Deep Learning (DL) system on simulated interferometer data and then apply it to the 40m interferometer is underway.
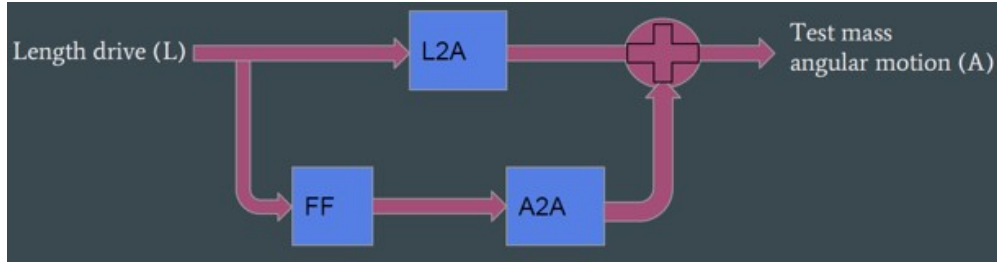
Figure 27: Local feedforward correction filter for length-to-angle decoupling.
FF = -L2A/A2A.

Op-8.2.2 Length-to-Angle (L2A) decoupling

The suspension systems exhibit frequency dependent coupling between length commands and angular motion due to cross-coupling as well as imbalance between the coil actuators. Although the angular control loops mitigate this coupling, improved control can result from implementing length to angle (L2A) feedforward correction. Local feedforward correction at the suspension level can be used to correct for mechanical cross-coupling in the suspensions, as depicted in figure 27. In addition to local feedforward correction, the length control signal can be fed forward to the angular control system to compensate for any residual cross-coupling (e.g. associated with sensing).

The local L2A feedforward correction may permit improved angular sensing and control (ASC) stability and performance by reshaping the ASC loop design. The Power Recycling Mirror (PRM) length-to-pitch decoupling example in figure 28 resulted in improved robustness to disturbances. Global feed forward correction has yet to be attempted, but coherence studies indicate potentially significant performance gains. Various time domain and frequency domain approaches to feed forward filter synthesis are being explored.

If the beam is decentered on the test mass, angular noise couples to strain. If we're able to sense beam position relative to the center of the test mass (optic), then we can steer the beam to center. Using the fixed pattern of scatter points embedded in the optic coating, convolved/modulated with the jittering Gaussian-shaped beam, gives us the potential to determine the beam centroid, either with standard image processing techniques, or via machine learning [449]. An experiment to try this DL approach on track the beam position on an image stream of a test mass at LHO is planned.

Op-8.2.3 Feedback optimization

Feedback optimization serves two goals:

1. to optimize our control loops directly in terms of the requirements of the interferometer, and

2. to automate the design process.

The first goal involves writing a cost function directly in terms of what matters to the interferometer, such as noise, control authority, and stability. The second goal requires utilization
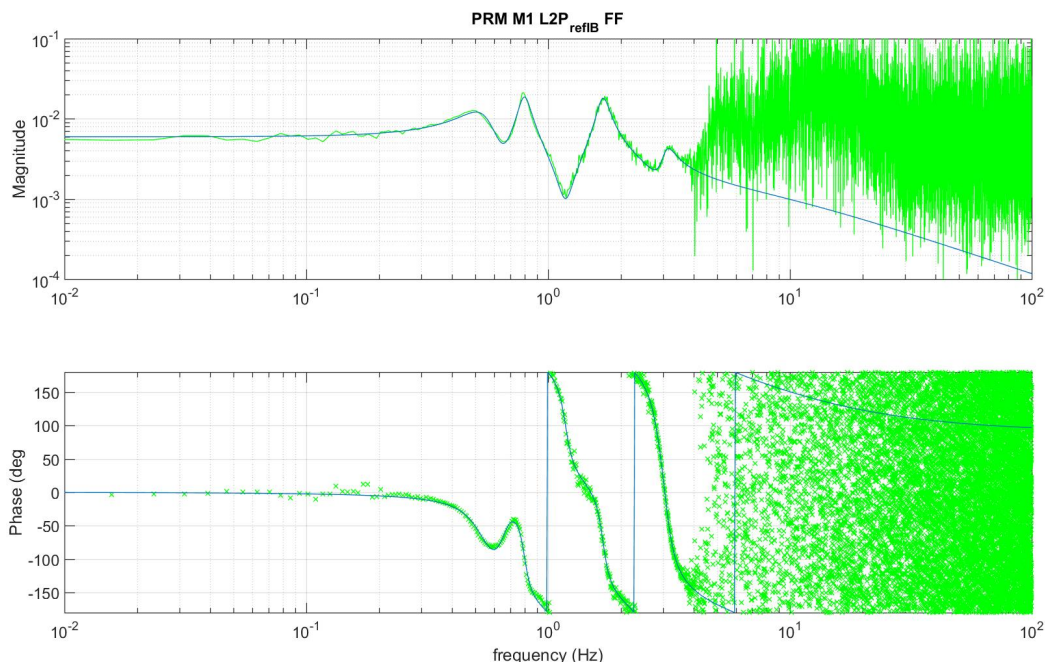
Figure 28: Local feedforward correction filter for length-to-pitch decoupling for the Power Recycling Mirror (PRM), M1 stage. Trend data indicates improved robustness to disturbances (wind, earthquakes) after implementing length-to-pitch (L2P) and length-to-yaw (L2Y) feedforward (FF) filters from the ReflB photodiode for the PRM.

of a general purpose optimization algorithm, such as a particle swarm method that is capable of finding global minimums amongst numerous local minima. This algorithm should reliably find a close to optimal solution in a reasonably short amount of time, alleviating the need for commissioners to create time consuming designs using loop shaping and guess and check techniques that result in suboptimal solutions. Traditional optimal control approaches, such as LQG and H-infinity, have not proven more useful than loop shaping and guess and check techniques for many applications due to the fact that the cost functions do not directly translate to interferometer requirements. Consequently, we are working on more generalized cost functions and optimization algorithms to meet the goals of this feedback optimization focus area.

Op-8.2.4 System Identification and Transfer Function Fitting

System identification is the process of developing or improving a mathematical representation of a physical system using experimental data. Techniques for system identification range from those which require physical insight to develop an underlying model structure to those which are model-independent fits of the experimental data.

All control implementations require some form of system identification, either explicitly or implicitly. As LIGO seeks to implement more robust control, better descriptions of the plant, and the associated plant model uncertainty, are required.

The basic system identification process steps, which incorporate physical insight, are as

follows:

- Build a physics-based model

- Design the transfer function measurement

- Collect the transfer function data

- Select, filter, de-trend the data, as appropriate

- Fit the model

- Validate the model (compare prediction to data)

- Iterate until converged on a validated model

Optimal transfer function measurement [452, 453] is basically concentrating the injection to the frequencies where the uncertainty in the model is greatest. Given a coarse model of the system, this method delivers lower system parameter uncertainties for a fixed excitation RMS and measurement time. In many cases, we have $< 50\%$ uncertainty in the roots, so this is less expensive in time than our usual technique of making a detailed swept-sine measurement with diaggui. As usual, we use awgstream or awg.py to inject this signal. Our next steps are to develop user friendly software for control room use - this software can also be prototyped using the Virtual Interferometer; see section Op-8.1.4.

Transfer function fitting in LIGO is often divorced from the physics-based model, i.e. we do not fit to model parameters, we instead curve fit the frequency domain transfer function response and do not validate the model and use it for subsequent control synthesis. Even in these scenarios, we can benefit from more accurate curve fits to the measured transfer functions, as indicated in figure 29.

System identification is a well established field rich with techniques suitable for various applications. We are working toward:

- determining the applicability of various system identification techniques to GW interferometer subsystems,

- defining a "'road map"' for application to our systems and further research,

- using frequency, time domain and state space techniques for model parameter identification, and

- developing methods to incorporate measurement uncertainty and underlying physical modeling to provide better fits to measurement data from which improved and robust control laws can be formulated.

Ultimately we seek a recursive, real-time parameter identification of our MIMO systems (in their operating states). Many techniques are available such as Generalized Least Squares and Maximum Likelihood Estimators, which are computationally simple. Virgo has been exploring the development of Observer/Kalman Filter identification techniques (time domain
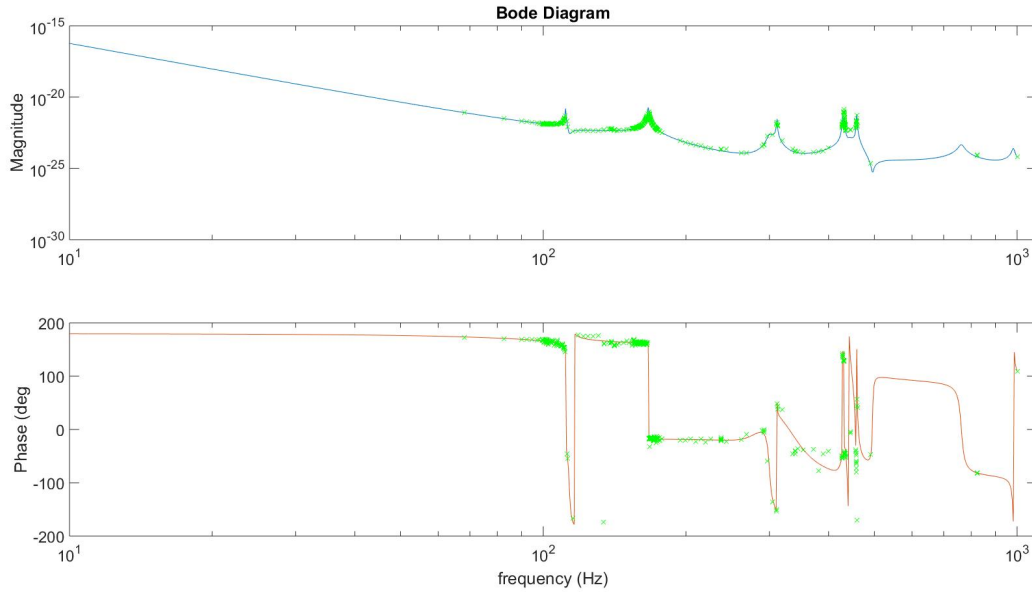
Figure 29: High Frequency Suspension Dynamics: A number of dynamical, resonant features have been found in the quadruple pendulum suspension (UIM/L1 actuation stage) in the frequency range of 100 to 500 Hz. Measurements are a combination of swept-sine (SS) and broad-band (BB) transfer function ratios. For system calibration, a pole-zero fit of this transfer function above 20 Hz, that can be used as a "correction" filter to a model that falls off as f^6, was needed. While this filter does not need to perfectly resolve the details of all of the high-Q features, but it must track the overall frequency dependence over the 20 - 500 Hz region well. The best pole:zero fit is the stable, non-minimum phase, zero delay, 22:28 order model shown (compatible with a Linear Time Invariant (LTI) representation).

based) extended to identification of a closed loop effective controller/observer combination for their seismic isolation system. We think that State-Space Frequency Domain (SSFD) identification techniques are a natural extension to our traditional frequency domain approaches and lead naturally to the application of modern control approaches to our MIMO systems.

Improvements of the existing models may be required in order to account for cross coupling or complex geometry effects, such physical features not being captured by the current models. We see finite element methods as good approach for this task, namely to model the full geometric complexity of the plant, as well as to cover its high frequency dynamical response. In addition, a reduced-order parametric model of the system, extracted from the the finite element model, would be tested against experimental characterizations, through comparison between modeled and measured transfer functions for instance, and the parameters would be adjusted consequently. Such a parameterization would help to identify and study the impact of key physical aspects of the suspension behavior. This modeling strategy, involving detailed physical modeling of the plant, a parametric model, the fitting and the verification against experimental data would not only be used to enhance the reliability of the model in the framework of robust control of the suspension, but will also be of great use in in the context of future detectors design.

Op-8.2.5   Interferometer robust configuration for earthquakes

The detectors are susceptible to teleseismic events, which can significantly impact a detector's duty cycle. Efforts by the SWG have produced an early-warning system, known as *Seismon*[454, 455], for gravitational-wave observatories, which relies on near real-time earthquake alerts provided by the U.S. Geological Survey (USGS) and the National Oceanic and Atmospheric Administration (NOAA). *Seismon* estimates the amplitude of the ground velocity at the site, and the time-of-arrival, to create warnings for the detectors.

Losing optical cavity lock leads to significant down time due to the time to reacquire lock and reestablish thermal equilibrium. Algorithms (including machine learning[451]) are being explored to set thresholds on predicted ground motion relative to probability of lock loss.

The goal of the early warning system is to allow time to reconfigure the control system if the probability of interferometer lock loss is high. The control system reconfiguration trades off sensitivity for added robustness in order to maintain lock. For this reason, it cannot be permanently activated and needs to be part of the Guardian switching system. Based on the information provided by *Seismon*, we could regain duty cycle otherwise lost during earthquake events. Advanced LIGO has an impressive array of sensors and a flexible control system, and different control strategies are being considered (see section Op-6.1.4). Studies are conducted to investigate optimal ways to reduce the impact of the extra-motion created by earthquakes at low frequencies while still providing isolation performance in the LIGO detection band. For example, tuning the seismic platform, control scheme to reduce the gain peaking at low frequencies has been studied [456]. Other control strategies are underway to increase the interferometer robustness via mechanical length to angle decoupling [457] and common mode rejection along the arms [458].

Op-8.2.6   State space control for Real-Time Code Generator (RCG) Software

The current primary mechanism in the RCG environment for implementing MIMO control is to use filter matrices. While these filter matrices work well for some applications, they are often suboptimal for implementing state space models for applications such as simulated plants, fault detection or 'Modern Controls' techniques such as Kalman filtering and LQG. Since these applications begin in state space form, it is natural to implement them in state space form. Converting them to filter matrices introduces computational redundancies such as numerous pole-zeros cancellations and/or unnecessary transformation steps in the implementation. The implementation of state space blocks in the RCG environment is envisioned to have a user interface similar to existing matrix blocks, with the added complexities that state spaces will consist of four matrices, the A, B, C, and D matrices, and the user will have to specify the number of inputs, outputs, and states. Since matrices are easy to update in real-time in the RCG environment, these state space tools may also open up new ways for implementing adaptive control techniques.

Op-8.2.7   Angular Sensing & Control

As mentioned in section Op-8.1.2, the control noise of the ASC system has consistently been one of the main limiting technical noises in the low frequency band for all interferometric

gravitational wave detectors. In fact angular control noise is dominant in the aLIGO spectrum below 25 Hz, due to a number of causes [459]. We plan to focus on the following research related to angular sensing & control:

- make the 'plant' appear to be power independent by digitally compensating for the power dependency [460]

- investigate means to reduce excess noise, and noise coupling, to the ASC sensors

- investigate new sensing schemes for the SRC (e.g. [461]) to overcome current sensing matrix limitations

- study means to mitigate initial alignment drift so that lock re-acquisition time is minimized

Op-8.2.8   Calibration

As motivated in section Op-8.1.3, we plan to focus on the following research:

- Detector Commissioning

  - Configuring detector controls so as to minimize sensitivity detector component uncertainty

  - Improving methods for estimating of unknown frequency dependent systematic error

  - Review and synthesis of models of the detector response at frequencies above 1 kHz.

- Absolute Reference Development: Photon Calibrator

  - See Section Op-7.5.5.

- Absolute Reference Development: Alternative Methods

  - Exploring ideas for integrated multiple, absolute reference system methods for determining displacement fiducials.

  - Continue development of direct gravitational actuators as absolute references.

  - Design exploration and prototyping for absolute reference techniques exploiting the lock acquisition system.

References

[1] Lisa Barsotti, Peter Fritschel, Matthew Evans, and Slawomir Gras. Updated Advanced LIGO Design Curve. *LIGO Document: LIGO-T1800044*, 2018.

[2] Lisa Barsotti, Lee McCuller, Matthew Evans, and Peter Fritschel. The A+ design curve. *LIGO Document: LIGO-T1800042*, 2018.

[3] Patricia Purdue and Yanbei Chen. Practical speed meter designs for quantum nondemolition gravitational-wave interferometers. *Phys. Rev. D*, 66:122004, 2002.

[4] Y. Chen. Sagnac interferometer as a speed-meter-type, quantum-nondemolition gravitational-wave detector. *Phys. Rev. D*, 67:122004, 2003.

[5] S. L. Danilishin. Sensitivity limitations in optical speed meter topology of gravitational-wave antennas. *Phys. Rev. D*, 69:102003, 2004.

[6] Helge Müller-Ebhardt. *On quantum effects in the dynamics of macroscopic test masses.* PhD thesis, Leibniz Universität Hannover, 2009.

[7] Mengyao Wang, Charlotte Bond, Daniel Brown, Frank Brückner, Ludovico Carbone, Rebecca Palmer, and Andreas Freise. Realistic polarizing Sagnac topology with DC readout for the Einstein Telescope. *Phys. Rev. D*, 87:096008, May 2013.

[8] Andrew Wade, Kirk Mckenzie, Yanbei Chen, Daniel Shaddock, Jong Chow, and David McClelland. A polarization speed meter for gravitational-wave detection. *LIGO Document: P1100205*, 2011.

[9] S. P. Voronchev, N. V.; Tarabrin and S. L Danilishin. Broadband detuned sagnac interferometer for future generation gravitational wave astronomy. *arXiv:1503.01062*, 2015.

[10] S H Huttner, S L Danilishin, B W Barr, A S Bell, C Gr??f, J S Hennig, S Hild, E A Houston, S S Leavey, D Pascucci, B Sorazu, A P Spencer, S Steinlechner, J L Wright, T Zhang, and K A Strain. Candidates for a possible third-generation gravitational wave detector: comparison of ring-sagnac and sloshing-sagnac speedmeter interferometers. *Classical and Quantum Gravity*, 34(2):024001, 2017.

[11] E. Knyazev, S. Danilishin, S. Hild, and F.Ya. Khalili. Speedmeter scheme for gravitational-wave detectors based on epr quantum entanglement. *Physics Letters A*, 2017.

[12] S. L. Danilishin, E. Knyazev, N. V. Voronchev, F. Y. Khalili, C. Gräf, S. Steinlechner, J.-S. Hennig, and S. Hild. A new quantum speed-meter interferometer: Measuring speed to search for intermediate mass black holes. *Light: Science & Applications*, 2018.

[13] Sheila Dwyer. personal communication, 2012.

[14] Thomas Corbitt, Yanbei Chen, and Nergis Mavalvala. Mathematical framework for simulation of quantum fields in complex interferometers using the two-photon formalism. *Physical Review A*, 72(1):013818+, July 2005.

[15] Rana X Adhikari. Gravitational radiation detection with laser interferometry. *Reviews of Modern Physics*, 2013.

[16] LIGO Scientific Collaboration and Virgo Collaboration. Observation of Gravitational Waves from a Binary Black Hole Merger. *Physical Review Letters*, 116:061102, 2016.

[17] LIGO Scientific Collaboration and Virgo Collaboration. Binary black hole mergers in the first advanced ligo observing run. *Physical Review X*, 6(4):041015, 2016.

[18] LIGO Scientific Collaboration and Virgo Collaboration. Gw170104: observation of a 50-solar-mass binary black hole coalescence at redshift 0.2. *Physical Review Letters*, 118(22):221101, 2017.

[19] LIGO Scientific Collaboration and Virgo Collaboration. Gw170608: Observation of a 19 solar-mass binary black hole coalescence. *The Astrophysical Journal Letters*, 851(2):L35, 2017.

[20] LIGO Scientific Collaboration and Virgo Collaboration. Gw170814: A three-detector observation of gravitational waves from a binary black hole coalescence. *Physical review letters*, 119(14):141101, 2017.

[21] B. P. Abbott et al. GWTC-1: A Gravitational-Wave Transient Catalog of Compact Binary Mergers Observed by LIGO and Virgo during the First and Second Observing Runs. 2018.

[22] BP Abbott, R Abbott, RX Adhikari, A Ananyeva, SB Anderson, S Appert, K Arai, MC Araya, JC Barayoga, BC Barish, et al. Multi-messenger observations of a binary neutron star merger. *Astrophysical Journal Letters*, 848(2):L12, 2017.

[23] LSC, Virgo and KAGRA Collaborations. LSC-Virgo-KAGRA Operations White Paper (2022-2023 edition). *LIGO Document: LIGO-T2200381*, 2022.

[24] The LSC Program Committee. LSC 2022 Program. *LIGO Document: LIGO-M2200183*, 2022.

[25] Einstein Telescope Science Team. Einstein gravitational wave Telescope conceptual design study. *ET Document: ET-0106C-10*, 2011.

[26] M. Evans et al. Cosmic explorer: Science, observatories, community. Technical Report CE–P2100003, Cosmic Explorer, 2021.

[27] Christian D Ott, Yanbei Chen, and Rana X. Adhikari. Astrophysical Motivations for the Third Generation LIGO Detectors. *LIGO Document: LIGO-P1200099*, 2012.

[28] David Reitze et al. The US Program in Ground-Based Gravitational Wave Science: Contribution from the LIGO Laboratory. *Bull. Am. Astron. Soc.*, 51:141, 2019.

[29] KAGRA Collaboration, LIGO Scientific Collaboration and Virgo Collaboration. Prospects for observing and localizing gravitational-wave transients with advanced ligo, advanced virgo and kagra. *LIGO Document: LIGO-P1200087*, 2020.

[30] John Miller, Lisa Barsotti, Peter Fritschel, and Matt Evans. Prospects for doubling the range of advanced ligo. *LIGO Document: LIGO-T0900144*, 2014.

[31] Patrick Brady, Dave Reitze, and Albert Lazzarini. Ligo post-o5 study group. *https://dcc.ligo.org/LIGO-M2100044*, 2021.

[32] The LSC Post-O5 Study Group. Report of the LSC Post-O5 Study Group. *LIGO Document: LIGO-T2200287*, 2022.

[33] Yoichi Aso, Yuta Michimura, Kentaro Somiya, Masaki Ando, Osamu Miyakawa, Takanori Sekiguchi, Daisuke Tatsumi, and Hiroaki Yamamoto. Interferometer design of the KAGRA gravitational wave detector. *Phys. Rev.*, D88(4):043007, 2013.

[34] R. Adhikari et al. A cryogenic silicon interferometer for gravitational-wave detection. *arXiv:2001.11173*, 2020.

[35] Matt Evans, Kevin Kuns, Evan Hall, Stefan Ballmer, Duncan Brown, and Joshua Smith. Design stage r&d for cosmic explorer: a review of critical technologies. *https://dcc.cosmicexplorer.org/CE-P2100005*, 2021.

[36] S. Chua, B. Slagmolen, D. Shaddock, and D. McClelland. Quantum squeezed light in gravitational-wave detectors. *Classical and Quantum Gravity*, 29:145015, 2012.

[37] J Abadie and et al. Enhanced sensitivity of the ligo gravitational wave detector by using squeezed states of light. *Nature Photonics*, 7:613–619, 2013.

[38] H. Grote, K. Danzmann, K.L. Dooley, R. Schnabel, J. Slutsky, and H. Vahlbruch. First long-term application of squeezed states of light in a gravitational-wave observatory. *Phys. Rev. Lett.*, 110, 2013.

[39] H. J. Kimble, Y. Levin, A. B. Matsko, K. S. Thorne, and S. P. Vyatchanin. Conversion of conventional gravitational-wave interferometers into quantum nondemolition interferometers by modifying their input and/or output optics. *Phys. Rev. D*, 65:022002, 2001.

[40] J. Harms and et al. Squeezed-input, optical-spring, signal-recycled gravitational-wave detectors. *Phys. Rev. D*, 68:042001, 2003.

[41] Hang Yu, Denis Martynov, Salvatore Vitale, Matthew Evans, David Shoemaker, Bryan Barr, Giles Hammond, Stefan Hild, James Hough, Sabina Huttner, Sheila Rowan, Borja Sorazu, Ludovico Carbone, Andreas Freise, Conor Mow-Lowry, Katherine L. Dooley, Paul Fulda, Hartmut Grote, and Daniel Sigg. Prospects for detecting gravitational waves at 5 hz with ground-based detectors. *Phys. Rev. Lett.*, 120:141102, Apr 2018.

[42] Denis Martynov. Should we use 2 um lasers and a-Si / SiO2 coatings on SiO2 mirrors at room temperature? *LIGO Document: LIGO-G1901141*, 2019.

[43] Conor Mow-Lowry, and Katherine Dooley, and Denis Martynov. Low-frequency workshop report. *LIGO Document: LIGO-G1801755*, 2018.

[44] Teng Zhang, and Denis Martynov, and Andreas, Freise, and Haixing Miao. Quantum Squeezing Schemes for Heterodyne Readout. *LIGO Document: LIGO-P2000132*, 2020.

[45] Vaishali Adya. Signal recycling control through the dark port. *LIGO Document: LIGO-G1801710*, 2018.

[46] Ackley, A. and others. Neutron star Extreme Matter Observatory (NEMO): A kilohertz-band gravitational-wave detector in the global network. *LIGO Document: LIGO-P2000200*, 2020.

[47] M Punturo, M Abernathy, F Acernese, B Allen, Nils Andersson, K Arun, F Barone, B Barr, M Barsuglia, M Beker, et al. The einstein telescope: a third-generation gravitational wave observatory. *Classical and Quantum Gravity*, 27(19):194002, 2010.

[48] Benjamin P Abbott, R Abbott, TD Abbott, MR Abernathy, K Ackley, C Adams, P Addesso, RX Adhikari, VB Adya, C Affeldt, et al. Exploring the sensitivity of next generation gravitational wave detectors. *Classical and Quantum Gravity*, 34(4):044001, 2017.

[49] Aidan Brooks. A+ Active Wavefront Control (AWC) Preliminary Design Document. *LIGO Document: LIGO-T2000244*, 2020.

[50] N. Smith-Lefebvre and N. Mavalvala. Modematching feedback control for interferometers with an output mode cleaner. *LIGO Document: LIGO-P1200034*, 2012.

[51] Fabian Magana-Sandoval, Thomas Vo, Daniel Vander-Hyde, Jax Sanders, Stefan Ballmer. Sensing Optical Cavity Mismatch with a Mode-Converter and Quadrant Photodiode. *LIGO Document: LIGO-P1900270*, 2019.

[52] Daniel Brown, Huy Tuong Cao, Alexei Ciobanu, Peter Veitch, and David Ottaway. Differential wavefront sensing and control using radio-frequency optical demodulation, May 2021.

[53] Ken Strain, Joseph Briggs, Mark Barton, Russell Jones, Stephen Webster, Eric Oelker. Conceptual Design: Balanced Homodyne Detection for A+. *LIGO Document: LIGO-E1900377*, 2020.

[54] Rana Adhikari, and Koji Arai. 40m BHD Review Docs. *LIGO Document: LIGO-E2000076*, 2020.

[55] P. Willems. Implications of ETM02 HR Coating Absorption for Thermal Compensation. *LIGO Document, LIGO-T1100250-v2*, 2011.

[56] Aidan Brooks, Hiro Yamamoto, Daniel Brown, Evan Hall, Gabriele Vajente, GariLynn Billingsley, Marie Kasprzack,. The point absorbers and aLIGO. *LIGO Document: LIGO-G1900203*, 2019.

[57] Aidan F. Brooks, Gabriele Vajente, Hiro Yamamoto, et al. Point absorbers in advanced ligo. *Appl. Opt.*, 60(13):4047–4063, May 2021.

[58] Kazuhiro Agatsuma, David Rabeling, Jo Van den Brand. Phase camera for Advanced Virgo. *LIGO Document: LIGO-G1801077*, 2018.

[59] Stefan Ballmer, Erik Muniz. A new approach for a Phase Camera. *LIGO Document: LIGO-G1801736*, 2018.

[60] Huy Tuong Cao, Daniel D. Brown, Peter J. Veitch, and David J. Ottaway. Optical lock-in camera for gravitational wave detectors. *Opt. Express*, 28(10):14405–14413, May 2020.

[61] Hiro Yamamoto. SIS: Stationary interferometer simulation. `https://labcit.ligo.caltech.edu/~hiro/SIS/`. Accessed: 2018-05-18.

[62] Jérôme Degallaix. Oscar a matlab based optical fft code. *Journal of Physics: Conference Series*, 228(1):012021, 2010. Code is available at `https://www.mathworks.com/matlabcentral/fileexchange/20607-oscar`.

[63] Alexei A. Ciobanu, Daniel David Brown, Peter J. Veitch, and David J. Ottaway. Modeling circulating cavity fields using the discrete linear canonical transform, 2021.

[64] Hiro Yamamoto et al. Ligo end to end simulation software. `http://www.ligo.caltech.edu/~e2e/`, 2015. Accessed: 2018-05-18.

[65] H. Yamamoto, B. Bhawal, M. Evans, E. Maros, M. Rakhmanov, Jr. R. L. Savage, G. Cella, S. Klimenko, and S. Mohanty. End to End Simulation Program for Gravitational-Wave Detectors. In Seiji Kawamura and Norikatsu Mio, editors, *Gravitational Wave Detection II*, volume 32 of *Frontiers Science Series*, pages 331–336. Universal Academy Press, 2000.

[66] Tomislav Andric and Jan Harms. Lightsaber: A simulator of the angular sensing and control system in ligo. *Galaxies*, 9(3), 2021.

[67] Matt Evans. Optickle simulation software. `https://github.com/Optickle/Optickle`, 2004. Accessed: 2018-05-18.

[68] Daniel David Brown and Andreas Freise. Finesse. `http://www.gwoptics.org/finesse`, May 2014. You can download the binaries and source code at `http://www.gwoptics.org/finesse`.

[69] A Freise, G Heinzel, H Lück, R Schilling, B Willke, and K Danzmann. Frequency-domain interferometer simulation with higher-order spatial modes. *Classical and Quantum Gravity*, 21(5):S1067, 2004.

[70] Kevin Kuns. Quantum optomechanics loop analysis and noise calculation engine, 2021.

[71] Gabriele Vajente. Fast modal simulation of paraxial optical systems: the mist open source toolbox. *Classical and Quantum Gravity*, 30(7):075014, 2013.

[72] LIGO Scientific Collaboration. Gravitational wave interferometer noise calculator. `https://awiki.ligo-wa.caltech.edu/aLIGO/GWINC`, 2015. Accessed: 2018-05-18.

[73] LIGO. pygwinc: Python based Gravitational Wave Interferometer Noise Calculator.

[74] Tomislav Andric and Jan Harms. Lightsaber: A simulator of the angular sensing and control system in LIGO. *https://dcc.ligo.org/LIGO-P2100229*, 2021.

[75] Jan Harms. Terrestrial Gravity Fluctuations. *Living Reviews in Relativity*, 18(3), 2015.

[76] Jennifer C. Driggers, Jan Harms, and Rana X. Adhikari. Subtraction of Newtonian noise using optimized sensor arrays. *Phys. Rev. D*, 86:102001, Nov 2012.

[77] M Coughlin, N Mukund, J Harms, J Driggers, R Adhikari, and S Mitra. Towards a first design of a Newtonian-noise cancellation system for Advanced LIGO. *Classical and Quantum Gravity*, 33(24):244001, 2016.

[78] M Coughlin, J Harms, N Christensen, V Dergachev, R DeSalvo, S Kandhasamy, and V Mandic. Wiener filtering with a seismic underground array at the Sanford Underground Research Facility. *Classical and Quantum Gravity*, 31(21):215003, 2014.

[79] Donatella Fiorucci, Jan Harms, Matteo Barsuglia, Irene Fiori, and Federico Paoletti. Impact of infrasound atmospheric noise on gravity detectors used for astrophysical and geophysical applications. *Phys. Rev. D*, 97:062003, Mar 2018.

[80] M. W. Coughlin, J. Harms, J. Driggers, D. J. McManus, N. Mukund, M. P. Ross, B. J. J. Slagmolen, and K. Venkateswara. Implications of dedicated seismometer measurements on newtonian-noise cancellation for advanced ligo. *Phys. Rev. Lett.*, 121:221104, Nov 2018.

[81] Jan Harms and Krishna Venkateswara. Newtonian-noise cancellation in large-scale interferometric GW detectors using seismic tiltmeters. *Classical and Quantum Gravity*, 33(23):234001, 2016.

[82] J. Harms, E. L. Bonilla, M. W. Coughlin, J. Driggers, S. E. Dwyer, D. J. McManus, M. P. Ross, B. J. J. Slagmolen, and K. Venkateswara. Observation of a potential future sensitivity limitation from ground motion at ligo hanford. *Phys. Rev. D*, 101:102002, May 2020.

[83] G. Cella. Off-Line Subtraction of Seismic Newtonian Noise. In B. Casciaro, D. Fortunato, M. Francaviglia, and A. Masiello, editors, *Recent Developments in General Relativity*, pages 495–503. Springer Milan, 2000.

[84] D J McManus, P W F Forsyth, M J Yap, R L Ward, D A Shaddock, D E McClelland, and B J J Slagmolen. Mechanical characterisation of the TorPeDO: a low frequency gravitational force sensor. *Classical and Quantum Gravity*, 34(13):135002, jun 2017.

[85] Thomas Corbitt and Nergis Mavalvala. Review: Quantum noise in gravitational-wave interferometers. *Journal of Optics B: Quantum and Semiclassical Optics*, 6(8):S675, 2004.

[86] D.E. McClelland, N. Mavalvala, Y. Chen, and R. Schnabel. Advanced interferometry, quantum optics and optomechanics in gravitational wave detectors. *Laser & Photonics Reviews*, 5:677, 2011.

[87] Stefan L. Danilishin and Farid Ya. Khalili. Quantum measurement theory in gravitational-wave detectors. *Living Reviews in Relativity*, 15:5, 2012.

[88] Gravitational wave detection using laser interferometry beyond the standard quantum limit. *Philosophical Transactions of the Royal Society A: Mathematical, Physical and Engineering Sciences*, 376(2120):20170289, 2018.

[89] Stefan L Danilishin, Farid Ya. Khalili, and Haixing Miao. Advanced quantum techniques for future gravitational-wave detectors. *Living Reviews in Relativity*, 22(1):2, 2019.

[90] C. M. Caves. Quantum-mechanical noise in an interferometer. *Phys. Rev. D*, 23:1693, 1981.

[91] M. T. Jaekel and S. Reynaud. Quantum Limits in Interferometric Measurements. *Europhys. Lett.*, 13:301, 1990.

[92] Roman Schnabel, Nergis Mavalvala, D.E. David E McClelland, and Ping K P.K. Lam. Quantum metrology for gravitational wave astronomy. *Nature communications*, 1(8):121, jan 2010.

[93] The LIGO Scientific Collaboration, J. Abadie, B. P. Abbott, R. Abbott, T. D. Abbott, M. Abernathy, C. Adams, R. Adhikari, C. Affeldt, B. Allen, and et al. A gravitational wave observatory operating beyond the quantum shot-noise limit. *Nature Physics*, 7:962–965, 2011.

[94] Roman Schnabel. Squeezed states of light and their applications in laser interferometers. *Physics Reports*, 684:1–51, apr 2017.

[95] Yiqiu Ma, Haixing Miao, Belinda Heyun Pang, Matthew Evans, Chunnong Zhao, Jan Harms, Roman Schnabel, and Yanbei Chen. Proposal for gravitational-wave detection beyond the standard quantum limit through EPR entanglement. *Nature Physics*, may 2017.

[96] Jan Südbeck, Sebastian Steinlechner, Mikhail Korobko, and Roman Schnabel. Demonstration of interferometer enhancement through Einstein–Podolsky–Rosen entanglement. *Nature Photonics*, 14(4):240, 2020.

[97] Min Jet Yap, Paul Altin, Terry G McRae, Bram J J Slagmolen, Robert L Ward, and David E McClelland. Generation and control of frequency-dependent squeezing via Einstein–Podolsky–Rosen entanglement. *Nature Photonics*, 14(4):223, 2020.

[98] H. J. Kimble, Yuri Levin, Andrey B. Matsko, Kip S. Thorne, and Sergey P. Vyatchanin. Conversion of conventional gravitational-wave interferometers into quantum nondemolition interferometers by modifying their input and/or output optics. *Phys. Rev. D*, 65:022002, 2001.

[99] A F Pace, M J Collett, and D F Walls. Quantum limits in interferometric detection of gravitational radiation. *Phys. Rev. A*, 47:3173, 1993.

[100] A. Wicht, K. Danzmann, M. Fleischhauer, M. Scully, G. M\\"uller, R.-H. R.H. Rinkleff, and G Müller. White-light cavities, atomic phase coherence, and gravitational wave detectors. *Opt. Commun.*, 134(1-6):431, 1997.

[101] H. Rehbein, J. Harms, R. Schnabel, and K. Danzmann. Optical transfer functions of Kerr nonlinear cavities and interferometers. *Phys. Rev. Lett.*, 95:193001, 2005.

[102] M. Korobko, L. Kleybolte, S. Ast, H. Miao, Y. Chen, and R. Schnabel. Beating the Standard Sensitivity-Bandwidth Limit of Cavity-Enhanced Interferometers with Internal Squeezed-Light Generation. *Physical Review Letters*, 118(14):143601, apr 2017.

[103] V. B. Braginsky, M. L. Gorodetsky, and F. Y. Khalili. Optical bars in gravitational wave antennas. *Phys. Lett. A*, 232:340, 1997.

[104] A. Buonanno and Y. Chen. Signal recycled laser-interferometer gravitational-wave detectors as optical springs. *Phys. Rev. D*, 65:042001, 2002.

[105] Haixing Miao, Nicolas D Smith, and Matthew Evans. Quantum Limit for Laser Interferometric Gravitational-Wave Detectors from Optical Dissipation. *Phys. Rev. X*, 9(1):11053, 2019.

[106] F. Ya. Khalili and Yu. Levin. Speed meter as a quantum nondemolition measuring device for force. *Phys. Rev. D*, 54:4735–4737, 1996.

[107] Patricia Purdue. Analysis of a quantum nondemolition speed-meter interferometer. *Phys. Rev. D*, 66:022001, 2002.

[108] Patricia Purdue and Yanbei Chen. Practical speed meter designs for quantum nondemolition gravitational-wave interferometers. *Phys. Rev. D*, 66:122004, 2002.

[109] Yanbei Chen. Sagnac interferometer as a speed-meter-type, quantum-nondemolition gravitational-wave detector. *Phys. Rev. D*, 67:122004, 2003.

[110] Christoffer B. Møller, Rodrigo A. Thomas, Georgios Vasilakis, Emil Zeuthen, Yeghishe Tsaturyan, Mikhail Balabas, Kasper Jensen, Albert Schliesser, Klemens Hammerer, and Eugene S. Polzik. Quantum back-action-evading measurement of motion in a negative mass reference frame. *Nature*, 547(7662):191–195, jul 2017.

[111] V. B. Braginsky, M. L. Gorodetsky, F. Ya. Khalili, and K. S. Thorne. Energetic Quantum Limit in Large-Scale Interferometers. *AIP Conf. Proc.*, 523:180–190, 2000.

[112] Mankei Tsang, Howard M. Wiseman, and Carlton M. Caves. Fundamental quantum limit to waveform estimation. *Phys. Rev. Lett.*, 106:090401, 2011.

[113] Haixing Miao, Rana X Adhikari, Yiqiu Ma, Belinda Pang, and Yanbei Chen. Towards the Fundamental Quantum Limit of Linear Measurements of Classical Signals. *Phys. Rev. Lett.*, 119(5):050801, 2017.

[114] M. Tse et al. Quantum-Enhanced Advanced LIGO Detectors in the Era of Gravitational-Wave Astronomy. *Phys. Rev. Lett.*, 123(23):231107, 2019.

[115] F. Acernese et al. Increasing the Astrophysical Reach of the Advanced Virgo Detector via the Application of Squeezed Vacuum States of Light. *Phys. Rev. Lett.*, 123(23):231108, 2019.

[116] L. McCuller, C. Whittle, D. Ganapathy, K. Komori, M. Tse, A. Fernandez-Galiana, L. Barsotti, P. Fritschel, M. MacInnis, F. Matichard, K. Mason, N. Mavalvala, R. Mittleman, Haocun Yu, M. E. Zucker, and M. Evans. Frequency-Dependent Squeezing for Advanced LIGO. *Phys. Rev. Lett.*, 124(17):171102, 2020.

[117] Yuhang Zhao et al. Frequency-Dependent Squeezed Vacuum Source for Broadband Quantum Noise Reduction in Advanced Gravitational-Wave Detectors. *Phys. Rev. Lett.*, 124(17):171101, 2020.

[118] Henning Vahlbruch, Moritz Mehmet, Karsten Danzmann, and Roman Schnabel. Detection of 15 dB squeezed states of light and their application for the absolute calibration of photoelectric quantum efficiency. *Phys. Rev. Lett.*, 117:110801, Sep. 2016.

[119] Andrew R. Wade, Georgia L. Mansell, Sheon S. Y. Chua, Robert L. Ward, Bram J. J. Slagmolen, Daniel A. Shaddock, and David E. McClelland. A squeezed light source operated under high vacuum. *Scientific Reports*, 5(December):18052, Dec. 2015.

[120] Haixing Miao, Huan Yang, and Denis Martynov. Towards the design of gravitational-wave detectors for probing neutron-star physics. *Phys. Rev. D*, 98(4):044044, 2018.

[121] Denis Martynov, Haixing Miao, Huan Yang, Francisco Hernandez Vivanco, Eric Thrane, Rory Smith, Paul Lasky, William E. East, Rana Adhikari, Andreas Bauswein, Aidan Brooks, Yanbei Chen, Thomas Corbitt, Andreas Freise, Hartmut Grote, Yuri Levin, Chunnong Zhao, and Alberto Vecchio. Exploring the sensitivity of gravitational wave detectors to neutron star physics. *Phys. Rev. D*, 99(10):102004, 2019.

[122] Michael Page, Jiayi Qin, James La Fontaine, Chunnong Zhao, Li Ju, and David Blair. Enhanced detection of high frequency gravitational waves using optically diluted optomechanical filters. *Phys. Rev. D*, 97(12):124060, jun 2018.

[123] Michael Page, Ma Yiqiu, Carl Blair, Yanbei Chen, Li Ju, David Blair, Michael Edmond Tobar, and Chunnong Zhao. Gravitational wave detectors with broadband high frequency sensitivity. *LIGO DCC-P1900353*, 2019.

[124] V B Adya, M J Yap, D Töyrä, T G McRae, P A Altin, L K Sarre, M Meijerink, N Kijbunchoo, B J J Slagmolen, R L Ward, and D E McClelland. Quantum enhanced kHz gravitational wave detector with internal squeezing. *Classical and Quantum Gravity*, 37(7):07LT02, 2020.

[125] J. Eichholz, N. A. Holland, V. B. Adya, J. V. van Heijningen, R. L. Ward, B. J. J. Slagmolen, D. E. McClelland, and D. J. Ottaway. Practical test mass and suspension configuration for a cryogenic kilohertz gravitational wave detector. *Phys. Rev. D*, 102:122003, Dec 2020.

[126] Nutsinee Kijbunchoo, Terry McRae, Daniel Sigg, Sheila Dwyer, Haocun Yu, Lee Mc-Culler, Lisa Barsotti, Carl Blair, Anamaria Effler, Matthew Evans, Alvaro Fernandez-Galiana, Peter Fritschel, Valery Frolov, Fabrice Matichard, Nergis Mavalvala, Adam Mullavey, Bram Slagmolen, Maggie Tse, Chris Whittle, and David McClelland. Low Phase Noise Squeezed Vacuum for Future Generation Gravitational Wave Detectors. *LIGO DCC-P2000064*, 2020.

[127] Georgia L. Mansell, Terry G. McRae, Paul A. Altin, Min Jet Yap, Robert L. Ward, Bram J. J. Slagmolen, Daniel A. Shaddock, and David E. McClelland. Observation of Squeezed Light in the 2 μ m Region. *Phys. Rev. Lett.*, 120(20):203603, 2018.

[128] M. J. Yap, D. W. Gould, T. G. McRae, P. A. Altin, N. Kijbunchoo, G. L. Mansell, R. L. Ward, D. A. Shaddock, B. J. J. Slagmolen, and D. E. McClelland. Squeezed vacuum phase control at 2 μm. *Optics Letters*, 44(21):5386, 2019.

[129] Tobias Eberle, Sebastian Steinlechner, Jöran Bauchrowitz, Vitus Händchen, Henning Vahlbruch, Moritz Mehmet, Helge Müller-Ebhardt, and Roman Schnabel. Quantum Enhancement of the Zero-Area Sagnac Interferometer Topology for Gravitational Wave Detection. *Phys. Rev. Lett.*, 104(25):251102, June 2010.

[130] Moritz Mehmet, Stefan Ast, Tobias Eberle, Sebastian Steinlechner, Henning Vahlbruch, and Roman Schnabel. Squeezed light at 1550 nm with a quantum noise reduction of 12.3 dB. *Optics Express*, 19(25):25763–72, December 2011.

[131] C Affeldt, K Danzmann, K L Dooley, H Grote, M Hewitson, S Hild, J Hough, J Leong, H Lück, M Prijatelj, S Rowan, A Rüdiger, R Schilling, R Schnabel, E Schreiber, B Sorazu, K A Strain, H Vahlbruch, B Willke, W Winkler, and H Wittel. Advanced techniques in geo 600. *Classical and Quantum Gravity*, 31(22):224002, 2014.

[132] K L Dooley, J R Leong, T Adams, C Affeldt, A Bisht, C Bogan, J Degallaix, C Gr??f, S Hild, J Hough, A Khalaidovski, N Lastzka, J Lough, H Lück, D Macleod, L Nuttall, M Prijatelj, R Schnabel, E Schreiber, J Slutsky, B Sorazu, K A Strain, H Vahlbruch, M W??s, B Willke, H Wittel, K Danzmann, and H Grote. Geo 600 and the geo-hf upgrade program: successes and challenges. *Classical and Quantum Gravity*, 33(7):075009, 2016.

[133] H Billing, K Maischberger, A Rudiger, R Schilling, L Schnupp, and W Winkler. An argon laser interferometer for the detection of gravitational radiation. *Journal of Physics E: Scientific Instruments*, 12(11):1043, 1979.

[134] H Vahlbruch, S Chelkowski, K Danzmann, and R Schnabel. Quantum engineering of squeezed states for quantum communication and metrology. *New Journal of Physics*, 9(10):371–371, October 2007.

[135] Melanie Meinders and Roman Schnabel. Sensitivity improvement of a laser interferometer limited by inelastic back-scattering, employing dual readout. *Classical and Quantum Gravity*, 32(19):195004, oct 2015.

[136] R. Adhikari. Upgrades to the Advanced LIGO Interferometer. *LIGO Document: LIGO-G1000524*, 2010.

[137] G. Rempe, R. J. Thompson, H. J. Kimble, and R. Lalezari. Measurement of Ultralow Losses in an Optical Interferometer. *Opt. Lett.*, 17:363–365, 1992.

[138] N. Uehara, A. Ueda, K. Ueda, H. Sekiguchi, T. Mitake, and et al. Ultralow-loss mirror of the parts-in 10^{-6} level at 1064 nm. *Opt. Lett.*, 20:530–532, 1995.

[139] Teng Zhang, Hang Yu, Vivishek Sudhir, Calum Torrie, Ken Strain, Hartmut Grote, Koji Arai, Michael Zucker, Rana Adhikari, Sebastian Steinlechner, Joseph Briggs, Peter Fritschel, and Stefan Hild. Plans for the a+ balanced homodyne readout. *LIGO Document: LIGO-G1800459*, 2018.

[140] Sebastian Steinlechner, Bryan W. Barr, Angus S. Bell, Stefan L. Danilishin, Andreas Gläfke, Christian Gräf, Jan-Simon Hennig, E. Alasdair Houston, Sabina H. Huttner, Sean S. Leavey, Daniela Pascucci, Borja Sorazu, Andrew Spencer, Kenneth A. Strain, Jennifer Wright, and Stefan Hild. Local-oscillator noise coupling in balanced homodyne readout for advanced gravitational wave detectors. *Physical Review D*, 92(7):072009, oct 2015.

[141] Teng Zhang, Denis Martynov, Andreas Freise, and Haixing Miao. Quantum Squeezing Schemes for Heterodyne Readout. *arXiv: 2004.10503*, 2020.

[142] Teng Zhang, Philip Jones, Haixing Miao, Denis Martynov, Andreas Freise, and Stefan Ballmer. A two-carrier detector: evading 3dB quantum penalty in heterodyne readout. *in preparation*, 2020.

[143] Boris Hage, Aiko Samblowski, and Roman Schnabel. Towards Einstein-Podolsky-Rosen quantum channel multiplexing. *Phys. Rev. A*, 81(6):62301, June 2010.

[144] Daniel D. Brown, Haixing Miao, Chris Collins, Conor Mow- Lowry, Daniel Töyrä, and Andreas Freise. Broadband sensitivity enhancement of detuned dual-recycled Michelson interferometers with EPR entanglement. *Phys. Rev. D*, 96:062003, Sep 2017.

[145] A. Thüring, R. Schnabel, H. Lück, and K. Danzmann. Detuned Twin-Signal-Recycling for ultra-high precision interferometers. *Opt. Lett.*, 32:985–987, 2007.

[146] A. Thuring, C. Graf, H. Vahlbruch, M. Mehmet, K. Danzmann, and R. Schnabel. Broadband squeezing of quantum noise in a michelson interferometer with twin-signal-recycling. *Opt. Lett*, page 181101, 2009.

[147] Haixing Miao, Huan Yang, Rana X Adhikari, and Yanbei Chen. Quantum Limits of Interferometer Topologies for Gravitational Radiation Detection. *Class. Quant Grav.*, 31(16):165010, 2014.

[148] V. B. Braginsky and F. Ya. Khalili. *Quantum Measurement.* ed. K. S. Thorne, Cambridge University Press, 1992.

[149] P. Purdue and Y. Chen. Practical speed meter designs for quantum nondemolition gravitational-wave interferometers. *Phys. Rev. D*, 66:122004, 2002.

[150] Henning Rehbein, Helge Müller-Ebhardt, Kentaro Somiya, Chao Li, Roman Schnabel, Karsten Danzmann, and Yanbei Chen. Local readout enhancement for detuned signal-recycling interferometers. *Phys. Rev. D*, 76:062002, 2007.

[151] N. A. Robertson, G. Cagnoli, D. R. M. Crooks, E. Elliffe, J. E. Faller, P. Fritschel, S. Goßler, A. Grant, A. Heptonstall, J. Hough, H. Lück, R. Mittleman, M. Perreur-Lloyd, M. V. Plissi, S. Rowan, D. H. Shoemaker, P. H. Sneddon, K. A. Strain, C. I. Torrie, H. Ward, and P. Willems. Quadruple suspension design for Advanced LIGO. *Class. Quantum Grav.*, 19:4043–4058, 2002.

[152] A V Cumming, A S Bell, L Barsotti, M A Barton, G Cagnoli, D Cook, L Cunningham, M Evans, G D Hammond, G M Harry, A Heptonstall, J Hough, R Jones, R Kumar, R Mittleman, N A Robertson, S Rowan, B Shapiro, K A Strain, K Tokmakov, C Torrie, and A A van Veggel. Design and development of the advanced ligo monolithic fused silica suspension. *Class. Quantum Grav.*, 29(3):035003, 2012.

[153] N. A. Robertson for the LSC. Seismic isolation and suspension systems for advanced ligo. *Proceedings of SPIE*, 5500:81, 2004.

[154] Peter R. Saulson. Terrestrial gravitational noise on a gravitational wave antenna. *Phys. Rev. D*, 30:732–736, 1984.

[155] Gregory M Harry, Matthew R Abernathy, Andres E Becerra-Toledo, Helena Armandula, Eric Black, Kate Dooley, Matt Eichenfield, Chinyere Nwabugwu, Akira Villar, D R M Crooks, Gianpietro Cagnoli, Jim Hough, Colin R How, Ian MacLaren, Peter Murray, Stuart Reid, Sheila Rowan, Peter H Sneddon, Martin M Fejer, Roger Route, Steven D Penn, Patrick Ganau, Jean-Marie Mackowski, Christophe Michel, Laurent Pinard, and Alban Remillieux. Titania-doped tantala/silica coatings for gravitational-wave detection. *Class. Quantum Grav.*, 24(2):405, 2007.

[156] T. Hong, H. Yang, E. K. Gustafson, R. Adhikari, and Y. Chen. Brownian thermal noise in multlayer coated mirrors. *in prep.*, 2012. in prep.

[157] Jonathan Cripe, Nancy Aggarwal, Robert Lanza, Adam Libson, Robinjeet Singh, Paula Heu, David Follman, Garrett D Cole, Nergis Mavalvala, and Thomas Corbitt. Measurement of quantum back action in the audio band at room temperature. *Nature*, 568(7752):364, 2019.

[158] Min Jet Yap, Jonathan Cripe, Georgia L Mansell, Terry G McRae, Robert L Ward, Bram J J Slagmolen, Paula Heu, David Follman, Garrett D Cole, Thomas Corbitt, and David E McClelland. Broadband reduction of quantum radiation pressure noise via squeezed light injection. *Nature Photonics*, 14(1):19, 2020.

[159] Haocun Yu et al. Quantum correlations between the light and kilogram-mass mirrors of LIGO. *arXiv: 2002.01519*, 2020.

[160] T P Purdy, P-L Yu, R W Peterson, N S Kampel, and C A Regal. Strong Optomechanical Squeezing of Light. *Phys. Rev. X*, 3(3):031012, September 2013.

[161] Nancy Aggarwal, Torrey Cullen, Jonathan Cripe, Garrett D. Cole, Robert Lanza, Adam Libson, David Follman, Paula Heu, Thomas Corbitt, and Nergis Mavalvala. Room temperature optomechanical squeezing. *arXiv: 1812.09942*, 2018.

[162] Mikhail Korobko, Yiqiu Ma, Yanbei Chen, and Roman Schnabel. Quantum expander for gravitational-wave observatories. *Light: Science & Applications*, 8:118, 2019.

[163] Mikhail Korobko, F.Ya. Khalili, and Roman Schnabel. Engineering the optical spring via intra-cavity optical-parametric amplification. *Physics Letters A*, 2017.

[164] Kentaro Somiya. Current status of the intracavity OPO experiments at Tokyo Tech. *LIGO DCC-G2000950*, 2020.

[165] Minchuan Zhou, Zifan Zhou, and Selim M. Shahriar. Quantum noise limits in white-light-cavity-enhanced gravitational wave detectors. *Phys. Rev. D*, 92:082002, Oct 2015.

[166] Yiqiu Ma, Haixing Miao, Chunnong Zhao, and Yanbei Chen. Quantum noise of a white-light cavity using a double-pumped gain medium. *Phys. Rev. A*, 92:023807, Aug 2015.

[167] Minchuan Zhou, Zifan Zhou, and Selim M. Shahriar. Catastrophic breakdown of the caves model for quantum noise in some phase-insensitive linear amplifiers or attenuators based on atomic systems. *Phys. Rev. A*, 93:033858, Mar 2016.

[168] Haixing Miao, Yiqiu Ma, Chunnong Zhao, and Yanbei Chen. Enhancing the bandwidth of gravitational-wave detectors with unstable optomechanical filters. *Phys. Rev. Lett.*, 115:211104, Nov 2015.

[169] Joe Bentley, Hendra Nurdin, Yanbei Chen, and Haixing Miao. A direct approach to realising quantum filters for high-precision measurements. *arXiv: 2002.07644*, feb 2020.

[170] Xiang Li, Rana X Adhikari, Yanbei Chen, Michael Tobar, and Chunnong Zhao. Broadband sensitivity improvement via coherent quantum feedback with PT symmetry. *LIGO DCC-G2000405*, 2020.

[171] Joe Bentley, Philip Jones, Denis Martynov, Andreas Freise, and Haixing Miao. Converting the signal-recycling cavity into an unstable optomechanical filter to enhance the detection bandwidth of gravitational-wave detectors. *Phys. Rev. D*, 99(10):102001, 2019.

[172] Yiqiu Ma, Shtefan L. Danilishin, Chunnong Zhao, Haixing Miao, W. Zach Korth, Yanbei Chen, Robert L. Ward, and D. G. Blair. Narrowing the filter-cavity bandwidth in gravitational-wave detectors via optomechanical interaction. *Phys. Rev. Lett.*, 113:151102, Oct 2014.

[173] Eugeniy E. Mikhailov, Keisuke Goda, Thomas Corbitt, and Nergis Mavalvala. Frequency-dependent squeeze-amplitude attenuation and squeeze-angle rotation by electromagnetically induced transparency for gravitational-wave interferometers. *Phys. Rev. A*, 73:053810, 2006.

[174] Minchuan Zhou, Zifan Zhou, and Selim M. Shahriar. Realizing the GEIT system using Zeeman sublevels in Rb for enhancing the sensitivity-bandwidth product in next generation LIGO, 2016.

[175] Mankei Tsang and Carlton M Caves. Coherent Quantum-Noise Cancellation for Optomechanical Sensors. *Phys. Rev. Lett.*, 105(12):123601, 2010.

[176] Maximilian H. Wimmer, Daniel Steinmeyer, Klemens Hammerer, and Michéle Heurs. Coherent cancellation of backaction noise in optomechanical force measurements. *Phys. Rev. A*, 89(5), 2014.

[177] Lu-Ming Duan, J. I. Cirac, P. Zoller, and E. S. Polzik. Quantum communication between atomic ensembles using coherent light. *Phys. Rev. Lett.*, 85:5643–5646, Dec 2000.

[178] Brian Julsgaard, Alexander Kozhekin, and Eugene S. Polzik. Experimental long-lived entanglement of two macroscopic objects. *Nature*, 413(6854):400–403, sep 2001.

[179] F. Ya. Khalili and E. S. Polzik. Overcoming the Standard Quantum Limit in Gravitational Wave Detectors Using Spin Systems with a Negative Effective Mass. *Phys. Rev. Lett.*, 121(3):031101, 2018.

[180] Emil Zeuthen, Eugene S. Polzik, and Farid Ya. Khalili. Gravitational wave detection beyond the standard quantum limit using a negative-mass spin system and virtual rigidity. *Phys. Rev. D*, 100(6):062004, 2019.

[181] Yu. Levin. Internal thermal noise in the ligo test masses: A direct approach. *Phys. Rev. D*, 57:659–663, 1998.

[182] W A Phillips. Two-level states in glasses. *Reports on Progress in Physics*, 50:1657, 1987.

[183] Spectral Shape of Relaxations in Silica Glass. *Physical Review Letters*, 84:2718, 2000.

[184] S. Chao et al. Low loss dielectric mirrors with ion beam sputtered $tio_2 - sio_2$ mixed films. *Opt. Lett*, 40:2177, 2001.

[185] S.V. Ushakov et al. Crystalization in hafnia and zirconia based systems. *Phys. Stat. Sol*, 241:2268, 2004.

[186] S. Chao et al. Thickness-dependent crystallization on thermal anneal for the titania/silica nano-layers deposited by ion-beam-sputter method. LIGO Document: LIGO G1300921.

[187] M. Liu et al. Microstructure and interfacial properties of hfo_2/al_2o_3 nanolaminate films. *Appl. Surf. Sci.*, 252:6206, 2006.

[188] M Abernathy, A Amato, A Ananyeva, S Angelova, B Baloukas, R Bassiri, G Billingsley, R Birney, G Cagnoli, M Canepa, M Coulon, J Degallaix, A Di Michele, M A Fazio, M M Fejer, D Forest, C Gier, M Granata, A M Gretarsson, E M Gretarsson, E Gustafson, E J Hough, M Irving, É Lalande, C Lévesque, A W Lussier, A Markosyan, I W Martin,

L Martinu, B Maynard, C S Menoni, C Michel, P G Murray, C Osthelder, S Penn, L Pinard, K Prasai, S Reid, R Robie, S Rowan, B Sassolas, F Schiettekatte, R Shink, S Tait, J Teillon, G Vajente, M Ward, and L Yang. Exploration of co-sputtered ta$_2$o$_5$-zro$_2$ thin films for gravitational-wave detectors. *Classical and Quantum Gravity*, 38(19):195021, sep 2021.

[189] Emile Lalande, Alexandre W. Lussier, Carl Lévesque, Marianne Ward, Bill Baloukas, Ludvik Martinu, Gabriele Vajente, Garilynn Billingsley, Alena Ananyeva, Riccardo Bassiri, Martin M. Fejer, and François Schiettekatte. Zirconia-titania-doped tantala optical coatings for low mechanical loss bragg mirrors. *Journal of Vacuum Science & Technology A*, 39(4):043416, 2021.

[190] R. Bassiri. Coating atomic structure investigations at stanford and glasgow, 2013.

[191] G Vajente, R Birney, A Ananyeva, S Angelova, R Asselin, B Baloukas, R Bassiri, G Billingsley, M M Fejer, D Gibson, L J Godbout, E Gustafson, A Heptonstall, J Hough, S MacFoy, A Markosyan, I W Martin, L Martinu, P G Murray, S Penn, S Roorda, S Rowan, F Schiettekatte, R Shink, C Torrie, D Vine, S Reid, and R X Adhikari. Effect of elevated substrate temperature deposition on the mechanical losses in tantala thin film coatings. *Classical and Quantum Gravity*, 35(7):075001, feb 2018.

[192] Rosalie Shink. Caracterisation et optimisation des parametres physiques du ta2o5 affectant le facteur de qualite de miroirs dielectriques, 2019.

[193] Steven D Penn, Peter H Sneddon, Helena Armandula, Joseph C Betzwieser, Gianpietro Cagnoli, Jordan Camp, D R M Crooks, Martin M Fejer, Andri M Gretarsson, Gregory M Harry, Jim Hough, Scott E Kittelberger, Michael J Mortonson, Roger Route, Sheila Rowan, and Christophoros C Vassiliou. Mechanical loss in tantala/silica dielectric mirror coatings. *Class. Quantum Grav.*, 20(13):2917, 2003.

[194] I. Pinto et al. Interdiffused coatings. LIGO Document G-1200976.

[195] Laurent Pinard, C. Michel, B. Sassolas, L. Balzarini, J. Degallaix, J. Dolique, R. Flaminio, D. Forest, M. Granata, B. Lagrange, N. Straniero, J. Teillon, and G. Cagnoli. The mirrors used in the ligo interferometers for the first-time detection of gravitational waves. In *Optical Interference Coatings 2016*, page MB.3. Optical Society of America, 2016.

[196] V. B. Braginsky, M. L. Gorodetsky, and S. P. Vyatchanin. Thermodynamical fluctuations and photo-thermal shot noise in gravitational wave antennae. *Phys. Lett. A*, 264:1, 1999.

[197] V. B. Braginsky, M. L. Gorodetsky, and S. P. Vyatchanin. Thermo-refractive noise in gravitational wave antennae. *Phys. Lett. A*, 271:303, 2000.

[198] Yuri Levin. Fluctuation-dissipation theorem for thermo-refractive noise. *Physics Letters A*, 372(12):1941 – 1944, 2008.

[199] M. Evans, S. Ballmer, M. Fejer, P. Fritschel, G. Harry, and G. Ogin. Thermo-optic noise in coated mirrors for high-precision optical measurements. *Phys. Rev. D*, 78:102003, 2008.

[200] Gregory H Ogin. *Measurement of thermo-optic properties of thin film dielectric coatings*. California Institute of Technology, 2013.

[201] Tara Chalermsongsak, Evan D Hall, Garrett D Cole, David Follman, Frank Seifert, Koji Arai, Eric K Gustafson, Joshua R Smith, Markus Aspelmeyer, and Rana X Adhikari. Coherent cancellation of photothermal noise in gaas/al0. 92ga0. 08as bragg mirrors. *Metrologia*, 53(2):860, 2016.

[202] VB Braginsky and SP Vyatchanin. Thermodynamical fluctuations in optical mirror coatings. *Physics Letters A*, 312(3-4):244–255, 2003.

[203] M Naci Inci. Simultaneous measurements of the thermal optical and linear thermal expansion coefficients of a thin film etalon from the reflection spectra of a superluminescent diode. *Journal of Physics D: Applied Physics*, 37(22):3151, 2004.

[204] DRM Crooks, G Cagnoli, MM Fejer, A Gretarsson, G Harry, J Hough, N Nakagawa, S Penn, R Route, S Rowan, et al. Experimental measurements of coating mechanical loss factors. *Classical and Quantum Gravity*, 21(5):S1059, 2004.

[205] Andri Gretarsson. Thermo-optic noise from doped tantala/silica coatings. *LIGO DCC, pages G080151–00*, 2008.

[206] Eda Çetinörgü, Bill Baloukas, Oleg Zabeida, Jolanta E Klemberg-Sapieha, and Ludvik Martinu. Mechanical and thermoelastic characteristics of optical thin films deposited by dual ion beam sputtering. *Applied optics*, 48(23):4536–4544, 2009.

[207] Huang-Wei Pan, Shun-Jin Wang, Ling-Chi Kuo, Shiuh Chao, Maria Principe, Innocenzo M. Pinto, and Riccardo DeSalvo. Thickness-dependent crystallization on thermal anneal for titania/silica nm-layer composites deposited by ion beam sputter method. *Opt. Express*, 22(24):29847–29854, Dec 2014.

[208] R. Bassiri, K. B. Borisenko, D. J. H. Cockayne, J. Hough, I. MacLaren, and S. Rowan. Probing the atomic structure of amorphous ta2o5 coatings. *Applied Physics Letters*, 98(3):031904, 2011.

[209] R Bassiri, K Evans, KB Borisenko, MM Fejer, J Hough, I MacLaren, IW Martin, RK Route, and S Rowan. Correlations between the mechanical loss and atomic structure of amorphous tio2-doped ta2o5 coatings. *Acta Materialia*, 61(4):1070–1077, 2013.

[210] Riccardo Bassiri, Franklin Liou, Matthew R Abernathy, Angie C Lin, Namjun Kim, Apurva Mehta, Badri Shyam, Robert L Byer, Eric K Gustafson, Martin Hart, et al. Order within disorder: The atomic structure of ion-beam sputtered amorphous tantala (a-ta2o5). *APL materials*, 3(3):036103, 2015.

[211] Riccardo Bassiri, Matthew R Abernathy, Franklin Liou, Apurva Mehta, Eric K Gustafson, Martin J Hart, Hafizah N Isa, Namjun Kim, Angie C Lin, Ian MacLaren, et al. Order, disorder and mixing: The atomic structure of amorphous mixtures of titania and tantala. *Journal of Non-Crystalline Solids*, 438:59–66, 2016.

[212] Badri Shyam, Kevin H Stone, Riccardo Bassiri, Martin M Fejer, Michael F Toney, and Apurva Mehta. Measurement and modeling of short and medium range order in amorphous ta 2 o 5 thin films. *Scientific reports*, 6:32170, 2016.

[213] Martin J Hart, Riccardo Bassiri, Konstantin B Borisenko, Muriel Véron, Edgar F Rauch, Iain W Martin, Sheila Rowan, Martin M Fejer, and Ian MacLaren. Medium range structural order in amorphous tantala spatially resolved with changes to atomic structure by thermal annealing. *Journal of Non-Crystalline solids*, 438:10–17, 2016.

[214] J. P. Trinastic, R. Hamdan, Y. Wu, L. Zhang, and Hai-Ping Cheng. Unified inter-atomic potential and energy barrier distributions for amorphous oxides. *The Journal of Chemical Physics*, 139(15):154506, 2013.

[215] Jonathan P Trinastic, Rashid Hamdan, Chris Billman, and Hai-Ping Cheng. Molecular dynamics modeling of mechanical loss in amorphous tantala and titania-doped tantala. *Physical Review B*, 93(1):014105, 2016.

[216] K. Prasai, J. Jiang, A. Mishkin, B. Shyam, S. Angelova, R. Birney, D. A. Drabold, M. Fazio, E. K. Gustafson, G. Harry, S. Hoback, J. Hough, C. Lévesque, I. MacLaren, A. Markosyan, I. W. Martin, C. S. Menoni, P. G. Murray, S. Penn, S. Reid, R. Robie, S. Rowan, F. Schiettekatte, R. Shink, A. Turner, G. Vajente, H-P. Cheng, M. M. Fejer, A. Mehta, and R. Bassiri. High precision detection of change in intermediate range order of amorphous zirconia-doped tantala thin films due to annealing. *Phys. Rev. Lett.*, 123:045501, Jul 2019.

[217] Le Yang, Gabriele Vajente, Mariana Fazio, Alena Ananyeva, GariLynn Billingsley, Ashot Markosyan, Riccardo Bassiri, Kiran Prasai, Martin M. Fejer, and Carmen S. Menoni. Enhanced medium range order in vapor deposited germania glasses at elevated temperatures, 2021.

[218] Gabriele Vajente. Low thermal noise tio2-doped geo2 coatings for high sensitivity gravitational wave interferometers. *https://dcc.ligo.org/LIGO-P2100075*, 2021.

[219] Carl Lévesque, Sjoerd Roorda, François Schiettekatte, and Normand Mousseau. Internal mechanical dissipation mechanisms in amorphous silicon. *Physical Review X, accepted*, 2022.

[220] Sadanand Singh, Mark D Ediger, and Juan J De Pablo. Ultrastable glasses from in silico vapour deposition. *Nature materials*, 12(2):139, 2013.

[221] Ivan Lyubimov, Mark D Ediger, and Juan J de Pablo. Model vapor-deposited glasses: Growth front and composition effects. *The Journal of chemical physics*, 139(14):144505, 2013.

[222] S. Gras, H. Yu, W. Yam, D. Martynov, and M. Evans. Audio-band coating thermal noise measurement for advanced ligo with a multimode optical resonator. *Phys. Rev. D*, 95:022001, Jan 2017.

[223] G. Cole S. Penn, G. Harry. Both time and financial budget for developing 30 cm algaas coatings based on engineering study with freiberger and quote from evg in march 2020, 2020.

[224] M. Principe et al. Chapter 12, reflectivity and thickness optimization. In G. Harry et al., editors, *Optical Coatings and Thermal Noise in Precision Measurements*. Cambridge University Press, 2012.

[225] A.E. Villar et al. Measurement of thermal noise in multilayer coatings with optimized layer thicknesses. *Phys. Rev. D*, 81:122001, 2010.

[226] William Yam, Slawek Gras, and Matthew Evans. Multimaterial coatings with reduced thermal noise. *Phys. Rev. D*, 91:042002, Feb 2015.

[227] Jessica Steinlechner, Iain W. Martin, Jim Hough, Christoph Krüger, Sheila Rowan, and Roman Schnabel. Thermal noise reduction and absorption optimization via multimaterial coatings. *Phys. Rev. D*, 91:042001, Feb 2015.

[228] Jessica Steinlechner and Iain W. Martin. How can amorphous silicon improve current gravitational-wave detectors? *Phys. Rev. D*, 103:042001, Feb 2021.

[229] Jessica Steinlechner and Iain W. Martin. High index top layer for multimaterial coatings. *Phys. Rev. D*, 93:102001, May 2016.

[230] M. Evans, L. Barsotti, and P. Fritschel. A general approach to optomechanical parametric instabilities. *Phys. Lett. A*, 374(4):665–671, 2010.

[231] C. Zhao et al. *Phys. Rev. Lett.*, 4:121102, 2005.

[232] S. Gras et al. *Class. Quantum Grav.*, 27:205019, 2010.

[233] S. Strigin et al. *Phys. Lett. A*, 372:5727, 2008.

[234] Brian Lantz. Simple calculations for charge noise for advanced ligo. *LIGO Document: LIGO-T080214*, 2010.

[235] Rainer Weiss. Note on electrostatics in the ligo suspensions. *LIGO Document: LIGO-T960137*, 1996.

[236] Dennis Ugolini and Colin Fitzgerald. Developing a charging testbed in an advanced ligo geometry. *LIGO Document: LIGO-G1200853*, 2012.

[237] Valery Mitrofanov and Leonid Prokhorov. Space charge polarization in fused silica test masses of gravitational wave detector associated with the electrostatic drive. *LIGO Document: LIGO-P1000077*, 2010.

[238] Rainer Weiss. ionic_neutralization. *LIGO Document: LIGO-G1000383*, 2010.

[239] Dennis Ugolini. Discharging optics with ionized gases. *LIGO Document: LIGO-T1000135*, 2010.

[240] Rainer Weiss. Surface charge control of the advanced ligo mirrors using externally introduced ions. *LIGO Document: LIGO-T1100332*, 2011.

[241] J. Gundlach. Charge management with uv leds, 2010.

[242] P. Campsie. Development of a torsion balance for measuring charging noise, 2011.

[243] P. Campsie. Measurements of charging noise with a torsion balance, 2013.

[244] P. Campsie. A measurement of instrument noise created by fluctuating electrostatic charges on dielectric surfaces using a torsion balance, 2013.

[245] L. Prokhorov. Experimental setup for measurement of fluctuating force acting between fused silica torsional oscillator and electrostatic drive, 2012.

[246] Iain W Martin, E Chalkley, R Nawrodt, H Armandula, R Bassiri, C Comtet, MM Fejer, A Gretarsson, G Harry, D Heinert, et al. Comparison of the temperature dependence of the mechanical dissipation in thin films of ta2o5 and ta2o5 doped with tio2. *Classical and Quantum Gravity*, 26(15):155012, 2009.

[247] Iain W Martin, R Bassiri, R Nawrodt, MM Fejer, A Gretarsson, E Gustafson, G Harry, J Hough, I MacLaren, S Penn, et al. Effect of heat treatment on mechanical dissipation in ta2o5 coatings. *Classical and Quantum Gravity*, 27(22):225020, 2010.

[248] G. D. Cole, W. Zhang, M. J. Martin, J. Ye, and M. Aspelmeyer. Tenfold reduction of Brownian noise in optical interferometry. *ArXiv e-prints*, February 2013.

[249] Garrett D Cole, Wei Zhang, Michael J Martin, Jun Ye, and Markus Aspelmeyer. Tenfold reduction of brownian noise in high-reflectivity optical coatings. *Nature Photonics*, 7(8):644, 2013.

[250] Angie C Lin, Riccardo Bassiri, Suraya Omar, Ashot S Markosyan, Brian Lantz, Roger Route, Robert L Byer, James S Harris, and Martin M Fejer. Epitaxial growth of gap/algap mirrors on si for low thermal noise optical coatings. *Optical Materials Express*, 5(8):1890–1897, 2015.

[251] AV Cumming, K Craig, IW Martin, R Bassiri, L Cunningham, MM Fejer, JS Harris, K Haughian, D Heinert, B Lantz, et al. Measurement of the mechanical loss of prototype gap/algap crystalline coatings for future gravitational wave detectors. *Classical and Quantum Gravity*, 32(3):035002, 2015.

[252] Iain W Martin, Ronny Nawrodt, Kieran Craig, Christian Schwarz, Riccardo Bassiri, Gregory Harry, James Hough, Steven Penn, Stuart Reid, Raymond Robie, et al. Low temperature mechanical dissipation of an ion-beam sputtered silica film. *Classical and Quantum Gravity*, 31(3):035019, 2014.

[253] Peter G. Murray, Iain W. Martin, Kieran Craig, James Hough, Raymond Robie, Sheila Rowan, Matt R. Abernathy, Teal Pershing, and Steven Penn. Ion-beam sputtered amorphous silicon films for cryogenic precision measurement systems. *Phys. Rev. D*, 92:062001, Sep 2015.

[254] R. Birney, J. Steinlechner, Z. Tornasi, S. MacFoy, D. Vine, A. S. Bell, D. Gibson, J. Hough, S. Rowan, P. Sortais, S. Sproules, S. Tait, I. W. Martin, and S. Reid. Amorphous silicon with extremely low absorption: Beating thermal noise in gravitational astronomy. *Phys. Rev. Lett.*, 121:191101, Nov 2018.

[255] J. Steinlechner, I. W. Martin, A. S. Bell, J. Hough, M. Fletcher, P. G. Murray, R. Robie, S. Rowan, and R. Schnabel. Silicon-based optical mirror coatings for ultrahigh precision metrology and sensing. *Phys. Rev. Lett.*, 120:263602, Jun 2018.

[256] I.Martin et al. Mechanical loss of crystalline and amorphous coatings. GWADW 2014.

[257] Shiuh Chao, Huang-Wei Pan, and Ling-Chi Kuo. Mechanical loss of silicon nitride films grown by plasma-enhanced chemical vapor deposition (PECVD) method. *LIGO Document: LIGO-G1300171*, 2013.

[258] Shiuh Chao, Huang-Wei Pan, Yu-Hang Juang, and Shu-Yu Huang. Mechanical loss of silicon cantilever coated with a high-stress sinx film. *LIGO Document: LIGO-G1400851*, 2014.

[259] Shiuh Chao, Wen-Jie Tsai, Zhen-Li Huang, Jia-qian Wu, and YU-HSUN Kao. Preliminary results of the low refractive index silicon-oxynitride thin films. LIGO dcc.

[260] Innocenzo Pinto. nm-layered coatings: status and perspectives. ELiTES: Second general meeting 2013.

[261] Juri Agresti, Giuseppe Castaldi, Riccardo DeSalvo, Vincenzo Galdi, Vincenzo Pierro, and Innocenzo M Pinto. Optimized multilayer dielectric mirror coatings for gravitational wave interferometers. In *Advances in Thin-Film Coatings for Optical Applications III*, volume 6286, page 628608. International Society for Optics and Photonics, 2006.

[262] Akira E Villar, Eric D Black, Riccardo DeSalvo, Kenneth G Libbrecht, Christophe Michel, Nazario Morgado, Laurent Pinard, Innocenzo M Pinto, Vincenzo Pierro, Vincenzo Galdi, et al. Measurement of thermal noise in multilayer coatings with optimized layer thickness. *Physical Review D*, 81(12):122001, 2010.

[263] Kunihiko Hasegawa, Tomotada Akutsu, Nobuhiro Kimura, Yoshio Saito, Toshikazu Suzuki, Takayuki Tomaru, Ayako Ueda, and Shinji Miyoki. Molecular adsorbed layer formation on cooled mirrors and its impacts on cryogenic gravitational wave telescopes. *Phys. Rev. D*, 99:022003, Jan 2019.

[264] Jessica Steinlechner and Iain W. Martin. Thermal noise from icy mirrors in gravitational wave detectors. *Phys. Rev. Research*, 1:013008, Aug 2019.

[265] Satoshi Tanioka, Kunihiko Hasegawa, and Yoichi Aso. Optical loss study of molecular layer for a cryogenic interferometric gravitational-wave detector. *Phys. Rev. D*, 102:022009, Jul 2020.

[266] B. Lantz, R. Schofield, B. O'Reilly, D. E. Clark, and D. DeBra. Review: Requirements for a Ground Rotation Sensor to Improve Advanced LIGO. *Bulletin of the Seismological Society of America*, 99:980–989, 2009.

[267] Michael P Ross, Krishna Venkateswara, Conor Mow-Lowry, Sam Cooper, Jim Warner, Brian Lantz, Jeffrey Kissel, Hugh Radkins, Thomas Shaffer, Richard Mittleman, Arnaud Pele, and Jens Gundlach. Towards windproofing LIGO: reducing the effect of

wind-driven floor tilt by using rotation sensors in active seismic isolation. *Classical and Quantum Gravity*, 37(18):185018, aug 2020.

[268] Michael Ross. In-Vacuum Inertial Rotation Sensors. *https://dcc.ligo.org/LIGO-G2100756*, 2021.

[269] Vladimir Dergachev and Riccardo DeSalvo. A high precision mechanical ground rotation sensor . *LIGO Document: LIGO-G1200187*, 2012.

[270] Krishna Venkateswara. TiltWash: Update on tiltmeter work at UW. *LIGO Document: LIGO-G1200225*, 2012.

[271] William Korth, Alastair Heptonstall, Rana Adhikari, Eric Gustafson, and Brian Lantz. Status of the Caltech Laser Gyro. *LIGO Document: LIGO-G1200261*, 2012.

[272] M. Evans and F. Matichard. Tilt free inertial sensing. *LIGO Document: LIGO-T0900628*, 2009.

[273] Brian Lantz. Thoughts on Hanford Wind. *LIGO Document: LIGO-G1501371*, 2015.

[274] Andrew Gao, Brian Lantz, and Jim Warner. Comparing Wind-Driven Motion at LHO's Corner and End Stations Between O3a and O3b. *LIGO DCC T2100269*, 2021.

[275] David Tshilumba, LK Nuttall, Tim Mac Donald, Rich Mittleman, Brian Lantz, Fabrice Matichard, and Christophe Collette. Vibration analysis and control of the ligo observatories large chambers and support piers. In *PROCEEDINGS OF ISMA2014 INCLUDING USD2014*, pages 187–200, 2014.

[276] T. MacDonald. BSC HEPI Motion Measurements and Modeling. *LIGO Document: LIGO-G1401167*, 2014.

[277] Jenne Driggers, Valery Frolov, Dani Atkinson, Haixing Miao, Michael Landry, Rana Adhikari, and Ryan DeRosa. Global feed-forward vibration isolation in a km scale interferometer. *LIGO-Document: LIGO-P1000088*, 2010.

[278] Thomas Dehaeze, Mohit Verma, and Christophe Collette. Complementary filters shaping using h-infinity synthesis. In *Proc. of the 7th Int. Conf. on Control, Mechatronics and Automation*, pages 457–461. IEEE, 2019.

[279] Brett Noah Shapiro. *Adaptive Modal Damping for Advance LIGO Suspensions*. PhD thesis, Massachusetts Institute of Technology, 2012.

[280] Christophe Collette, Guoying Zhao, Binlei Ding, and Jennifer Watchi. Study of mimo control laws for seismic isolation of flexible payload. *LIGO Document: LIGO-P1900212*, 2019.

[281] Ruslan Kurdyumov, Christopher Kucharczyk, and Brian Lantz. Blend Switching User Guide. *LIGO-Document: LIGO-T1200126*, 2012.

[282] M. Coughlin et al. Earthquake monitoring for aLIGO. *LIGO Document: LIGO-G1400811*, 2014.

[283] Nikhil Mukund. update on lockloss monitoring & prediction. 2018. LIGO-G1800569.

[284] Brian Lantz, Sebastien Biscans, Jim Warner, Arnaud Pele, Hugh Radkins, Nikhil Mukund, and Michael Coughlin. Seismic control during earthquakes: Review of new technique. 2018. LIGO-G1800399.

[285] Eyal Schwartz, Arnaud Pele, Jim Warner, Brian Lantz, Joseph Betzwieser, Katherine Dooley, Sebastien Biscans, Michael Coughlin, Nikhil Mukund, et al. Improving Robustness of the LIGO Detectors to Earthquakes. *LIGO DCC-P2000072*, 2020.

[286] Christophe Collette and Fabrice Matichard. Sensor fusion methods for high performance active vibration isolation systems. *Journal of Sound and Vibration*, (P1400022), 2014.

[287] Christophe Collette and Fabrice Matichard. Vibration control of flexible structures using fusion of inertial sensors and hyper-stable actuator/sensor pairs. *LIGO Document: LIGO-P1400099*, 2014.

[288] Kuo-Feng Jimson Tseng. System Failure Diagnosis for the Advanced LIGO HAM Chamber Seismic Isolation System. *LIGO Document: LIGO-P1000086*, 2010.

[289] B N Shapiro, R Adhikari, J Driggers, J Kissel, B Lantz, J Rollins, and K Youcef-Toumi. Noise and control decoupling of advanced ligo suspensions. *Classical and Quantum Gravity*, 32(1):015004, 2015.

[290] Edgard Bonilla. Improving darm with isi -> sus feedforward. 2018. LIGO-G18003467.

[291] Peter Fritschel and Brian Lantz. Report on the Low Frequency Workshop, April 6 & 7, 2021. *LIGO DCC L2100055*, 2021.

[292] Rate of scattering glitches as a function of microseism. https://alog.ligo-la.caltech.edu/aLOG/index.php?callRep=51613. Accessed: 2020.

[293] Sam Cooper, Arnaud Pele, Conor Mow-Lowry, Jim Warner, Rich Mittleman, Jeffry Kissel, and Brian Lantz. Modeling of Ham ISIs. *LIGO DCC T1800092*, 2018.

[294] Sam Cooper, Brian Lantz, Jim Warner, Chiara DiFronzo, and Conor Mow-Lowry. Modeling of Ham ISIs. *LIGO DCC T1900107*, 2019.

[295] Chiara DiFronzo, Conor Mow-Lowry, and Sam Cooper. Reducing differential motion of Advanced LIGO seismic platforms to improve interferometer control signals:analysis of feasibility. *LIGO DCC T2000365*, 2020.

[296] Full diff cps seems to help for high wind, even if microseism is bad. https://alog.ligo-wa.caltech.edu/aLOG/index.php?callRep=54322. Accessed: 2020.

[297] Darm doesn't seem to be strongly affected by cps diff controls. https://alog.ligo-wa.caltech.edu/aLOG/index.php?callRep=54775. Accessed: 2020.

[298] Hoqi damping at m2. https://alog.ligo-la.caltech.edu/SEI/index.php?callRep=1732. Accessed: 2021.

[299] B. Lantz. Measurements and mysteries of the srcl noise, 2021.

[300] B. Sorazu et al. Characterisation of the aligo monolithic suspensions. *LIGO G1601163*, 2016.

[301] G. D. Hammond et al. Suspension activities in glasgow. *LIGO G1800423*, 2018.

[302] Peter Fritschel. Potential Advanced LIGO post-Project upgrades. Technical Report T1300176, LIGO Laboratory, Mar 2013.

[303] Norna Robertson. Beamsplitter Actuation: A Note on Sweetspot Positioning and Magnet Size Considerations. *LIGO Document: LIGO-T1600328*, 2016.

[304] Norna A Robertson, Harrison Miller, and Calum Torrie. Risk reduction work on advanced ligo suspensions. *LIGO Document: LIGO-G1400804*, 2014.

[305] Norna Robertson and Mark Barton. Design of a Larger Beamsplitter Suspension. *LIGO Document: LIGO-T1400296*, 2014.

[306] Norna Robertson and Harrison Miller. Revised Design of HSTS with Improved Vertical Isolation. *LIGO Document: LIGO-T1400290*, 2014.

[307] Norna Robertson. Relook at Signal Recycling Cavity Displacement Noise. *LIGO Document: LIGO-T1500323*, 2015.

[308] Norna Robertson, Calum Torrie, Eddie Sanchez, and Rich Abbott. BRDs for HSTS: Design, Results and Conclusions. *LIGO Document: LIGO-T1700111*, 2017.

[309] Norna Robertson, Calum Torrie, and Eddie Sanchez. BRDs for HLTS: Design, Results and Conclusions. *LIGO Document: LIGO-T1700155*, 2017.

[310] N. A. Robertson and J. Hough. Gas Damping in Advanced LIGO Suspensions. *LIGO Document: LIGO-T0900416-v2*, 2009.

[311] A. Cavalleri, G. Ciani, R. Dolesi, A. Heptonstall, M. Hueller, D. Nicolodi, S. Rowan, D. Tombolato, S. Vitale, P. J. Wass, and W. J. Weber. Increased Brownian Force Noise from Molecular Impacts in a Constrained Volume. *Phys. Rev. Lett.*, 103:140601, 2009.

[312] R. Dolesi, M. Hueller, D. Nicolodi, D. Tombolato, S. Vitale, P. J. Wass, W. J. Weber, M. Evans, P. Fritschel, R. Weiss, J. H. Gundlach, C. A. Hagedorn, S. Schlamminger, G. Ciani, and A. Cavalleri. Brownian force noise from molecular collisions and the sensitivity of advanced gravitational wave observatories. *Phys. Rev. D*, 84:063007, 2011.

[313] GariLynn Billingsley, Norna Robertson, and Brett Shapiro. Annular End Reaction Mass Conceptual/Final Design Document. *LIGO Document: LIGO-E1500264*, 2015.

[314] Norna Robertson and Calum Torrie. Recent Results and Conclusions from Tests of the UIM Blade Non-Magnetic Damper. *LIGO Document: LIGO-T1600046*, 2016.

[315] Norna Robertson and Calum Torrie. A Tale of Two Dampers: Bounce and Roll Mode Damping for the Quads. *LIGO Document: LIGO-G1600371*, 2016.

[316] Norna Robertson, Peter Fritschel, Brett Shapiro, Calum Torrie, and Matt Evans. Design of a Tuned Mass Damper for High Quality Factor Suspension Modes in Advanced LIGO. *Review of Scientific Instruments*, 88(3):035117, 2017.

[317] Marie Kasprzack, Norna Robertson, and Calum Torrie. BS BRD installation update. *LIGO DCC G2001699*, 2020.

[318] Marie Kasprzack and Norna Robertson. BS BRDS Status Update. *LIGO DCC G200539*, 2020.

[319] R. Mittleman et al. Violin mode damper. *LIGO document G1701702*, 2017.

[320] Norna A Robertson. Simple model for analysing passive violin mode damping. *LIGO document T1800161*, 2018.

[321] B. Sorazu, K. A. Strain, I. S. Heng, , and R. Kumar. Violin mode amplitude glitch monitor for the presence of excess noise on the monolithic silica suspensions of geo 600. *Class. Quantum Grav.*, 27:155017, 2010.

[322] Xiaoyue Ni, Eric Quintero, and Gabriele Vajente. Proposal for an upgrade of the crackle experiment. *LIGO Document: LIGO-T1400407*, 2014.

[323] G. Vajente, E. A. Quintero, X. Ni, K. Arai, E. K. Gustafson, N. A. Robertson, E. J. Sanchez, J. R. Greer, and R. X. Adhikari. An instrument to measure mechanical upconversion phenomena in metals in the elastic regime. *Review of Scientific Instruments*, 87(6), 2016.

[324] G Vajente. Crackling noise in advanced gravitational wave detectors: A model of the steel cantilevers used in the test mass suspensions. *Phys. Rev D*, 96:022003, 2017.

[325] G Vajente. Crackling noise scaling: from the crackle2 experiment to the quad suspension. *LIGO document G1700347*, 2017.

[326] Norna Robertson and Calum Torrie. Redesign of blades for improved vertical isolation for triple suspensions in advanced ligo. *LIGO Document: LIGO-T080267*, 2008.

[327] M. Barsanti, M. Beghini, F. Frasconi, R. Ishak, B. D. Monelli, R. Valentini. Experimental study of hydrogen embrittlement in maraging steels. *Procedia Structural Integrity*, 2018.

[328] Damping cryobaffle - two options. https://alog.ligo-la.caltech.edu/aLOG/index.php?callRep=53868. Accessed: 2020.

[329] M.P. Ross and et al. Low frequency tilt seismology with a precision ground rotation sensor. *arXiv:1707.03084*, 2018.

[330] M. Zucker et al. The a+ upgrade: Expanding the advanced ligo horizon. *LIGO Document: LIGO-M1800040*, 2018.

[331] M. Zucker et al. A+ overview. *LIGO Document: LIGO-G1800514*, 2018.

[332] Mark Barton, Adam Huddart, and Joseph Odell. A+UK WP3 HRTS Document Tree. *https://dcc.ligo.org/LIGO-E2000149*, 2020.

[333] Kyung-ha Lee, Giles Hammond, James Hough, Russell Jones, Sheila Rowan, and Alan Cumming. Improved fused silica fibres for the advanced ligo monolithic suspensions. *Classical and Quantum Gravity*, in press, 2019.

[334] Y. Aso, M. Ando, K. Kawabe, S. Otsuka, and K. Tsubono. Stabilization of a Fabry–Perot interferometer using a suspension-point interferometer. *Phys. Lett. A*, 327(1):1–8, 2004.

[335] Daniel Clark, Brian Lantz, and Dan DeBra. Seismic Platform Interferometer - Progress at Stanford. *LIGO Document: LIGO-G1200178*, 2012.

[336] Daniel Clark. Control of Differential Motion Between Adjacent Advanced LIGO Seismic Isolation Platforms. Technical Report P1300043, LIGO Laboratory, Mar 2013.

[337] K. Dahl, A. Bertolini, M. Born, Y Chen, D Gering, S Goßler, C. Gräf, G. Heinzel, S. Hild, F. Kawazoe, O. Kranz, G Kühn, H. Lück, K. Mossavi, R. Schnabel, K. Somiya, K. A. Strain, J. R. Taylor, A. Wanner, T. Westphal, B. Willke, and K. Danzmann. Towards a Suspension Platform Interferometer for the AEI 10 m Prototype Interferometer. *J. Phys.: Conf. Ser.*, 228:012027, 2010.

[338] Sheon Chua and Bram Slagmolen. Sensing seismic platform relative motion using Digital Interferometry. *https://dcc.ligo.org/LIGO-G2100987*, 2021.

[339] Sheon Chua and Bram Slagmolen. Relative Platform Sensing using Digital Interferometry - Prospectives. *https://dcc.ligo.org/LIGO-G2100765*, 2021.

[340] J. Kissel. Displacement noise comparison between srm and fc1 suspoint displacement. aLIGO LHO Logbook log 64466, 2022.

[341] E. Bonilla. State estimators for integrated sei-sus control, 2022.

[342] Jennfier Watchi, Sam Cooper, Binlei Ding, Conor Mow-Lowry, and Christophe Collette. A review of compact interferometers. *Review of Scientific Instruments*, 89:121501, 2018.

[343] S. J. Cooper, C. J. Collins, A. C. Green, D. Hoyland, C. C. Speake, A. Freise and C. M. Mow-Lowry. A compact, large-range interferometer for precision measurement and inertial sensing. *Classical and Quantum Gravity]*, 35:095007, 2018.

[344] Jesse Dongen, Sam Cooper, and Conor Mow-Lowry. Mechanical Design of a HoQI Interferometer for the LIGO Big Beamsplitter Suspension. *https://dcc.ligo.org/LIGO-G2100400*, 2021.

[345] Birmingham update (swg meeting may 2021. `https://alog.ligo-la.caltech.edu/SWG/index.php?callRep=11836`. Accessed: 2021.

[346] Katharina-Sophie Isleif, Gerhard Heinzel, Moritz Mehmet, and Oliver Gerberding. Compact Multifringe Interferometry with Subpicometer Precision. *Physical Review Applied*, 12(3):034025, September 2019.

[347] Oliver Gerberding. Deep frequency modulation interferometry. *Optics Express*, 23(11):14753–14762, 2015. tex.ids: gerberding2015c.

[348] Oliver Gerberding and Katharina-Sophie Isleif. Ghost beam suppression in deep frequency modulation interferometry for compact on-axis optical heads. *Sensors*, 21(5):1708, 2021.

[349] M. Beker, G. Bobbink, B. Bouwens, N. Deelen, P. Duinker, J. van Eldik, N. de Gaay Fortman, R. van der Geer, H. van der Graaf, H. Groenstege, R. Hart, K. Hashemi, J. van Heijningen, M. Kea, J. Koopstra, X. Leijtens, F. Linde, J.A. Paradiso, H. Tolsma, and M. Woudstra. The rasnik 3-point optical alignment system. *Journal of Instrumentation*, 14(08):P08010–P08010, aug 2019.

[350] Harry van der Graaf and et al. The ultimate performance of the rasnik 3-point alignment system. *arXiv:2104.03601*, 2021.

[351] D. Martynov et al. Sensitivity of the advanced ligo detectors at the beginning of gravitational wave astronomy. *Physical Review D*, 93:112004, 2016.

[352] Y. Hang et al. Prospects for detecting gravitational waves at 5 hz with ground-based detectors. *Physical Review Letters*, 120:141102, 2018.

[353] C. M. Mow-Lowry and D. Martynov. A 6d interferometric inertial isolation system. *arXiv:1801.01468 [astro-ph.IM]*, 2018.

[354] Amit Ubhi, Jiri Smetana, Sam Cooper, Leonid Prokhorov, Haixing Miao, and Denis Martynov. Compact 6D Sensor Preliminary Results. *https://dcc.ligo.org/LIGO-G2100771*, 2021.

[355] Sam Cooper and Conor Mow-Lowry. An interferometrically sensed L4C seismometer. *https://dcc.ligo.org/P2100226*, 2021.

[356] Sam Cooper, Conor Mow-Lowry, Christopher Collins, and Chiara DiFronzo. Improving HAM ISI performance with Interferometric sensors. *https://dcc.ligo.org/LIGO-G1801759*, 2018.

[357] C Collette, F Nassif, J Amar, C Depouhon, and S-P Gorza. Prototype of interferometric absolute motion sensor. *Sensors and Actuators A: Physical*, 2015.

[358] Binlei Ding, Jennifer Watchi, Christophe Collette. Development of a high resolution optical inertial sensor. *LIGO Document: LIGO-P1800096-v1*, 2018.

[359] J.V. van Heijningen et al. A novel interferometrically read out inertial sensor for future gravitational wave detectors. *IEEE SAS proc., pp 76-80*, 2018.

[360] Binlei Ding, Jennifer Watchi, and Christophe Collette. Development of a high resolution optical inertial sensor. *LIGO Document: LIGO-P1800096*, 2018.

[361] Binlei Ding, Guoying Zhao, Jennifer Watchi, and Christopher Collette. Huddle test of optical inertial sensors combined with slightly damped mechanics. *LIGO Document: LIGO-P1800193*, 2018.

[362] Guoying Zhao, Binlei Ding, Jennifer Watchi, and Christophe Collette. Experimental study on active seismic isolation using interferometric inertial sensors. *LIGO Document: LIGO-P1900054*, 2019.

[363] Jonathan Carter, Sina Kohlenbeck, Pascal Birckigt, Ramona Eberhardt, Gerhard Heinzel, and Oliver Gerberding. A High Q, Quasi-Monolithic Optomechanical Inertial Sensor. page 4. tex.ids: carter2020.

[364] Thomas S Schwarze, Germán Fernández Barranco, Daniel Penkert, Marina Kaufer, Oliver Gerberding, and Gerhard Heinzel. Picometer-Stable Hexagonal Optical Bench to Verify LISA Phase Extraction Linearity and Precision. *Physical Review Letters*, 122(8):081104, 2019. tex.ids: schwarze2019a publisher: American Physical Society.

[365] Oliver Gerberding, Katharina-Sophie Isleif, Moritz Mehmet, Karsten Danzmann, and Gerhard Heinzel. Laser-Frequency Stabilization via a Quasimonolithic Mach-Zehnder Interferometer with Arms of Unequal Length and Balanced dc Readout. *Phys. Rev. Applied*, 7(2):024027, February 2017. tex.ids: gerberding2017.

[366] Felipe Guzmán Cervantes, Lee Kumanchik, Jon Pratt, and Jacob Taylor. High sensitivity optomechanical reference accelerometer over 10 khz. *Applied Physics Letters*, 104:221111, 2014.

[367] Binlei Ding, Jennifer Watchi, Guoying Zhao, and Christophe Collette. Development of a high resolution liquid absolute tilt-meter (lat). *LIGO Document: LIGO-T1900460*, 2019.

[368] J. J. McCann, J. Winterflood, L. Ju, and C. Zhao. A multi-orientation low-frequency rotational accelerometer. *Review of Scientific Instruments*, 92(6):064503, 2021.

[369] G. Hammond et al. Progress on silica and silicon suspensions. *LIGO Document: LIGO-G1400849*, 2014.

[370] D. Madden-Fong. LIGO III Quad Pendulum Conceptual Design Optimization. *LIGO Document: LIGO-T1300786*, 2013.

[371] Brett Shapiro. Alternative design approach for caging, sensing and control next generation suspensions. *LIGO Document: LIGO-G1601426*, 2016.

[372] A. Cumming, R. Jones, M. Barton, G. Cagnoli, C. A. Cantley, D. R. M. Crooks, G. D. Hammond, A. Heptonstall, J. Hough, S. Rowan, and K. A. Strain. Apparatus for dimensional characterization of fused silica fibers for the suspensions of advanced gravitational wave detectors. *Rev. Sci. Instrum.*, 82:044502, 2011.

[373] A. Heptonstall, M. Barton, C. Cantley, A. Cumming, G. Cagnoli, J. Hough, R. Jones, R. Kumar, I. Martin, S. Rowan, C. Torrie, and S. Zech. Investigation of mechanical dissipation in co2 laser-drawn fused silica fibres and welds. *Class. Quantum Grav.*, 27:035013, 2010.

[374] A. Heptonstall, M. A. Barton, A. Bell, G. Cagnoli, C. A. Cantley, and et al. Invited Article: CO2 laser production of fused silica fibers for use in interferometric gravitational wave detector mirror suspensions. *Rev. Sci. Insrum.*, 82:011301, 2011.

[375] L. Cunningham, P.G. Murray, A. Cumming, E.J. Elliffe, G.D. Hammond, K. Haughian, J. Hough, M. Hendry, R. Jones, I.W. Martin, S. Reid, S. Rowan, J. Scott, K.A. Strain, K. Tokmakov, C. Torrie, and A.A. van Veggel. Re-evaluation of the mechanical loss factor of hydroxide-catalysis bonds and its significance for the next generation of gravitational wave detectors. *Phys. Lett. A*, 374(39):3993 – 3998, 2010.

[376] J. Winterflood, D.G. Blair, and B. Slagmolen. High performance vibration isolation using springs in euler column buckling mode. *Physics Letters A*, 300:122–130, 2002.

[377] J.V. van Heijningen, J. Winterflood, and L. Ju. Geometric contoured euler springs for vertical vibration isolation in future gravitational wave detector, 2019.

[378] LSC. LIGO Voyager: A Cryogenic Silicon Interferometer for Gravitational-wave Detection. *LIGO Document: LIGO-P1800072*, 2019.

[379] Yuki Ikushima, Rui Li, Takayuki Tomaru, Nobuaki Sato, Toshikazu Suzuki, Tomiyoshi Haruyama, Takakazu Shintomi, and Akira Yamamoto. Ultra-low-vibration pulse-tube cryocooler system - cooling capacity and vibration. *Cryogenics*, 48(9-10):406 – 412, 2008.

[380] B. Shapiro. Cryogenic Test Mass Work at Stanford. *LIGO Document: LIGO-G1400926*, 2014.

[381] O. Aguiar. Multi-Nested Pendula System: measured, calculated and simulated cooling performances. *LIGO Document: LIGO-G1400845*, 2014.

[382] O. Aguiar, M. Constancio, E. Ferreira, A. Silva, and M. Okada. Multi-Nested Pendula System: Mechanics and Cryogenics Update. *LIGO Document: LIGO-G1500172*, 2015.

[383] B. Shapiro. A Cryogenic LIGO Mirror for 3rd Generation Observatories. *LIGO Document: LIGO-G1600766*, 2016.

[384] Brett Shapiro. Ligo voyager cryogenics at stanford. 2017. LIGO-G1700404.

[385] David I. G. Jones. *Handbook of Viscoelastic Vibration Damping.* Chichester: J. Wiley, 2001. pp. 171-174.

[386] Y. Sakakibara et al. A study of cooling time reduction of interferometric cryogenic gravitational wave detectors using a high-emissivity coating. *AIP Conf. Proc*, 1573:176, 2013.

[387] Acktar Ltd. Acktar black coating services.

[388] J. Lehman, C. Yung, N. Tomlin, D. Conklin, and M. Stephens. Carbon nanotube-based black coatings. *Applied physics reviews*, 5:011103, 2018.

[389] M R Abernathy, N Smith, W Z Korth, R X Adhikari, L G Prokhorov, D V Koptsov and V P Mitrofanov. Measurement of mechanical loss in the acktar black coating of silicon wafers. *Classical and Quantum Gravity*, 33:185002.

[390] L.G. Prokhorov, V.P. Mitrofanov, B. Kamai, A. Markowitz, Xiaoyue Ni, R. X. Adhikari. Measurement of mechanical losses in the carbon nanotube nasa black coating of silicon wafers. *LIGO-G1800447*, 2018.

[391] Joris van Heijningen. A fifty-fold improvement of thermal noise limited inertial sensitivity byoperating at cryogenic temperatures. *Journal of Instrumentation*, 15:P06034, 2020.

[392] Giles Hammond. Suspension Thermal Noise. *LIGO Document: LIGO-G1200579*, 2012.

[393] Disha Kapasi, Bram Slagmolen, Terry McRae, Robert Ward, Paul Altin, Andrew Wade, Johannes Eichholz, and David McClelland. Preparing thermal noise measurements in gram-scale silicon flexures at 123K. *https://dcc.ligo.org/LIGO-G2100478*, 2021.

[394] Y. Klochkov and V. Mitrofanov. Temperature dependence of loss caused by an electric field in silicon disk mechanical resonators, 2022.

[395] R. Birney, A. V. Cumming, P. Campsie, D. Gibson, G. D. Hammond, J. Hough, I. W. Martin, S. Reid, S. Rowan, S. Song. Coatings and surface treatments for enhanced performance suspensions for future gravitational wave detectors. *Classical and Quantum Gravity*, 34:235012, 2017.

[396] L.G. Prokhorov, D.V. Koptsov, M.S. Matiushechkina, V.P. Mitrofanov, K. Haughian, J. Hough, S. Rowan, A.A. van Veggel, P.G. Murray, G.D. Hammond, K. Tokmakov. Cryogenic measurement of hydroxide catalysis bond loss using a silicon tuning fork oscillator. *LIGO-G1700340*, 2017.

[397] Evan Hall. Cosmic Explorer: a 40 km gravitational-wave detector. *LIGO Document: LIGO-G1901563-v2*, 2018.

[398] V. Guerrero. Monitoring void fraction and bubble formation in flowing liquid nitrogen. *LIGO G1701534*, 2017.

[399] Odylio Aguiar, Marcio Constancio, Elvis Ferreira, and Marcos Okada. Cryogenic updates for voyager. *LIGO Document: LIGO-G1800357*, 2018.

[400] Odylio Aguiar, Marcio Constancio, Rana Adhikari, Koji Arai, Aaron Markowitz, Marcos Okada, and Christopher Wipf. Ligo voyager rd: Silicon emissivity as a function of temperature. *LIGO Document: LIGO-G1900394*, 2019.

[401] Marcio Constancio, Rana Adhikari, Odylio Aguiar, Koji Arai, Aaron Markowitz, Marcos Okada, and Christopher Wipf. Silicon emissivity as a function of temperature. *International Journal of Heat and Mass Transfer*, 157:119863, 2020.

[402] L. Winkelmann, O. Puncken, R. Kluzik, C. Veltkamp, P. Kwee, J. Poeld, C. Bogan, B. Willke, M. Frede, J. Neumann, P. Wessels, and D. Kracht. Injection-locked single-frequency laser with an output power of 220 W. *Applied Physics B: Lasers and Optics*, 102:529–538, 2011.

[403] Maik Frede, Ralf Wilhelm, Dietmar Kracht, and Carsten Fallnich. Nd:YAG ring laser with 213 W linearly polarized fundamental mode output power. *Opt. Express*, 13:7516–7519, 2005.

[404] Gregory D. Goodno, Lewis D. Book, and Joshua E. Rothenberg. Low-phase-noise, single-frequency, single-mode 608 w thulium fiber amplifier. *Opt. Lett.*, 34(8):1204–1206, Apr 2009.

[405] D. P. Kapasi, J. Eichholz, T. McRae, R. L. Ward, B. J. J. Slagmolen, S. Legge, K. S. Hardman, P. A. Altin, and D. E. McClelland. Tunable narrow-linewidth laser at 2 μm wavelength for gravitational wave detector research. *Opt. Express*, 28(3):3280–3288, Feb 2020.

[406] Yue Tao, Man Jiang, Can Li, Pu Zhou, and Jiang Zongfu. Low threshold 1150 nm single-polarization single-frequency yb-doped dfb fiber. In *Colloquium on Optical Fibre Gratings (Ref. No. 1999/023)*, volume 16, page 1999, 1915.

[407] Wiktor Walasik, Daniya Traore, Alexandre Amavigan, Robert E Tench, Jean-Marc Delavaux, and Emmanuel Pinsard. 2-m narrow linewidth all-fiber dfb fiber bragg grating lasers for ho-and tm-doped fiber-amplifier applications. *Journal of Lightwave Technology*, 2021.

[408] Shijie Fu, Wei Shi, Yan Feng, Lei Zhang, Zhongmin Yang, Shanhui Xu, Xiushan Zhu, Robert A Norwood, and N Peyghambarian. Review of recent progress on single-frequency fiber lasers. *JOSA B*, 34(3):A49–A62, 2017.

[409] Peter Hofmann, Christian Voigtlander, Stefan Nolte, N Peyghambarian, and Axel Schulzgen. 550-mw output power from a narrow linewidth all-phosphate fiber laser. *Journal of lightwave technology*, 31(5):756–760, 2012.

[410] Jiageng Chen, Qingwen Liu, and Zuyuan He. Feedforward laser linewidth narrowing scheme using acousto-optic frequency shifter and direct digital synthesizer. *Journal of Lightwave Technology*, 37(18):4657–4664, 2019.

[411] Patrick Kwee, Benno Willke, and Karsten Danzmann. Shot-noise-limited laser power stabilization with a high-power photodiode array. *Opt. Lett.*, 34:2912–2914, 2009.

[412] D. A. Bryan, R. Gerson, and H. E. Tomaschke. Increase optical damage resistance in lithium niobate. *Appl. Phys. Lett.*, 44:847, 1984.

[413] Miftar Ganija, David Ottaway, Peter Veitch, and Jesper Munch. Cryogenic, high power, near diffraction limited, yb:yag slab laser. *Opt. Express*, 21(6):6973–6978, Mar 2013.

[414] S. Karki, D. Tuyenbayev, S. Kandhasamy, B.P. Abbott, T.D. Abbott, E.H. Anders, J. Berliner, J. Betzwieser, C. Cahillane, L. Canete, C. Conley, H.P. Daveloza, N. De Lillo, J.R. Gleason, E. Goetz, K. Izumi, J.S. Kissel, G. Mendell, V. Quetschke, M. Rodruck, S. Sachdev, T. Sadecki, P.B. Schwinberg, A. Sottile, M. Wade, A.J. Weinstein, M. West, and R.L. Savage. The advanced ligo photon calibrators. *Review of Scientific Instruments*, 87:114503, 2016. (LIGO-P1500249).

[415] M. Evans and P. Fritschel. TCS and the Golden Shield. *LIGO Document: LIGO-T0900359-v2*, 2009.

[416] G. Mueller, M. Arain, P. Sainathan, and G. Ciani. aLIGO TCS Ring Heater development at UF - Krakow 2010 talk. *LIGO Document: LIGO-G1000945-v1*, 2010.

[417] Rich Abbott, Rana Adhikari, Stefan Ballmer, Lisa Barsotti, Matt Evans, Peter Fritschel, Valera Frolov, Guido Mueller, Bram Slagmolen, and Sam Waldman. Advligo interferometer sensing and control conceptual design. *LIGO Document: LIGO-T070247-01*, 2007.

[418] K. Arai, M. Ando, S. Moriwaki, K. Kawabe, and K. Tsubono. New signal extraction scheme with harmonic demodulation for power-recycled fabry-perot-michelson interferometers. *Phys. Lett. A*, 273:15–24, 2000.

[419] T. Fricke, N. Smith-Lefebvre, R. Abbott, R. Adhikari, K. L. Dooley, M. Evans, P. Fritschel, V. Frolov, K. Kawabe, J. S. Kissel, and S. Waldman. DC readout experiment in Enhanced LIGO. *Class. Quantum Grav.*, 2012.

[420] S Hild, H Grote, J Degallaix, S Chelkowski, K Danzmann, A Freise, M Hewitson, J Hough, H Lück, M Prijatelj, K A Strain, J R Smith, and B Willke. Dc-readout of a signal-recycled gravitational wave detector. *Class. Quantum Grav.*, 26(5):055012, 2009.

[421] K. Goda, O. Miyakawa, E. E. Mikhailov, S. Saraf, R. Adhikari, K. McKenzie, R. Ward, S. Vass, A. J. Weinstein, and N. Mavalvala. A quantum-enhanced prototype gravitational-wave detector. *Nature Physics*, 4:472–476, 2008.

[422] Osamu Miyakawa, Robert Ward, Rana Adhikari, Matthew Evans, Benjamin Abbott, Rolf Bork, Daniel Busby, Jay Heefner, Alexander Ivanov, Michael Smith, Robert Taylor, Stephen Vass, Alan Weinstein, Monica Varvella, Seiji Kawamura, Fumiko Kawazoe, Shihori Sakata, and Conor Mow-Lowry. Measurement of optical response of a detuned resonant sideband extraction gravitational wave detector. *Phys. Rev. D*, 74:022001, 2006.

[423] R L Ward, R Adhikari, B Abbott, R Abbott, D Barron, R Bork, T Fricke, V Frolov, J Heefner, A Ivanov, O Miyakawa, K McKenzie, B Slagmolen, M Smith, R Taylor, S Vass, S Waldman, and A Weinstein. DC readout experiment at the caltech 40m prototype interferometer. *Class. Quantum Grav.*, 25(11):114030, 2008.

[424] Matt Evans, Peter Fritschel, David McClelland, John Miller, Adam Mullavey, Daniel Shaddock, Bram Slagmolen, Sam Waldman, and et al. Adv. ligo arm length stabilization design. *LIGO Document: LIGO-T0900144*, 2012.

[425] Adam J. Mullavey, Bram J. J. Slagmolen, John Miller, Matthew Evans, Peter Fritschel, Daniel Sigg, Sam J. Waldman, Daniel A. Shaddock, and David E. McClelland. Arm-length stabilisation for interferometric gravitational-wave detectors using frequency-doubled auxiliary lasers. *Opt. Express*, 20:81–89, 2012.

[426] Kiwamu Izumi, Koji Arai, Bryan Barr, Joseph Betzwieser, Aidan Brooks, Katrine Dahl, Suresh Doravari, Jennifer C. Driggers, W. Zach Korth, Haixing Miao, Jameson Graef Rollins, Stephen Vass, David Yeaton-Massey, and Rana Adhikari. Multicolor cavity metrology. *LIGO Document: LIGO-P1200019*, 2012.

[427] Vajente Gabriele. Machine learning testbed interferometer. *LIGO Document Control Center*, 2020. LIGO-E2000273.

[428] John A. Sidles and Daniel Sigg. Optical torques in suspended Fabry–Perot interferometers. *Phys. Lett. A*, 354:167–172, 2006.

[429] N. Smith-Lefebvre, S. Ballmer, M. Evans, S. Waldman, K. Kawabe, V. Frolov, and N. Mavalvala. Optimal alignment sensing of a readout mode cleaner cavity. *Opt. Lett.*, 36(22):4365–4367, 2011.

[430] Walter Del Pozzo. Inference of cosmological parameters from gravitational waves: Applications to second generation interferometers. *Phys. Rev. D*, 86:043011, Aug 2012.

[431] Salvatore Vitale, Walter Del Pozzo, Tjonnie G. F. Li, Chris Van Den Broeck, Ilya Mandel, Ben Aylott, and John Veitch. Effect of calibration errors on bayesian parameter estimation for gravitational wave signals from inspiral binary systems in the advanced detectors era. *Phys. Rev. D*, 85:064034, Mar 2012.

[432] Salvatore Vitale, Ryan Lynch, John Veitch, Vivien Raymond, and Riccardo Sturani. Measuring the spin of black holes in binary systems using gravitational waves. *Phys. Rev. Lett.*, 112:251101, Jun 2014.

[433] Emanuele Berti, Enrico Barausse, Vitor Cardoso, Leonardo Gualtieri, Paolo Pani, Ulrich Sperhake, Leo C Stein, Norbert Wex, Kent Yagi, Tessa Baker, C P Burgess, Flávio S Coelho, Daniela Doneva, Antonio De Felice, Pedro G Ferreira, Paulo C C Freire, James Healy, Carlos Herdeiro, Michael Horbatsch, Burkhard Kleihaus, Antoine Klein, Kostas Kokkotas, Jutta Kunz, Pablo Laguna, Ryan N Lang, Tjonnie G F Li, Tyson Littenberg, Andrew Matas, Saeed Mirshekari, Hirotada Okawa, Eugen Radu, Richard O'Shaughnessy, Bangalore S Sathyaprakash, Chris Van Den Broeck, Hans A Winther, Helvi Witek, Mir Emad Aghili, Justin Alsing, Brett Bolen, Luca Bombelli, Sarah Caudill, Liang Chen, Juan Carlos Degollado, Ryuichi Fujita, Caixia Gao, Davide Gerosa, Saeed Kamali, Hector O Silva, João G Rosa, Laleh Sadeghian, Marco Sampaio, Hajime Sotani, and Miguel Zilhao. Testing general relativity with present and future astrophysical observations. *Classical and Quantum Gravity*, 32(24):243001, dec 2015.

[434] Benjamin D. Lackey and Leslie Wade. Reconstructing the neutron-star equation of state with gravitational-wave detectors from a realistic population of inspiralling binary neutron stars. *Phys. Rev. D*, 91:043002, Feb 2015.

[435] B. P. Abbott, R. Abbott, T. D. Abbott, F. Acernese, K. Ackley, C. Adams, T. Adams, P. Addesso, R. X. Adhikari, V. B. Adya, C. Affeldt, B. Agarwal, M. Agathos, K. Agatsuma, N. Aggarwal, O. D. Aguiar, L. Aiello, A. Ain, P. Ajith, B. Allen, G. Allen, A. Allocca, M. A. Aloy, P. A. Altin, A. Amato, A. Ananyeva, S. B. Anderson, W. G. Anderson, S. V. Angelova, S. Antier, S. Appert, K. Arai, M. C. Araya, J. S. Areeda, M. Arène, N. Arnaud, K. G. Arun, S. Ascenzi, G. Ashton, M. Ast, S. M. Aston, P. Astone, D. V. Atallah, F. Aubin, P. Aufmuth, C. Aulbert, K. AultONeal, C. Austin, A. Avila-Alvarez, S. Babak, P. Bacon, F. Badaracco, M. K. M. Bader, S. Bae, P. T. Baker, F. Baldaccini, G. Ballardin, S. W. Ballmer, S. Banagiri, J. C. Barayoga, S. E. Barclay, B. C. Barish, D. Barker, K. Barkett, S. Barnum, F. Barone, B. Barr, L. Barsotti, M. Barsuglia, D. Barta, J. Bartlett, I. Bartos, R. Bassiri, A. Basti, J. C. Batch, M. Bawaj, J. C. Bayley, M. Bazzan, B. Bécsy, C. Beer, M. Bejger, I. Belahcene, A. S. Bell, D. Beniwal, M. Bensch, B. K. Berger, G. Bergmann, S. Bernuzzi, J. J. Bero, C. P. L. Berry, D. Bersanetti, A. Bertolini, J. Betzwieser, R. Bhandare, I. A. Bilenko, S. A. Bilgili, G. Billingsley, C. R. Billman, J. Birch, R. Birney, O. Birnholtz, S. Biscans, S. Biscoveanu, A. Bisht, M. Bitossi, M. A. Bizouard, J. K. Blackburn, J. Blackman, C. D. Blair, D. G. Blair, R. M. Blair, S. Bloemen, O. Bock, N. Bode, M. Boer, Y. Boetzel, G. Bogaert, A. Bohe, F. Bondu, E. Bonilla, R. Bonnand, P. Booker, B. A. Boom, C. D. Booth, R. Bork, V. Boschi, S. Bose, K. Bossie, V. Bossilkov, J. Bosveld, Y. Bouffanais, A. Bozzi, C. Bradaschia, P. R. Brady, A. Bramley, M. Branchesi, J. E. Brau, T. Briant, F. Brighenti, A. Brillet, M. Brinkmann, V. Brisson, P. Brockill, A. F. Brooks, D. D. Brown, S. Brunett, C. C. Buchanan, A. Buikema, T. Bulik, H. J. Bulten, A. Buonanno, D. Buskulic, C. Buy, R. L. Byer, M. Cabero, L. Cadonati, G. Cagnoli, C. Cahillane, J. Calderón Bustillo, T. A. Callister, E. Calloni, J. B. Camp, M. Canepa, P. Canizares, K. C. Cannon, H. Cao, J. Cao, C. D. Capano, E. Capocasa, F. Carbognani, S. Caride, M. F. Carney, G. Carullo, J. Casanueva Diaz, C. Casentini, S. Caudill, M. Cavaglià, F. Cavalier, R. Cavalieri, G. Cella, C. B. Cepeda, P. Cerdá-Durán, G. Cerretani, E. Cesarini, O. Chaibi, S. J. Chamberlin, M. Chan, S. Chao, P. Charlton, E. Chase, E. Chassande-Mottin, D. Chatterjee, K. Chatziioannou, B. D. Cheeseboro, H. Y. Chen, X. Chen, Y. Chen, H.-P. Cheng, H. Y. Chia, A. Chincarini, A. Chiummo, T. Chmiel, H. S. Cho, M. Cho, J. H. Chow, N. Christensen, Q. Chu, A. J. K. Chua, S. Chua, K. W. Chung, S. Chung, G. Ciani, A. A. Ciobanu, R. Ciolfi, F. Cipriano, C. E. Cirelli, A. Cirone, F. Clara, J. A. Clark, P. Clearwater, F. Cleva, C. Cocchieri, E. Coccia, P.-F. Cohadon, D. Cohen, A. Colla, C. G. Collette, C. Collins, L. R. Cominsky, M. Constancio, L. Conti, S. J. Cooper, P. Corban, T. R. Corbitt, I. Cordero-Carrión, K. R. Corley, N. Cornish, A. Corsi, S. Cortese, C. A. Costa, R. Cotesta, M. W. Coughlin, S. B. Coughlin, J.-P. Coulon, S. T. Countryman, P. Couvares, P. B. Covas, E. E. Cowan, D. M. Coward, M. J. Cowart, D. C. Coyne, R. Coyne, J. D. E. Creighton, T. D. Creighton, J. Cripe, S. G. Crowder, T. J. Cullen, A. Cumming, L. Cunningham, E. Cuoco, T. Dal Canton, G. Dálya, S. L. Danilishin, S. D'Antonio, K. Danzmann, A. Dasgupta, C. F. Da Silva Costa, V. Dattilo, I. Dave, M. Davier, D. Davis, E. J. Daw, B. Day, D. DeBra, M. Deenadayalan, J. Degallaix, M. De Laurentis, S. Deléglise, W. Del Pozzo, N. Demos, T. Denker, T. Dent, R. De Pietri, J. Derby, V. Dergachev, R. De Rosa, C. De Rossi, R. DeSalvo, O. de Varona, S. Dhurandhar, M. C. Díaz, T. Dietrich, L. Di Fiore, M. Di Giovanni, T. Di Girolamo, A. Di Lieto, B. Ding, S. Di Pace, I. Di Palma, F. Di Renzo, A. Dmitriev, Z. Doctor, V. Dolique, F. Donovan,

K. L. Dooley, S. Doravari, I. Dorrington, M. Dovale Álvarez, T. P. Downes, M. Drago, C. Dreissigacker, J. C. Driggers, Z. Du, R. Dudi, P. Dupej, S. E. Dwyer, P. J. Easter, T. B. Edo, M. C. Edwards, A. Effler, H.-B. Eggenstein, P. Ehrens, J. Eichholz, S. S. Eikenberry, M. Eisenmann, R. A. Eisenstein, R. C. Essick, H. Estelles, D. Estevez, Z. B. Etienne, T. Etzel, M. Evans, T. M. Evans, V. Fafone, H. Fair, S. Fairhurst, X. Fan, S. Farinon, B. Farr, W. M. Farr, E. J. Fauchon-Jones, M. Favata, M. Fays, C. Fee, H. Fehrmann, J. Feicht, M. M. Fejer, F. Feng, A. Fernandez-Galiana, I. Ferrante, E. C. Ferreira, F. Ferrini, F. Fidecaro, I. Fiori, D. Fiorucci, M. Fishbach, R. P. Fisher, J. M. Fishner, M. Fitz-Axen, R. Flaminio, M. Fletcher, H. Fong, J. A. Font, P. W. F. Forsyth, S. S. Forsyth, J.-D. Fournier, S. Frasca, F. Frasconi, Z. Frei, A. Freise, R. Frey, V. Frey, P. Fritschel, V. V. Frolov, P. Fulda, M. Fyffe, H. A. Gabbard, B. U. Gadre, S. M. Gaebel, J. R. Gair, L. Gammaitoni, M. R. Ganija, S. G. Gaonkar, A. Garcia, C. García-Quirós, F. Garufi, B. Gateley, S. Gaudio, G. Gaur, V. Gayathri, G. Gemme, E. Genin, A. Gennai, D. George, J. George, L. Gergely, V. Germain, S. Ghonge, Abhirup Ghosh, Archisman Ghosh, S. Ghosh, B. Giacomazzo, J. A. Giaime, K. D. Giardina, A. Giazotto, K. Gill, G. Giordano, L. Glover, E. Goetz, R. Goetz, B. Goncharov, G. González, J. M. Gonzalez Castro, A. Gopakumar, M. L. Gorodetsky, S. E. Gossan, M. Gosselin, R. Gouaty, A. Grado, C. Graef, M. Granata, A. Grant, S. Gras, C. Gray, G. Greco, A. C. Green, R. Green, E. M. Gretarsson, P. Groot, H. Grote, S. Grunewald, P. Gruning, G. M. Guidi, H. K. Gulati, X. Guo, A. Gupta, M. K. Gupta, K. E. Gushwa, E. K. Gustafson, R. Gustafson, O. Halim, B. R. Hall, E. D. Hall, E. Z. Hamilton, H. F. Hamilton, G. Hammond, M. Haney, M. M. Hanke, J. Hanks, C. Hanna, M. D. Hannam, O. A. Hannuksela, J. Hanson, T. Hardwick, J. Harms, G. M. Harry, I. W. Harry, M. J. Hart, C.-J. Haster, K. Haughian, J. Healy, A. Heidmann, M. C. Heintze, H. Heitmann, P. Hello, G. Hemming, M. Hendry, I. S. Heng, J. Hennig, A. W. Heptonstall, F. J. Hernandez, M. Heurs, S. Hild, T. Hinderer, D. Hoak, S. Hochheim, D. Hofman, N. A. Holland, K. Holt, D. E. Holz, P. Hopkins, C. Horst, J. Hough, E. A. Houston, E. J. Howell, A. Hreibi, E. A. Huerta, D. Huet, B. Hughey, M. Hulko, S. Husa, S. H. Huttner, T. Huynh-Dinh, A. Iess, N. Indik, C. Ingram, R. Inta, G. Intini, H. N. Isa, J.-M. Isac, M. Isi, B. R. Iyer, K. Izumi, T. Jacqmin, K. Jani, P. Jaranowski, D. S. Johnson, W. W. Johnson, D. I. Jones, R. Jones, R. J. G. Jonker, L. Ju, J. Junker, C. V. Kalaghatgi, V. Kalogera, B. Kamai, S. Kandhasamy, G. Kang, J. B. Kanner, S. J. Kapadia, S. Karki, K. S. Karvinen, M. Kasprzack, W. Kastaun, M. Katolik, S. Katsanevas, E. Katsavounidis, W. Katzman, S. Kaufer, K. Kawabe, N. V. Keerthana, F. Kéfélian, D. Keitel, A. J. Kemball, R. Kennedy, J. S. Key, F. Y. Khalili, B. Khamesra, H. Khan, I. Khan, S. Khan, Z. Khan, E. A. Khazanov, N. Kijbunchoo, Chunglee Kim, J. C. Kim, K. Kim, W. Kim, W. S. Kim, Y.-M. Kim, E. J. King, P. J. King, M. Kinley-Hanlon, R. Kirchhoff, J. S. Kissel, L. Kleybolte, S. Klimenko, T. D. Knowles, P. Koch, S. M. Koehlenbeck, S. Koley, V. Kondrashov, A. Kontos, M. Korobko, W. Z. Korth, I. Kowalska, D. B. Kozak, C. Krämer, V. Kringel, B. Krishnan, A. Królak, G. Kuehn, P. Kumar, R. Kumar, S. Kumar, L. Kuo, A. Kutynia, S. Kwang, B. D. Lackey, K. H. Lai, M. Landry, P. Landry, R. N. Lang, J. Lange, B. Lantz, R. K. Lanza, A. Lartaux-Vollard, P. D. Lasky, M. Laxen, A. Lazzarini, C. Lazzaro, P. Leaci, S. Leavey, C. H. Lee, H. K. Lee, H. M. Lee, H. W. Lee, K. Lee, J. Lehmann, A. Lenon, M. Leonardi, N. Leroy, N. Letendre, Y. Levin, J. Li, T. G. F. Li, X. Li, S. D. Linker, T. B. Littenberg, J. Liu, X. Liu, R. K. L. Lo, N. A. Lockerbie,

L. T. London, A. Longo, M. Lorenzini, V. Loriette, M. Lormand, G. Losurdo, J. D. Lough, C. O. Lousto, G. Lovelace, H. Lück, D. Lumaca, A. P. Lundgren, R. Lynch, Y. Ma, R. Macas, S. Macfoy, B. Machenschalk, M. MacInnis, D. M. Macleod, I. Magaña Hernandez, F. Magaña Sandoval, L. Magaña Zertuche, R. M. Magee, E. Majorana, I. Maksimovic, N. Man, V. Mandic, V. Mangano, G. L. Mansell, M. Manske, M. Mantovani, F. Marchesoni, F. Marion, S. Márka, Z. Márka, C. Markakis, A. S. Markosyan, A. Markowitz, E. Maros, A. Marquina, F. Martelli, L. Martellini, I. W. Martin, R. M. Martin, D. V. Martynov, K. Mason, E. Massera, A. Masserot, T. J. Massinger, M. Masso-Reid, S. Mastrogiovanni, A. Matas, F. Matichard, L. Matone, N. Mavalvala, N. Mazumder, J. J. McCann, R. McCarthy, D. E. McClelland, S. Mc-Cormick, L. McCuller, S. C. McGuire, J. McIver, D. J. McManus, T. McRae, S. T. McWilliams, D. Meacher, G. D. Meadors, M. Mehmet, J. Meidam, E. Mejuto-Villa, A. Melatos, G. Mendell, D. Mendoza-Gandara, R. A. Mercer, L. Mereni, E. L. Merilh, M. Merzougui, S. Meshkov, C. Messenger, C. Messick, R. Metzdorff, P. M. Meyers, H. Miao, C. Michel, H. Middleton, E. E. Mikhailov, L. Milano, A. L. Miller, A. Miller, B. B. Miller, J. Miller, M. Millhouse, J. Mills, M. C. Milovich-Goff, O. Minazzoli, Y. Minenkov, J. Ming, C. Mishra, S. Mitra, V. P. Mitrofanov, G. Mitselmakher, R. Mittleman, D. Moffa, K. Mogushi, M. Mohan, S. R. P. Mohapatra, M. Montani, C. J. Moore, D. Moraru, G. Moreno, S. Morisaki, B. Mours, C. M. Mow-Lowry, G. Mueller, A. W. Muir, Arunava Mukherjee, D. Mukherjee, S. Mukherjee, N. Mukund, A. Mullavey, J. Munch, E. A. Muñiz, M. Muratore, P. G. Murray, A. Nagar, K. Napier, I. Nardecchia, L. Naticchioni, R. K. Nayak, J. Neilson, G. Nelemans, T. J. N. Nelson, M. Nery, A. Neunzert, L. Nevin, J. M. Newport, K. Y. Ng, S. Ng, P. Nguyen, T. T. Nguyen, D. Nichols, A. B. Nielsen, S. Nissanke, A. Nitz, F. Nocera, D. Nolting, C. North, L. K. Nuttall, M. Obergaulinger, J. Oberling, B. D. O'Brien, G. D. O'Dea, G. H. Ogin, J. J. Oh, S. H. Oh, F. Ohme, H. Ohta, M. A. Okada, M. Oliver, P. Oppermann, Richard J. Oram, B. O'Reilly, R. Ormiston, L. F. Ortega, R. O'Shaughnessy, S. Ossokine, D. J. Ottaway, H. Overmier, B. J. Owen, A. E. Pace, G. Pagano, J. Page, M. A. Page, A. Pai, S. A. Pai, J. R. Palamos, O. Palashov, C. Palomba, A. Pal-Singh, Howard Pan, Huang-Wei Pan, B. Pang, P. T. H. Pang, C. Pankow, F. Pannarale, B. C. Pant, F. Paoletti, A. Paoli, M. A. Papa, A. Parida, W. Parker, D. Pascucci, A. Pasqualetti, R. Passaquieti, D. Passuello, M. Patil, B. Patricelli, B. L. Pearlstone, C. Pedersen, M. Pedraza, R. Pedurand, L. Pekowsky, A. Pele, S. Penn, C. J. Perez, A. Perreca, L. M. Perri, H. P. Pfeiffer, M. Phelps, K. S. Phukon, O. J. Piccinni, M. Pichot, F. Piergiovanni, V. Pierro, G. Pillant, L. Pinard, I. M. Pinto, M. Pirello, M. Pitkin, R. Poggiani, P. Popolizio, E. K. Porter, L. Possenti, A. Post, J. Powell, J. Prasad, J. W. W. Pratt, G. Pratten, V. Predoi, T. Prestegard, M. Principe, S. Privitera, G. A. Prodi, L. G. Prokhorov, O. Puncken, M. Punturo, P. Puppo, M. Pürrer, H. Qi, V. Quetschke, E. A. Quintero, R. Quitzow-James, F. J. Raab, D. S. Rabeling, H. Radkins, P. Raffai, S. Raja, C. Rajan, B. Rajbhandari, M. Rakhmanov, K. E. Ramirez, A. Ramos-Buades, Javed Rana, P. Rapagnani, V. Raymond, M. Razzano, J. Read, T. Regimbau, L. Rei, S. Reid, D. H. Reitze, W. Ren, F. Ricci, P. M. Ricker, G. Riemenschneider, K. Riles, M. Rizzo, N. A. Robertson, R. Robie, F. Robinet, T. Robson, A. Rocchi, L. Rolland, J. G. Rollins, V. J. Roma, R. Romano, C. L. Romel, J. H. Romie, D. Rosińska, M. P. Ross, S. Rowan, A. Rüdiger, P. Ruggi, G. Rutins, K. Ryan, S. Sachdev, T. Sadecki, M. Sakellariadou, L. Salconi, M. Saleem, F. Salemi, A. Samajdar, L. Sammut, L. M.

Sampson, E. J. Sanchez, L. E. Sanchez, N. Sanchis-Gual, V. Sandberg, J. R. Sanders, N. Sarin, B. Sassolas, B. S. Sathyaprakash, P. R. Saulson, O. Sauter, R. L. Savage, A. Sawadsky, P. Schale, M. Scheel, J. Scheuer, P. Schmidt, R. Schnabel, R. M. S. Schofield, A. Schönbeck, E. Schreiber, D. Schuette, B. W. Schulte, B. F. Schutz, S. G. Schwalbe, J. Scott, S. M. Scott, E. Seidel, D. Sellers, A. S. Sengupta, D. Sentenac, V. Sequino, A. Sergeev, Y. Setyawati, D. A. Shaddock, T. J. Shaffer, A. A. Shah, M. S. Shahriar, M. B. Shaner, L. Shao, B. Shapiro, P. Shawhan, H. Shen, D. H. Shoemaker, D. M. Shoemaker, K. Siellez, X. Siemens, M. Sieniawska, D. Sigg, A. D. Silva, L. P. Singer, A. Singh, A. Singhal, A. M. Sintes, B. J. J. Slagmolen, T. J. Slaven-Blair, B. Smith, J. R. Smith, R. J. E. Smith, S. Somala, E. J. Son, B. Sorazu, F. Sorrentino, T. Souradeep, A. P. Spencer, A. K. Srivastava, K. Staats, M. Steinke, J. Steinlechner, S. Steinlechner, D. Steinmeyer, B. Steltner, S. P. Stevenson, D. Stocks, R. Stone, D. J. Stops, K. A. Strain, G. Stratta, S. E. Strigin, A. Strunk, R. Sturani, A. L. Stuver, T. Z. Summerscales, L. Sun, S. Sunil, J. Suresh, P. J. Sutton, B. L. Swinkels, M. J. Szczepańczyk, M. Tacca, S. C. Tait, C. Talbot, D. Talukder, D. B. Tanner, M. Tápai, A. Taracchini, J. D. Tasson, J. A. Taylor, R. Taylor, S. V. Tewari, T. Theeg, F. Thies, E. G. Thomas, M. Thomas, P. Thomas, K. A. Thorne, E. Thrane, S. Tiwari, V. Tiwari, K. V. Tokmakov, K. Toland, M. Tonelli, Z. Tornasi, A. Torres-Forné, C. I. Torrie, D. Töyrä, F. Travasso, G. Traylor, J. Trinastic, M. C. Tringali, L. Trozzo, K. W. Tsang, M. Tse, R. Tso, D. Tsuna, L. Tsukada, D. Tuyenbayev, K. Ueno, D. Ugolini, A. L. Urban, S. A. Usman, H. Vahlbruch, G. Vajente, G. Valdes, N. van Bakel, M. van Beuzekom, J. F. J. van den Brand, C. Van Den Broeck, D. C. Vander-Hyde, L. van der Schaaf, J. V. van Heijningen, A. A. van Veggel, M. Vardaro, V. Varma, S. Vass, M. Vasúth, A. Vecchio, G. Vedovato, J. Veitch, P. J. Veitch, K. Venkateswara, G. Venugopalan, D. Verkindt, F. Vetrano, A. Viceré, A. D. Viets, S. Vinciguerra, D. J. Vine, J.-Y. Vinet, S. Vitale, T. Vo, H. Vocca, C. Vorvick, S. P. Vyatchanin, A. R. Wade, L. E. Wade, M. Wade, R. Walet, M. Walker, L. Wallace, S. Walsh, G. Wang, H. Wang, J. Z. Wang, W. H. Wang, Y. F. Wang, R. L. Ward, J. Warner, M. Was, J. Watchi, B. Weaver, L.-W. Wei, M. Weinert, A. J. Weinstein, R. Weiss, F. Wellmann, L. Wen, E. K. Wessel, P. Weßels, J. Westerweck, K. Wette, J. T. Whelan, B. F. Whiting, C. Whittle, D. Wilken, D. Williams, R. D. Williams, A. R. Williamson, J. L. Willis, B. Willke, M. H. Wimmer, W. Winkler, C. C. Wipf, H. Wittel, G. Woan, J. Woehler, J. K. Wofford, W. K. Wong, J. Worden, J. L. Wright, D. S. Wu, D. M. Wysocki, S. Xiao, W. Yam, H. Yamamoto, C. C. Yancey, L. Yang, M. J. Yap, M. Yazback, Hang Yu, Haocun Yu, M. Yvert, A. Zadrożny, M. Zanolin, T. Zelenova, J.-P. Zendri, M. Zevin, J. Zhang, L. Zhang, M. Zhang, T. Zhang, Y.-H. Zhang, C. Zhao, M. Zhou, Z. Zhou, S. J. Zhu, X. J. Zhu, A. B. Zimmerman, Y. Zlochower, M. E. Zucker, and J. Zweizig. Properties of the binary neutron star merger gw170817. *Phys. Rev. X*, 9:011001, Jan 2019.

[436] B. P. Abbott, R. Abbott, T. D. Abbott, M. R. Abernathy, F. Acernese, K. Ackley, C. Adams, T. Adams, P. Addesso, R. X. Adhikari, V. B. Adya, C. Affeldt, M. Agathos, K. Agatsuma, N. Aggarwal, O. D. Aguiar, L. Aiello, A. Ain, P. Ajith, T. Akutsu, B. Allen, A. Allocca, P. A. Altin, A. Ananyeva, S. B. Anderson, W. G. Anderson, M. Ando, S. Appert, K. Arai, A. Araya, M. C. Araya, J. S. Areeda, N. Arnaud, K. G. Arun, H. Asada, S. Ascenzi, G. Ashton, Y. Aso, M. Ast, S. M. Aston, P. Astone,

S. Atsuta, P. Aufmuth, C. Aulbert, A. Avila-Alvarez, K. Awai, S. Babak, P. Bacon, M. K. M. Bader, L. Baiotti, P. T. Baker, F. Baldaccini, G. Ballardin, S. W. Ballmer, J. C. Barayoga, S. E. Barclay, B. C. Barish, D. Barker, F. Barone, B. Barr, L. Barsotti, M. Barsuglia, D. Barta, J. Bartlett, M. A. Barton, I. Bartos, R. Bassiri, A. Basti, J. C. Batch, C. Baune, V. Bavigadda, M. Bazzan, B. Bécsy, C. Beer, M. Bejger, I. Belahcene, M. Belgin, A. S. Bell, B. K. Berger, G. Bergmann, C. P. L. Berry, D. Bersanetti, A. Bertolini, J. Betzwieser, S. Bhagwat, R. Bhandare, I. A. Bilenko, G. Billingsley, C. R. Billman, J. Birch, R. Birney, O. Birnholtz, S. Biscans, A. Bisht, M. Bitossi, C. Biwer, M. A. Bizouard, J. K. Blackburn, J. Blackman, C. D. Blair, D. G. Blair, R. M. Blair, S. Bloemen, O. Bock, M. Boer, G. Bogaert, A. Bohe, F. Bondu, R. Bonnand, B. A. Boom, R. Bork, V. Boschi, S. Bose, Y. Bouffanais, A. Bozzi, C. Bradaschia, P. R. Brady, V. B. Braginsky, M. Branchesi, J. E. Brau, T. Briant, A. Brillet, M. Brinkmann, V. Brisson, P. Brockill, J. E. Broida, A. F. Brooks, D. A. Brown, D. D. Brown, N. M. Brown, S. Brunett, C. C. Buchanan, A. Buikema, T. Bulik, H. J. Bulten, A. Buonanno, D. Buskulic, C. Buy, R. L. Byer, M. Cabero, L. Cadonati, G. Cagnoli, C. Cahillane, J. Calderón Bustillo, T. A. Callister, E. Calloni, J. B. Camp, K. C. Cannon, H. Cao, J. Cao, C. D. Capano, E. Capocasa, F. Carbognani, S. Caride, J. Casanueva Diaz, C. Casentini, S. Caudill, M. Cavaglià, F. Cavalier, R. Cavalieri, G. Cella, C. B. Cepeda, L. Cerboni Baiardi, G. Cerretani, E. Cesarini, S. J. Chamberlin, M. Chan, S. Chao, P. Charlton, E. Chassande-Mottin, B. D. Cheeseboro, H. Y. Chen, Y. Chen, H.-P. Cheng, A. Chincarini, A. Chiummo, T. Chmiel, H. S. Cho, M. Cho, J. H. Chow, N. Christensen, Q. Chu, A. J. K. Chua, S. Chua, S. Chung, G. Ciani, F. Clara, J. A. Clark, F. Cleva, C. Cocchieri, E. Coccia, P.-F. Cohadon, A. Colla, C. G. Collette, L. Cominsky, M. Constancio, L. Conti, S. J. Cooper, T. R. Corbitt, N. Cornish, A. Corsi, S. Cortese, C. A. Costa, M. W. Coughlin, S. B. Coughlin, J.-P. Coulon, S. T. Countryman, P. Couvares, P. B. Covas, E. E. Cowan, D. M. Coward, M. J. Cowart, D. C. Coyne, R. Coyne, J. D. E. Creighton, T. D. Creighton, J. Cripe, S. G. Crowder, T. J. Cullen, A. Cumming, L. Cunningham, E. Cuoco, T. Dal Canton, S. L. Danilishin, S. D'Antonio, K. Danzmann, A. Dasgupta, C. F. Da Silva Costa, V. Dattilo, I. Dave, M. Davier, G. S. Davies, D. Davis, E. J. Daw, B. Day, R. Day, S. De, D. DeBra, G. Debreczeni, J. Degallaix, M. De Laurentis, S. Deléglise, W. Del Pozzo, T. Denker, T. Dent, V. Dergachev, R. De Rosa, R. T. DeRosa, R. DeSalvo, R. C. Devine, S. Dhurandhar, M. C. Díaz, L. Di Fiore, M. Di Giovanni, T. Di Girolamo, A. Di Lieto, S. Di Pace, I. Di Palma, A. Di Virgilio, Z. Doctor, K. Doi, V. Dolique, F. Donovan, K. L. Dooley, S. Doravari, I. Dorrington, R. Douglas, M. Dovale Álvarez, T. P. Downes, M. Drago, R. W. P. Drever, J. C. Driggers, Z. Du, M. Ducrot, S. E. Dwyer, K. Eda, T. B. Edo, M. C. Edwards, A. Effler, H.-B. Eggenstein, P. Ehrens, J. Eichholz, S. S. Eikenberry, R. A. Eisenstein, R. C. Essick, Z. Etienne, T. Etzel, M. Evans, T. M. Evans, R. Everett, M. Factourovich, V. Fafone, H. Fair, S. Fairhurst, X. Fan, S. Farinon, B. Farr, W. M. Farr, E. J. Fauchon-Jones, and M. Favata. Prospects for observing and localizing gravitational-wave transients with advanced ligo, advanced virgo and kagra. *Living Reviews in Relativity*, 21(1):3, Apr 2018.

[437] Katerina Chatziioannou, Carl-Johan Haster, and Aaron Zimmerman. Measuring the neutron star tidal deformability with equation-of-state-independent relations and gravitational waves. *Phys. Rev. D*, 97:104036, May 2018.

[438] Juan Calderón Bustillo, Pablo Laguna, and Deirdre Shoemaker. Detectability of gravitational waves from binary black holes: Impact of precession and higher modes. *Phys. Rev. D*, 95:104038, May 2017.

[439] C. Cahillane1, J. Betzwieser, D.A. Brown, E. Goetz, E.D. Hall, K. Izumia, S. Kandhasamy, S. Karki, J.S. Kissel, G. Mendell, R.L. Savage, D. Tuyenbayev, A. Urban, A. Viets, M. Wade, and A.J. Weinstein. Calibration uncertainty for advanced ligo's first and second observing runs. *Physical Review D*, 96:102001, 2017. (LIGO-P1600139).

[440] Ling Sun, Evan Goetz, Jeffrey S. Kissel, Joseph Betzwieser, Sudarshan Karki, Aaron Viets, Madeline Wade, Dripta Bhattacharjee, Vladimir Bossilkov, Pep B. Covas, Laurence E. H. Datrier, Rachel Gray, Shivaraj Kandhasamy, Yannick K. Lecoeuche, Gregory Mendell, Timesh Mistry, Ethan Payne, Richard L. Savage, Alan J. Weinstein, Stuart Aston, Aaron Buikema, Craig Cahillane, Jenne C. Driggers, Sheila E. Dwyer, Rahul Kumar, and Alexander Urban. Characterization of systematic error in advanced ligo calibration, 2020.

[441] D. Tuyenbayev, T. Sadecki, and R. Savage. Photon calibrator procedure for measuring response ratios of power calibration standards. 2018. (LIGO-T1400442).

[442] D Bhattacharjee, Y Lecoeuche, S Karki, J Betzwieser, V Bossilkov, S Kandhasamy, E Payne, and R L Savage. Fiducial displacements with improved accuracy for the global network of gravitational wave detectors, 2020.

[443] D Estevez, B Lieunard, F Marion, B Mours, L Rolland, and D Verkindt. First tests of a newtonian calibrator on an interferometric gravitational wave detector. *Classical and Quantum Gravity*, 35(23):235009, nov 2018.

[444] Yuki Inoue, Sadakazu Haino, Nobuyuki Kanda, Yujiro Ogawa, Toshikazu Suzuki, Takayuki Tomaru, Takahiro Yamanmoto, and Takaaki Yokozawa. Improving the absolute accuracy of the gravitational wave detectors by combining the photon pressure and gravity field calibrators. *Phys. Rev. D*, 98:022005, Jul 2018.

[445] R. Adhikari et al. Grant application for moore foundation funding in calibration. 2020. LIGO-L1800369.

[446] J. C. Driggers, M. Evans, K. Pepper, and R. Adhikari. Active noise cancellation in a suspended interferometer. *Rev. Sci. Instrum.*, 83, 2012.

[447] J. C. Driggers et al. Improving astrophysical parameter estimation via offline noise subtraction for advanced ligo. *Phys. rev. D*, page 042001, 2019.

[448] G. Vajente, Y. Huang, M. Isi, J. C. Driggers, J. S. Kissel, M. J. Szczepańczyk, and S. Vitale. Machine-learning nonstationary noise out of gravitational-wave detectors. *Phys. Rev. D*, 101:042003, Feb 2020.

[449] G. Vajente. Machine learning and controls in gw detectors. 2018. LIGO-G1800874.

[450] Koji Arai, Joe Betzwieser, Peter Kalmus, and Rana Adhikari. Simulated plant approach. *LIGO Document: LIGO-G1000546*, 2010.

[451] N. Mukund. update on lockloss monitoring & prediction. 2018. LIGO-G1800569.

[452] L. Price. Optimal transfer functions. 2014. LIGO-G1400084.

[453] R. Pintelon and J. Schoukens. *System Identification: A Frequency Domain Approach.* John Wiley & Sons, 2012.

[454] M. Coughlin, P. Earle, J. Harms, S. Biscansa, C. Buchanan, E. Coughlin, F. Donovan, J. Fee, H. Gabbard, M. Guy, and *et al.* Limiting the effects of earthquakes on gravitational-wave interferometers. Classical and Quantum Gravity, page 044004, 2017. LIGO-P1600321.

[455] N. Mukund, M. Coughlin, J. Harms, N. Arnaud, D. Barker, S. Biscans, E. Coughlin, F. Donovan, P.S. Earle, J. Fee, I. Fiori, H. Gabbard, M.R. Guy, B. Lantz, R. Mittleman, A. Pele, H. Radkins, B. Swinkels, K. Thorne, and J. Warner. Status of seismon. 2018. LIGO-G1800118.

[456] S Biscans, J Warner, R Mittleman, C Buchanan, M Coughlin, M Evans, H Gabbard, J Harms, B Lantz, N Mukund, A Pele, C Pezerat, P Picart, H Radkins, and T Shaffer. Control strategy to limit duty cycle impact of earthquakes on the ligo gravitational-wave detectors. *Classical and Quantum Gravity*, 35(5):055004, 2018. LIGO-P1700163.

[457] A. Pele, M. Kasprzack, R. Adhikari, H. Yu, E. Quintero, and J. Driggers. L2a decoupling webpage. Classical and Quantum Gravity.

[458] B. Lantz, S. Biscans, J. Warner, A. Pele, H. Radkins, N. Mukund, and M. Coughlin. Seismic control during earthquakes: Review of new technique. LIGO-G1800399.

[459] M. Kasprzack. Angular control issues in advanced ligo. 2018. LIGO-G1800989.

[460] H. Yu and D. Martynov. Optimal and robust control of the arm alignment with mu-synthesis. 2018. LIGO-T1800077.

[461] H. Yu and D. Sigg. Alignment sensing in the signal recycling cavity using a new 118.3 mhz sideband scheme. 2017. LIGO-T1700215.